UNIVERSITY OF SOUTHAMPTON

FACULTY OF MEDICINE

Mechanical Forces and Collagen in Asthma

by

Wiparat Manuyakorn

Thesis for the degree of Doctor of Philosophy

October 2011

UNIVERSITY OF SOUTHAMPTON

ABSTRACT

FACULTY OF MEDICINE

Doctor of Philosophy

MECHANICAL FORCES AND COLLAGEN IN ASTHMA

by Wiparat Manuyakorn

Asthma is an airway inflammatory disease with functional and structural changes, leading to bronchial hyperresponsiveness (BHR) and airflow obstruction. Collagen is the most abundant extracellular matrix (ECM) protein in the airways and its cross-linking by lysyl oxidase (LOX) influences its strength and stability. An increase in collagen deposition in the subepithelial layer is a characteristic feature of airway remodelling in asthma. Even though inhaled corticosteroids can suppress airway inflammation, the natural history of asthma is still unaltered after inhaled corticosteroid treatment. It was hypothesized that (i) mechanical stimulation of the airways (eg. during bronchoconstriction or deep inspiration) may activate submucosal fibroblasts to produce collagen and LOX; (ii) the profibrotic effects of TGFβ on collagen and LOX expression are insensitive to corticosteroids and (iii) these responses may contribute to alterations in the properties of collagen in asthmatic airways.

Bronchial fibroblasts from healthy and asthmatic subjects were exposed to cyclical mechanical strain. To investigate the impact of corticosteroids, bronchial fibroblasts from healthy and asthmatic subjects and lung fibroblasts from one interstitial lung disease patient were treated with dexamethasone in the presence and absence of TGFβ2. Soluble collagen was measured by Sircol assay. LOX mRNA expression was measured using RT-qPCR. The level of LOX in cell culture supernatants and in bronchoalveolar lavage (BAL) fluid from healthy, mild and severe asthma was measured using western blot analysis. Airway collagen from healthy and asthmatic subjects was extracted and its structure and mechanical properties were investigated using atomic force microscopy (AFM).

Mechanical strain enhanced the production of soluble collagen ($p < 0.01$). Active LOX was increased after mechanical strain. TGFβ2 up-regulated LOX mRNA expression and enhanced the production of pro and active LOX in fibroblasts from all groups ($p<0.02$). Dexamethasone up-regulated LOX mRNA expression only in fibroblasts from asthmatic and ILD subjects, but dexamethasone enhanced the production of pro and active LOX in fibroblasts from all groups ($p<0.05$). Active LOX was only detected in BAL fluid from severe asthmatic subjects. The structure of airway collagen from a healthy non-asthmatic and an asthmatic subject was not different. Both of them exhibited a characteristic banding pattern with similar size as demonstrated by AFM. However, airway collagen from the asthmatic subject had a greater stiffness than collagen from the healthy non-asthmatic subject.

Mechanical strain of airway fibroblasts enhanced the production of collagen. Dexamethasone, TGFβ2 and mechanical strain up-regulated LOX production. Exposure to mechanical stimulation and/or a high level of TGFβ and corticosteroids (for asthma treatment) in asthmatic airways may result in more LOX production with the potential for increased cross-linked collagen deposition in asthmatic airways. This may alter collagen stiffness to affect airway wall mechanics. These findings suggest that apart from their immediate anti-inflammatory effects, corticosteroids may have a long term detrimental effect on collagen cross-linking. Should such an action be evident in vivo this could have a detrimental effect on decline in lung function and disease persistence in asthma.

Table of contents

List of figures

List of tables

DECLARATION OF AUTHORSHIP

I, Wiparat Manuyakorn, declare that the thesis entitled

“Mechanical Forces and Collagen in Asthma”

and the work presented in the thesis are both my own, and have been generated by me as the result of my own original research. I confirm that:

- this work was done wholly or mainly while in candidature for a research degree at this University;
- where any part of this thesis has previously been submitted for a degree or any other qualification at this University or any other institution, this has been clearly stated;
- where I have consulted the published work of others, this is always clearly attributed;
- where I have quoted from the work of others, the source is always given. With the exception of such quotations, this thesis is entirely my own work;
- I have acknowledged all main sources of help;
- where the thesis is based on work done by myself jointly with others, I have made clear exactly what was done by others and what I have contributed myself;
- none of this work has been published before submission, or [delete as appropriate] parts of this work have been published as: [please list references]

Signed: ……..

Date:…….

Acknowledgements

All work presented in this thesis was performed by me except in the following instances:

Dr David Summit and Dr Sarah Field: provided fibroblasts samples
Dr Laurie Lau: provided BAL fluid samples
Dr Susan Wilson: provided nasal polyp sample, pellets culture TEM samples processing and helping in imaging TEM samples
Dr Aton Page: processed SEM samples, helping in TEM negative staining and imaging and SEM samples imaging
Dr Jane Warner: provided lung parenchyma and COPD airways samples
Drs Nivenka Jayasekara and Patrick Dennison: provided bronchial biopsy samples for AFM imaging
Mr Orestis Katsamenis: analysed nanoindentation load and displacement curve of collagen from nasal polyp and rat tail samples
Mr Tsiloon Li: imaged collagen from rat tail and performed nanoindentation
Mr Orestis Antriotis: analysed nanoindentation load and displacement curve of collagen from healthy non-asthmatic and asthmatic airways
Dr Philipp Thurner: supervised all AFM works at School of Engineering Science
Dr Mick Phillips: helped in imaging collagen from healthy and asthmatic airways

I would like to thank you all my colleagues in Brooke lab for their helps: Ms Camelia Molnar, Ms Sue Martin, Dr Nicole Bedke and Ms Gemma Cambell. Special thanks to Drs Antonio Noto and Hans-Michael Haitchi for helping me in the beginning of my PhD work. I wouldn't be able to complete my study without the supports from family: Papa, Mama, J' Lin and H' Seng. Thank you for all helps from friends in Southampton especially Miao-chiu, Xiaoli, P'Ying, P'Tan, P'Aui, P'Pom, P'Pui, Jom, Dear, N'M and Kate. Special thanks to Ning and N'Pik for listening and supporting. My studentship wouldn't be happened without the funding support from Faculty of Medicine, Ramathibodi Hospital, Bangkok, Thailand. Special thanks to all my colleagues in Division of Allergy and Immunology: A.Suwat, A.Charerat, P'Som and P'Ba for allowing me to leave from work for my study. Special thanks to Doa and P'Pat who helped in looking after my parents while I was away. I wouldn't have come to Southampton without the help of Professor Stephen Holgate. This work wouldn't have been finished without the excellent supervisions from my supervisors: Dr Peter Howarth and Professor Donna Davies. Thank you very much Peter and Donna. Thank you Medical Research Council for the funding of this work.

Abbreviations

A2	phospholipase A2
AFM	atomic force microscopy
ASM	airway smooth muscles
α-SMA	α-smooth muscle actin
BAL	bronchoalveolar larvage
BAPN	β-aminopropionitrile
BDP	Beclometasone Dipropionate
BHR	Bronchial hyper-responsiveness
BM	basement membrane
BSA	Bovine Serum Albumin
cDNA	complementary deoxyribonucleic acid
CCM	conditioned media
COPD	chronic obstructive pulmonary disease
CPM	cycle per minute
Ct	threshold cycle in a polymerase reaction
CTGF	connective tissue growth factor
DAPI	4',6-diamidino-2-phenylindole
Dex	dexamethasone
Δ-DHLNL	dehydro-dihydroxylysinonorleucine
DMEM	Dubelcco's modified Eagle's medium
DMSO	dimethyl sulphoxide
DNA	deoxyribonucleotide triphosphate
DOC	deoxycholate
dNTP	deoxyribonucleotide triphosphate
DPD	deoxypyridinolone
3D	3 dimensional
ECM	extracellular matrix components
EDTA	Ethylenediaminetetraacetic acid
EGFR	epidermal growth factor receptor
EMT	epithelial-mesenchymal transition
EMTU	epithelial-mesenchymal trophic unit
ELISA	Enyzyme-linked Immunosorbent Assay
E	elastic (young)'s modulus
Er	reduced modulus
Es	sample modulus
F	female

FBS	foetal bovine serum
FEV_1	forced expiratory volume at 1 second
FGF	fibroblast growth factor
FITC	fluorescein isothiocyanate
Fmax	maximum force applied
FOT	forced oscillation technique ()
GAG	glycosaminoglycan
GAPDH	Glyceraldehyde 3-phosphate dehydrogenase
GINA	global initiative for asthma
GFP	green fluorescent protein
GWASs	genome-wide association studies
HBSS	Hank's balanced saline solution
HHL	histidinohydroxylysinonorleucine
HIF1-α	Hypoxia-inducible factor-1α
Δ-HLNL	dehydro-hydroxylysinonorleucine
hc	contact depth
hmax	penetration depth
hf	final depth
HRCT	high-resolution computed tomography
HRP	horseradish peroxidase ()
Hz	Hertz
IFNγ	interferon-γ
IL	interleukin
ILD	interstitial lung disease
LABA	long acting beta2 agonist
LH	lysyl hydroxylase
LOX	lysyl oxidase
M	male
MMLV	Moloney murine leukemia virus
MMPs	matrix metalloproteinases
MUC5AC	mucin-5AC
NEAA	nonessential amino acids
Oligo-dT	oligodeoxythymidylic acid
OGNs	oligonucleotides
P	probability value
PAGE	PolyAcrylamide Gel Electrophoresis
PBS	phosphate buffer saline
PCR	Polymerase chain reaction
PDGF	platelet derived growth factor
PGE_2	prostaglandin E_2 synthesis

PIPES	piperazine-N,N′-bis(2-ethanesulfonic acid)
P4H	propyl 4-hydroxylase
PVDF	Polyvinylidene Fluoride
PYD	pyridinoline
rDNase I	recombinant dexoyribonuclease I
RBM	reticular basement membrane
RNA	ribonucleic acid
RT	reverse transcription
RT-qPCR	Real time-Quantitative PCR Analysis
ROS	reactive oxygen species
S	stiffness
SDS	Sodium dodecyl sulphate
SEM	Scanning electron microscopy
SLRPs	small leucine-rich proteoglycans
Taq	Thermus aquaticus
TBS	tris-buffered saline
TEM	Transmission electron microscopy
TGFβ	transforming growth factor-β
Th1	T helper cell type 1
Th2	T helper cell type 2
Th17	T helper cell type 17
TIMP	tissue inhibitors of MMPs
TMB	tetramethylbezidine
UBC	Ubiquitin C
VAT	Video-assisted thoracoscopy
VEGF	vascular endothelial growth factor
Yr	year

Chapter 1: Introduction and Review of Literature

1.1) Asthma definition

Asthma is a disease that defined by its typical clinical, physiological and pathological characteristics. The major feature of clinical history is episodic shortness of breath, particularly at night or cannot exercise and accompanied by cough. Wheezing is also a common clinical feature. The characteristic physiological feature of asthma is variable airway obstruction and it measures bronchial hyperresponsiveness. The main pathological findings are airway inflammation and structural airway changes (1). The global initiative for asthma (GINA) has defined asthma as "*a chronic inflammatory disorder of the airways in which many cells and cellular elements plays a role. The chronic inflammation is associated with airway hyperresponsiveness that leads to recurrent of wheezing, breathlessness, chest tightness, and coughing, particularly at night or in the early morning. These episodes are usually associated within the lung that is often reversible either spontaneously or with treatment*".

1.2) Asthma epidemiology and the burden of asthma

Asthma is a worldwide problem, particularly in industrialised countries. The prevalence has increased dramatically over the last 40 years with the prevalence from 1% to 18% of the population in different countries (1). It is one of the commonest chronic conditions in Western countries affecting 1 in 7 children and 1 in 12 adults (2). A recent assessment of asthma across Europe (Brussels Declaration) has identified substantial unmet clinical need which accounts for approximately 50% of the health costs (3).

1.3) Factors influencing the development and expression of asthma

Asthma is thought to arise through the action of environmental factors on a genetically susceptible host. Early environmental exposures, such as viral infections, tobacco smoke (passive and active), and allergens, in children with genetic predisposition result in the development of asthma (1). Epidemiologic studies have identified some unexpected environmental trigger for the development of asthma, such as exposure to chemicals in the home (4), paracetamol use (5), air pollution (6), and obesity (7). The intra-uterine environment also has a role in asthma development. For example, it has been shown that maternal smoking and diet during pregnancy as well as intra-uterine growth and birth weight are associated with later life asthma development (8-10). There are multiple genes associated with asthma pathogenesis and different genes may be involved in different ethnicity. Most, but not all, asthma is associated with atopy (the inherited predisposition to generate IgE against common environmental allergens). With the era of genome-wide association studies (GWASs), there has been a better understanding of the genetic factors that underlie inherited susceptibility to asthma (11). Several studies have demonstrated the genetic influence in natural history of asthma, from susceptibility to atopy, susceptibility to asthma, progression to severe disease and the response of treatment. A number of genes have been identified the association with susceptibility to atopy such as a polymorphic variant of human *IL13* (12), and gene encoding a chain of the high-affinity receptor for IgE (*FCER1A*) (13). A disintegrin and metalloproteinase 33 gene (*ADAM33*) was identified as an asthma susceptible gene. A genetic polymorphism in *ADAM33* has been shown to associate with an accelerated decline in lung function in asthmatic adults (14) or impaired lung function in atopic asthmatic children (15). There are multiple genes that were suggested to determine the overall risk of asthma, such as *ADAM33*, Dipeptidyl peptidase X (*DPP10*), PHD Finger Protein 11 (*PHF11*), Human Leukocyte Antigen G (*HLAG*), Neuropeptide - S Receptor 1 (*NSPR1*), Urokinase Plasminogen Activated Receptor (*PLAUR*), Protocadherin 1 (*PCDH1*), and Interleukin 1 Receptor-Associated Kinase 3 (*IRAK3*) (16). The interactions between environmental factors and individual genetic variation in genes that controls environmental response, such as innate immune responses (*CD14 and TLR4*) (17;18), oxidant response (*GSTM1 GSTT1, and GSTP1*)(19-21), have been shown to associate with increased risk of asthma. Polymorphisms of genes, such as the β2-adrenergic receptor (*ADRB2) (22;23)*, tumor necrosis factor α (*TNFA)* (24), have been shown to associate with measures of asthma severity, such as exacerbation frequency or treatment indices. A recent large scale, consortium based, genomewide association study of asthma has identified the association between asthma and the following gene: *ORMDL3, IL1RL1/IL18R1, HLA-DQ, SMAD3, IL2RB* (25). Genes involved in asthma are summarized in Table 1-1.

Table 1-1 : Susceptible genes associated with asthma (11;25)

Stages of asthma progression	Examples of genes associated with disease
The susceptibility to disease	
-Susceptibility to atopy	*IL13, FCER1A*
-Susceptibility to asthma through altered lung development	*ADAM33, HHIP, MMP12*
-Susceptibility to asthma	*ADAM33, PHF11, DPP10, HLA-G, GPRA (GPCR 154),IRAK3,ORMDL3, IL1RL1/IL18R1, HLA-DQ, SMAD3, IL2RB*
-Susceptibility to asthma through altered response to environment	*CD14, TLR4, GSTM1 GSTT1, GSTP1*
Progression of disease	
-Progression to severe disease	*ADRB2, TNFA*
-Fixed airway obstruction and accelerated decrease in lung function	*ADAM33, GSTM1* and *GSTT1*, estrogen receptor, possibly *TNS1,GSTCD, AGER, HTR4, THSD4,GPR126, ADAM19, FAM13A,PTCH1, PID1*
Response to treatment	
-Altered response to treatment	*ADRB2, CRHR1, ALOX5, ALOX5AP*

1.4) Asthma pathogenesis

Asthma is a common chronic disorder of the airway that is characterized by the complex interaction of airway obstruction, bronchial hyper-responsiveness (BHR), and airway inflammation which leads to recurrent episodes of wheezing, breathlessness, chest tightness, and coughing. The airway inflammation is typically eosinophillic and accompanied by elevation of Th2 cytokines (1). Eosinophils are a key feature of Th2 inflammation and are a useful biomarker in guiding treatment (26). However, Th2 inflammation alone cannot explain all features of asthma. For example airway hyperresponsiveness and tissue remodelling are not entirely linked to this inflammation (27). There are a number of asthmatic patients in whom anti-inflammatory therapy does not lead to symptom control and who are considered treatment resistant. Furthermore, asthmatic patients treated with an IL-5 mAb (mepolizumab) or T cell directed therapy have failed to demonstrate symptomatic improvement (27;28). Furthermore whilst recognized to modify eosinophilic inflammation, inhaled corticosteroids treatment in atopic children with recurrent wheezing has shown to have no effect on declining in lung function and the natural history of asthma (29-31). This irreversible airflow obstruction has been shown to develop despite appropriate use of inhaled corticosteroids, as advocated by international disease management guidelines (32).

Apart from eosinophilic inflammation, neutrophilic inflammation, which is Th1 and/or Th17 mediated inflammation, has also been suggested to play an important role in asthma pathogenesis especially in severe corticosteroids dependent asthma (33). The number of neutrophils in the airway lavage from severe asthmatic patients has been reported to be higher than normal patients (33). Furthermore, airway neutrophilia has been shown to link with chronic airway narrowing in asthma (34), occupational asthma (35), exercise induced asthma (36), and nocturnal asthma (37). Sputum levels of IL-8 in severe asthmatic patients have been reported to be also higher than in non-severe asthmatic patients (38), and an increase sputum IL-8 is also found in severe asthmatics subjects with neutrophilia (39). This suggests that an increase in neutrophils in severe asthma may be secondary to IL-8 generation. As a result, it has been recognized at least in severe asthma that asthma is not a purely Th2 mediated disease. Furthermore, there is increasing evidence for the role of structural airway cells in the pathogenesis of asthma.

The epithelium has a role as a physical barrier and is known to be significant in translating gene-environment interactions (40). Epithelial cells in asthmatic subjects have been shown to be more susceptible to oxidant induced apoptosis and have increased permeability after exposure to ozone or nitrogen dioxide (41;42). The leakiness of the asthmatic epithelium may lead to greater access of inhaled allergens, pollutants and other irritants. Injuries to the epithelium cause the release of fibroproliferative and profibrogenic growth factors. These include transforming growth factor-β (TGFβ), fibroblast growth factor (FGF), platelet derived growth factor (PDGF), and endothelin-1 (43;44). Among these growth factors, TGFβ is notably significant because it is able to further impair epithelial repair response and promote the differentiation of fibroblast into myofibroblasts (45). Increased numbers of myofibroblasts have been demonstrated in the subepithelial and submucosal region of asthmatic airways and increase in proportion to disease chronicity and severity (45). Myofibroblasts can secrete collagen, extracellular matrix components and growth factors such as endothelin-1 and vascular endothelial growth factor (VEGF) (40). The communication between the epithelial and mesenchymal cells or the epithelial-mesenchymal trophic unit (EMTU) has been proposed to drive the remodelling of the asthmatic airways (40). Apart from environmental injury to epithelial cells, Th2 mediated airway inflammation can trigger and perpetuate a vicious cycle of epithelial injury, and thus the remodelling processes can occur as a consequence of repeated injuries, inflammation and impaired healing processes (Figure 1-1).

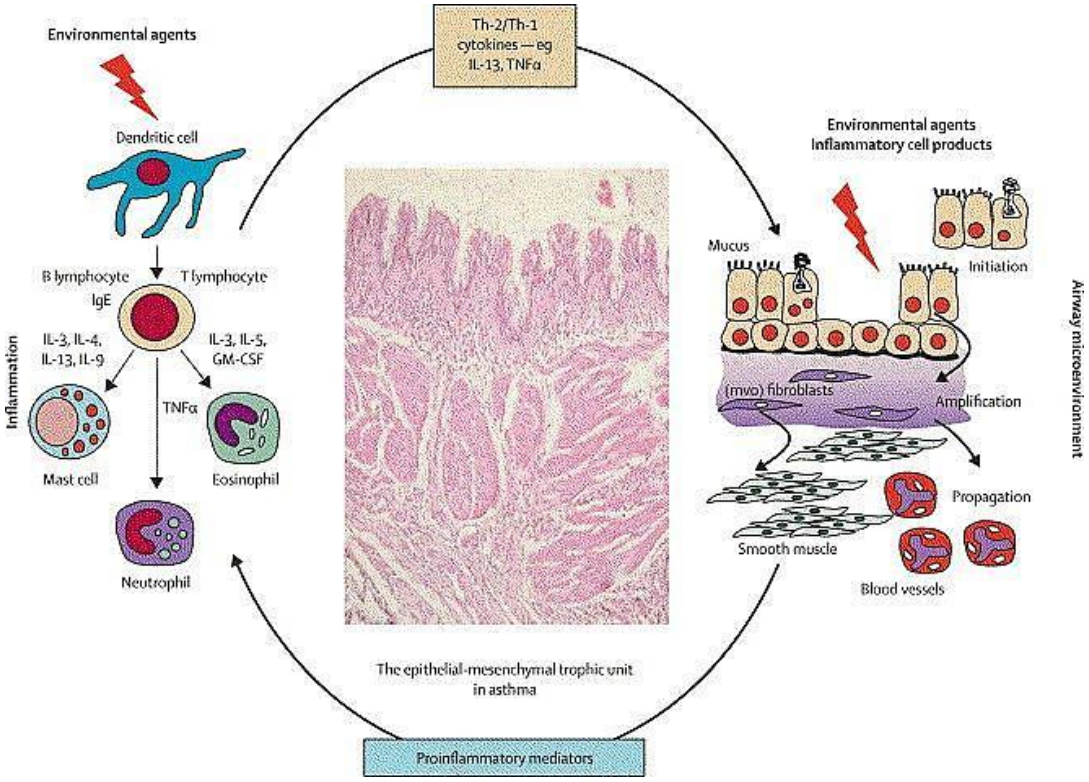

Figure 1-1: Communication between Th2 inflammation and epithelial-mesenchymal tropic unit in response to airway injury. This image was reprinted from The Lancet, Vol 368, Number 9537, Holgate et al., The mechanisms, diagnosis, and management of severe asthma in adults, Page No 383. Copyright (2006), with permission from Elsevier.

1.5) Airway remodelling in asthma

Pathological repair of the airways leads to structural changes that are called airway remodelling. Airway remodelling which has been proposed to result in lower lung function is characterised by subepithelial thickening from collagen deposition, epithelial denudation with goblet cell metaplasia, increased airway smooth muscle mass, bronchial gland enlargement, angiogenesis and alterations in the extracellular matrix components (ECM) such as collagens, proteoglycans and glycoproteins throughout the airway wall (46) (Figure 1-2). Structural remodelling of the airways has been found in children with recurrent wheezing regardless their atopic status (21). It has also been reported that airway epithelial cells in asthmatic children express makers of injury, such as the epidermal growth factor receptor (EGFR), even in the absence of significant eosinophilic inflammation (47). These studies suggest that remodelling can occur independently of inflammation (48). Furthermore, evidence of airway remodelling, such as epithelial layer damage, thickening of basement membrane, angiogenesis has been demonstrated in children as early as 4 years of age in asthmatic subjects (49-51). It is thus an early feature of the disease and not only a marker of long standing chronic disease. However, the subepithelial thickening was not demonstrated in wheezer infants (48). These indicate that airway thickening begins early in the development of asthma and may play role in the disease progression in some patients (52).

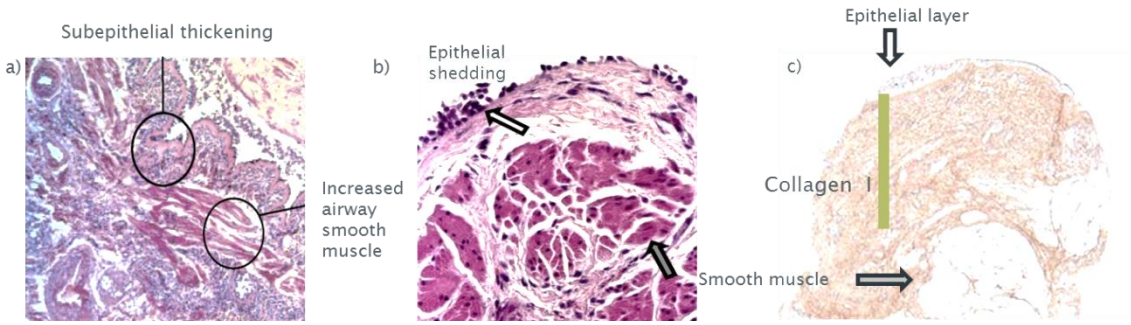

Figure 1-2: Structural changes of airway wall in asthma. Image a) and b) demonstrate epithelial shedding, subepithelial thickening and increased airway smooth muscle mass. Image c) demonstrates increased collagen deposition in subepithelial layer. Image a) and b) were reprinted from Journal of Allergy and Clinical Immunology, Vol 128, Al-Muhsen S, et al., Remodelling in asthma, Page No 453, Copyright (2011), with permission from Elsevier. Image c) was given from Dr Peter Howarth.

1.6) Structural changes in the asthmatic airway wall

The asthmatic airway wall is thicker than the normal airway wall and has been linked to asthma severity. It has been shown that the airway wall thickness is increased by up to 100-300% in patients with non-fatal and fatal asthma when compared with non-asthmatic subjects (35). The asthmatic airways become thickened due to the increase in airway smooth muscle, the laying down of new matrix proteins including collagen fibres and proteoglycans resulting in the thickening of the lamina reticularis, goblet cell hyperplasia, along with proliferation of micro-vessels and vascular leakage (26).

1.6.1) Epithelial layer alterations

Epithelial layer damages in asthma airways include shedding of the epithelium, loss of ciliated cell layer, goblet cell hyperplasia and up-regulation of several growth factors, cytokines and chemokines (45). Previous studies have also demonstrated the change in epithelial tight junction integrity following injury (53). However, epithelial changes are not specific for asthma as they are also observed in several airway diseases.

1.6.2) Subepithelial layer thickening

Subepithelial layer thickening is considered a characteristic feature of airway remodelling in asthma. It has been shown in post-mortem studies that the basement membrane region of patients who died of asthma are two times thicker than those of non-asthmatic airways as demonstrated by light microscopy (54). However, electron microscopy studies revealed that this thickness is really attributable to subepithelial basement membrane thickening (55). The apparent basement membrane thickening is confined to the lamina reticularis, or reticular basement membrane (RBM). The true basement membrane, consisting of the lamina rara and lamina densa, divides the airway epithelium from the mesenchyme which is not altered in the thickness in asthma. Roche et al has shown that this thickened subepithelial basement membrane consists of a dense layer of fibrillar collagens (56). Immunohistochemistry revealed that the thickened reticular layer is largely composed of collagen I, III and V and fibronectin (56). The distribution of laminin and collagen IV is unaltered in asthma. Collagen I was also localised in the interstitium of the submucosal layer through the muscular layer (56-58). Collagen IV is the major constituent of the basement membrane. The major component of the thickened layer are interstitial collagens (collagen I, III, and V), suggesting that the bronchial epithelial cells are not responsible for this collagen deposition. Epithelial cells are responsible for synthesis and maintenance of the true basement membrane. The submucosal layer collagen is most

likely be produced by fibroblasts/myofibroblasts which lie beneath the epithelial layer (59). It has been found that the number of subepithelial myofibroblasts correlates with the thickness of reticular basement membrane (57). Inflammatory cells, such as mast cells, eosinophils, and T cells, also accumulate in the submucosal layer, where the fibroblasts/myofibroblasts are situated. The interaction between inflammatory cells, structural cells (eg, epithelial cells and fibroblasts) and the turnover rate of extracellular matrix protein (ECM) determines the net balance of remodelling and fibrosis within the airways (58). This may suggest an essential role for fibroblasts/myofibroblasts in communicating inflammatory signals from the epithelium through the airway wall (60). Therefore, the chronically injured epithelium and improper repair may contribute to the thickening of the *lamina reticularis* in the asthmatic airways (47). It has been shown that epithelial cells release numerous profibrotic mediators in response to damage that directly influence the synthesis of matrix proteins by fibroblasts/myofibroblasts (61). As a result, this leads to the concept of the epithelial mesenchymal trophic unit (EMTU) as an integrated component within the airways of relevance to asthma. Fibroblasts from asthmatic airways have been shown to produce more extracellular matrix proteins (perlecan, versican, decorin, and biglycan) than those from normal airway fibroblasts when cultured in vitro (62).

Subepithelial layer thickening has been demonstrated to occur in pre-school wheezers as early as 29 months of age (48). It also has shown to associate with asthma severity (63). However, there is no evidence of association with asthma duration both in fatal and stable asthma studies (63;64). Apart from evaluating airway wall thickness using biopsy samples, high-resolution computed tomography (HRCT) has been used to measure the internal size of the airways. Airway wall thickness evaluated by HRCT has demonstrated the association of the airway wall thickness and asthma severity (65;66). Paradoxically, the airway wall thickness as assessed by HRCT and the RBM thickness in the asthmatic airway were demonstrated to inversely correlate with airway hyperresponsiveness (67;68). Additionally, asthmatic patients who have highly variable airway obstruction or brittle asthma has been shown to have a less airway wall thickening, while those who had less variable or fixed airway obstruction exhibited more thickened airways (69). It was proposed that the thickening with deposition of the matrix proteins may be a protective mechanism by increasing the stiffness of the airways to attenuate the sporadic bronchoconstriction (45).

1.6.3) **Airway smooth muscle hyperplasia and hypertrophy**

An increase in smooth muscle layer in asthma is demonstrated to related to hyperplasia rather than hypertrophy (35). The migration of airway smooth muscle cells (ASM) toward the epithelium was recently suggested to be one of the feature of airway remodelling in asthma (70). Increased airway smooth muscle mass has been suggested to be responsible for the pathophysiology of airway hyperresponsiveness (71;72). ASM cells participate in the remodelling process through the synthesis of ECMs: fibronectin, perlecan, laminin and collagen I in response to growth factors (TGFβ, VEGF, and CTGF) and serum from asthmatic patients (73-76).

1.7) Candidate mediators in airway remodelling

1.7.1) **TGFβ**

TGFβ has been recognized as the central mediator of tissue fibrosis and structural remodelling (77). There are three TGFβ isoforms identified in mammals, namely TGFβ1, TGFβ2 and TGFβ3 (78). All these three isoforms are expressed in the normal human airways. Previous studies have shown increased TGFβ1 and TGFβ2 expression in asthmatic airways (79-82). There is little information on TGFβ3, but it was suggested the similar expression in non-asthmatic and asthmatic airway. Both TGFβ1 and TGFβ2 were shown to equally regulate airway collagen deposition in an animal model (83). Overexpression of TGFβ in a murine model resulted in a marked increase in collagen deposition within the lungs (84). Mice treated with TGFβ intratracheally have been demonstrated to have up-regulation of collagen I and III mRNA expression (85). Additionally, both TGFβ1 and TGFβ2 have been reported to up-regulate collagen III gene expression in human lung fibroblasts (86). TGFβ was shown to induce an apoptotic effect in airway epithelial cells. This results in the detachment of epithelial cells, one of the characteristic of airway remodelling in asthma. On the other hand, TGFβ has been demonstrated to be responsible for epithelial-mesenchymal transition (EMT), a process by which fully differentiated epithelial cells undergo phenotypic transition to fully differentiated mesenchymal cells (fibroblasts and myofibroblasts), (87;88). It was shown that TGFβ induced EMT both primary airway epithelial cells from asthmatic and normal subjects, but the number of airway epithelial cells undergoing EMT was greater in those from asthmatic subjects (88). This suggests that TGFβ may be linked to the dysregulated epithelial repair in asthmatic airways.

Furthermore, baseline levels of TGFβ1 are higher in bronchoalveolar lavage (BAL) fluid from asthmatic subjects as compared to that in BAL fluid from non-asthmatic controls. Additionally, both TGFβ1 and TGFβ2 have been reported to be increased in BAL fluid after segmental allergen challenge (89). Human bronchial epithelial cells have been shown to release predominantly TGFβ2 (44). It was also shown that mechanical stress to human bronchial epithelial cells enhanced the release of TGFβ2 but not TGFβ1 (43;90). TGFβ2 was also shown to be involved in wound healing, subepithelial matrix homeostasis and regulation of airway mucin expression (79;91). Hence, epithelial cell derived TGFβ is likely to act on subepithelium and plays a significant role in airway remodelling.

TGFβ can promote the transformation from fibroblasts to myofibroblasts and enhance the survival of fibroblasts/myofibroblasts by inhibiting the apoptosis (92). Myofibroblasts are morphological intermediates of fibroblasts and smooth muscle cells. They express α-smooth muscle actin (αSMA) and microfilament bundles which are regulated by TGFβ1 and TGFβ2 (86;93;94). Myofibroblasts can be distinguished from smooth muscle cells by their lack of smooth muscle cells markers such as desmin and smooth muscle myosin (95). Fibroblasts/myofibroblasts play a key role for extracellular matrix deposition and structural remodelling (77;95).

Current asthma treatment guidelines recommend inhaled corticosteroids as the most effective anti-inflammatory medications for the treatment of chronic asthma (1). Corticosteroids have been reported to inhibit TGFβ production by human foetal lung fibroblasts (96) and to modulate myofibroblast accumulation and TGFβ1 expression in chronic allergen challenge mice (97). Corticosteroids appear to have less impact *in vivo* in human asthma. A recent study in patients with moderate to severe asthma has reported that oral corticosteroids had no effect on the TGFβ expression in bronchial mucosa (80). Currently several approaches to modulate airway remodelling by targeting TGFβ are being investigated. Pre-treatment with a pan-specific TGFβ antibody has been demonstrated to reduce subepithelial ECM deposition as well as, the number and proliferation of airway smooth muscles in an allergic asthmatic murine model (98). A monoclonal anti- TGFβ antibody (GC1008) targeting all three TGFβ isoforms is being tested for treating idiopathic pulmonary fibrosis in a Phase I clinical trial (99). Antisense oligonucleotides (OGNs) against TGFβ1 were shown to significantly reduce the postoperative scarring in an animal model of glaucoma filtration surgery (100). Collectively, these evidences underline the essential role of TGFβ in promoting tissue remodelling. However, apart from a potent profibrotic effect, TGFβ also has an important role in promoting the suppressive function of regulatory T cells and the inhibitory effect on Th1 and Th2 cells (101). Treatment targeting TGFβ thus needs to consider this regulatory function of TGFβ.

1.7.2) **IL-4 and IL-13**

IL-4 and IL-13 are the key cytokines in Th2 differentiation and the pathogenesis of asthma. IL-4 regulates the allergen-specific IgE production whilst IL-13 amongst other actions has been implicated in the regulation of airway hyperresponsiveness (70). IL-4 and IL-13 share a common receptor subunit and have overlap in function. Studies in IL-4 and IL-13 transgenic mice have demonstrated that only IL-13, but not IL-4, has an effect on airway wall fibrosis (102-104). However, the role of IL-4 and IL-13 in regulating subepithelial thickening is still controversial. Batra et al (86) have demonstrated that IL-4, but not IL-13, stimulates human lung fibroblasts to produce collagen III and α-smooth muscle actin (αSMA). In contrast, work by Saito et al (105) have shown that both IL-13 and IL-4 are efficient in induction αSMA protein expression in lung fibroblasts. However, in this study interferon-γ (IFNγ) was found to attenuate this effect. Additionally, a recent study has shown the effect of IL-13 in induction epithelial apoptosis and increase in αSMA and collagen III gene expression in human lung fibroblasts (106). Both IL-4 and IL-13 were shown to enhance TGFβ2 release, but not TGFβ1, from epithelial cells. This effect is insensitive to corticosteroid but can be suppressed by IFNγ (107;108). IL-13 was also shown to enhance fibroblasts in releasing TGFβ2 (107).

1.7.3) **IL-5**

IL-5 is known to responsible for eosinophil growth, differentiation, mobilization, recruitment, activation and survival. Eosinophil has been considered to be important in airway remodelling. An increase in the number of submucosa eosinophils has been shown to be associated with the thickness of the reticular basement membrane (109). In IL-5 deficient mice that are chronically challenged with allergen, there is a significantly lower level of peribronchial fibrosis and smooth muscle layer than similarly challenged wild type mice (110). In a human study in mild asthma, anti-IL-5 treatment was reported to significantly reduce eosinophils and TGFβ1 in BAL fluid as well as the expression of tenascin, lumican and procollagen III in the airway wall. However, these biological effects were not associated with any changes in lung function after treatment (111). Recent studies focusing on steroid dependent-severe asthma with sputum eosinophilia have demonstrated a significantly reduction in asthma exacerbations after treatment with anti-IL-5 that is linked to the reduction of eosinophils (112;113). Furthermore, this study found a significantly improvement in the airway wall area and total airway area when evaluated by computed tomographic scans (112). These findings suggest a role for IL-5 in airway remodelling and asthma exacerbations.

1.7.4) **Matrix metalloproteinase**

Matrix metalloproteinases (MMPs), a family of zinc-dependent endopeptidase, play an important role for the net ECM composition in the airways. They have an ability to cleave ECM components especially collagen. MMPs can be classified according to their substrate specificity such as interstitial collagenase including MMP-1, MMP-8, MMP-13 and gelatinase including MMP-2 and MMP-9. MMPs are firstly synthesized as an inactive pro-form and need to be activated in the extracellular space by other MMPs or serine proteases (114). The activities of MMPs are regulated by their natural inhibitors, tissue inhibitors of MMPs (TIMPs). TIMPs bind to active MMPs in a 1:1 stoichiometric ratio (115). MMPs and TIMPs can be secreted by both structural cells and inflammatory cells in the lung and airways. Airway fibroblasts are the cellular source for MMP-1, MMP-3, MMP-2 and TIMP-1. Bronchial epithelial cells also can release MMP-2, MMP-9 and TIMP-1 (114). Airway smooth muscle cells can secrete MMP-1 and MMP-2 (116). Apart from structural cells, inflammatory cells such as neutrophils are the cellular sources of MMP-8, MMP-9 and TIMP-1 (117). Collagenase MMPs such as MMP-1, MMP-3 and MMP-8 have a major role in degrading interstitial collagen (collagen I and III). It has been suggested that MMP-1 secreted by asthmatic airway smooth muscle cells has a role in airway smooth muscle hyperplasia (118). A recent study has demonstrated an association of MMP-1 polymorphism with persistent airway obstruction in asthma (119). The level of MMP-8 in BAL fluid has been shown to correlate with the degree of airway obstruction in asthma as measured by FEV_1 (120). Gelatinase MMPs (MMP-2 and MMP-9) have a crucial role in lung repair after injury (115). MMP-2 and MMP-9 both play an important role in degrading collagen IV which is the main component of airway basement membrane. Mechanical stimulation to airway epithelial cells in vitro has been shown the increase in MMP-2 and MMP-9 as demonstrated by gelatin zymography (121;122). A low serum MMP-9/TIMP-1 ratio has been identified in asthmatic patients with fixed airway obstruction (123). Additionally, the sputum MMP-9 /TIMP-1 ratio has been reported to be inversely correlated with airway wall thickness (124). The net deposition of collagen I, III in the reticular layer of basement membrane is a result of cycles of matrix degradation and impaired repair and also is favoured by an overproduction of activated TGFβ. This process involves MMP-2 and MMP-9 which have the ability to disrupt normal basement membrane (114).

1.8) ECM deposition and mechanical properties of the lungs and airways

The ECM components such as collagens and proteoglycans are important for the mechanical properties of the tissue. The most abundant and most critical ECM for structural integrity is collagen. In an animal model of bleomycin induced fibrosis, the increase in ECM (collagen and proteoglycan) deposition within the lungs and airways correlates with the increase in airway stiffness (125;126). Increases in ECMs especially collagen deposition, and reorganization in the subepithelial layer has been reported in asthmatic airways (56-58). This reorganization of ECM fibres has been suggested to be responsible for a change tissue mechanical properties (127). However, little is known about the effects of remodelling on the mechanical function of asthmatic airways. Physiological studies have suggested that it may stiffen the airways, making them less distensible during forced inspiration (128-130) or less collapsible during forced expiration (131) than those of normal subjects. Airway distensibility is calculated by the change in airway calibre per unit change in lung volume (132). Ward et al have reported a negative correlation between the thickness of the reticular basement membrane and airway distensibility in asthma (128). A recent study has found a reduction in airway distensibility in asthmatic subjects, as compared to non-asthmatic subjects, with no changes in airway distensibility after bronchodilator administration (133). The authors of this study suggested the reduction in airway distensibility in subjects with asthma may represent the effects of airway structural changes rather than those of airway smooth muscle tone. Thus increased collagen deposition in the subepithelial layer of asthma airways may affect airway mechanics.

1.9) Collagen biosynthesis and post translational modification

Collagen is the most abundant and important ECM in the airway wall. Collagen comprises three parallel polypeptide strands with a helical conformation that coil about each other with a one-residue stagger to form a right-handed triple helix. Within the triple helix, there is a repeating XaaYaaGlycine sequence, where Xaa and Yaa can be any amino acid. Proline-Hydroxyproline-Glycine is the most common triplet in collagen. Mutations in the collagen I gene resulting in substitution of Glycine to other amino acids have an impact on collagen stability as seen in osteogenesis imperfecta (134). There are over 20 different types of collagen molecule which can be found in both fibril and non-fibril forming forms. The fibrillar collagens such as collagen I, II, III, V and XI provide the structural framework of the tissue.

Collagen has complex post-translational modifications. It is synthesized within the cells in a precursor form as protocollagen which is the non-hydroxylated, non-triple-helical form of collagen. This protocollagen is then modified by propyl 4-hydroxylase (P4H) to form a procollagen triple helix containing the N-and C- terminal nontriple-helical domains that direct triple helix folding prior to fibrillogenesis. After secretion into the extracellular space, the procollagen N-and C- terminals are cleaved by proteinases to form the collagen molecule triple helix monomer. Collagen fibrillogenesis begins from self-assembly by the interaction of C-terminal telopeptidase with specific binding sites on the collagen molecule monomer. The next step is cross-linking. Lysine or hydroxylysine side chains in the telopeptides are cross-linked by lysyl oxidase (LOX) (Figure 1-3) (134). Collagen organization and fibre thickness appear to be changed in asthmatic when compared to normal subjects (56). It has been suggested that it is the collagen post-translation modifications that may be different in asthma as compared with non-asthmatic subjects, as the production of procollagen has not been found to be different between non-asthmatic and asthmatic fibroblasts (135).

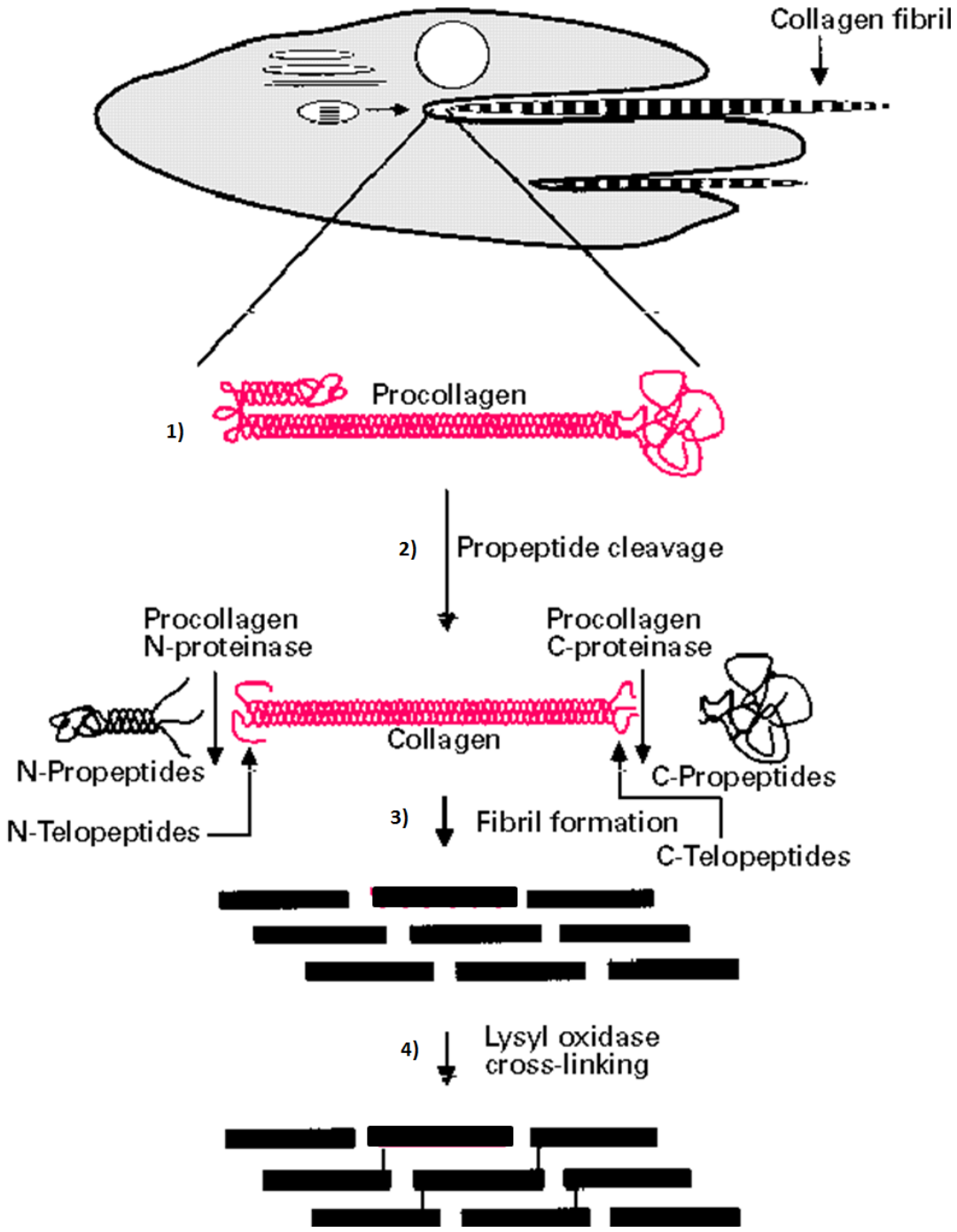

Figure 1-3: Collagen post-translational modifications. Collagen is synthesized within the cells as a non-hydroxylated, non-triple helix structure. 1) During the intracellular modification the first collagen triple helix structure "procollagen" is excreted to the extracellular space. 2) Procollagen processing occurs shortly after secretion followed by the assembly of fibrils. 3) Fibrils are stabilized by the formation of covalent cross-links. 4) Collagen cross-linking gives rise the strength and stability for collagen. The image was reproduced with permission, from Kadler et al, 1996, Biochemical Journal, 316, 1-11 © the Biochemical Society.

1.10) Collagen crosslinking

The cross-linking processes give the mature collagen strength and stability. Lysyl oxidase (LOX) is pivotal in initiating the collagen cross-linking. It has been demonstrated that there is a reduction in collagen stiffness in rats treated with β-aminopropionitrile (BAPN), an irreversibly lysyl oxidase inhibitor (136). The tissue specificity of collagen cross-linking depends on whether the telopeptide lysine, as in skin, or the telopeptide hydroxylysine, as in cartilage, is oxidized by lysyl oxidase. In the skin pathway, after the lysyl oxidase-dependent oxidative deamination of the lysine residue in the telopeptides, the difunctional crosslink dehydro-hydroxylysinonorleucine (Δ-HLNL) or aldimines are formed by condensation with another hydroxylysine from the helical part of a second collagen molecule. Aldimines are condensed with a helical histidine which leads to the formation of a histidine-base crosslink, and the formation of histidinohydroxylysinonorleucine (HHL). In the cartilage pathway, the lysyl oxidase-dependent oxidative deamination of hydroxylysine in the telopeptides generates hydroxylysine aldehyde. After condensation with hydroxylysine on the helical part, this gives rise to the dehydro-dihydroxylysinonorleucine (Δ-DHLNL) or ketoamines. When ketoamines interact with hydroxylysine aldehyde in the telopeptides of another collagen, there is resultant generation of the end products, pyridinoline (PYD) and deoxypyridinolone (DPD) (137) (Figure 1-4). Changing from the lysine pathway to the hydroxylysine pathway appears to be a fibrotic phenomenon, as an increase in production of pyridinoline has been demonstrated in various tissues and organs in which there is fibrosis: e.g. skin (hypertrophic scar, keloid and systemic sclerosis (138-140), lungs (infant and adult respiratory distress syndrome and animal models induced pulmonary fibrosis) (141-143), liver cirrhosis (144), kidney (glomerulosclerosis and interstitial fibrosis) (145). Increase in pyridinoline crosslink formation has been demonstrated to relate to the irreversible accumulation of collagen in fibrotic tissues. This can imply that collagen containing pyridinoline crosslink is more difficult to degrade and so may alter the tissue mechanical properties. As a consequence, stiffer collagen is deposited in the tissue (127). The hydroxylation of lysine to hydroxylysine depends on lysyl hydroxylase (LH) enzyme. There are 3 isoforms of lysyl hydroxylase: LH1, LH2 and LH3. LH1 converts triple helical lysine to hydroxylysine. LH2 is responsible for converting telopeptide lysine to be telopeptide hydroxylysine allowing the cross-linking to be shifted to the pyridinoline pathway. LH3 has glucosyltransferase and galactosytransferase activities (146).

LH2 gene has 2 alternative RNA splice variants: LH2a and LH2b. LH2b mRNA expression has been shown to be predominantly up-regulated in fibroblasts from fibrotic tissue (keloid, hepatic stellate cells and hypertrophic scar) but only minor amounts of LH2a were present while there was no expression of LH1 or LH3 mRNA. The formation of pyridinoline (PYD) has been demonstrated by the same fibrotic cells (147). This suggests that LH2b is the primary regulator of the pattern of pyridinoline cross-linking in collagen.

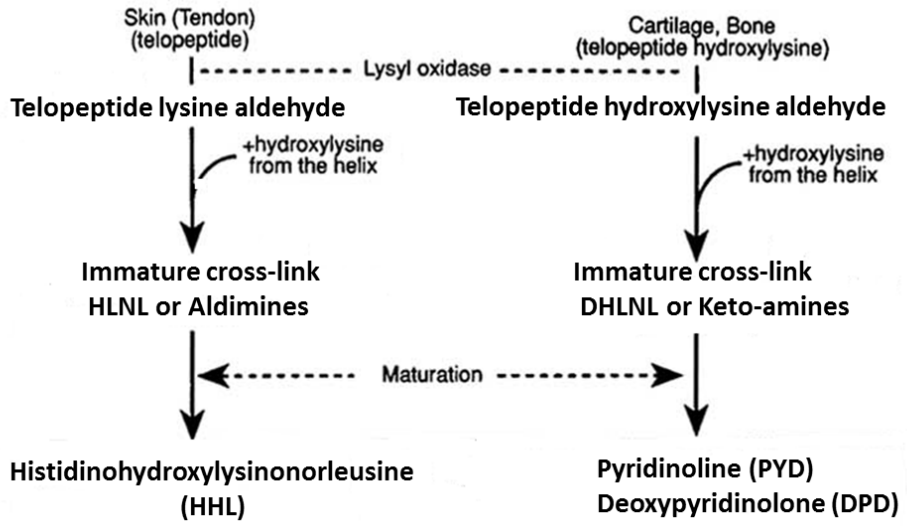

Figure 1-4: The collagen cross-linking pathway. Reaction of telopeptide lysine (skin pathway) and telopeptide hydroxylysine pathway initiate by lysyl oxidase with the end product of HHL, PYD and DPD, respectively. This diagram is modified from Robins SP. Biochem Soc Trans. 2007;35:849-52.

1.11) Collagen morphology

The amount of collagen in the tissue is the key factor for its mechanical property (127). The lungs and airways contain mostly collagen I and III. Collagen IV is also expressed in the airway basement membrane. Collagen I is the most abundant collagen in the most tissues and collagen III is the second most abundant. A model of five collagen molecule or collagen molecule staggered side by side gives rise the typical offset of D=65-67 nm seen in collagen fibrils (Figure 1-5). Collagen fibrils can be assembled from one type of collagen (homotypic fibril formation) or different types of collagen (heterotypic fibril formation) (Figure 1-6). The heterotypic fibril formation between collagen I and collagen III is often found in soft tissue such as skin and gastro-intestinal mucosa (148;149). There is no previous report regarding the type of collagen fibrils formation in the airways and lungs. Several collagen fibrils assemble with proteoglycans (PGs) and glycosaminoglycans (GAGs) to form collagen fibres (150) (Figure 1-7).

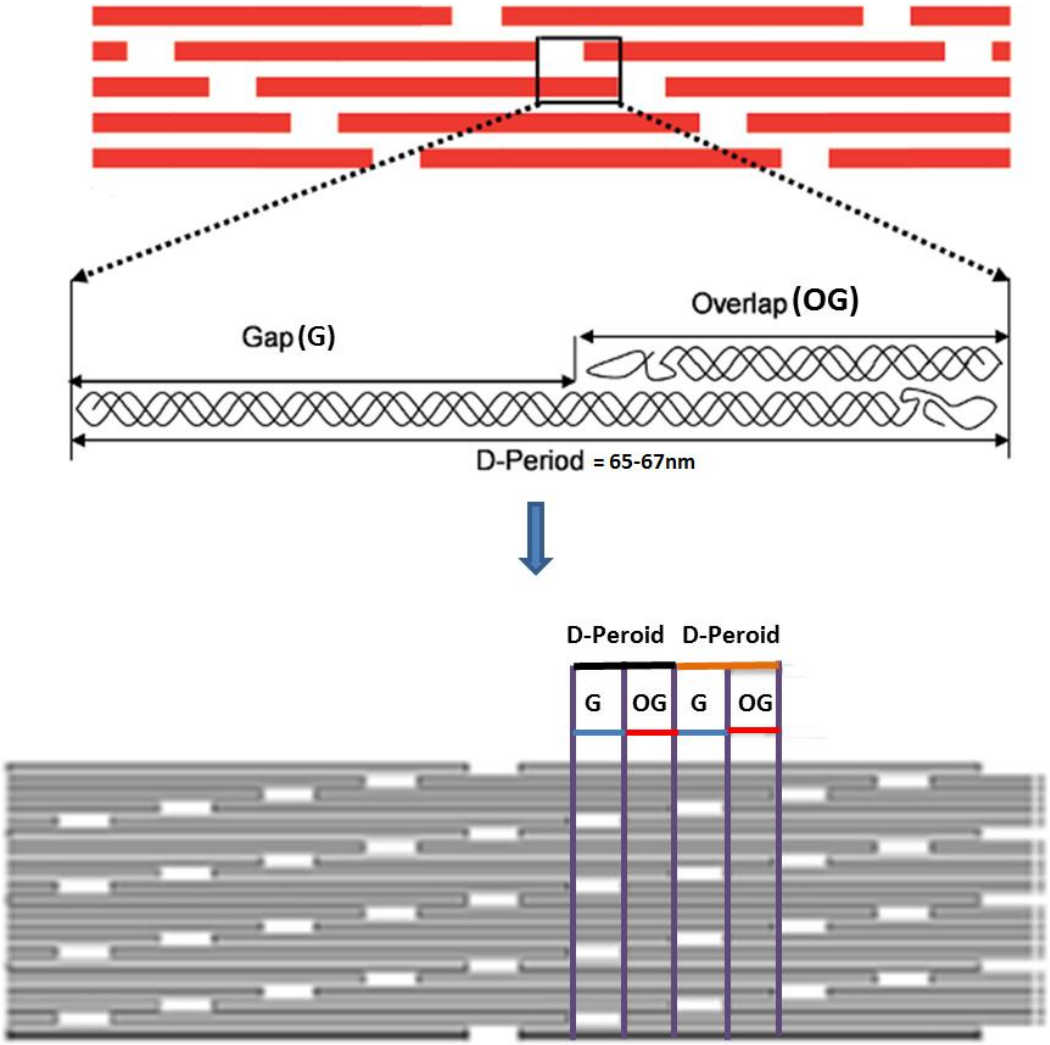

Figure 1-5: A model of collagen molecule give rise a characteristic D periodicity. In a) five collagen molecule or collagen molecule staggered side by side gives rise the typical offset of D=65-67 nm. This image was reprinted from Progress in Materials Science, Vol 52, Fratzl et al., Nature's hierarchical materials, 1263-1334, Copyright (2007), with permission from Elsevier.

Figure 1-6: Image of a cutaway of the 70-nm-diameter collagen fibril construct, where collagen I molecules are shown in magenta and the randomly distributed collagen III molecules are shown in cyan. This image was reprinted from Journal of Structural Biology, Vol 137, Cameron et al, Structure of Type I and Type III Heterotypic Collagen Fibrils: An X-Ray Diffraction Study, Page No 137, Copyright (2002), with permission from Elsevier.

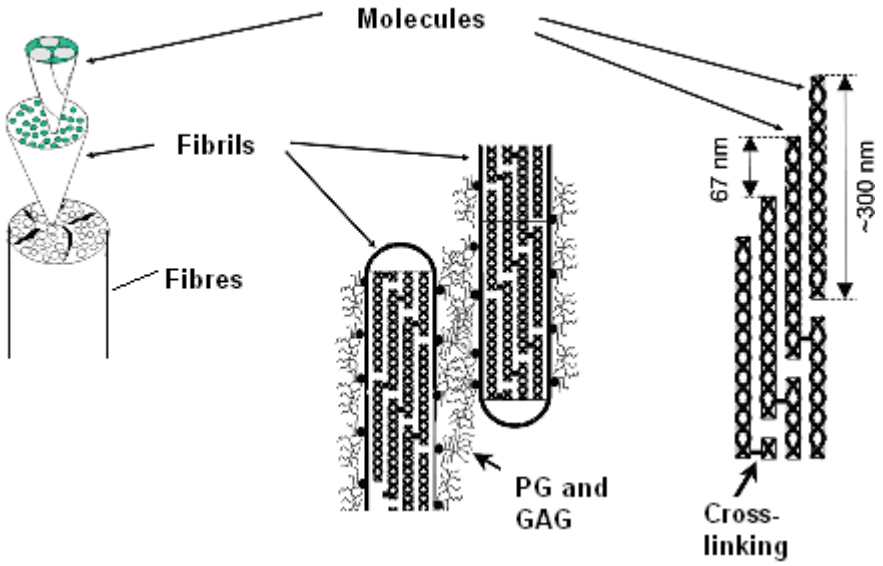

Figure 1-7: Collagen hierarchical structure from collagen molecules to collagen fibres. This image was reprinted from Progress in Materials Science, Vol 52, Fratzl et al., Nature's hierarchical materials, 1263-1334, Copyright (2007), with permission from Elsevier.

1.12) Factors involving collagen fibril diameter and length

The diameter and length of collagen fibrils varies depending on anatomical location. For example collagen fibrils have a diameter range from a micron in tendon to 40 nm in cornea and 10 nm in cartilage. In mature Achilles tendons, there is a bimodal distribution of thicker fibrils with the diameter of 150–250 nm and a group of thinner fibrils with the diameter of 50–80 nm (151). In other tissues such as skin there is, however, a uniform distribution of collagen fibrils with a diameter of 60 nm. The lengths and diameter of the collagen fibrils also increase with maturation of tissue (152). Collagen fibril diameter distribution has an influence on the mechanical properties of tendons. The large fibrils are responsible for withstanding high tensile forces and the smaller fibrils have a role in resisting resist distortion under load and have more stiffness (151). Other extracellular matrix components, such as, the proteoglycans also regulate size of collagen fibrils or fibres. Previous studies have demonstrated that small leucine-rich proteoglycans (SLRPs), such as decorin and biglycan, have an effect on collagen assembly (153), stability (154) and also protect collagen fibrils from proteolytic cleavage by collagenases (155). Decorin knockout mice had abnormal skin fragility with collagen fibrils that are broader in diameter containing loose collagen networks (156). Decorin has also been shown to coat the fibrils surface and prevent them from further expansion. It was suggested that the amount of decorin determines how tightly or loosely collagen fibrils assemble (157). In contrast to decorin, biglycan knockout mice suffered from a thin dermis due to the larger and irregular collagen fibrils but did not suffered from skin fragility (158). Thus the interaction between collagen fibrils and proteoglycans is important to overall collagen structure.

1.13) Mechanical properties of collagen

The mechanical properties of the collagen fibril can be expressed as Young's modulus and stiffness. Young's modulus (E) represents the property of the material which is its resistance against deformation when subjected to a given stress. In contrast, stiffness is a property of a structure. It depends on the material, shape and boundary conditions (150). Young's modulus (E) is calculated by the ratio of stress and strain. Stress is the ratio of applied force F and cross section A, defined as "force per area". Strain is defined as "deformation of a solid due to stress" (Figure 1-8). Stress and strain curves also depend on the material behaviour: elastic, plastic or viscoelastic (Figure 1-9). Collagen has a viscoelastic property which the Young's modulus (E) is defined as the slope of the loading curve near the origin. The Young's modulus of a collagen fibril range from 0.2-21.5 GPa depending on the method of measurement and the source of the collagen (159). However, there are limited studies regarding the structure and the mechanical properties of collagen in the lungs and airways on a nanoscale. In vitro measurement the mechanical properties of the lungs and airways of rat following bleomycin induced pulmonary fibrosis using oscillatory mechanics have demonstrated up to a 3 times increase in tissue stiffness with the increase in ECM deposition (125;126). These studies highlight the important role of ECM on the lung and airway mechanics.

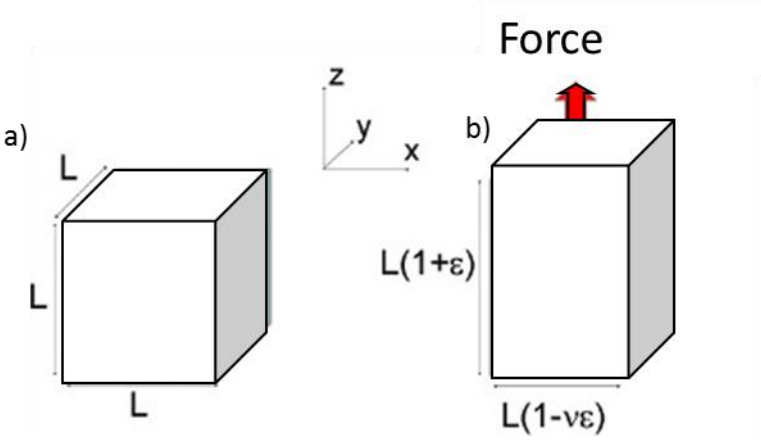

Figure 1-8: Stress and strain. Image a) shows a material before applying a force, and image b) shows material after applying the force. Stress is the ratio of applied force F and cross section area (L^2). When a material is subjected to a force along the Z axis, its length is increased by Lϵ. The relative elongation, ϵ, is called strain. The image was modified from Fratz P. Collgen: Structure and Mechanics, an Introduction. In: Peter Fratzl, editor. Collagen: Structure and Mechanics. New York USA: Springer Science+Business Media; 2008.

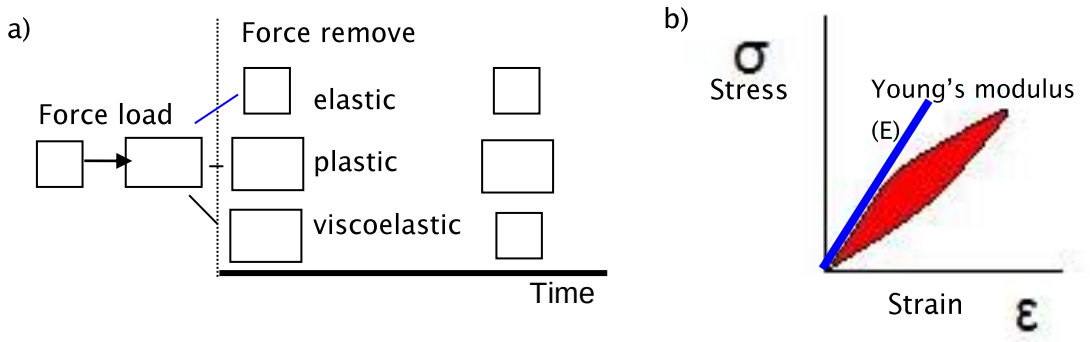

Figure 1-9: Materials behave differently according to their elastic, plastic and viscoelastic properties when the force is removed. In diagram a), after removing the force, the elastic material return to the original shape immediately, but the morphology of plastic material change permanently. Collagen has a viscoelastic property which means the material can return to the original shape over time after removing the force. Graph b) demonstrates stress and strain curve of collagen. The slope of blue line shows the Young's modulus. The image was modified from Fratz P. Collgen: Structure and Mechanics, an Introduction. In: Peter Fratzl, editor. Collagen Structure and Mechanics. New York USA: Springer Science+Business Media; 2008.

1.14) Effect of mechanical strain to the airways

Human airway development requires a mechanical environment to promote proliferation and airway elongation. The major structural cells of the airways (epithelial cells, fibroblasts, and smooth muscle cells) are responsible for these mechanical environments. During *in utero* development, mechanical stress results from epithelial fluid secretion to the airways, peristaltic movement of fluid and intermittent foetal breathing. At the time of birth, the mechanical environment alters suddenly as the air-liquid interface is a novel factor contributing to the dynamic balance between muscle contraction, airway lumen patency and wall structure (160). Airway smooth muscle contraction produces a compressive stress on the airway epithelium, fibroblasts and smooth muscle itself. Therefore, abnormal mechanical loading conditions may result in altered cellular activations and modify the composition of ECM leading to fibrosis in the airways (161). The detail of the effect of mechanical force to airway epithelium and fibroblasts on airway remodelling will be discussed on section 1.15) and 1.16)

There are three strategies that can be employed to study the influence of mechanical forces on cells: 1) culture of cells in matrix-coated two dimensional elastic substrates that can be cyclically stretched in monolayer, 2) a compressive model involving cell culture in which the direction of the force is vertical, and 3) culture of cells within 3 dimensional (3D) sponges that can be uni-axially compressed (Figure 1-10). There are many variations to be considered in mechanical studies as the cellular responses depend significantly on the mechanical conditions (frequency, magnitude, uniformity, and duration), the nature of the underlying matrix, serum supplementation of the media, type of mechanical apparatus and source of the cells studied (primary or cell line, embryonic stage, and human or mouse) (160-162). Consequently, the variation in the method of mechanical stimulation may result in the difference in cellular responses.

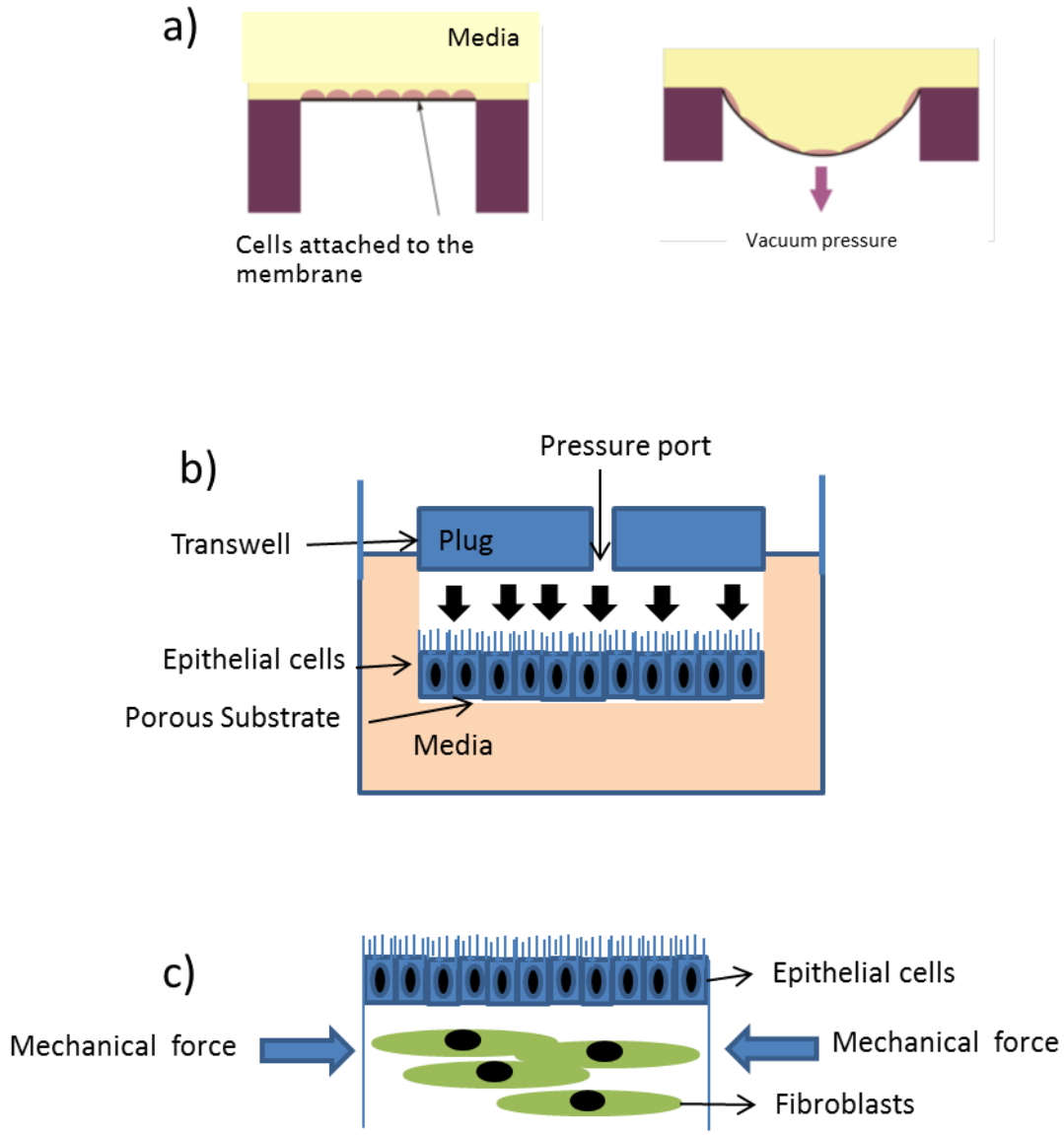

Figure 1-10: Schematic models of different types of mechanical stimulation to airway epithelial cells and fibroblasts. Image a) shows a model of culture of cells in matrix-coated two dimensional elastic substrates that can be cyclically stretched which is the model used in the present study. Image b) demonstrates a model of compressive stress to airway epithelium. And image c) shows a model of 3 D lateral compressive stress. Image b) was adapted from Tschumperlin et al Am J Respir Cell Mol Biol.2003;28:142-149. Image c) was adapted from Choe et al Am J Respir Cell Mol Biol.2006;35:306-313.

1.15) Effect of mechanical strain on the airway epithelium: role in airway remodelling

Recent studies have shown that mechanical strain activates epithelial cells causing release of factors that are involved in airway remodelling. Savla et al have shown that cyclical mechanical strain and compressive stress to human and cat airway epithelium cells inhibited epithelial layer repair after wounded by scraping (163). A model of compressive stress on differentiated normal human bronchial epithelial cells cultured at air-liquid interface has been shown to promote airway remodelling by increasing the gene expression of TGFβ, endothelin-1, and plasminogen activator gene (90;121), enhancing the release of profibrotic cytokines: TGFβ2 and endothelin (90), increasing intracellular mucin-5AC (MUC5AC) levels (164), increasing expression of EGFR and EGFR ligand (165), as well as enhancing the production of MMP-2 and MMP-9 (121). Cyclical mechanical strain of airway epithelium cells has also been shown to increase the production of reactive oxygen species (ROS) (166), and to down-regulate prostaglandinE_2 synthesis (PGE_2) (167). PGE_2 was found to inhibit fibroblast proliferation and collagen production in vitro (168;169). Comparative studies have shown that mechanical strain enhances DNA synthesis in rat foetal epithelial cells and fibroblasts when cultured in three-dimensional organotypic cultures and in this respect has greater influence than 2D monolayer mechanical strain (170). Mechanical injury to guinea-pig epithelial cells, co-cultured with fibroblasts in the human amnion chamber, results in fibroblast differentiation to myofibroblast and the expression of procollagen I and III (171). Compressive mechanical stress of human epithelial cell with fibroblasts has been shown to have a greater effect on increasing the MMP-9/TIMP-1 ratio than when epithelial cells or fibroblasts are cultured alone (122). Similar effects have been seen on collagen production, where mechanical stress applied to three dimensional epithelial cells co-cultured with fibroblasts causes enhanced collagen expression more than if fibroblasts are cultured alone (172). Application of three dimensional dynamic lateral compressive stress to foetal rat lungs cells in organotypic cultures has also been shown to increase the production of fibronectin in the culture supernatants (173). These studies highlight the importance of epithelial-mesenchymal cross talk in airway remodelling. Studies examining the effect of mechanical stress of airway epithelium, airway epithelial cells co-cultured with fibroblasts are summarized in Table 1-2.

Table 1-2: Mechanical strain on airway epithelium, epithelium and fibroblast co-culture

Cell type	**Type of strain, magnitude and frequency**	**Duration**	**Result**	**Reference**
Human bronchial epithelial cell (NHBE)	Compressive stress 30 cmH2O Continuous	8hr	Increase level of MMP-9 and MMP-2	(121)
Human bronchial epithelial cell (NHBE)	Compressive stress 30 cmH2O Continuous	8hr	Increase gene expression and protein level of TFFβ2 and endothelin	(90)
Co-culture NHBE and human lung fibroblast (CCL-186)	Compressive stress 10, 20, 30, 40 cmH2O Continuous	4hr	Increase in collagen III, V and fibronectin protein production by fibroblast	(122)
Co-culture Human bronchial epithelial cell (HBEC) and human foetal lung fibroblast (IMR-90)	3D in collagen I Lateral compressive strain 50% Continuous	48hr	Increase in thickness of the epithelial layer	(162)

Cell type	Type of stretching, magnitude and frequency	Duration	Result	Reference
Co-culture Foetal rat lung epithelial and fibroblast cells	3D in gelfoam sponge Dynamic lateral compressive strain 5% 60 cpm for 15 min/h	48hr	Increase fibronectin in culture media	(173)
Co-culture Human bronchial epithelial cells (HBEC) and human foetal lung fibroblasts(IMR-90) compared to fibroblast alone	3D in collagen I Dynamic lateral compressive strain 10%or 30% 1cycle/hr or 60 cycle/h	48hr	Co-culture had more deposition of collagen III, IV measured by immunoflurescent staining and more MMP-2,9 than fibroblast alone -Decrease in fibronectin deposition -Increase in αSMA staining both co-culture and fibroblast alone -10% amplitude promoted more ECM and αSMA expression	(172)

1.16) Effect of mechanical strain to airway fibroblasts

Fibroblasts are the major cell that responds to mechanical signals, translating them into biological events especially in expression of ECM genes. As a result, fibroblasts play a pivotal role in tissue remodelling and wound healing (174). Previous studies have highlighted the role of airway fibroblasts in the production of ECM in response to mechanical stress, including up-regulation of versican and decorin mRNA expression (175;176), as well as up-regulation of procollagen mRNA expression (177). Airway fibroblasts from normal and asthmatic subject have been shown to respond to mechanical stimuli differently. Mechanical strain increased versican mRNA expression only asthmatic bronchial fibroblasts but not in normal bronchial fibroblasts (175). In contrast, Ludwig et al found that mechanical strain up-regulated versican mRNA expression both in normal and asthmatic bronchial fibroblasts, but decorin was up-regulated only in asthmatic bronchial fibroblasts. However, these investigators reported the mRNA expression using northern blot analysis without showing the house keeping gene, so the difference in gene expression may have been due to the difference in RNA content (176). There are few studies evaluating the effect of mechanical strain on fibroblast cytokine secretion. Le Bellego et al. have reported that asthmatic bronchial fibroblasts secrete more IL-6 than fibroblasts from normal controls after 24 h of mechanical strain (175). Furthermore, mechanical strain has been found to up-regulate IL-8 mRNA expression in both normal and asthmatic fibroblasts (175). The impact of mechanical strain on fibroblast proliferation is controversial. Whilst Bishop et al (178) reported an increase in foetal lung fibroblast cell numbers after mechanical strain, Sanchez-Esteban et al (179) found that mechanical strain led to both an increase in apoptosis and a decrease in cell proliferation. In a study of the effect of mechanical stress on foetal rat lung fibroblasts, it has been found that a 3D model promoted more DNA synthesis than a 2D monolayer model (170). Therefore, the mechanical conditions are essential to the cellular responses. Studies examining the effect of mechanical strain on airway fibroblasts were summarized in (Table 1-3)

Mechanical stress can impact on airway structural cells (epithelial cells, fibroblasts, and ASM) to influence their proliferation, differentiation, cytokine productions as well as ECM production. Airway smooth muscle contraction in response to stimuli such as allergen will cause significant mechanical stress to the airway wall. Previous reports have shown that tidal breathing produces a 4% stretch of ASM and a deep inspiration causes a 25-30% stretch (180). However, bronchial hyperresponsiveness has been shown to be inversely related with the airway wall thickness (67;68). It was also shown that asthmatic patients who have highly variable airway obstruction showed less airway wall thickening, while those who had less variable or fixed airway obstruction exhibited more thickened airways (69). Thus the thickening with deposition of the matrix proteins may be a protective mechanism by increasing the stiffness of the airways to attenuate the force from smooth muscle contraction (45). As a result, it is hypothesized that airway fibroblasts from healthy non-asthmatic, mild and severe asthmatic subjects may respond to mechanical strain differently.

Table 1-3: Mechanical strain on fibroblasts

Cell type	Type of strain, frequency and magnitude	Duration	Result	Reference
Primary bronchial -Asthma -Normal	Cyclical strain in collagen I coated 1Hz 30%	3hr, 6hr, 24hr	Increase in versican mRNA expression at 6hr in asthma patients	(175)
Primary bronchial -Asthma -Normal	Cyclical strain in collagen I coated 1Hz 30%	24h	In asthma : increase in versican and decorin mRNA In normal: only versican mRNA increased	(176)
Human foetal lung fibroblast (IMR-90)	Cyclical strain in fibronectin, laminin, elastin coated 1Hz 20%	48hr	Only in laminin and elastin coated increase in procollagen mRNA expression	(177)
Human foetal lung fibroblast (IMR-90)	Cyclical strain in collagen I coated 1Hz 10%	5 day	Increase in cells number	(178)

Cell type	Type of strain, frequency and magnitude	Duration	Result	Reference
Foetal rat lung fibroblast cell	3D in gelfoam sponge and 2D in collagen I coated 1 Hz for 15 min/h 5%	48hr	Increase in DNA synthesis in 3D	(170)
Foetal rat lung fibroblast	Cyclical strain in collagen I coated 1Hz,15min/hr 5%	24hr	Increase apoptosis and inhibit cell proliferation	(179)

1.17) Hypotheses

That 1) Mechanical forces to the airways may activate submucosal fibroblasts and thereby contribute to airway remodelling and airway inflammation. 2) Biochemical cross-linking alters the properties of collagen in asthmatic airways. 3) Differences in airway collagen properties can be demonstrated by atomic force microscopy (AFM).

1.18) Aims of study

- To study the effect of mechanical strain on airway fibroblasts in vitro.
- To investigate the effect of mechanical strain on the generation of extracellular matrix proteins and inflammatory cytokines from airway fibroblasts in vitro.
- To investigate if asthmatic fibroblasts respond to mechanical strain differently than normal fibroblasts.
- To investigate the changes in collagen cross-linking enzymes produced by airway fibroblasts after treatment with TGFβ.
- To investigate if the asthmatic bronchial fibroblasts respond to TGFβ treatment differently than normal bronchial fibroblasts.
- To investigate the level of collagen cross-linking enzymes in BAL fluid.
- To investigate changes in collagen cross-linking enzyme expression in airway fibroblasts following dexamethasone treatment.
- To investigate the structure of airway collagen using AFM.
- To evaluate the structure of collagen extracted from asthmatic and healthy non-asthmatic airway and measure its impact on tissue stiffness.

Chapter 2: Materials and Methods

2.1) Materials

Acetic acid (Sigma, Dorset, UK# 27221-1L)
Acrylamide/methylene bisacrylamide solution (Geneflow, Stratfordshire, UK#A2-0072)
7-Aminoactinomycin D (Sigma, Dorset, UK# A9400-1MG)
Amonium hydroxide (Sigma, Dorset, UK# 6899)
Alexa Fluor488® conjugated Phallodin (Invitrogen, Paisley, UK # A12379
Ammonium persulphate (Sigma, Dorset, UK# A3678)
Anti-α-Smooth Muscle antibody (Sigma, Dorset, UK# A2547)
Anti-Lysyl Oxidase antibody produced in rabbit (Sigma, Dorset, UK# L4794-200UL)
Atomic force microscopy, MFP-3D™ Stand Alone AFM (Asylum research,Oxfordshire)
Bovine collagen solution, PureCol® (Advanced BioMatrix, US #5005)
Bovine Serum Albumin (Sigma, Dorset, UK#A3059)
Bovine hyaluronidase type I (Sigma, Dorset, UK#H3506-100MG)
Brij 35 solution (Sigma, Dorset, UK#B4184)
bromophenol blue (Sigma, Dorset, UK#B5525)
Calcium chloride (Sigma, Dorset, UK#C3306)
Carbonate-Bicarbonate Buffer9 Sigma, Dorset, UK#C3041)
CFX96™ real time PCR system (Biorad, Hertfordshire, UK)
Chloroform (Sigma, Dorset, UK#C2432)
Complete protease inhibitor cocktail tablets (Roche, West Sussex, UK # 04693116001)
Coomaasie Blue R-250 (Sigma, Dorset, UK)
Dexamethasone (Sigma-Aldrich, Gillingham, UK#D4902)
DMEM (Invitrogen, Paisley, UK#11960044)
DNA-*free*™ reagent (Applied Biosystems, Warrington, UK#1906)
Dulbecco A tablet/ phosphate buffered saline (Oxoid, Basingstoke, UK#RR00146)
ECL Plus Western Blotting Detection System (Amersham, Buckinghamshire, UK#RPN2132)
EDTA (Sigma, Dorset, UK#63690)
Ethanol (Sigma, Dorset, UK#32221)
Foetal bovine serum (Invitrogen, Hertfordshire, UK#10108165)
Filter unit (Millipore, Watford, UK#SLGPO33RS)
Fluorescence microscope (Leica DMI 6000B)
Flexercell-4000T TensionPlus (Flexcell International, Mckeesport, PA, USA
Fotospeed DV10 Varigrade Print Developer (Corsham, UK#02530)
Fotospeed FX20 Rapid Fixer (Corsham, UK#02530)

GAPDH/G3PDH Polyclonal Ab, Rabbit IgG (R&D, Abingdon, UK#2275-PC-100)
Gelatin (Sigma, Dorset, UK#G9382)
Glycerol (Sigma, Dorset, UK#G5150)
Glycine (Sigma, Dorset, UK#G7126)
HBSS (Hanks Balanced Salt Solution without Ca^{2+} or Mg^{2+})(Invitrogen, Paisley, UK #14170-0880)
Human CXCL8/IL-8 DuoSet (R&D, Abingdon, UK# DY208)
Hypond P (PVDF) transfer membranes (Amersham, Buckinghamshire, UK#RPN303F)
Hyperfilm cassette (Amersham, Buckinghamshire, UK)
Human Transforming Growth Factor-β_2 (Hu TGFβ2) (Peprotech, London, UK#100-35)
Imager Gel Doc System (Biorad, Hertfordshire, UK)
Lab-Tek Chamber Slide Permanox Slide (NUNC, UK#1777445)
Lab-Tek Chamber Slide Glass Slide (NUNC, UK#154917)
L-Glutamine (Invitrogen, Hertfordshire, UK#25030-024)
Mini Protean II system (Biorad, Hertfordshire, UK)
2-mercaptoethanol (Sigma, Dorset, UK#M7154)
Multiskan Ascent plate reader (Lab systems)
NanoDrop spectrophotometer (Thermo Fisher Scientific, Loughborough, UK)
NEAA 100X (Invitrogen, Paisley, UK #11140-35)
Orbital shaker (Stuart Scientific SO1)
96-well PCR plates (Biorad, Hetrfordshire, UK)
Penicillin G Sodium/Streptomycin sulphate (Invitrogen, Hertfordshire, UK#25030-024)
PonceauS solution (Sigma, Dorset, UK#P170-1L)
Power pack (Biorad power Pac 300, Hertfordshire, UK)
Precision™ qPCR (Primer Design, Southampton, UK)
Prolong antifade (Invitrogen, Hertfordshire, UK#P36934)
2-Propanol (Sigma, Dorset, UK#I9516)
Precision Plus Protein Kaleidoscope standards (Biorad, Hertfordshire, UK#161-0375)
Reverse transcription kit (Primer Design, Southampton, UK)
Scanning electron microscope (Hitachi S800)
Sircol soluble collagen assay (Biocolor, Belfast, Northen Ireland)
Sodium chloride (Sigma, Dorset, UK# S7653-1KG)
Sodium deoxycholate (Sigma, Dorset, UK# D6750)
Sodium dodecyl sulphate (SDS) (Sigma, Dorset, UK# L6026)
Sodium Pyruvate (Invitrogen, Paisley, UK #11360)
Strataclean Resin (Agilent Technologies, Stockport, UK#400714)
Tetramethylethylenediamine (Sigma, Dorset, UK# T7024)
TGFβ1 Emax® ImmunoAssay System (Promega, UK# G7590)
Tissue culture flask Nunc EasY Flask angled neck polystyrene radiation sterilised filter cap (Fisher Scientrific, UK)

TMB solution (Sigma, Dorset, UK#T0440)
Transmission electron microscope (Philips EM 201)
Triz base (Sigma, Dorset, UK#T1503)
Trizma HCl (Sigma, Dorset, UK#T3253)
Triton-X-100 (Pharmacia Biotech#17-1315-01)
Tween-20 (Sigma, Dorset, UK#H3506)
Type I trypsin from bovine pancrease(Sigma, Dorset, UK# T8003-100MG)
Trypan blue (Sigma, Dorset, UK#93595)
0.05% Trypsin EDTA (Invitrogen, Hertfordshire, UK#15400054)
TRIzol® reagent (Invitrogen, Hertfordshire, UK#15596-0185)
Whatman filter paper (3MM CHR, GE Healthcare, UK #3030672)
X-ray film (Amersham Hyperfilm™ ECL, Buckinhamshire, UK#28906837)

2.2) Subject characteristics of primary bronchial fibroblasts

Bronchial fibroblasts were grown from bronchial biopsies obtaining from fibre optic bronchoscopies in healthy and asthmatic volunteers and lung fibroblasts were grown from video-assisted thoracoscopy (VAT) biopsies in an interstitial lung disease patient following informed consents with ethical approval. Subject characteristics of fibroblasts used in mechanical strain and lysyl oxidase experiments are summarized in Table 2-1 and 2-2.

Table 2-1: Subject characteristics of primary fibroblasts used in mechanical strain experiments

	Age (yr)	Sex	FEV_1 (%predicted)	Atopy	Inhaled steroid (µg/day BDP equivalent)	Prednisolone (mg/day)	Current smoking
Healthy							
DS029	64	M	89.8	N	N	N	N
DS056	20	M	102.4	N	N	N	N
DS028	59	F	133.8	N	N	N	N
BG183	36	F	102	N	N	N	N
A32	20	M	112	N	N	N	N
A50	31	M	115	N	N	N	N
A16	23	M	103	N	N	N	N
Mild asthma							
DS052	36	F	95.5	Y	N	N	N
DS047	27	F	102.9	Y	N	N	N
DS048	26	M	113.4	Y	N	N	N
B14	33	F	103	Y	N	N	N
B06	45	M	131	Y	N	N	N
B22	21	F	104	Y	N	N	N
B33	23	M	103	Y	N	N	N
Severe asthma							
DS030	45	F	47.7	Y	1800	0	N
DS033	17	M	71.3	NA	2800	0	N
BG224	57	M	64.9	Y	1600	0	N
BG221	69	F	101	N	1000	0	N
BG178	54	F	19 .8	Y	1600	10	N
BG128	60	F	87	N	2000	19	Y
BG170	28	M	34.9	Y	1320	0	N
BG180	51	F	29.7	N	4000	15	N

BDP= Beclomethasone Dipropionate

Table 2-2: Subject characteristics of primary fibroblasts used in lysyl oxidase experiments

	Age (yr)	Sex	FEV_1 (%predicted)	Atopy	Inhaled steroid (µg/day BDP* equivalent)	Prednisolone (mg/day)	Current smoking
Healthy							
A32	20	M	112	N	N	N	N
A16	25	M	121	N	N	N	N
DS056	20	M	102.4	N	N	N	N
DS029	64	M	89.8	N	N	N	N
DS028	59	F	133.8	Y	N	N	N
BG183	36	F	113	Y	N	N	N
A50	31	M	114.6	N	N	N	N
Severe Asthma							
BG170	28	M	34.9	Y	1320	0	N
BG180	51	F	29.7	N	4000	15	N
BG221	67	F	101	N	1000	0	N
BG224	57	M	64.9	Y	1600	0	N
BG178	54	F	19.8	Y	1600	15	N
DS030	45	F	47.7	Y	1800	0	N
BG128	60	F	87	N	2000	20	Y
ILD							
***KOR-ILD55**	67	F	64	N	800	0	N

BDP= Beclometasone Dipropionate

***KOR-ILD55:** The patient was diagnosed chronic bronchiolitis with constrictive obliterative bronchiolitis.

2.3) Subject characteristics of bronchoalveolar lavage (BAL) fluid samples

BAL fluid was obtained from fibre optic bronchoscopy performed in healthy, mild and severe asthmatic volunteers following informed consents with ethical approval.

Table 2-3: Subject characteristics of BAL fluids samples

	Age (yr)	Sex	FEV_1 (% predicted)	Atopy	Inhaled steroid (µg/day BDP equivalent)	Prednisolone (mg/day)	Current smoking
Healthy							
BG227	55	F	116	N	N	N	N
BG228	31	F	110	N	N	N	N
BG183	36	M	102	N	N	N	N
DS067	21	F	99	N	N	N	N
DS072	20	F	108	N	N	N	N
DS081	22	F	83	N	N	N	N
MJ2	NA	M	84.9	NA	N	N	N
MJ3	26	M	98	NA	N	N	N
MJ4	NA	F	96.6	NA	N	N	N
Mild asthma							
CG1	27	F	99	Y	N	N	N
CG3	24	M	95	Y	N	N	N
CG4	27	M	82	Y	N	N	N
CG5	22	F	92	Y	N	N	N
CG15	25	F	116	Y	N	N	N
CG19	23	F	107	Y	N	N	N
CG30	22	M	111	Y	N	N	N
CG52	19	M	134	Y	N	N	N
DS052	36	F	96	Y	N	N	N
DS051	34	F	70	Y	N	N	N
Severe asthma							
BG178	54	F	19.8	Y	1600	10	N
BG225	50	F	84.8	Y	3080	15	N
BG224	57	M	64.9	Y	1600	0	N
BG129	20	F	60	N	8000	25	N
BG180	51	F	29.7	N	4000	15	N
BG157	40	F	80	Y	2400	0	Y
BG170	28	M	34.9	Y	1320	0	N
BG173	32	F	78.6	Y	2380	20	Y
DS070	42	F	59	N	2000	0	Y
DS075	28	M	83	Y	2800	1	Y
DS077	45	F	64	N	1600	0	Y
DS083	51	F	76	Y	2400	1	Y

2.4) Methods

2.4.1) Culture of primary bronchial fibroblasts

2.4.1.a) Reconstitution of cryopreserved fibroblasts

Primary bronchial fibroblasts from asthmatic and normal subjects (all were gift from Drs David Sammut and Sarah Field) were reconstituted from cryopreserved fibroblasts. The cryovials were retrieved from liquid nitrogen storage. Pre-warmed complete DMEM culture media [Dubelcco's modified Eagle's medium (DMEM), 50 IU/ml penicillin, 50 mg/ml streptomycin, 2 mM L-glutamine, 1 mM Sodium pyruvate and 1 mM nonessential amino acids (NEAA)] supplemented with 10% (v/v) heat inactivated foetal bovine serum (FBS) was added to the cryovials then the cell suspension was transferred to a 75cm^2 tissue culture flask. 10 ml of complete DMEM containing 10% FBS were added to the flask. The flasks were then incubated at 37°C in the presence of 5% CO_2 for 6 hours to allow the fibroblasts to attach to the surface of the flask. After 6 hours, the media was changed to remove the non-viable cells. The cells were incubated at 37°C in the presence of 5% CO_2 with 3 changes of complete DMEM containing 10% FBS per week until 90% confluence was reached. The cells were then trypsinised for subculture.

2.4.1.b) Sub-culturing of fibroblasts

When the fibroblasts reached 90% confluence, the media was removed from the flask and 10 ml of Hank's balanced saline solution without calcium or magnesium (HBSS) pre-warmed at 37 °C was carefully added to wash the cell layer two times. To detach to cell layer, 1 ml of 1% trypsin/ EDTA in HBSS was added and the flask was swirled around to cover trypsin all the surface. Trypsin was then removed. The flask was incubated at 37 °C for 60 seconds. After cell detachment was checked by phase contrast microscopy, 5ml of complete DMEM containing 10% FBS were added to neutralise trypsin and the cells were transferred to a 50 ml-conical bottom centrifuge tube. A further 5 ml complete DMEM was added to the empty flask swirled around and pipetted into the centrifuge tube to maximise retrieval of cells. A cell count was then performed. A minimum of 0.2X10^6 cells were used to grow into a 75cm^2 tissue culture flask. Experiments were performed by using cells from passages 4-7.

2.4.2) **Mechanical stimulation of cultured fibroblasts**

Cells were seeded on type I collagen-coated six-well BioFlex silastic bottom culture plates 24h prior to the experiments at a density of 100,000 cells/well. The plates were placed on the baseplate of the cell stretching device (Flexercell-4000T TensionPlus; Flexcell International, Mckeesport, PA, USA) in a 37 °C, 5% CO_2 incubator. The machine produces a negative pressure pulling down the flexible membrane where the cells were attached (Figure 2-1). A sinusoidal cyclical strain of 30% elongation was applied at the frequency of 12 cycles per minute for 6 hr-144 hr. Control cells were cultured under the same conditions but without mechanical strain.

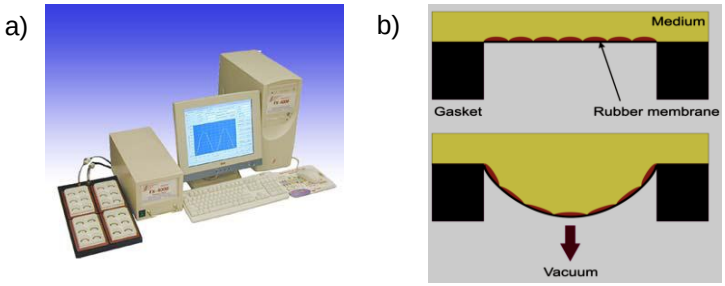

Figure 2-1: a) Representative of the FlexerCell FX4000 strain unit. b) The machine produces a negative pressure pulling down the flexible membrane where the cells were attached.

2.4.3) **TGBβ2 stimulation of cultured fibroblasts**

For experiments analysing LOX and LH production by fibroblasts, cells were seeded at a density of 100,000 cells/well in 12 well plates and incubated in 37°C in the presence of 5% CO_2 until fully confluent. The cells were then treated with TGFβ2 (10ng/ml) with or without dexamethasone (10-1000 nM) in serum free or 0.4% (v/v) FBS in complete DMEM for 6h to 96h. In fibroblast pellet culture experiments (181), fibroblasts (1 x 10^6 cells) were centrifuged at 500 g for 5 minutes in a 15 ml polypropylene tube. The pellets were then cultured in same tube with TGFβ2 (10ng/ml) in 2 ml of complete DMEM containing 10% FBS.

2.4.4) **RNA extraction**

Principle

RNA extraction was performed using the TRIzol® method. TRIzol® Reagent is a monophasic solution of phenol, guanidine isothiocyanate, and other proprietary components which facilitate the isolation of a variety of RNA species of large or small molecular size. TRIzol® disrupts the cell components but maintains the integrity of the RNA due to highly effective inhibition of RNase activity while disrupting cells and dissolving cell components. Chloroform is added to separate the RNA out by differential solubilisation. The acidification of the phenol keeps the DNA in the organic phase whilst the RNA dissolves in the water component. The samples are centrifuged and the liquid is separated into three phases- a lower red phenol-chloroform phase, an interphase, and a colourless upper aqueous phase. RNA remains exclusively in the aqueous phase. The RNA is then precipitated out of the solution by isopropanol. Any residual genomic DNA is eliminated by DNAse treatment.

Methodology

Fibroblasts cultured in 6 wells or 12 wells were harvested in 500 µl or 1000 µl of TRIzol® reagent by incubation for 5 minutes at room temperature. Chloroform (100 or 200 µl) was then added to the samples and shaken for 15 seconds. Samples were incubated for 10 minutes at room temperature, and then centrifuged at 12,000 g, 4°C for 15 minutes. The aqueous phase was transferred to an RNase-DNase-free Eppendorf tube. 500 µl or 1000 µl of isopropanol was added to each sample, and the samples were then stored at -80°C overnight to facilitate precipitation of the RNA. After thawing and vortexing, the samples were centrifuged at 12,000 g for 30 minutes at 4°C. The supernatant was decanted and the pallet was washed with 75% ethanol. The samples were spun at 7500 g for 5 minutes at 4°C. Ethanol was carefully removed and the pellets were air dried for 15 minutes. RNA samples were DNAse-treated with DNA-free™ reagent at 37°C for 1 hour, using the following amounts per sample: 1 µl rDNase I, 2 µl 10XDnase Buffer, 17 µl nuclease-free water. After 1 hour, 5 µl of DNAse Inactivation Reagent were added to each sample, and incubated at room temperature for 2 minutes. Samples were centrifuged at 12,000 g and the quality of RNA was verified by a NanoDrop spectrophotometer. 1.5 µl of sample were used to measure for RNA concentration. The absorbance reading was recorded at 260 nm and 280 nm which depend on the presence different proportion nucleotides in RNA and DNA (260 nm) and protein (280 nm). The ratio of 260nm to 280nm absorbance indicates the purity of RNA, whilst RNA concentration is calculated from the 260nm absorbance value. A ratio between 1.8 -2.0 is accepted as pure RNA.

2.4.5) **Reverse transcription**

Principle

Reverse transcription is the process that extracted RNA is transcribed to complementary DNA (cDNA) through the use of an RNA-dependent DNA polymerase or commonly known as a reverse transcriptase. The technique involves two steps: the annealing step in which a primer binds to the RNA and the extension step in which the reverse transcriptase adds nucleotides to the primer.

Methodology

1 µg of RNA was reverse transcribed to cDNA using the following reagents and conditions. The annealing step: 1µl random Hexamers, 1µl oligo-dT primer, 1mM dNTPs and 2 µl of nuclease-free water were added to the RNA and incubated at 65°C for 5 minutes to denature the RNA secondary structure. Samples were snap cooled on ice for 3 minutes. The following reagents were added to each sample for the extension step: 200 units of Moloney murine leukemia virus (MMLV) reverse transcriptase enzyme, 4 µl of MMLV 5X buffer, 0.2 µl of nuclease-free water (all from PrimerDesign, Southampton, UK). Samples were incubated at 42 °C for 1 hour. Then the cDNA was 1 in 10 diluted with dH_20 before quantitative PCR analysis.

2.4.6) **Real time-Quantitative PCR Analysis (RT-qPCR)**

Principle

Polymerase chain reaction (PCR) involves exponential amplification of a specific DNA sequences to enable its detection and quantification. Double stranded DNA need to be denatured to become single strand to be able to bind with primers. Primers are short sequence of nucleotides that are complementary to a sequence in the DNA of interest. Two primers, a 'sense' and an 'anti-sense' primer, are designed to attach to each of the two strands of DNA. With the action of DNA Taq- polymerase, nucleotides are added at the 3' end of the primer then extending it and finally produce a new copy of DNA stand amplicon. By repeating this process, exponential expansion of the DNA of interest can be achieved. Apart from Taq polymerase, primers and DNA samples, the PCR reaction needs deoxyribonucleotide triphosphate (dNTP) and magnesium ions in the buffer in order to ensure the optimal pH for the polymerase activity and the nucleotides need to be in excess for the proper extension. The reaction is performed by temperature cycling to allow denaturation, annealing and extension.

For denaturation, 95.0°C is applied to separate the double stranded DNA, the temperature is reduced to 45.0°C to 60.0 °C to allow the primers bind to DNA template for annealing, and finally the temperature is increased to 72.0°C, which is the optimum for the Taq to extend the primers by incorporating the dNTPs (Figure 2-2). Then all cycles are repeated for 25-50 times (182).

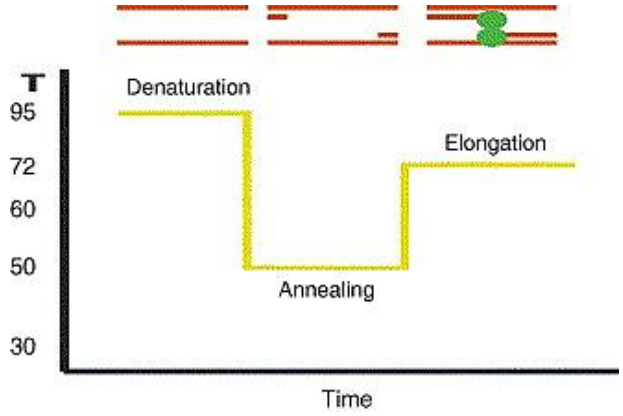

Figure 2-2: The PCR temperature cycle: denaturation- the temperature is raised to about 95.0°C to melt the double stranded DNA, annealing- the temperature is lowered to 45.0c - 60.0 °C to let primers anneal, and extension-the temperature is set to 72.0°C to let the polymerase extend the primers.

The real time quantitative PCR requires a fluorescent reporter that binds to the DNA formed and reports it presence by fluorescence emission. There are two types of fluorescent reporter: fluorescent dyes such as SybrGreen and a target specific fluorescent probe. SybrGreen becomes brightly fluorescent when it binds to double stranded DNA, so the amount of fluorescence increases with the amount of double stranded DNA formed. Fluorescent probes are pieces of DNA complimentary to the gene of interest that are labelled with a fluorescent dye. These probes are labelled with a fluorescent reporter molecule at one end and a quencher molecule (capable of quenching the fluorescence of the reporter) at the other. During the PCR the probe binds to the gene of interest and is cleaved by the Taq polymerase as it extends the DNA strand. As a consequence, the reporter and quencher are physically separated and the fluorescence increases. The fluorescent reporter generates a fluorescent signal that reflects the amount of the target DNA product and so it is more specific than SybrGreen which may also react with non-specifically amplified DNA. During the initial cycles the signal is weak and cannot be distinguished from the background. As the product accumulates a signal increase exponentially, a threshold value is determined when the fluorescent signal goes above the background. The number of cycles requires to reach threshold is called the Ct value (Figure 2-3). The lower the Ct value means the higher expression of the gene of interest. The data from real time quantitative PCR can

be analysed using absolute quantification and relative quantification. Absolute quantification determines the product copy number of the gene of interest by relating to the PCR signal of a standard curve. Relative quantification, such as delta delta Ct method, relates the PCR signal of the gene of interest in a treatment group to that of an untreated control sample.

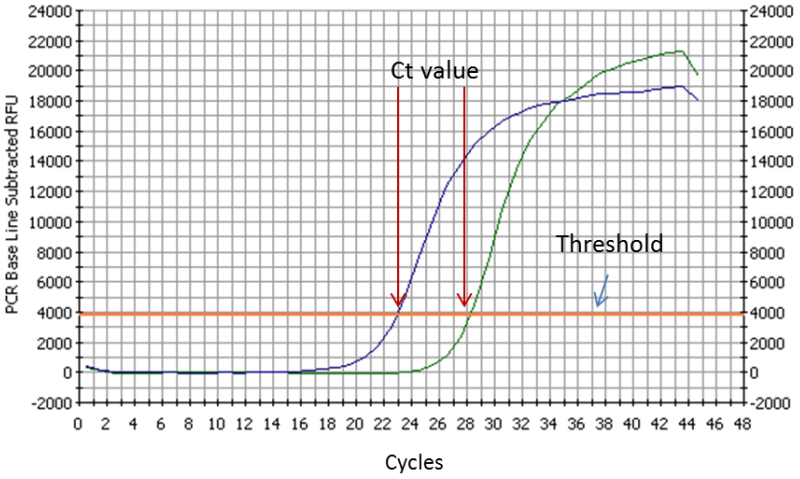

Figure 2-3: Representative of real-time PCR curves. A threshold level is set sufficiently above the background and the number of cycles required to reach the threshold is called Ct.

Methodology

cDNA were used for analysing single genes by qPCR reaction in 96 well-PCR plates using the following amounts: 1 µl Primer and Probe, 5 µl cDNA, 7.5 µl Precision™qPCR Mastermix containing 2X reaction buffer, 0.025 U/ µl Taq Polymerase, 5 mM $MgCl_2$, 200 µ of each dNTP and 1.5 µl nuclease-free water. For multiplex reactions the following amounts were used: 1 µl of Primer and Probe, 5 µl of cDNA, 12.5 µl Precision™qPCR Mastermix and 6.5 µl of nuclease-free water (all from PrimerDesign, Southampton, UK). Gene specific primer with SYBR Green: collagen I, III, V, versican, biglycan, decorin, and PerfectProbe were used to measure ECM: IL-8, αSMA, LOX, LH2b expression (all are from PrimerDesign, Southampton, UK). Genes of interest were normalized to the geometric means of the reference genes: Ubiquitin C (UBC) and phospholipase A2 (A2) for fibroblasts treated with TGFβ and dexamethasone experiments, or Glyceraldehyde 3-phosphate dehydrogenase (GAPDH) for mechanical strain experiments. The data were calculated relative to one control sample of a single patient using the relative expression: delta delta Ct method (183). As the Ct value depends on the amount of gene of interest expression of the sample, the difference in Ct value of two different samples corresponds to the difference in their gene expression. Relative expression of a gene of interest is calculated by normalising for

loading differences in the amount of DNA by determining Ct values for a reference gene (a gene whose expression is known to remain constant under the studied conditions) and then comparing with an untreated control samples.

2.4.7) **Protocol used for RT-qPCR**

2.4.7.a) Housekeeping gens Multiplex (Perfect Probe)

Cycle 1:	(1X)	Temperature	Time(min:sec)
	Step 1:	95.0°C	for 08:00
Cycle 2:	(50X)		
	Step 1:	95.0°C	for 00:15
	Step 2:	50.0°C	for 00:45
	Data collection enabled		
	Step 3:	72.0°C	for 00:10

2.4.7.b) Singleplex (Perfect Probe)

Cycle 1:	(1X)	Temperature	Time (min:sec)
	Step 1:	95.0°C	for 08:00
Cycle 2:	(52X)		
	Step 1:	95.0°C	for 00:10
	Step 2:	50.0°C	for 00:20
	Data collection enabled		
	Step 3:	72.0°C	for 00:10

2.4.7.c) Single probe (Sybergreen)

Cycle 1:	(1X)	Temperature	Time (min:sec)
	Step 1:	95.0°C	for 10:00
Cycle 2:	(49X)		
	Step 1:	95.0°C	for 00:15
	Step 2:	60.0°C	for 01:00
	Data collection enabled		
	Step 3:	95.0°C	for 3:10
	Step 4:	60.0°C	For 1:00
	Melt curve 60.0°C to 95.0°C increment 0.5°C for 0:50		

2.4.8) Gene Sequences of Primers and Probes, all are human

Gene product	Gene	Gene ID	Sense Primer	Anti-sense Primer
α-Smooth muscle actin	ACTA2	NM_001613	AAGCACAGAGCAAAAGAGGAAT	ATGTCGTCCCAGTTGGTGAT
IL-6	IL6	NM_000600	GCAGAAAACAACCTGAACCTT	ACCTCAAACTCCAAAAGACCA
IL-8	IL8	NM_000584	CAGAGACAGCAGAGCACAC	AGCTTGGAAGTCATGTTTACAC
Versican	VCAN	NM_004385	GGAGAAGTGGATATTGTTGATTCAT	CTTGGCACCTCAGGATGTTT
Collagen I	COL1A1	NM_000088	AGACAGTGATTGAATACAAAACCA	GGAGTTTACAGGAAGCAGACA
CollagenIII	COL3A1	NM_000090	GTCCCGCTGGCATTCCTG	CTCTCCTTTGGCACCATTCTTAC
Collagen V	COL5A1	NM_000093	GATGTGTATTTCCCCTGACCTT	CCTCTAAATGGATCGGTGTTGGA
Decorin	DCN	NM_001920	GCCACTATCATCCTCCTTCTG	TAGCATAAAGTCAAATAAGCCTCTC
Biglycan	BGN	NM_001711	GTCTGAAGTCTGTGCCCAAAG	GCTCGGAGATGTCGTTGTTC
Lysyl oxidase	LOX	NM_002317	GATATAGTCTAAATTAGCAAAGCACATAG	ATTACGCAGCACAGTCCTTG
Lysyl hydroxylase 2b	PLOD2	NM_182943	ACTATTTTGTTCGTGATAAACTGGATC	GGGGGCTGAGCATTTGGAA

2.4.9) Cell number quantification

Cell number was evaluated by determination of total cell count after 24, 48 and 96 hr after mechanical strain using a hemocytometer and trypan blue. After mechanical strain, the cell layer was washed with 1ml of HBSS X 2 times, then 250 µl of 1% trypsin was added, incubated in the incubator for 30 seconds. Cell detachment was checked under a phase contrast microscope. The trypsin reaction was stopped by adding 1000 µl of DMEM/10%FBS. The cell suspension was mixed thoroughly then 20 µl of cell suspension was added in 30 µl of HBSS and 50 µl of of 0.4 % (w/v) trypan blue, so the total dilution is 1:5. A neubauer haemocymetry was used for the counting. The diluted cell suspension with trypan blue was introduced by capillary action beneath the coverslip on the both sides of the slide. Under the microscope, a cell count was performed in the central 1mm x 1mm square and the surrounding corner squares. An average of these 5 counts is taken. Since the haemocytometer has a known depth of 0.1 mm, this is equivalent to $0.1mm^3$. The viable cell number per ml was calculated by mean cell count in 0.1 mm^3 X 10^4 X 5 (taking into account the dilution factor).

2.4.10) **Enzyme-linked Immunosorbent Assay (ELISA)**

Principle

The basic principle of an ELISA is to use an enzyme such as horseradish peroxidase (HRP) to detect the binding of antigen (Ag)-antibody (Ab). The enzyme converts a colourless substrate to a colour product, indicating the presence of Ag-Ab binding. These assays require an immunosorbent i.e., antigen or antibody immobilized on solid surface such as wells of micro-plates. The sandwich Enzyme-linked Immunosorbent Assay (ELISA) is called a "sandwich" assay because the antigen to be measured is bound between two primary antibodies - the capture antibody and the detection antibody (Figure 2-4).

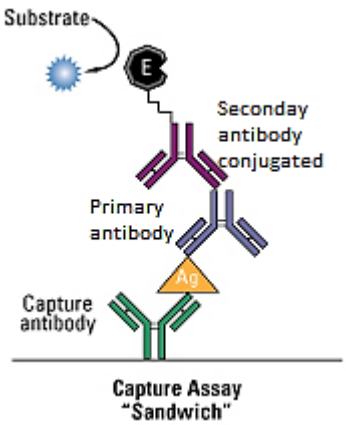

Figure 2-4: Sandwich ELISA. Antigen is bound to capture and detection antibody.

2.4.10.a) Human IL-8 Enzyme-linked Immunosorbent Assay (ELISA)

To determine the level of IL-8 released from fibroblasts after mechanical strain, culture supernatants were analysed for IL-8 by sandwich enzyme-linked Immunosorbent Assay (ELISA) using Human CXCL8/IL-8 DuoSet. NUNC Maxisorb 96-well plates were coated overnight at room temperature with capture antibody (4.0µg/mL) in PBS without carrier protein. The plates were then washed 4 times with wash buffer (1XPBS/0.05%v/v Tween 20) before blocking residual binding sites using blocking buffer (1% w/v BSA, in PBS with 0.05% w/v NaN_3) for 1 hour at room temperature. Doubling dilutions of IL-8 standards were prepared in assay buffer [0.1% BSA, 0.05% Tween 20 in Tris-buffered Saline (20 mM Trizma base, 150 mM NaCl), pH 7.4, 0.2 µm filtered]. Culture supernatants were diluted 1:5 in assay buffer. After blocking, the ELISA plates were washed 4 times with wash buffer. 100µl of samples or standards were added to wells in duplicate. The ELISA plates then were covered with an adhesive strip and incubated 2 hours at room temperature. The ELISA plates were washed 4 times with wash buffer. 100 µL of detection antibody solution (20 ng/mL in assay buffer) was added to each well. The ELISA plates were covered with a new adhesive strip and incubated for 2 hours at room temperature. The ELISA plates were washed 4 times with wash buffer. 100 µL of Streptavidin-HRP was added to each well. The ELISA plates were covered and incubated for 20 minutes at room temperature with protection from direct light. The ELISA plates were washed 4 times with wash buffer. 100 µl of TMB substrate solution were added to each well. The plates were incubated for 20 minutes at room temperature with protecting from direct light. 50 µL of Stop Solution (1M H_2SO_4) were added to each well. The plates were gently tapped to ensure thorough mixing. The optical density of each well was determined immediately, using a Multiskan Ascent plate reader at 450 nm with a 570 reference filter. Figure 2-5 shows a typical IL-8 standard curve derived from doubling dilution of a 2 ng/ml stock IL-8 solution. The lower detection limit was 32 pg/ml. This assay is designed for the analysis of cell culture supernatants. There is no cross-reactivity or interference with recombinant human: GROα, GROβ, GROγ, IP-10, MIP-1α, MIP-1β, MCP-1, MCP-2, MCP-3 and RANTES.

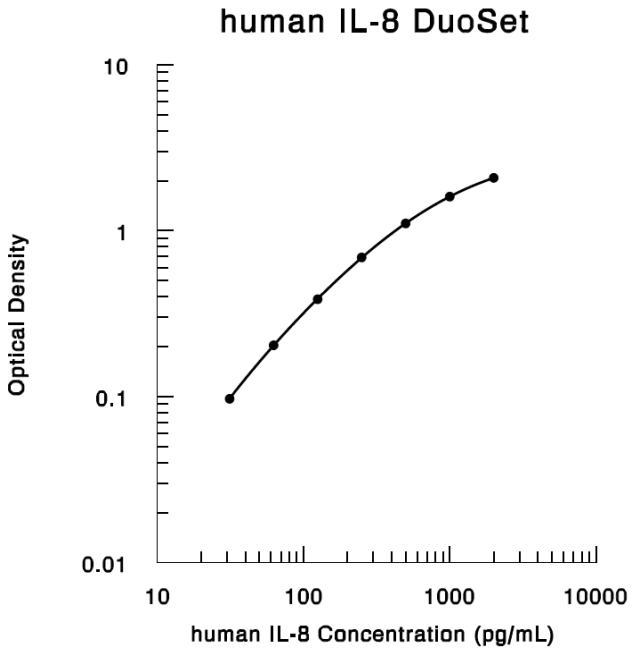

Figure 2-5: Graph demonstrates an IL-8 standard curve.

2.4.10.b) TGFβ 1 enzyme-linked Immunosorbent Assay (ELISA)

To determine the level of active TGFβ1 released from fibroblasts after mechanical strain, culture supernatants were analysed for active TGFβ1 by sandwich enzyme-linked Immunosorbent Assay (ELISA) using TGFβ1 Emax® ImmunoAssay System. NUNC Maxisorb 96-well plates were coated overnight at 4°C with 100µl of TGFβ coating antibody [(10 µl TGFβ Coat mAb + 10ml carbonate-bicarbonate coating buffer (1 capsule of carbonate-bicarbonate + 100 ml of dH_2O, pH9.6)]. On the next day, the coated plate was allowed to warm to room temperature (approximately 10-15 minutes). The coating content was removed by slapping the plate upside down three times on a paper towel. 270 µl of TGFβ Block 1X Buffer was added to each well using a multichannel pipettor. The plates were then incubated at 37°C for 35 minutes without shaking. The plates were washed 4 times with wash buffer (20mM Tris-HCl pH 7.6, 150mM NaCl and 0.05% (v/v) Tween® 20). 100µl of samples or standards were added to wells in duplicate. The plates then were covered with an adhesive strip and incubated 2 hours at room temperature with shaking. The plates were washed 4 times with wash buffer. 100 µL of detection antibody solution (10 µl of detection antibody in 10 ml of assay buffer) was added to each well. The plates were covered with a new adhesive strip and incubated for 2 hours at room temperature. The plates were washed 4 times with wash buffer and incubated for 2 hours at room temperature. After washing 4 time with wash buffer, 100 µL of Streptavidin-HRP was added to each well. The plates were covered and incubated for 2 hours at room temperature with protection from direct light. After incubation, the plates were washed 4 times with wash buffer. 100 µl of TMB substrate solution were added to each well. The plates were incubated for 20 minutes at room temperature with protection from direct light. 100 µL of Stop Solution (1M HCl) were added to each well. The plates were gently tapped to ensure thorough mixing. The optical density of each well was determined immediately, using a Multiskan Ascent plate reader at 450 nm filter. Figure 2-6 shows a typical TGFβ1 standard curve derived from doubling dilution of a 1 ng/ml stock TGFβ1 solution. The lower detection limit was 32 pg/ml.

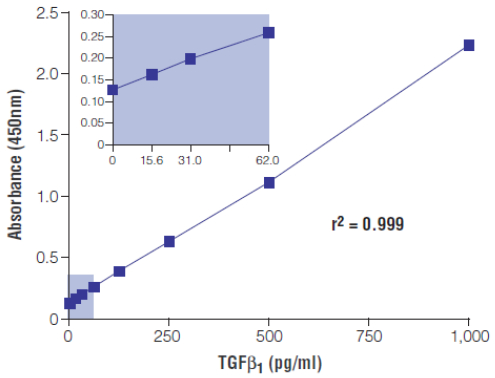

Figure 2-6: Graph demonstrates a TGFβ1 standard curve.

2.4.11) **Immunofluorescent staining for F-actin and α-SMA**

Principle

Immunofluorescence is a technique allowing the visualization of a specific protein or antigen in cells or tissue sections by binding a specific antibody chemically conjugated with a fluorescent dye such as fluorescein isothiocyanate (FITC). There are two major types of immunofluorescent staining methods: direct immunofluorescence staining in which the primary antibody is labelled with fluorescence dye, and indirect immunofluorescence staining in which a secondary antibody labelled with fluorochrome is used to recognize a primary antibody (Figure 2-7).

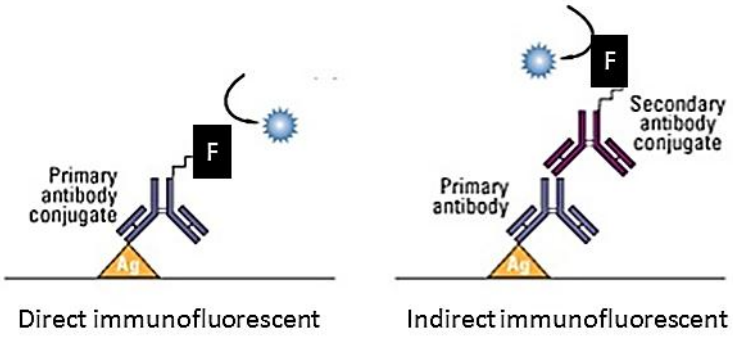

Figure 2-7: Direct and indirect immunofluorescent staining

Methodology

To demonstrate the presence of F-actin and α-SMA in fibroblasts after mechanical strain, the media was remove and washed the cell layer on silastic membrane with PBS before fixation with 4% paraformaldehyde in PBS for 15 minutes at room temperature. The cells were then washed with PBS (4 times for two minutes each) before permeabilization with 0.1% Triton in PBS for 5 min at room temperature. The samples were then blocked with 1%BSA, 0.1% Triton-X in PBS for 30 minutes at room temperature, washed with PBS x 3 times for 2 minutes each, and then the cells were incubated for 90 minutes on orbital shaker using an antibody with or without fluorophore: Alexa Fluor488® conjugated Phallodin (excitation 490 nm, emission 519 nm) (1:150) for F-actin characterization and anti α-SMA (1:150) for characterization of myofibroblast differentiation. The samples were protected from the light. After washing with PBS X 4 time for 2 minutes each, the samples stained for α-SMA were incubated with the secondary antibody anti-mouse IgG/FITC (excitation 495 nm, emission 521 nm) (1:50) for 1 hour at room temperature on orbital shaker and protected from sun light. The samples were washed with PBS X 4 time for 2 minutes each before counterstaining with 7-actinomycin D (7-AAD) (excitation 546 nm, emission 647 nm) (1:100) or Hoechest 33342 (excitation 343nm, emission 483 nm) (1:200) for 5 minutes at room temperature. After washing the cell layer on silastic membrane with PBS, the membrane were then cut from the culture plate and put on glass slide. 1 drop of Prolong anti-fade was added on the samples before covering with a cover slip. The samples were imaged by fluorescent microscopy (Leica DMI 6000B).

2.4.12) **Soluble collagen measurements**

Principle

Total newly synthesised collagen secreted from cultured cells was determined using the Sircol™ soluble collagen assay (Biocolor, Belfast, Northern Ireland). The Sircol™ dye reagent contains Sirius Red. The colour commission name is Direct Red 80. Sirius Red is an anionic dye with sulphonic acid chain groups. These groups react with the side chain groups of the basic amino acids present in collagen. The specificity affinity of the dye for collagen, under the assay conditions is due to the elongated dye molecules becoming aligned parallel to the long, rigid structure of native collagens that have intact triple helix organization. The presence of other soluble proteins in the samples, including proteoglycans, tropoelastin, and other soluble ECMs, does not interfere with the Sircol™ Assay (184). The assay can measured mammalian collagen type I to V (184).

Methodology

An equal volume of 4M NaCl was added to 1000ul of test sample to precipitate the collagen out of the solution, and this was harvested by centrifugation at 12,000 g for 10 min at 4°C. The pallets were re-solubilised in 0.5 M acetic acid (100 µl). Samples were then mixed with 1ml of Sirius red dye. The contents of each tube were mixed by inverting and the samples were incubated on an orbital shaker for 30 minutes. The collagen-dye complex was then precipitated by centrifugation at 12,000 g for 10 minutes. The unbound dye solution was removed by carefully inverting and draining the tubes. The remaining dye droplets were removed from the tubes using a cotton wool bud. 1 ml of alkali reagent was added to each sample and the tubes were recapped and vortexed. When the bound dye was fully dissolved, the samples were transfer to 96 well plates and the absorbance was measured at 540 nm. As a standard, collagen type I solution was diluted with 0.5 M acetic acid 100 µl and processed the same as samples. Figure 2-8 shows a typical collagen reference standard curve. The lower detection value was 2.5 µg of collagen.

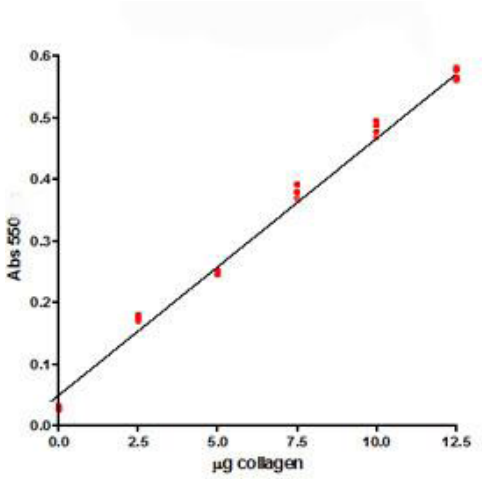

Figure 2-8: Graph demonstrates collagen reference standard curve.

2.4.13) Preparing samples for SDS-PAGE (PolyAcrylamide Gel Electrophoresis)

After exposure to mechanical strain for 96h, cells were washed with HBSS and scraped into Sodium dodecyl sulfate (SDS) lysis buffer (62.5 mM Tris-HCl, 10% Glycerol, 2% SDS, cocktail protease inhibitor (0.37mg/ml)). Supernatants were collected and sonicated. The quantity of the protein was measured using a NanoDrop spectrophotometer. 20 µg of protein was prepared in 1X sample buffer (20 µl) and heated to 95°C for 5 minutes prior to electrophoresis on a 12.5% SDS polyacrylamide gel with a 4% stacking gel for α-SMA detection. For the experiments measuring LOX protein in conditioned media (CCM) or in bronchoalveolar lavage fluid (BAL), Strataclean® Resin was added to 100 µl of CCM or 200 µl of BAL in the ratio of 1:10 in order to concentrate total protein. These samples were vortexed and mixed for 30 min at 4 °C. After centrifugation at 16,000 g for 5 minutes, the supernatants were removed and 20 µl of 2X sample buffer was added to the resin, boiled for 5 min and centrifuged before loading to the 10% SDS polyacrylamide gel with a 4% stacking gel (185). StrataClean® resin is a phenol-free technique for protein concentration. The solid phase silica-based resin contains hydroxyl groups that react with proteins in much the same manner as the hydroxyl group of phenol.

2.4.14) SDS-PAGE (PolyAcrylamide Gel Electrophoresis) and Western blotting

Principle

SDS-PAGE (PolyAcrylamide Gel Electrophoresis) is used to separate proteins according to their molecular weight. SDS-PAGE, coupled with western blotting (immunoblotting) is typically used to determine the presence of specific proteins. Electrophoresis involves applying an electric current to the gel and allowing the proteins to migrate though the gel. For SDS PAGE, the proteins are denatured and have a negative charge by binding of SDS. This allows the proteins bands to be separated depending on their electrophoretic mobility which is a function of their individual molecular weight. Following the electrophoresis, the proteins can be transferred to a Polyvinylidene Fluoride (PVDF) or nitrocellulose membrane. The transfer process uses the same principle as SDS-PAGE. The proteins migrate out of the gel towards the anode and are transferred onto the membrane. Once the proteins are separated and bound to the membrane, then the western blotting can begin. Western blotting is used to detect a target protein in a sample by using a polyclonal or monoclonal antibody specific to that protein. Western blotting involves in 4 steps: blocking, primary antibody incubation, secondary antibody incubation and developing. Blocking is to reduce non-specific protein interactions between the membrane and the antibody using a solution of bovine serum albumin (BSA) or non-fat dry milk. The primary antibody is specific for the protein of interest. Secondary antibody binds to the primary antibody and is typically linked to an enzyme that allows for visual identification. Developing is done by incubating the enzyme substrate to the membrane so that the positions of membrane-bound secondary antibodies will emit light (Figure 2-9). Bands corresponding to the detected protein of interest will appear as dark regions on the developed film.

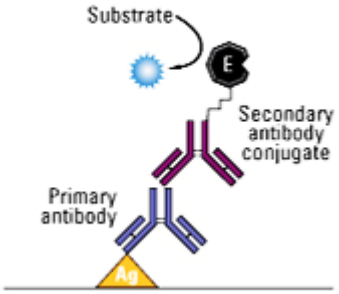

Figure 2-9: Antigen -antibody interaction in western blotting. Primary antibody binds to protein of interest. Secondary antibody tagged with enzyme binds to primary antibody. The enzyme -substrate reaction produces light causing a dark band on developed film.

Methodology

A Mini Protean II system was used to cast two 1 mm thick gels for SDS-PAGE. 10 ml of separation gel mix were prepared (Table 2-4), poured into casting plates and overlaid with isopropanol. Gels were left to polymerize for 30 minutes. Isopropanol was then removed and the surface of the gel was washed with dH_2O. 5 ml of stacking gel mix was poured over the separation gel. A 15 well or 10 well comb was inserted into the stacking gel mix which was left to set for 15 minutes. Once set, the comb was removed. The gel cassette was placed into the electrode assembly, which was placed into a mini tank containing 1X running buffer. After filling the upper electrode chamber, 20 µl of sample in sample buffer or 5 µl of protein marker (Precision Plus Protein Kaleidoscope standards 10-250 kDa) was loaded onto the gel. The mini tank was covered with a lid that connected to the power pack. Electrophoresis was run at 90V until the dye reached the bottom of the gel. Then the gel was removed and processed for electrophoretic transfer onto Polyvinylidene Fluoride (PVDF) transfer membrane.

Pre-cut PVDF membranes (hydrated with methanol), Whatman filter paper (3MM CHR, GE Healthcare, UK) and scotchbrite pads were soaked in transfer buffer for 15 minutes. In the transfer cassette from black side, a sandwich of one layer of scotchbrite, Whatman filter paper, gel, PVDF membrane, another layer of whatman filter paper, and one layer of scotchbrite at the white side. Air bubbles were carefully removed using a falcon during assembling the PVDF membrane in the transfer cassette. The cassette was inserted into the Transblot tank containing transfer buffer, with the clear side of the cassette situated closest to the anode (+red) and the black side of the cassette situated toward the cathode (- black). A magnetic flea and ice cartridge were placed

into the tank and filled with transfer buffer. The tank was placed in an iced filled tray on a magnetic stirrer. Electrophoretic transfer was carried out for 90 minutes at 90V. After transfer, the PVDF membranes were removed and stained with PonceauS for 3 minutes in order to confirm transfer of the protein. To prepare the membrane for western blotting, the PonceauS stain was removed by rinsing with dH_2O until the membrane was clear. Then the membranes were rehydrated with methanol for 3 minutes and washed with dH_2O for 3 minutes and wash buffer for 10 minutes. Non-specific binding was blocked using blocking buffer (Table 2-8) for 45 minutes on an orbital shaker. Before incubating with the primary antibody, the membranes were washed with wash buffer for 5 minutes. Membranes were incubated overnight at 4 °C with the proper dilution of primary antibody on an orbital shaker (Table 2-9). The next day, the membranes were washed with wash buffer for 10 minutes X 2 times with shaking at room temperature before incubating with appropriate secondary antibody conjugated to horseradish peroxidase (HRP) for 1 hour at room temperature (Table 2-10). Membranes were then washed 3 times with wash buffer for 10 minutes. The immunoreactivity was detected using enhanced chemiluminescence according to the manufacturer's protocol. This involved removing excess wash buffer was removed by tapping the membrane on tissue paper before covering the membranes with 2 ml of ECL Plus solution (2 ml of solution A + 50 µl of solution B) for 5 minutes. The excess fluid was removed and the membranes were placed onto cling film fixed into the inside of a hyperfilm cassette with tape, then another sheet of cling film was carefully laid over the membrane without trapping any air bubbles. X-ray films (Amersham Hyperfilm™ ECL, Buckinghamshire) were exposed to the membrane for 3-15 minutes in the dark room. Films were developed immediately using the developing solution (30ml developer + 270 ml dH_20) for 1 minute, followed by incubation in fixative solution (75 ml Fixer + 225 ml of dH_20) for 1 minute. X-ray films were then air dried and the protein bands were quantified using ImageJ (NIH, Bethesda, MD, USA).

Table 2-4: Composition of separation gel mix used for SDS-PAGE

Separation gel mix (for two 1mm thick mini gels)	10%	12.5%
dH_2O	4.1 ml	3.1 ml
1.5 M Tris-HCl pH 8.8	2.5 ml	2.5 ml
30% (w/v) Acrylamide/0.8%(w/v) bisacrylamide	3.3 ml	4.17 ml
10% SDS	100 µl	100 µl
10% (w/v) ammonium persulphate	50 µl	50 µl
TEMED	5 µl	5 µl

Table 2-5: Composition of stacking gel mix used for SDS-PAGE

Stacking gel mix	
dH_2O	3.5 ml
30% (w/v) Acrylamide/0.8%(w/v) bisacrylamide	0.5 ml
0.5 M Tris-HCl pH 6.8	1.25 ml
10% SDS	50 µl
10% (w/v) ammonium persulphate	25 µl
Tetramethylethylenediamine	10 µl

Table 2-6: Composition of SDS lysis buffer used to prepare cell lysate for SDS-PAGE

SDS lysis buffer	
62.5 mM Tris-HCl pH 6.8	2.1 ml of 1.5 M Tris-HCl pH 6.8
10% glycerol	5 ml
2%(w/v) SDS	5 ml of 20% SDS
dH_2O	33.75 ml

Complete protease inhibitor cocktail 1 tablet was dissolved in 1 ml of dH_2O and added 20 µl per 1 ml of SDS lysis buffer.

Table 2-7: Composition of 5X sample buffer used in sample preparation for SDS-PAGE

5X Sample buffer	
0.3125 M Tris-HCl pH 6.8	10.41 ml of 1.5M Tris-HCl pH 6.8
50% glycerol	25 ml
25% 2-mercaptoethanol	12.5 ml
10%(w/v) SDS	5g
0.01% bromophenol blue	5mg
dH_2O	Up to 50 ml

Table 2-8: Composition of SDS-PAGE western blotting buffer

10 X Tris Buffered Saline (TBS)	1L adjust pH to 7.6 with HCl
50mM Tris base	60.5g
150mM NaCl	87.6g

1X Running buffer pH 8.3	1L
0.025 M Tris	3.03g
0.192 M Glycine	14.4g
0.1%(w/v)SDS	1g

Transfer buffer pH 8.3	5L
0.025 M Tris	15.15g
0.192 M Glycine	72g
20% (v/v) methanol	1000ml

Wash buffer	
1X TBS	1000ml
0.1% Tween 20	1ml

Antibody buffer& blocking buffer	100 ml
1 X TBS	100 ml
0.1% Tween20	100µl
5%(w/v) non-fat milk powder	5g

Table 2-9: Primary antibodies used for western blotting

Antibody	Species	Company	Catalogue No.	Dilution
α-Smooth muscle actin	mouse	Sigma	A2547	1:10,000
Lysyl oxidase (LOX)	rabbit	Sigma	L4794	1:750
GAPDH	rabbit	R&D	2275-PC-100	1:1000

Table 2-10: Secondary antibodies used for western blotting

Antibody	Species	Company	Catalogue No.	Dilution
α-Mouse-HRP	rabbit	Dako Cytomation	P0260	1:2000
α-rabbit-HRP	swine	Dako Cytomation	P0217	1:2000

2.4.15) **Matrix metalloproteinase (MMPs) analysis**

Principle

The expression of MMPs can be analysed by substrate zymography, which identifies MMPs by the degradation of their preferential substrate and by their molecular weight. MMPs are separated by electrophoresis under nonreducing denaturing condition with SDS. During electrophoresis, the SDS causes the MMPs to denature and become inactive. After electrophoresis, the gel is washed with Triton X-100, which renatures and recovers the enzymes' activity. During incubation with developing buffer, the concentrated, renatured MMPs in the gel will digest the substrate. After staining with Coomaasie Blue R-250, the MMPs activity is detected as clear bands against a blue background of undegraded substrate (186).

Methodology

MMP2 and MMP9 released into the media were detected using gelatin zymography. Culture supernatant from fibroblasts pellets culture treated with TGFβ2 was used as a positive control. 15 µl of non-reducing sample buffer was added to culture supernatant 15 µl and let stand at room temperature for 10 minutes. Then 25 ul of samples was loaded onto 10% w/v acrylamide gel containing 1mg/mL gelatin. The gel preparation and electrophoresis protocol is the same as SDS-PAGE in previous section. Following electrophoresis, gels were denatured with 50ml/gel of renaturing solution at room temperature for 30 min. The renaturing solution then was decanted. Gels were subsequently rinsed with developing buffer and incubated in developing buffer overnight at 37 °C. On the next day, gels were stained with 0.5% Coomaasie Blue R-250 for 30 minutes and destained with destaining solution until clear band were visible. The MMP activity was visualized as clear bands against a dark blue background. Then the gels were photograph and analysed by the inverted densitometry using ImageJ (NIH, Bethesda, MD). The density was normalized to the lowest density of the non-strain group per 10,000 cells.

Table 2-11: Composition of buffer and solution used in gelatin zymography

Sample buffer 2X	
0.5 M Tris HCl pH 6.8	2.5ml
Glycerol	2 ml
10% (w/v) SDS	4ml
0.1% Bromophenol blue	0.5ml
dH_2O	Up to 10 ml

Renaturing solution	
2.5% Triton X -100	2.5ml
dH_2O	Up to 10 ml

10X Developing buffer	
Tris base	12.1 g
Tris-HCl	63.0g
NaCl	117g
$CaCl_2$	7.4g
Brij35	0.2%
dH_2O	Uo to 1 L

Destain solution	1L
Methanol	250ml
Acetic acid	50ml
Water	200ml

2.4.16) Preparation of fibroblast derived extracellular matrix for atomic force microscopy image

Cell-synthesized extracellular matrix was prepared by stimulating fibroblasts (10,000 cells/well) cultured in 8 wells chamber slide with TGFβ2 (10 ng/ml) for 7 days. Before, seeding the cells, the chamber glass slides were coated with bovine collagen I solution (1: 500 dilution in dH_2O) 1 ml/well for 1 hour at 37°C. After 7 days stimulation with TGFβ2, the culture medium was removed. The cell layers were then washed with calcium-and magnesium-free PBS. The cellular component was removed by following methods.

1) The cells were incubated with 25 mmol/l NH_4OH for 10 minutes at room temperature (187).
2) The cells were incubated with 0.5% deoxycholate (DOC) in immunoprecipitation assay buffer (50 mM Tris pH 8, 150 mM NaCl, and 1% Nonidet P-40) for 5 minutes at 4°C under gentle shaking (188).
3) The cells were incubated with 5 mM EDTA in calcium- and magnesium-free PBS for 5 minutes at 37°C (189) .

For all methods, the cell detachment was checked under light microscope, detached cells we then discarded and remaining ECM proteins attached to the surface of slides were washed with dH_20. The slides were then left to dry overnight before imaging using atomic force microscopy.

2.4.17) Collagen extraction from the tissue for atomic force microscopy image

Collagens in the tissue were extracted from nasal polyp, lung parenchyma or airway using a modification of the protocol described for extraction of collagen from cartilage: 100 mM Sorensen's phosphate buffer (pH 7.2) containing 1mg/ml bovine hyaluronidase and 1 mg/ml trypsin (190). Samples were incubated at 37°C for 24 h, washed with dH_20 for 2 times, and then put on glass slides and left to dry overnight before imaging by atomic force microscopy.

Table 2-12: Composition of Sorensen's phosphate buffer

Sorensen Phosphate Buffer 0.1M	
A. 0.2M Sodium Phosphate Monobasic **NaH2P04**	24g / 1000mL
B: 0.2M Sodium Phosphate Dibasic	28.4 g / 1000mL
STOCK BUFFER 0.2M,	Combine:
pH 7.2-7.4	Solution A 20 ml
	Solution B 80 ml
WORKING BUFFER 0.1M, pH 7.2-7.4	Dilute stock buffer (0.2M) 1:1 with distilled water

2.4.18) Transmission electron microscopy (TEM) sample preparation

After treatment with TGFβ2 for 7 days, fibroblasts pellet cultures were fixed with 3% glutaraldehyde and 4% formaldehyde in 0.1 M PIPES buffer pH 7.2 at room temperature for 1 hour. Samples were further processed by Dr Susan Wilson before imaging with a Philips EM 201 transmission electron microscope.

2.4.19) Scanning electron microscopy (SEM) samples preparation

Samples were fixed with 3% glutaraldehyde and 4% formaldehyde in 0.1 M PIPES buffer pH 7.2 at room temperature for 1 hour. The samples were then postfixed in 1% osmium tetroxide and dehydrated in an ascending series of alcohol. Next, the samples were further processed for critical point drying, mounting on the stubs and sputter coating by Dr Anton Page. Specimens were imaged using a Hitachi S800 scanning electron microscope.

2.4.20) Negative staining for transmission electron microscopy

To demonstrate the structure of collagen by TEM negative staining, 5µl of bovine collagen I solution (2 mg/ml) were put on 200 mesh formvar, carbon coated grids and left for 5-30 minutes. Then the grids were gently blotted by touching the edge of each onto a piece of tissue using reverse forceps. 5 µl of negative stain (containing 1% ammonium molybdate in 0.1 M ammonium acetate buffer pH 7.0 plus 1 grain of sucrose per ml) were put on the grids for 10 seconds. The grids then were gently blotted and allowed to dry. The samples were then imaged using a Philips EM 201 transmission electron microscope.

2.4.21) **Atomic force microscopy and nanoindentation**

Principle

Atomic force microscopy is an imaging instrument that can measure both three dimensional topography and mechanical properties of the surface with a sharpened probe. The probe is attached to a cantilever where the output from a laser is focused on and reflected into the photo-detector. In the microscope, the force between the probe and the sample surface is measured with a force sensor, and then the output is sent to a feedback controller that then drives a Z motion generator. The feedback controller uses the force sensor output to maintain a fixed distance between the probe and the sample. The motion of the probe is monitored and used to create an image of the surface (Figure 2-10) (191).

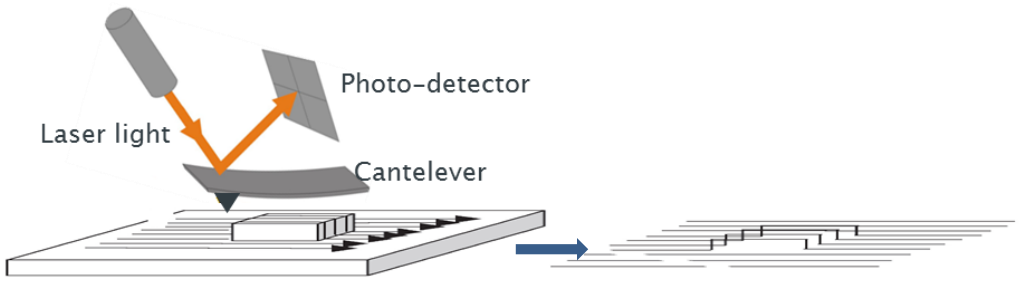

Figure 2-10: Schematic representation of how AFM creates an image. A probe with the force sensor is attached to the cantilever where the laser is focused on the backside of a cantilever and reflected into a photo-detector. The image on the left shows the motion of the probe from each passing across the surface, and a 2-D line profile is generated. The image on the right shows how the line profiles are combined to create a three dimensional image of the surface. This image was modified from Paul West. Introduction to Atomic Force Microscopy Theory Practices Applications. Paul West, editor, 2009. Available from http://www.paulwestphd.com/index.html.

2.4.21.a) Nanoindentation

Principle

Nanoindentaion, which is an application of controlled force to the surface to induce surface deformation by atomic force microscopy, is a recognized tool for measurement the mechanical properties of fibrillar structures such as collagen fibrils (159). Load and displacement curves are monitored during loading and unloading, and the mechanical properties such as stiffness and Young's modulus are calculated using the Oliver and Pharr method (192). During indentation, the force will be applied to the tip then the tip is moved into the sample tissue causing a deformity of the surface. Load and displacement are monitored continuously during the indentation process, resulting in a load-displacement curve (Figure 2-11b). The interaction between the tip and the sample during the indentation process is illustrated in Figure 2-11a.

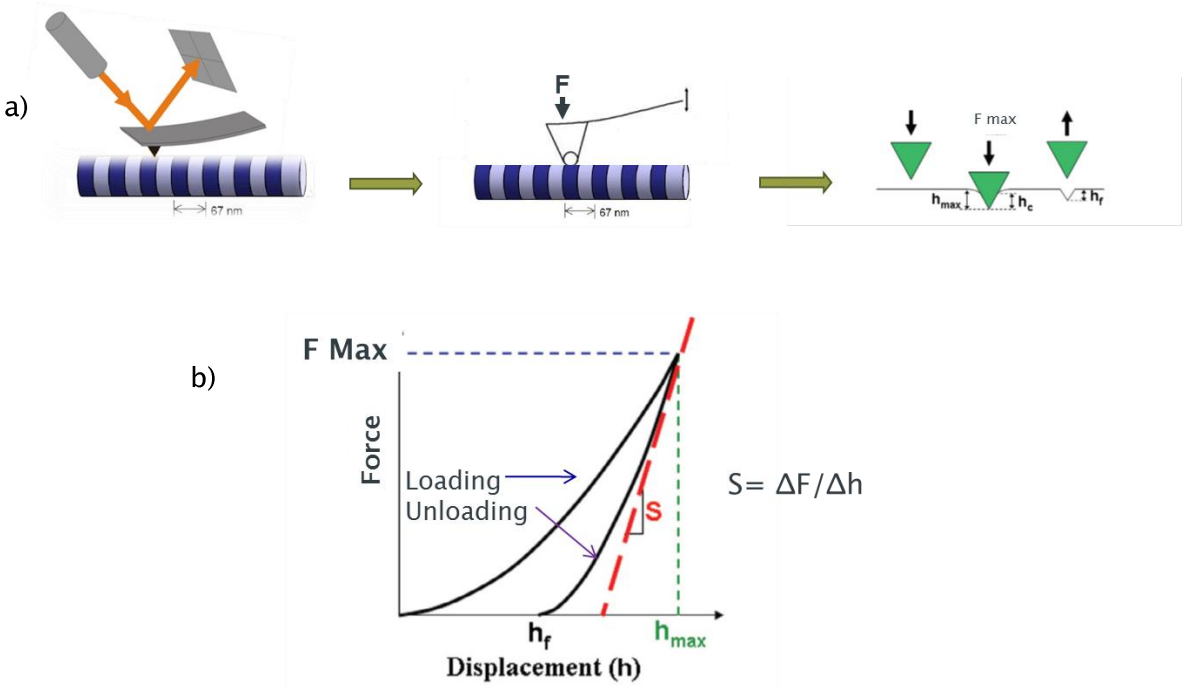

Figure 2-11: Schematic representation of how to measure nanoindentation of the sample surface and a typical load-displacement curve. a) During indentation, the force will be applied to the tip then the tip is moved into the sample tissue causing a deformity of the surface and b) the load and displacement curve can be generated. Fmax = maximum force applied; hmax = penetration depth; hc = contact depth (the height of the contact between the tip and the sample); hf = final depth; S = unloading stiffness.

During indentation, both the indenter (AFM tip) and sample (collagen fibril) with their characteristic stiffness are connected in series (Figure 2-12). Therefore, the reduced modulus which means the combine modulus of indenter and sample can be calculated from equation (1).

$$\frac{1}{E_r} = \left(\frac{1-\nu_i^2}{E_i} + \frac{1-\nu_s^2}{E_s} \right) \qquad (1)$$

Er is the reduced modulus of the combined indenter and sample, E is the elastic (Young)'s modulus, ν is the Poisson's ratio, and i and s refer to the indenter and sample, respectively.

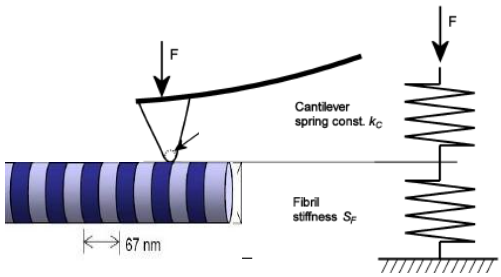

Figure 2-12: Schematic representation of the arrangement of AFM tip, cantilever and collagen fibril during nanoindentation. This can be described as two springs connected in series.

Collagen fibrils' stiffness (S) can be calculated by the slope of the unloading load and displacement curve (ΔF/Δh). Then the reduced modulus (Er) can be calculated from equation (2).

$$E_r = \frac{\sqrt{\pi}}{2} \frac{S}{\sqrt{A}} \qquad (2)$$

A is the measured, projected, or cross-sectional contact area,

Contact area (A) also depends on AFM tip shape and the depth of contact, so the AFM tip shape was imaged before the indentation process as shown in Figure 2-13. Then, the contact area (A) was calculated from the manufacturer's software (Figure 2-14). The reduced modulus (Er) and sample modulus (Es) can be calculated from the equation (2) and the equation (1).

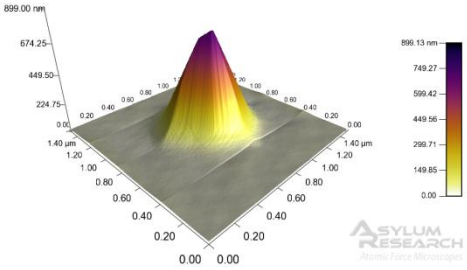

Figure 2-13: Image of AFM tip.

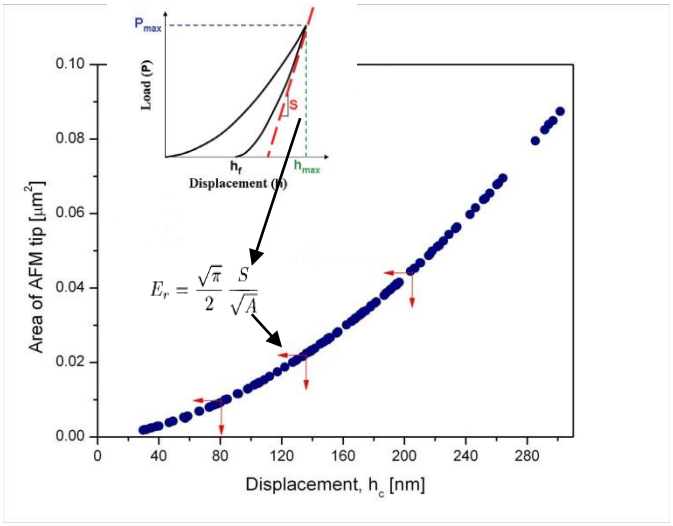

Figure 2-14: Graph demonstrates the contact area calculation from the manufacturer software and then Er can be calculated from the equation. Inset shows stiffness (S) calculation from load-displacement curve.

Methodology

Samples were imaged by AC mode and collagen fibril indentation was done using MFP-3D atomic force microscope (Asylum research, CA, USA). All measurements were taken in air and at room temperature. All data analysis was performed with the Asylum Research software.

2.5) Statistical analysis

The data were analysed using SigmaPlot 11.0 (Systat Software Inc, Hounslow, UK). Data are reported as mean± standard error if they are normally distributed or median± interquartile range if they are not normally distributed. One-way ANOVA or Kruskall-Wallis tests were used for analysing the difference between groups. The paired student *t* test or the Wilcoxon signed rank test were used to analyse the difference in mRNA expression and protein level between strain and non-strain group. Repeated ANOVA were used to analyse the difference among treatment conditions. Results were considered statistically significant at p levels< 0.05.

Chapter 3: Cyclical Mechanical Strain Enhances Pro-Fibrotic and Inflammatory Responses of Bronchial Fibroblasts

3.1) Rationale

Asthma is a clinical syndrome that is principally defined from a set of symptoms namely episodic shortness of breath, especially at night, and cough and wheezing. Chronic airway inflammation, airway hyper-responsiveness and structural changes are recognized as important features of chronic asthma (193). The airway inflammation is typically eosinophilic and accompanied by elevation of Th2 cytokines (1). However, Th2 inflammation alone cannot explain the development of airway remodelling in asthma (27). In chronic asthma with airway remodelling, the airways become thickened from an increase in airway smooth muscle, the laying down of new matrix proteins including collagen fibres and proteoglycans resulting in thickening of the *lamina reticularis*, epithelial layer denudation, goblet cell hyperplasia and proliferation of microvessels along with vascular leakage (45). The interaction between inflammatory cells, structural cells (e.g. epithelial cells and fibroblasts) and the turnover rate of extracellular matrix protein (ECM) leads to remodelling and fibrosis of the airway (58).

Human airway development requires a mechanical environment to promote airway growth and bronchial tree development. The key structural cells of the airways (epithelial cells, fibroblasts, and smooth muscle cells) are responsible for creating these mechanical environments (160). The normal airways and lungs are constantly exposed to mechanical forces during normal inspiration-expiration cycles and are exposed to an excessive force during airway constriction and deep inspiration. Submucosal airway fibroblasts are the major cells in transforming mechanical signals into biological events especially in driving expression of ECM gene. Consequently, they play a pivotal role in tissue remodelling and wound healing (174). Previous studies have highlighted the role of airway fibroblasts in production ECM in response to mechanical forces (175-177). Furthermore, bronchial hyperresponsiveness has been shown to be inversely related with the airway wall thickness (67). Therefore, it was hypothesized that airway fibroblasts from asthmatic and normal subjects may respond to mechanical strain differently.

3.2) Hypothesis

Mechanical forces may activate airway fibroblasts to produce ECM components and pro-inflammatory mediators. These may contribute to airway remodelling and airway inflammation in asthma.

3.3) Aims

This chapter was to study the effect of mechanical strain that mimics the deep inspiration-expiration cycles on primary bronchial fibroblasts obtained from asthmatic and healthy non-asthmatic subjects. Changes in collagen I, III, versican, and decorin, as markers of extracellular matrix proteins synthesis, TGFβ as a marker of growth factor release, and IL-8 as a marker of proinflammatory cytokine response were measured. The influence of mechanical strain on promoting myofibroblast differentiation by measuring αSMA expression was also investigated.

3.4) Methods

3.4.1) Mechanical stimulation of cultured fibroblasts

Fibroblasts were seeded on type I collagen-coated six-well BioFlex silastic bottom culture plates at a density of 200,000 cells/well and cultured for 24hr. The plates were placed on the baseplate of the cell stretching device (Figure 3-1) (Flexercell-4000T TensionPlus; Flexcell International, Mckeesport, PA, USA) in a 37 °C, 5% CO_2 incubator. The machine used a vacuum to produce a negative pressure pulling down the flexible membrane where the cells were attached (Figure 3-2). The cells were exposed to the mechanical strain that resembled respiratory cycles (Figure 3-3). A sinusoidal cyclical strain of 30% elongation was applied at a frequency of 12 cycles per minute for varying times between 6 hr-144 hr. Control cells were cultured in the similar trays but without mechanical strain. This strain regimen was chosen because it corresponds approximately to the inspiratory capacity and normal adult respiratory rate (175).

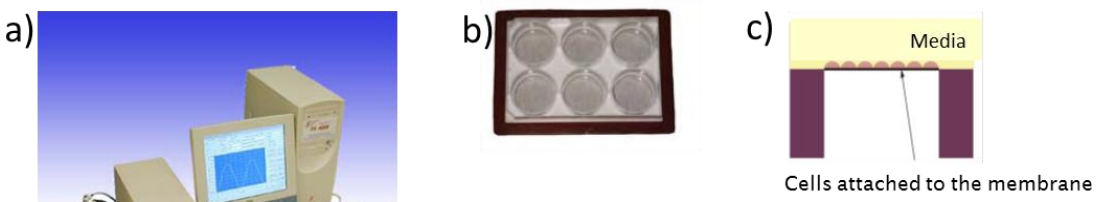

Figure 3-1: Image a) represents the FlexerCell FX4000 strain unit and image b) shows the Bioflex plate with silastic bottom. In c) a schematic image represents lateral view of cells attached to the membrane of the plate during resting stage.

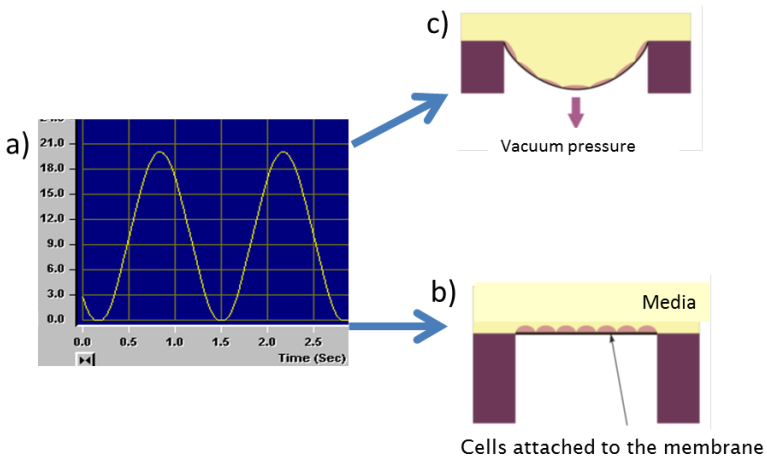

Figure 3-2: Images illustrating how the cells are exposed to mechanical strain. In a) The sinusoidal strain cycles are generated by the FlexerCell FX4000 strain unit, image b) represents the cells during resting stage and image c) represents the cells during exposed to mechanical strain.

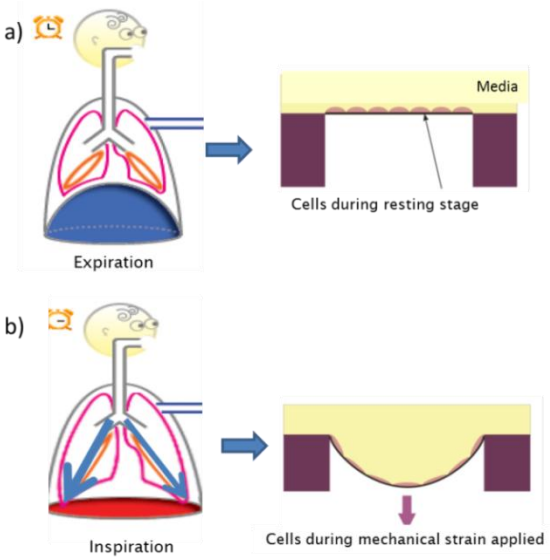

Figure 3-3: Schematic representation of the mechanical strain cycles resemble the respiratory cycles. In a) the expiration cycle equivalent to the cells during the resting stage and in b) the inspiration cycle equivalent to the cells during the mechanical strain applied.

3.4.2) **Subject characteristics**

Airway fibroblasts from 6 normal and 12 asthmatic (6 mild and 6 severe asthma) subjects were studied. The characteristics of the subjects are outlined in Table 3-1. There was no significant difference in age among group. Severe asthmatic subject had a significantly lower FEV_1 (%predicted) than healthy and mild asthmatic subjects. There were more female subjects in asthmatic group and only severe asthmatic subjects received corticosteroids in their treatment.

Table 3-1: Subjects characteristic studied on mechanical strain of airway fibroblasts

Disease	No.	Age* (yrs)	Sex (F:M)	FEV_1 (%predicted)	Inhaled steroid (µg/day BDP equivalent)	Prednisolone (mg/day)
Normal	6	38 (20-64)	2:4	109.2 (89.8-133.8)	0	0
Mild asthma	6	31 (21-45)	4:2	108.3 (95.5-131)	0	0
Severe Asthma	6	50 (17-69)	4:2	68.10* (19.8-71.1)	1800 (1000-2800)	5 (0-20)

* $p < 0.01$. Data were shown as mean with range in brackets. FEV_1= forced expiratory volume in 1 second. BDP =Beclomethasone Dipropionate

3.5) Results

3.5.1) Initial experiments

Initial experiments were performed to optimize the conditions for further studies to compare the difference in response to mechanical strain between fibroblasts from healthy non-asthmatic and asthmatic subjects. A mechanical strain of 30% elongation at a frequency of 12 cycles per minute was applied for 6h to 144h.

3.5.1.a) Morphologic changes of fibroblasts after exposure to mechanical strain at different time points

To establish the morphologic change of fibroblasts in response to mechanical strain over time, primary bronchial fibroblasts from one normal subject were cultured in complete DMEM containing 10% FBS and subjected to the mechanical strain (30% elongation, 12 cycles per minute) from 6 h to 144 h (Figure 3-4). After exposure to mechanical strain, the cell morphology was recorded in different regions of the well. This revealed that the morphology of strained cells changed, becoming smaller and linear in shape and they rearranged their direction according to the force of strain as early as 6 h after mechanical strain exposure. However, the silastic membranes where the cells attached were in a resting position when the cells were taken images. This may explain why the cells became smaller. After 144 h strain, the cells started to detach. Therefore, the further experiments were done until at 96h.

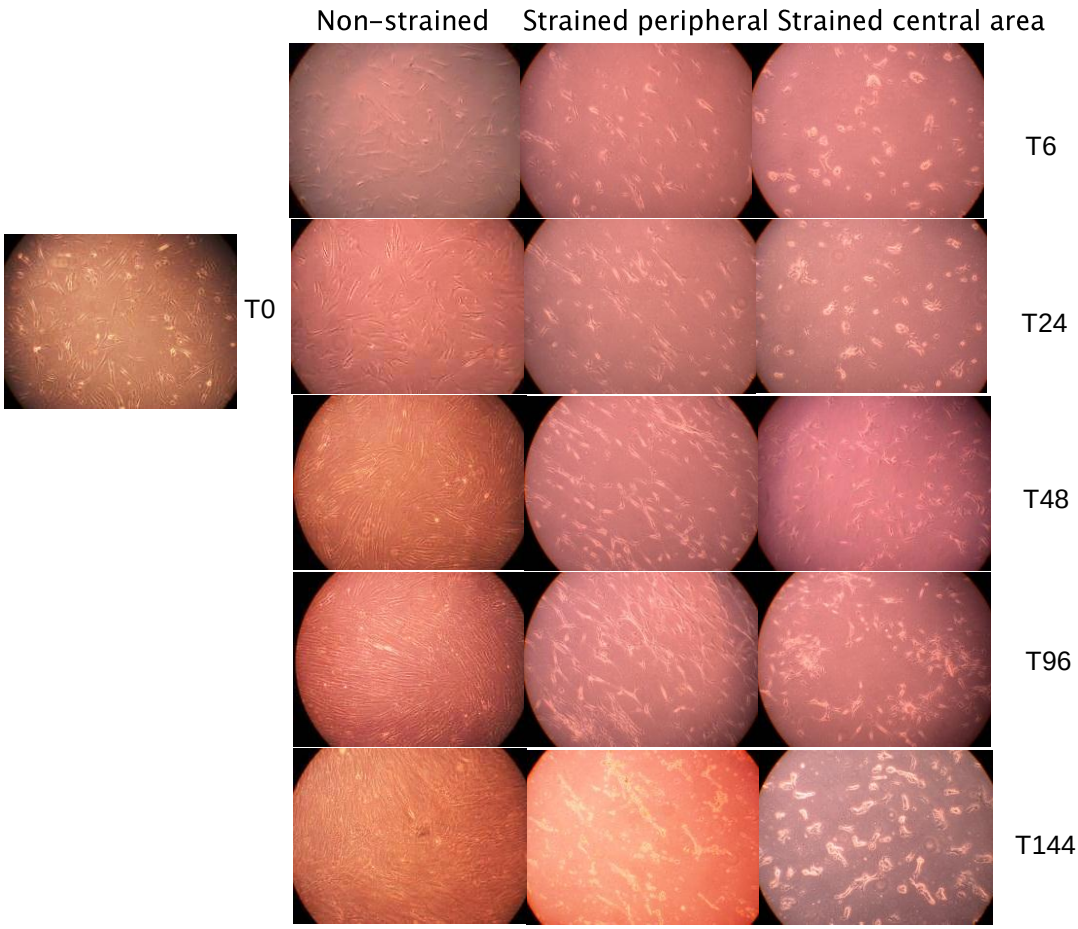

Figure 3-4: Photomicrographs of fibroblasts after exposure to mechanical strain from 6h to 144h. Fibroblasts were subjected to mechanical strain for 6h to 96 h. After exposure to mechanical strain, the cell morphology was recorded in different regions of the well. The cells were viewed by phase contrast microscopy using 10X magnification.

3.5.1.b) Dynamic changes of Collagen I and αSMA mRNA changed after mechanical strain for 6 h-144 h

To determine the optimal duration for detecting changes in gene expression, bronchial fibroblasts from one normal subject were cultured in complete DMEM containing 10% FBS and subjected to mechanical strain (30% elongation, 12 cycles per minute) from 6h to 144 h and analysed for collagen I and αSMA mRNA expression by RT-qPCR. This revealed that in the strained group, collagen I mRNA expression decreased 3 fold when compared to the non-strain group at 48 h but there was no effect at 6 h. αSMA mRNA expression also decreased around 3 fold in the strained group when compared to the non-strained group (Figure 3-5). Consequently, the further experiments were done at 48 and 96 h time points.

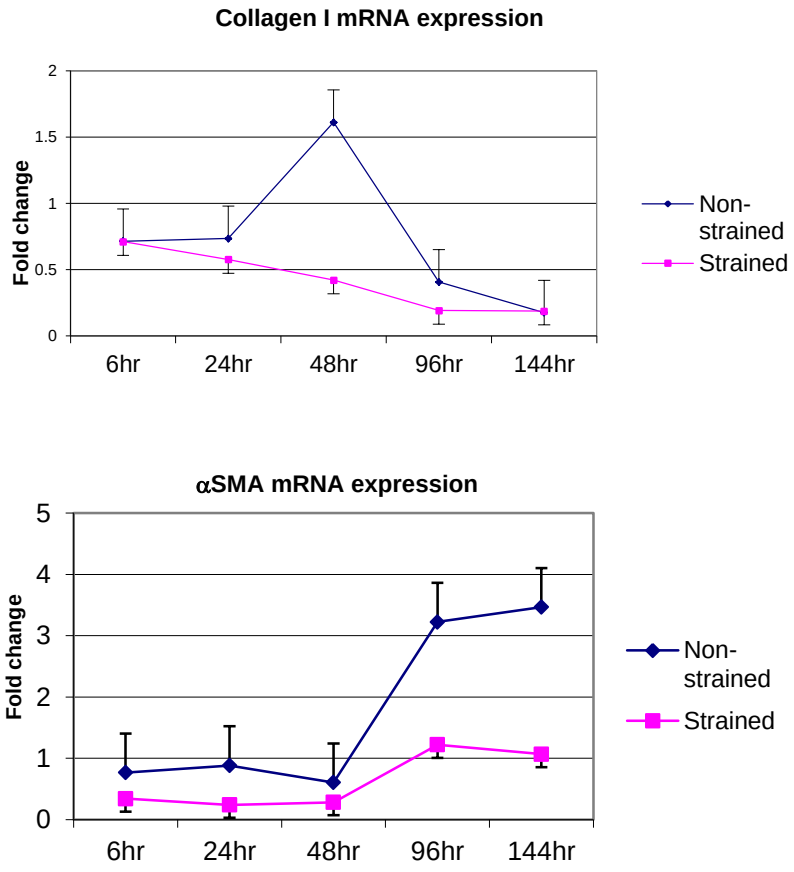

Figure 3-5: Collagen I and αSMA mRNA expression in primary bronchial fibroblasts after mechanical strain for 6 h-144 h. Bronchial fibroblasts from one normal subject were exposed to mechanical strain (30% elongation, 12 cycles per minute) from 6h to 144 h. Total RNA was extracted and analysed for collagen I and αSMA mRNA. The mRNA expression was normalized to GAPDH and expressed relative to the lowest expression of a non-strained sample at 6h using ΔΔCt method. Graphs show mean and standard error from 2 separate experiments performed in triplicate samples.

3.5.1.c) Effect of serum in culture media on gene expression

All experiments in previous sections were done in the cells cultured in DMEM containing 10% FBS. However, several studies suggested using minimal serum in the culture media to render the cells quiescent and to minimize the interference caused by serum to the cellular responses. To determine the effect of foetal bovine serum (FBS) on gene expression, bronchial fibroblasts from a normal subject (different from the subject studied in section 3.5.1b) were cultured in complete DMEM containing either 1% or 10% FBS and subjected to mechanical strain (30% elongation, 12 cycles per minute) for 48 h or 96 h. Cells were evaluated for the changes of gene expression by RT-qPCR and for the changes in cell morphology. This revealed that cells changed their morphology to become linear and elongated according to the direction of mechanical strain; this was more pronounced in 10% versus 1% FBS (Figure 3-6). There were similar trends of the changes of collagen I, collagen V, and αSMA mRNA expression (Figure 3-7) and collagen III, versican and IL-8 mRNA expression (Figure 3-8) after exposure to mechanical strain both in 10% and 1% FBS experiments. In contrast to the finding in section 3.5.1b, it was shown that collagen I mRNA expression was up-regulated after mechanical strain for 48h in medium containing 10% FBS. The discrepancy in collagen I mRNA expression may be explained by the variation in the response of primary fibroblasts obtained from different subjects thereby may affecting the reproducibility between experiments. In the pilot works, when the same fibroblasts from the same donors were studied repeatedly, the trend of the responses was similar finding. The heterogeneity of sample responses then may have affected the experimental reproducibility. Overall there was no major difference in mRNA expression between media containing 1% and 10% FBS experiments. However, from the cell morphology changes, it appeared that cells in 10% FBS responded to the mechanical strain more than 1% FBS. As a result further experiments were undertaken using culture media containing 10% FBS.

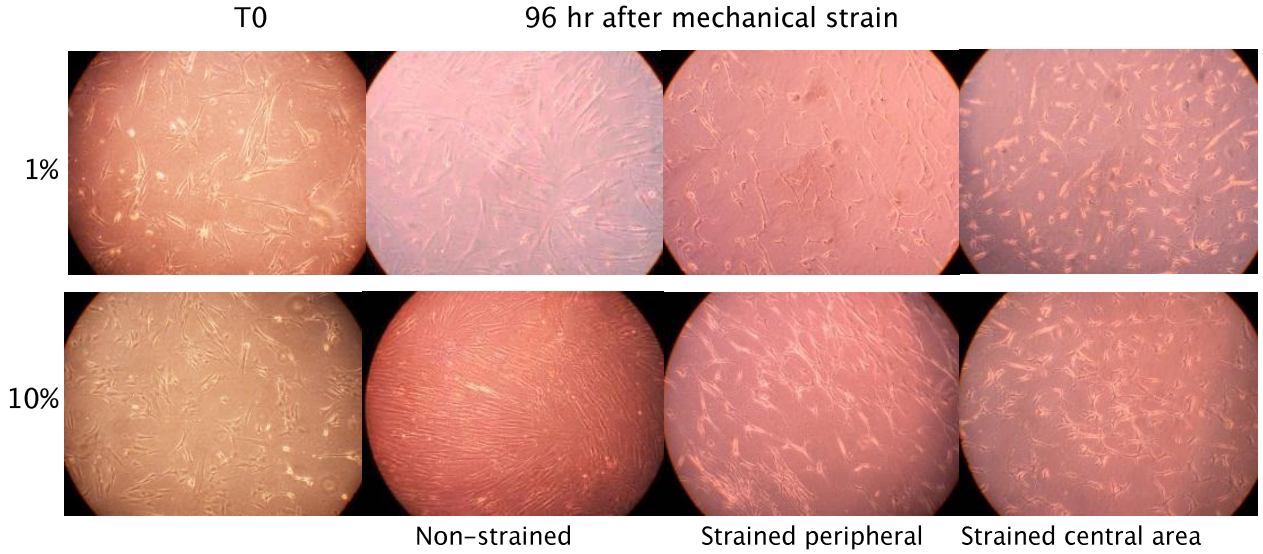

Figure 3-6: Photomicrographs of fibroblasts after exposure to mechanical strain. Bronchial fibroblasts cultured in complete DMEM containing 1% or 10% FBS were subjected to mechanical strain (30% elongation, 12 cpm) for 96 h and recorded the changes in cell morphology. The cells were viewed by phase contrast microscopy using 10X magnification.

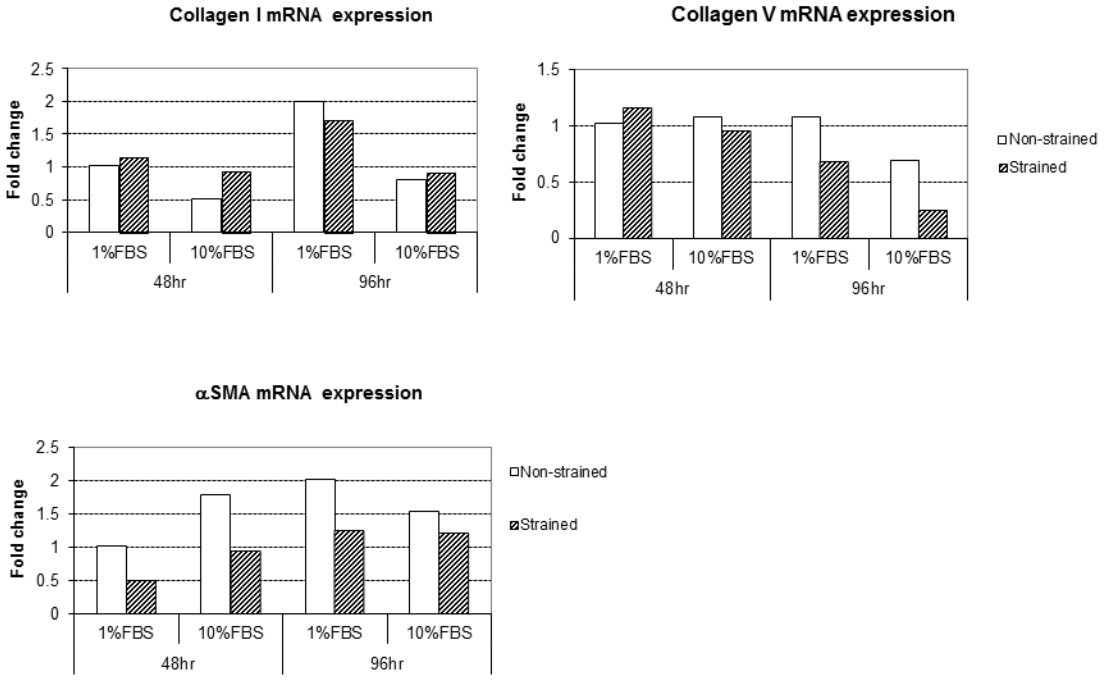

Figure 3-7: Collagen I, V and αSMA mRNA expression comparing between complete DMEM containing 1% and 10% FBS. Bronchial fibroblasts from one asthmatic subject cultured in DMEM containing 1% or 10% FBS were subjected to mechanical strain (30% elongation, 12 cpm) for 48 h or 96 h. Total RNA was extracted and evaluated for the changes of gene expression by RT-qPCR. Data were normalized to GAPDH and expressed relative to the lowest expression observed in a non-strained normal sample in 1% FBS at 48 using ΔΔCt method. Graphs represent mean of RNA change from one experiment performed in triplicate samples.

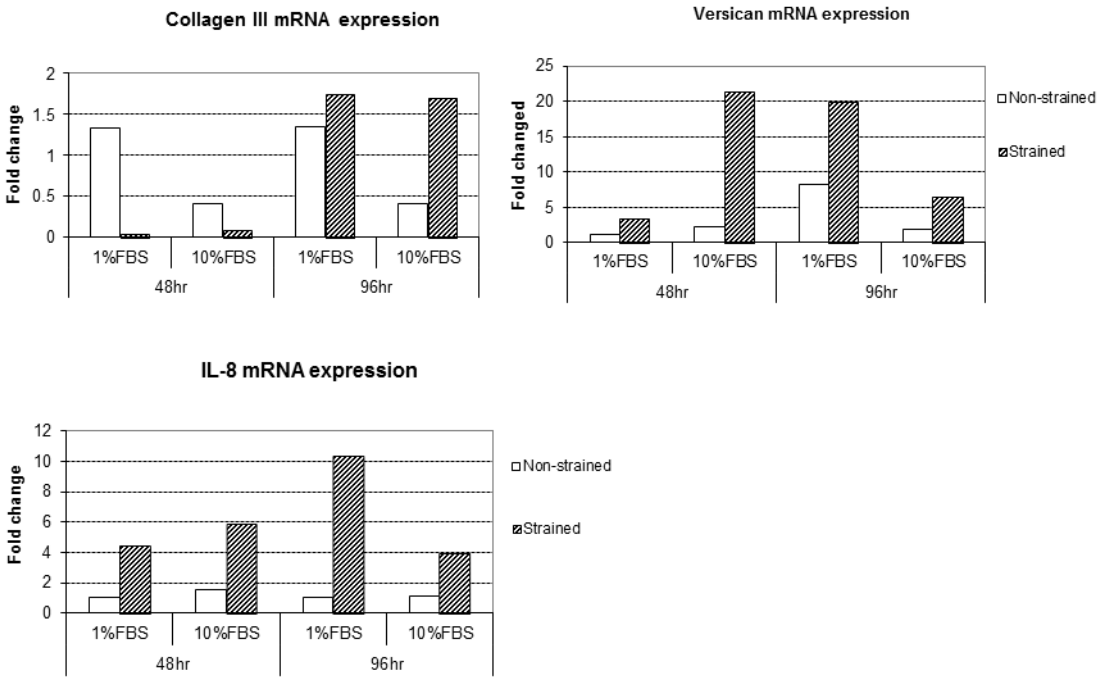

Figure 3-8: Collagen III, Versican and IL-8 mRNA expression comparing between complete DMEM containing 1% and 10% FBS. cDNA from the experiment shown in Figure 3-7 were analysed for collagen III, versican and IL8 mRNA expression using RT-qPCR. Data were normalized to GAPDH and expressed relative to the lowest expression observed in a non-strained normal sample in 1% FBS at 48h using ΔΔCt method. Graphs represent mean of RNA change from one experiment performed in triplicate samples.

3.5.1.d) Cell number after mechanical strain from 24 to 96h

To determine the effect of mechanical strain on cell number over time, bronchial fibroblasts from one normal, one severe, and one mild asthmatic subject were subjected to mechanical strain (30% elongation, 12 cycles per minute) for 24- 96 h. Cell number was determined by direct cell counting using a hemocytometer and trypan blue. There was no significant change in cell number in the strained group while cell number in the non-strained group increased significantly after 48 and 96h (Figure 3-9).

Figure 3-9: Cell number after exposure to mechanical strain. Bronchial fibroblasts from

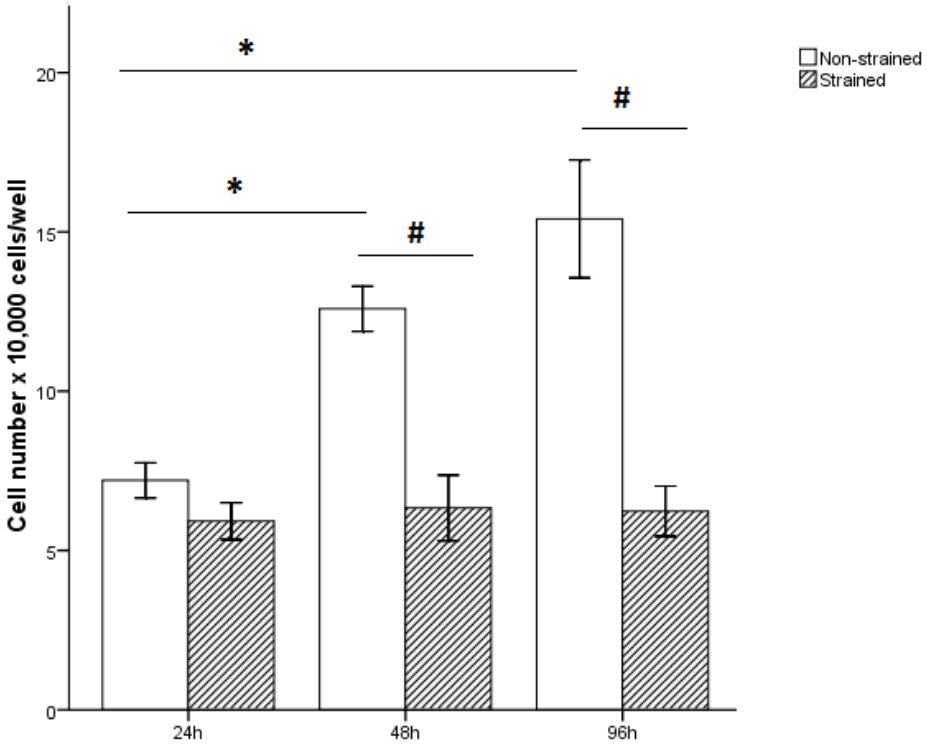

one normal, one mild, and one severe asthmatic subject were exposed to mechanical strain (30% elongation, 12 cycles per minute) for 24- 96 h. Cell number was evaluated by determination of total cell count using a hemocytometer and trypan blue. Graph represents mean and standard error from N=3. *=p <0.05 and #=p<0.01. The difference between strained and non-strained cell number was tested for statistical significance using paired-*t* test, and the difference among time points was tested for statistical significance using one way ANOVA.

3.5.1.e) Photomicrographs of fibroblasts after exposure to mechanical strain in different area of the well

In addition to assessment of cell number, the morphology of the strained cells in the experiments described in section 3.5.1.d) was investigated. After mechanical strain, the cell morphology was recorded in different regions of the well. This showed that there was a significant difference in cell morphology in the central compared with the peripheral area. A linear morphologic change and rearrangement in the orientation of the cell according to the direction of the mechanical strain was seen predominantly in the peripheral area (Figure 3-10). The similar responses were observed in fibroblasts from normal, mild and severe asthmatic subjects. This was supported by the F-actin fluorescent staining. F-actin fibres also rearranged the fibres according to the direction of mechanical forces. This finding was corresponded with a previous study where the cells at the periphery experienced the highest strain, whereas cells grown in at 0-5 mm from the centre of the well experience a little to no strain (194).

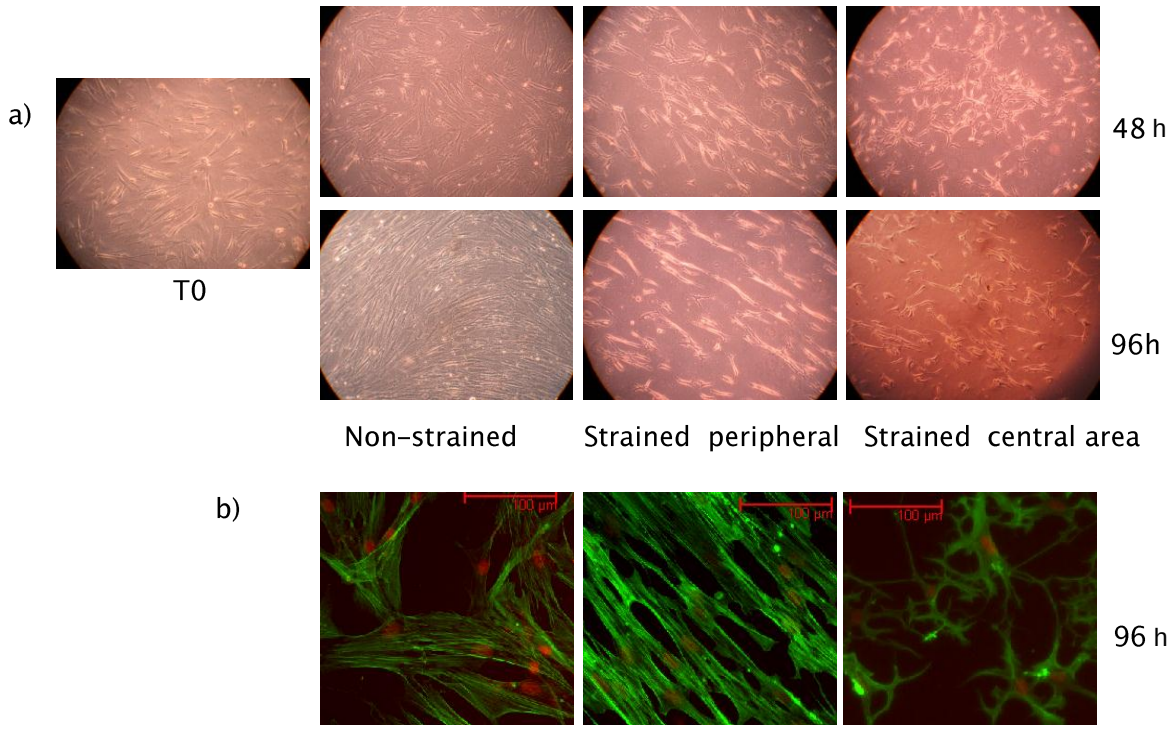

Figure 3-10: Photomicrographs of cell morphology in a) and F-actin fluorescent staining in b) after exposure to mechanical strain. Fibroblasts were subjected to mechanical strain for 48 and 96 h, after which they were fixed and stained with Alexa Flour 488®- conjugated Phalloidin for F-actin and actinomycin D stain for nuclear stain. Green channel = Alexa Flour 488 Phalloidin. Red channel = actinomycin D (nuclear stain). Cells showed in a) were viewed by phase contrast microscopy 10X magnification. Cells showed in b) were viewed by fluorescence microscopy. Scale bar = 100 µm.

3.5.2) The effect of mechanical strain on extracellular matrix mRNA expression

To assess whether asthmatic fibroblasts responded to mechanical strain differently from normal fibroblasts, fibroblasts from asthmatic subjects (n=12 [6 mild and 6 severe asthma]) and fibroblasts from normal subjects (n=6) were exposed to cyclical mechanical strain (30% elongation, 12 cycle per minute) for 48 and 96 h and evaluated for the changes of proteoglycans: versican and decorin and collagens mRNA expression by RT-qPCR. There was no significant change in versican and decorin mRNA expression after mechanical strain for 48h or 96h either in the normal or asthmatic group (Figure 3-11). However, collagen I and III mRNA expression increased significantly after mechanical strain for 48h only in the asthmatic group (Figure 3-12). The absence of significant changes in the normal group may be explained from the low statistic power. There was no significant change in collagen mRNA expression after mechanical strain for 96h. There was no significant difference in versican, decorin, and collagen mRNA expression between normal and asthmatic subject.

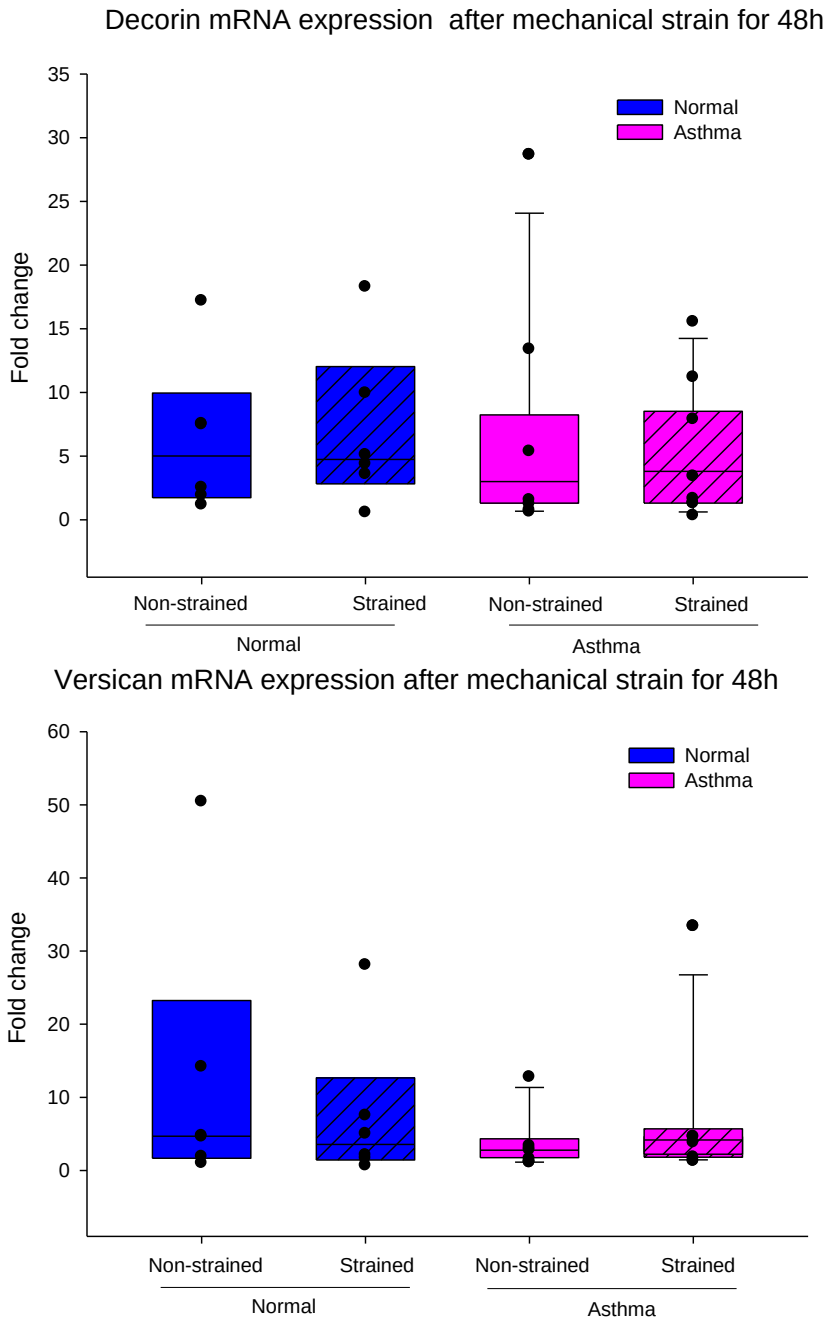

Figure 3-11: Decorin and versican mRNA expression after mechanical strain. Airway fibroblasts from normal and asthmatic subjects were exposed to mechanical strain for 48h. The cells were collected for RNA extraction. Decorin and versican mRNA expression were measured by RT-qPCR. Data were normalized to GAPDH and expressed relative to the lowest expression observed in a non-strained control from a normal subject using ΔΔCt method. The individual data points are superimposed on a box plot showing median and IQR. Blue boxes indicate normal subjects, pink boxes indicate asthmatic subjects, and hash boxes indicated cells exposed to mechanical strain. The data were tested for statistical significance using Wilcoxon's Signed Rank Test.

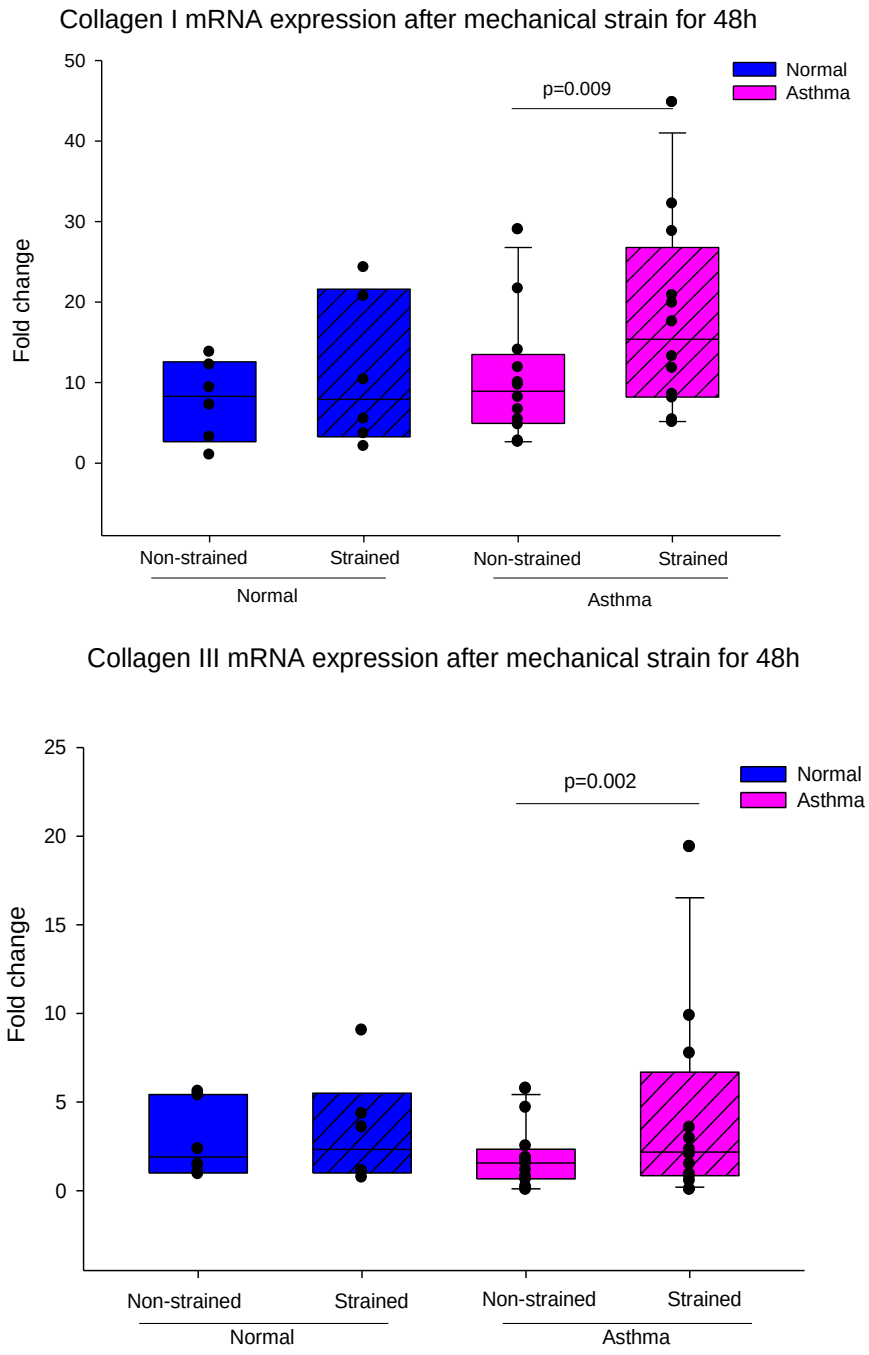

Figure 3-12: Mechanical strain up-regulated collagen mRNA expression. cDNA from experiments shown in Figure 3-11 were measured for collagen I and III mRNA expression using RT-qPCR. Data were normalized to GAPDH and expressed relative to the lowest expression observed in a non-strained control from a normal subject using ΔΔCt method. The individual data points are superimposed on a box plot showing median and IQR. Blue boxes indicate cells from normal subjects, pink boxes indicate cells from asthmatic subjects, and hash boxes indicated cells exposed to mechanical strain. The data were tested for statistical significance using Wilcoxon's Signed Rank Test.

3.5.3) **The effect of mechanical strain on soluble collagen production**

To investigate the production of soluble collagen by airway fibroblasts, culture supernatants from experiments described in section 3.5.2) after mechanical strain for 96h were measured for soluble collagen using Sircol® assay. The level of soluble collagen was demonstrated as µg per 10,000 cells. This revealed that mechanical strain enhanced the production of soluble collagen by airway fibroblasts from both normal and asthmatic subjects (Figure 3-13). There was no significant difference in the level of soluble collagen between normal and asthmatic group.

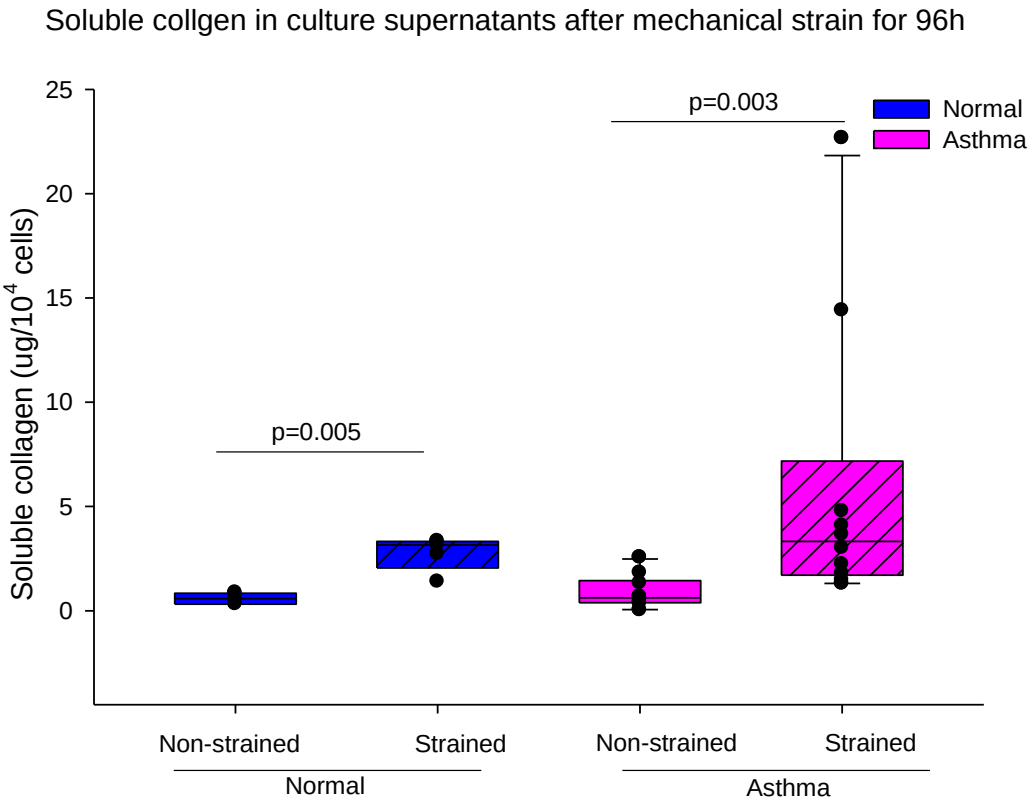

Figure 3-13: Soluble collagen in culture supernatants after mechanical strain. Culture supernatants from experiments shown in Figure 3-11 were collected at 96h and analysed for soluble collagen using Sircol® assay. The individual data points are superimposed on a box plot showing median and IQR. Blue boxes indicate cells from normal subjects, pink boxes indicate cells from asthmatic subjects, and hash boxes indicated cells exposed to mechanical strain. The data were tested for statistical significance using Wilcoxon's Signed Rank Test.

3.5.4) **Metalloproteinases (MMPs) after mechanical strain**

The balance between matrix synthesis and degradation is regulated by the interplay of matrix metalloproteinase (MMPs), and its tissue inhibitors of matrix metalloproteinase (TIMPs). An abnormal ECM turnover rate plays an essential role in airway wall thickening (59). As a result, the effect of mechanical strain on MMP2 and MMP9 were measured in culture supernatants from experiments in section 3.5.2) using gelatin zymography. As a consequence of serum supplementation in the culture media, the gelatinolytic activity in the culture media was measured as a baseline activity. Culture supernatants from fibroblasts treated with TGFβ were measured for MMP as a positive control. There was a significant increase in proMMP2 density after mechanical strain both in asthmatic and normal groups (Figure 3-14). There was no different in normalized density of proMMP2 between groups. Neither active MMP2 nor MMP9 was detected.

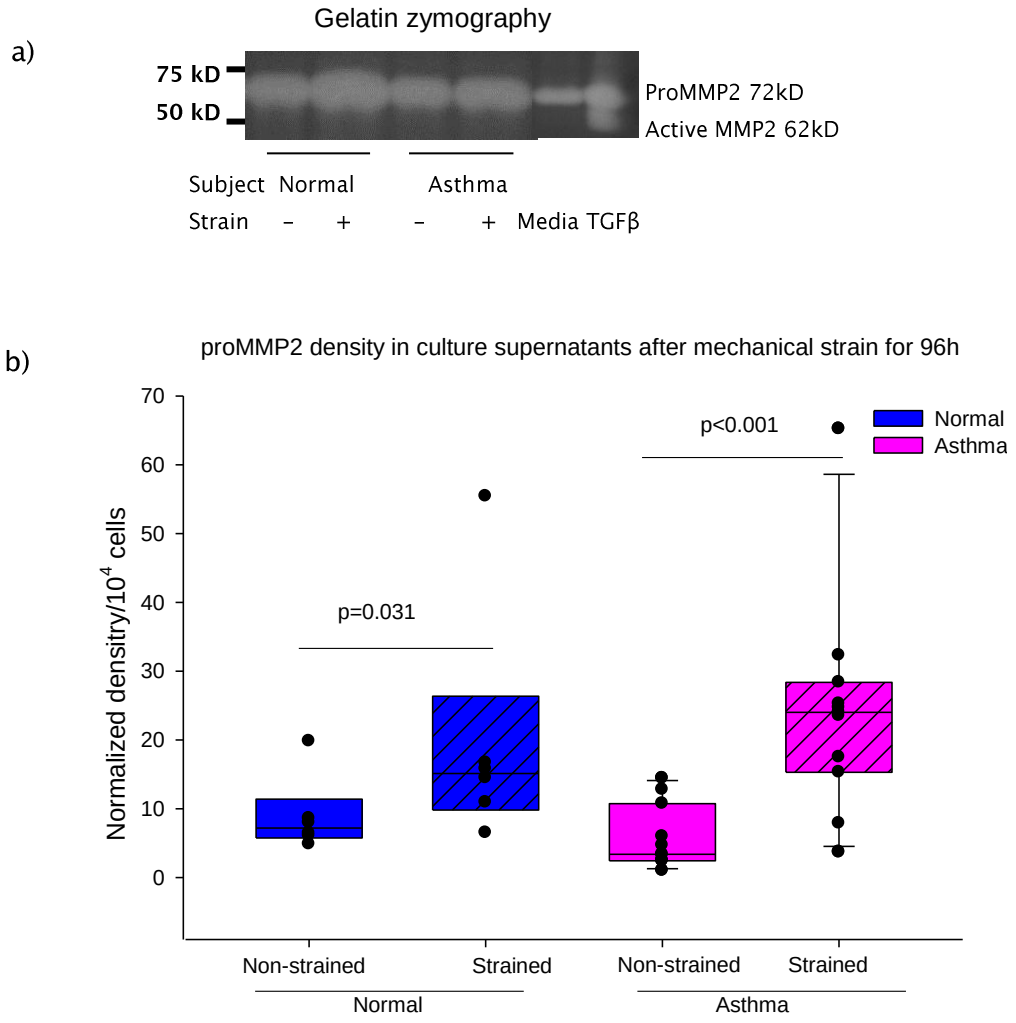

Figure 3-14: Mechanical strain induced the production of ProMMP2. ProMMP-2 secretion in the culture supernatants from experiments shown in Figure 3-11 after mechanical strain for 96 h was measured using gelatin zymography. a) Representative of MMP-2 gelatine zymograms from culture supernatants following 96 h mechanical strain and non-strained control. ProMMP-2 bands were quantified by inverted densitometry using ImageJ software b). Graph presents the density of proMMP-2. Data were normalized to the lowest density observed in a non-strained control sample per 10,000 cells. The individual data points are superimposed on a box plot showing median and IQR. Blue boxes indicate samples from normal subjects, pink boxes indicate samples from asthmatic subjects, and hash boxes indicated cells exposed to mechanical strain. The data were tested for statistical significance using Wilcoxon's Signed Rank Test.

3.5.5) αSMA expression in response to mechanical strain

As an increase in collagen production was observed after mechanical strain, the next question was to determine whether the cells responded to mechanical strain by becoming myofibroblasts. To assess myofibroblast differentiation, αSMA expression was measured in cDNA from experiments described in section 3.5.2). Surprisingly, it was revealed that there was a significant suppression in αSMA mRNA expression after exposure to mechanical strain for 48h in all groups (Figure 3-15a). A similar result was seen after mechanical strain for 96h. There was no significant difference in αSMA mRNA expression between normal and asthmatic group. However, when αSMA protein in cell lysates after mechanical strain for 96h was measured using western blot analysis, there was no difference in the normalized density for αSMA between the strained and non-strained groups (Figure 3-15b). On account of the inequality of the mechanical forces that the cells are exposed in different areas of the well, immunofluorescent staining for αSMA was also undertaken to allow assessment the cells in the central and peripheral area of the well. This revealed that strained cells had less αSMA fibres than non-strained cells. However, the strained cells were stained and imaged in a resting membrane after being stretched. This may explain the increase in the fluorescent signal in some area of strained cells. There was no difference in αSMA staining between strained cells in peripheral and central area of the well (Figure 3-16).

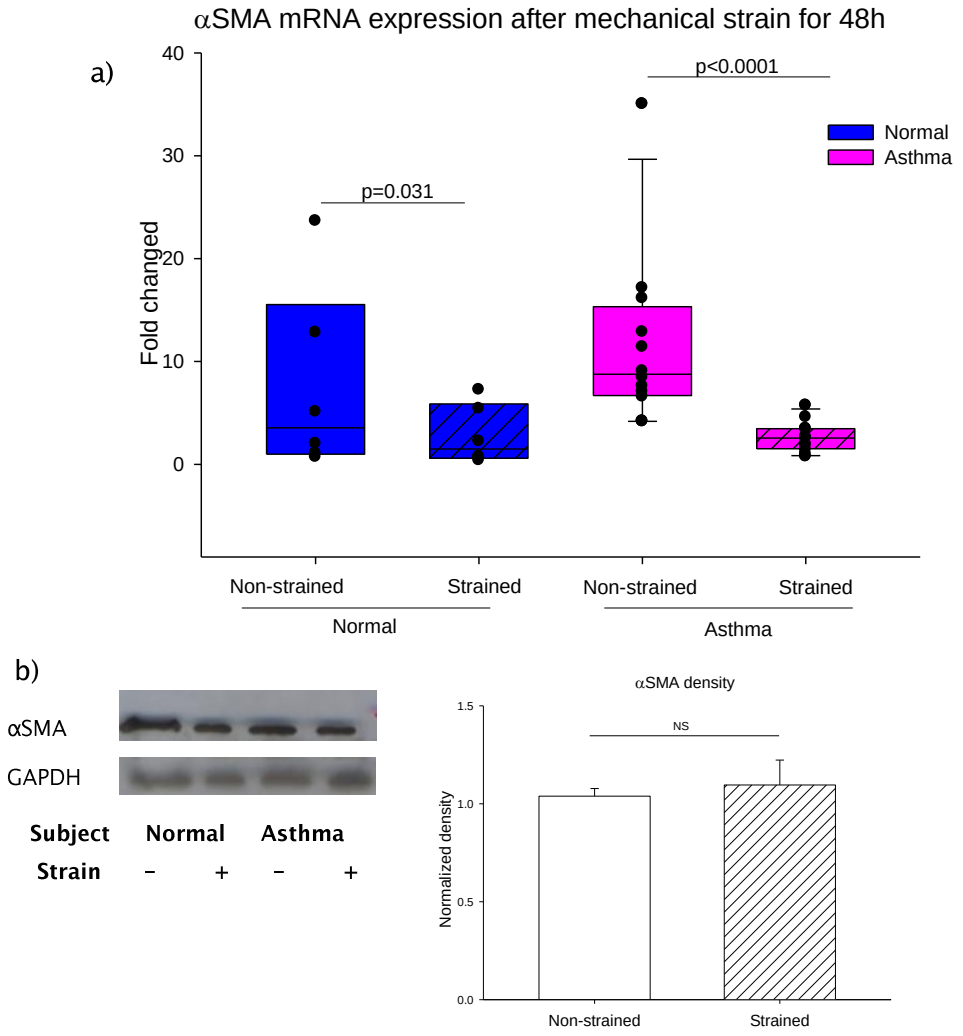

Figure 3-15: Mechanical strain suppressed αSMA expression. In a) cDNA from experiments shown in Figure 3-11 were measured for αSMA mRNA expression using RT-qPCR. Data were normalized to GAPDH and expressed relative to the lowest expression observed in a non-strained control from a normal subject using ΔΔCt method. The individual data points are superimposed on a box plot showing median and IQR. Blue boxes indicate cells from normal subjects, pink boxes indicate cells from asthmatic subjects, and hash boxes indicated cells exposed to mechanical strain. The data were tested for statistical significance using Wilcoxon's Signed Rank Test. In b) airway fibroblasts from one normal, one mild asthmatic, and severe asthmatic subjects were exposed to mechanical strain for 96h. Cell lysates after mechanical strain were analysed by SDS-PAGE and western blotting using αSMA antibody and GAPDH antibody. Protein bands were quantified by densitometry using ImageJ software and the ratio of αSMA to GAPDH was obtained. Graph represents mean and standard error of normalized density of αSMA. The data were tested for statistical significance using a paired *t*-test

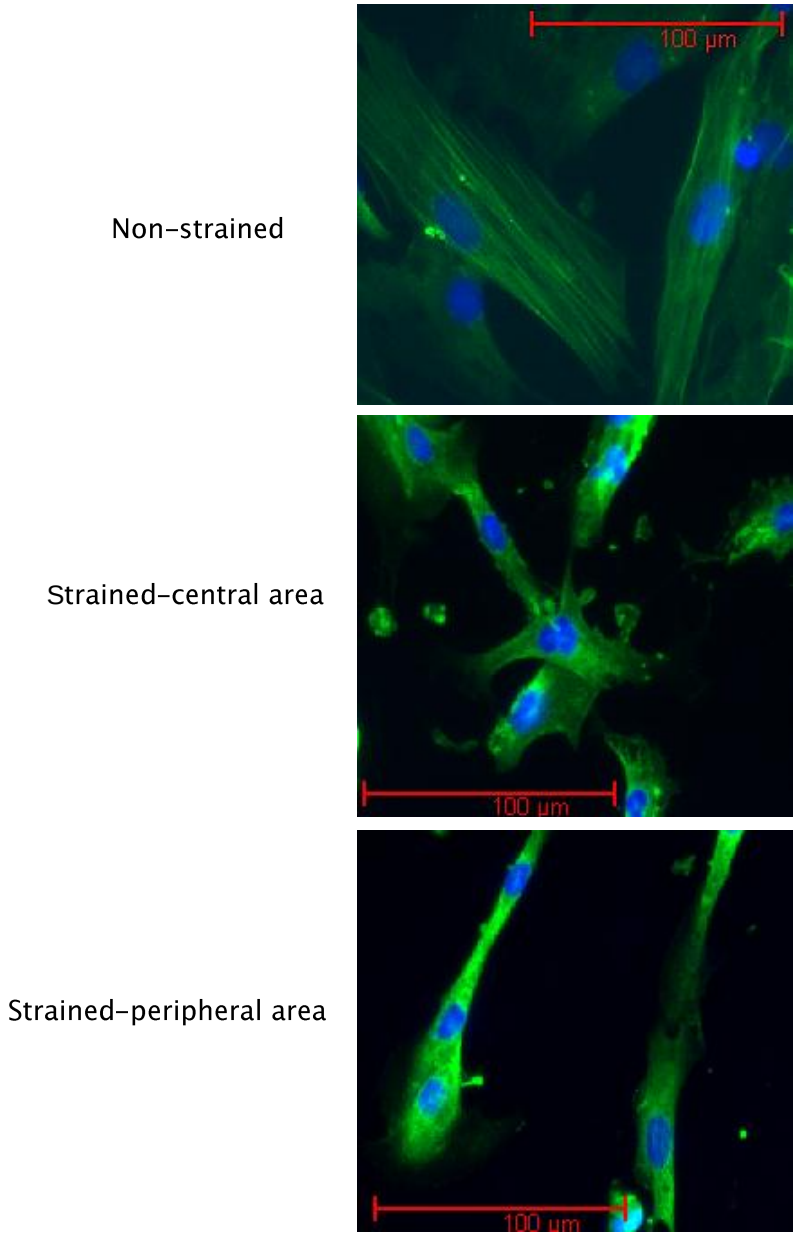

Figure 3-16: αSMA immunofluorescent staining in fibroblasts after mechanical strain. Cells were seeded on 6 well collagen coated silastic membrane plates and subjected to mechanical strain for 48h. The cells then were fixed and stained with αSMA and nuclear staining. αSMA staining in green (GFP channel), nuclear staining (Hoechest stain) in blue (DAPI channel). Scale bar =100µm.

3.5.6) Mediators released from airway fibroblasts in response to mechanical strain

3.5.6.a) The level of TGFβ1 in culture supernatants after mechanical strain

TGFβ is a potent profibrotic mediator and TGFβ has been shown to stimulate procollagen production by airway fibroblasts (195). To investigate the response of airway fibroblasts on mechanical strain on TGFβ production, culture supernatants from experiments in section 3.5.2) after mechanical strain for 96h were measured for the level of TGFβ1 using TGFβ1 Emax® immune assay system. As the supplementation of 10% FBS was used in the experiments and it was previously shown that serum contains substantial amount of latent TGFβ, active TGFβ1 in culture supernatants was evaluated and the level of active TGFβ1 in culture medium containing 10% FBS was measured as a baseline value. From a total of 18 paired (non-strained and strained) samples, it was only possible to detect active TGFβ1 in 8 of these paired (non-strained and strained) samples (3 from normal, 2 from mild asthmatic, and 3 from severe asthmatic subjects). Based on data from these 8 paired samples, it was found that mechanical strain enhanced the production of TGFβ1 by airway fibroblasts (Figure 3-17). Failure to detect active TGFβ1 in the remaining samples may reflect the insensitive of the TGFβ1 assay used in the present work or there may have been binding of TGFβ1 to the ECM preventing its detection.

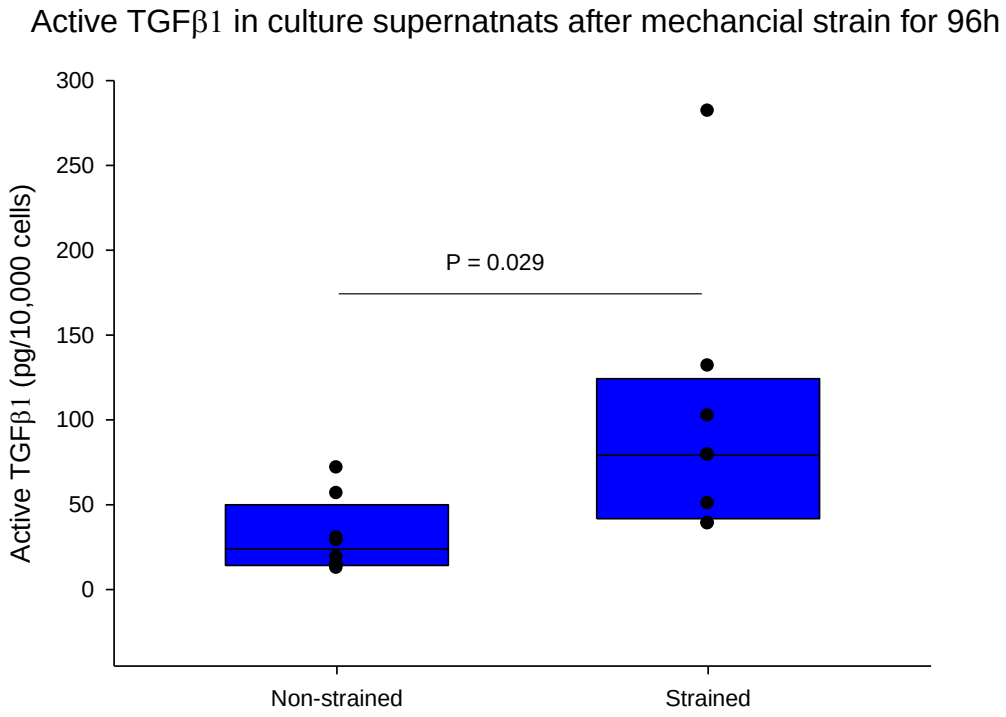

Figure 3-17: Mechanical strain enhanced the production of TGFβ1. Culture supernatants from experiments shown in Figure 3-11 were measured for TGFβ1 using ImmunoAssay system. The individual data points are superimposed on a box plot showing median and IQR. The data were tested for statistical significance using a Wilcoxon's Signed Rank.

3.5.6.b) IL-8 mRNA and protein after mechanical strain

Apart from eosinophilic inflammation, neutrophilic inflammation has also been suggested to play an important role in asthma pathogenesis especially in severe asthma. It has been shown that sputum levels of IL-8, a potent neutrophilic chemoattractance, are higher in severe asthmatic patients than non-severe asthmatic patients (38). As a consequence, the effect of mechanical strain on IL-8 production by airway fibroblasts was investigated. cDNA and culture supernatants samples from experiments described in section 3.5.2) were measured for IL-8 mRNA expression using RT-qPCR and IL-8 protein released into culture supernatants was measured using ELISA. It was shown that IL-8 mRNA expression and IL-8 level in culture supernatants were significantly higher in the strained group as compared to the non-strained group both in asthmatic and normal subjects (Figure 3-18). Comparing between groups, there was no significant difference in IL-8 mRNA expression or protein level between normal and asthmatic subjects.

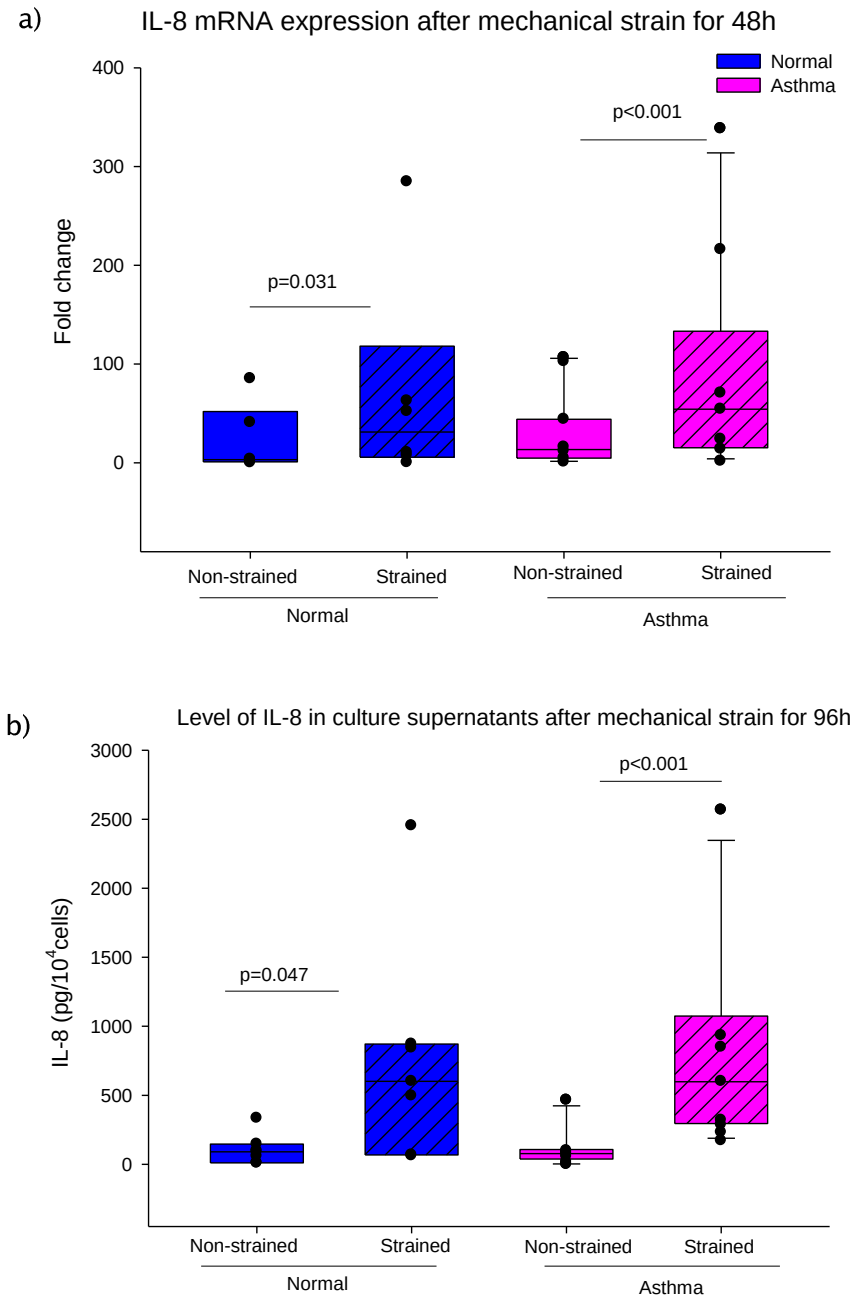

Figure 3-18: Mechanical strain induced IL-8 mRNA and protein expression. cDNA from experiments shown in Figure 3-11 were measured for IL-8 mRNA expression using RT-qPCR as shown in a). Data were normalized to GAPDH and expressed relative to the lowest expression observed in a non-strained control from a normal subject using ΔΔCt method. In b) culture supernatants from the same experiments were analysed for the level of IL-8. The individual data points are superimposed on a box plot showing median and IQR. Blue boxes indicate samples from normal subjects, pink boxes indicate samples from asthmatic subjects, and hash boxes indicated samples exposed to mechanical strain. The data were tested for statistical significance using Wilcoxon's Signed Rank.

3.6) Discussion

Summary of findings

- Mechanical strain up-regulated collagen mRNA expression in fibroblasts from asthmatic subjects but enhanced the production of soluble collagen by airway fibroblasts from both normal and asthmatic subjects.
- ProMMP2 production by airway fibroblasts was increased by mechanical strain.
- Mechanical strain to airway fibroblasts enhanced the production of active TGFβ1 in a proportion of cultures tested.
- Mechanical strain to airway fibroblasts did not promote myofibroblast differentiation.
- Mechanical strain promoted IL-8 production of airway fibroblasts both in mRNA and protein level.
- Mechanical strain suppressed airway fibroblasts proliferation.
- Airway fibroblasts from healthy non-asthmatic and asthmatic subjects responded to mechanical stimulation in the same pattern

The deposition of extracellular matrix protein beneath the basement membrane (BM), in the reticular BM (RBM) of the airway wall, is one of the hallmarks of airway remodelling in asthma. The BM of normal airways is composed of laminin and collagen IV. In contrast, collagen I, collagen III and proteoglycans are the main components of abnormal RBM in asthmatic airways (59). It has been shown that fibroblasts sense mechanical strain via the integrin adhesion receptors which connect the cytoskeleton stress fibres to the ECM such as collagen and laminin in the asthmatic and normal airways, respectively (196). Royce et al have shown that ECM composition has an effect on fibroblasts proliferation and morphology (197). Breen et al have also found that the environment also influence how airway fibroblasts responded to mechanical strain (177). The mechanical strain was found to up-regulate procollagen type I mRNA in fibroblasts cultured on laminin- and elastin-coated membrane but not when cultured on fibronectin-coated membrane (177). These studies highlight the importance of fibroblast-matrix interaction in response to mechanical strain. In the work presented here, airway fibroblasts were cultured on collagen type I coated membrane to reproduce a component of the ECM environment within the asthmatic airways. To investigate the involvement of mechanical strain in ECM generation the fibroblasts were exposed to mechanical strain, which represent the mechanical strain occurring to the airway during deep inspiration (175). As collagen synthesis and degradation is a dynamic process, matrix metalloproteinase (MMPs) play a prominent role for the net ECM composition in the airways, in addition to that of fibroblast collagen synthesis.

MMP-2 and MMP-9 have been shown to associate with lung injury (115). MMP-2 (72 kDa gelatinase or gelatinase A) is secreted by structural cells (fibroblasts, endothelial and epithelial cells), while MMP-9 (92 kDa gelatinase or gelatinase B) is secreted mainly by inflammatory cells (neutrophils, monocyte-microphages) but MMP-9 can be released by structural cells under stimulation (198). MMP-2 and MMP-9 play a vital role in degrading type IV collagen which is the main component of basement membrane. The present study demonstrated that cyclical mechanical strain to airway fibroblasts enhanced the remodelling process by increasing the production of collagen and proMMP-2 but not MMP-9 nor active MMP-2. ProMMP-2 is inactive and needs to be activated by MMPs such as membrane bound membrane type-1 MMP (MT1-MMP) when secreted into the extracellular environment. Compressive stress to epithelial cells or epithelial cell co-cultured with fibroblasts has been shown to increase the production of MMP-2 and MMP-9 (122;165). Similar results were reported in experiments employing a three dimensional lateral compressive strain study of epithelial cells and fibroblasts (172). These findings suggest that epithelial cells have a role in activating proMMP-2. This may explain why active MMP-2 was not detected in the present study. Alternatively the level of active MMP-2 may have been too low to be able to detect by gelatin zymography. However, the activity of MMP-2 is also regulated by its inhibitors, tissue inhibitor of metalloproteinase-2 (TIMP-2). TIMP-2 can also promote an effective activation of proMMP-2 by formation of a ternary complex with MT1-MMP at cell surface. However, an excess of TIMP-2 inhibited proMMP-2 activation (114). A recent study has demonstrated that mechanical stimulation to foetal mouse lung fibroblasts promotes the secretion of active MMP-2 which is associated with a decreased level of the MMP-2 inhibitor (TIMP-2) in concentrated culture supernatants. This resulted in an increase in MMP-2 activity (199). Consequently, to determine the net effect of MMP on collagen, the level of its inhibitor should also be considered.

The present study also demonstrated a significant increase in collagen production both in asthmatic and normal fibroblasts in response to cyclical mechanical strain. In addition, it was also found that in some cases mechanical strain enhanced the production of active TGFβ1 by airway fibroblasts. Whether this is a general phenomenon requires further investigation, perhaps using more sensitive ELISA or assessing matrix bound matrix bound TGFβ using nonradioactive quantitative bioassay based on the capacity of TGFβ to induce plasminogen activator inhibitor-1 (PAI-1) expression (200). In conjunction with an increase TGFβ1 produced by airway fibroblasts after mechanical strain, it can postulated that mechanical strain stimulated airway fibroblasts to produce more collagen via this increase in TGFβ1. Since TGFβ has been shown to stimulate procollagen production by airway fibroblasts (195). Such a consideration is consistent with a previous study in rat cardiac fibroblasts, which has demonstrated the inhibitory effect of a pan-specific TGFβ neutralizing antibody on the

induction of collagen I gene expression (201). To prove this postulation, a specific TGFβ1 neutralizing antibody should be added to the mechanical stimulation and the change in collagen production is measured.

Choe et al has shown that three dimensional lateral compressive stress to epithelial co-culture with fibroblasts promotes myofibroblasts differentiation (172). In contrast, the present work has found that cyclical mechanical strain of fibroblasts, cultured in monolayer, did not enhance αSMA expression, a marker of myofibroblast differentiation. This was evident even when there was an increase in TGFβ1 production. TGFβ is known to promote the transformation of fibroblasts to myofibroblasts (92). This result is consistent with a recent study which has revealed the suppressive effect of mechanical strain on TGFβ1 up-regulation of αSMA expression in airway fibroblasts (202). The different finding from other studies may be accounted for by the different type of mechanical loading: cyclical mechanical strain vs lateral compressive stress. Potentially as, epithelial cells can release of TGFβ after injury (43;44), this may overcome the suppressive effect of myofibroblast transformation induced by mechanical strain. In addition, in the present work, it was possible to detect TGFβ in the culture supernatants in 8 samples from 18 samples after exposure to mechanical strain. This suggests that the stimulation signal from mechanical strain may not be potent enough to enhance the production of TGFβ in airway fibroblasts from all subjects or the level is too low to be detected with conventional ELISA. Since the myofibroblast differentiation could not be demonstrated in the present work, the increase in collagen mRNA expression and increase in collagen protein may reflect fibroblast activation per se rather than myofibroblast transformation. It has been proposed that mechanical forces activate fibroblasts towards a fibrogenic phenotype which increase in proliferation, ECM synthesis, and protease activities (203). This suggests that in the present study, the fibroblasts have a synthetic rather than proinflammatory phenotype.

In the present study, mechanical strain also has been demonstrated to have a potential to promote neutrophilic airway inflammation by increased production of IL-8 which is a potent neutrophil chemoattractant. Neutrophilic airway inflammation plays a prominent role in asthma pathogenesis especially in severe refractory asthma and exercise induced asthma (35). The number of neutrophils in the airway lavage from severe asthmatic patients has been reported to be higher than normal (33). Although several chemokines such as IL-8 (CXCL-8), ENA-78 (CXCL-5) and GRO-α (CXCL-1) have been demonstrated to contribute to airway neutrophilia in asthmatic patients (204), a recent study has demonstrated that only sputum IL-8, but not ENA-78 or GRO-α is increased in sputum of severe asthma with neutrophilia (205). IL-8 may be a better airway neutrophils chemoattractant. Thus these in vitro findings demonstrate

that mechanical strain increases fibroblasts derived IL-8 generation. This may imply that mechanical strain could enhance the neutrophilic airway inflammation in asthma.

In the current study, there were no differences in the responses of fibroblasts from normal and asthmatic subjects to mechanical strain. This suggests that these responses were normal features of fibroblast response to mechanical strain, independent of disease status. It was suggested that an increase in collagen deposition in asthmatic airways would increase airway stiffness which in turn prevents the airways narrowing during airway smooth muscle contraction (45;193). This suggests that even fibroblast respond to mechanical stimuli independent of disease status, and that the impact on the airways may depend on the underlying disease status. Apart from enhancing the production of collagen, previous studies have shown that mechanical strain to airway fibroblasts has a role in promoting proteoglycan mRNA production both in normal and asthmatic subjects, as demonstrated by previous studies (175;176). In addition, a recent *in vivo* study has shown an increase in subepithelial collagen in asthmatic airway following bronchoconstriction without increase in airway inflammation (206). Patients with chronic cough without asthma were also shown to have a thicker subepithelial basement membrane than healthy control subjects (207). As a result, mechanical forces to the airways may play a crucial role in airway wall remodelling in asthma.

In the current study, it was demonstrated that mechanical strain altered fibroblasts' morphology and alignment. This was confirmed by rearrangement in F-actin stress fibres of fibroblasts that were exposed to mechanical strain. A recent study has suggested that such an alteration in fibroblasts morphology is directly related to the degree of actin polymerization (208). In contrast to the effect on morphology, the present study has found that mechanical strain prevented an increase in cell number which was observed in the non-strained group after 48-96 h. Thus mechanical strain appears to drive the development of a synthetic phenotype which involves loss of their proliferation potential. Nishimura et al. have demonstrated that the decrease in cell number by mechanical strain was due to the decrease in DNA synthesis, as measured by 5-bromo-2'-deoxyuridine (BrdU) staining. Cell apoptosis did not increase with mechanical strain, as assessed by terminal deoxynucleotidyl transferase-mediated sUTP nick-end labelling staining (TUNEL) (209). This suggests that mechanical strain has a growth inhibitory effect rather than a pro-apoptotic effect on fibroblasts. Consequently, the lower cell number in the strain group should have a minimal effect on the results as the results were corrected per cells exposed to mechanical strain.

Taken together, this chapter had demonstrated that mechanical strain to airway fibroblasts enhances both profibrotic and inflammatory response by enhancing the production of collagen and IL-8. This suggests a role for mechanical strain in promoting airway inflammation and airway remodelling as summarised in Figure 3-19. If these increased collagens have been cross-linked, stiff collagen will be deposited in the airways. As a result, collagen cross-linking enzyme produced by airway fibroblasts was investigated in the next chapter.

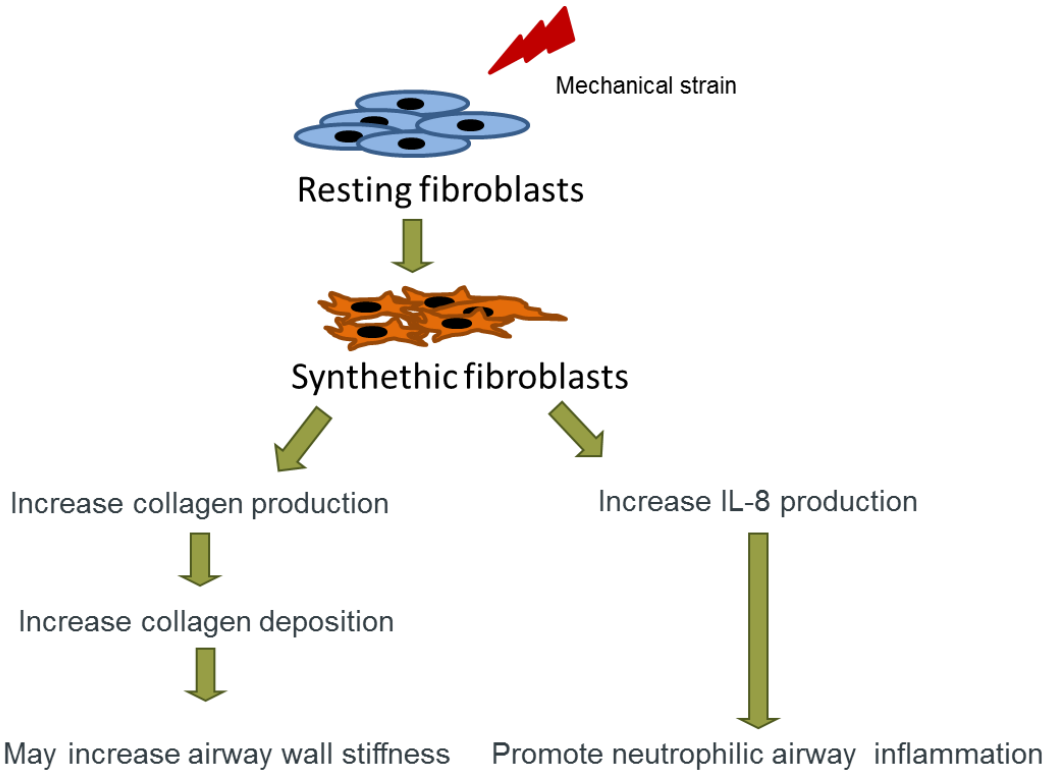

Figure 3-19: Schematic diagram of mechanical strain induced the synthetic phenotype fibroblasts that response in producing collagen and IL-8.

Chapter 4: TGFβ and Collagen Cross-linking Enzymes

4.1) Rationale

Subepithelial thickening involving collagen deposition and alterations in the extracellular matrix (ECM) components such as collagen, proteoglycan and glycoprotein are characteristic features of airway remodelling in asthma (46). Among these ECM components, collagen is the most abundant and influential ECM in the airway wall. It has been shown that the thickened subepithelial layer in asthmatic airway consists of a dense layer of fibrillar collagens, which are collagen I, III and V, but not the basement membrane collagen (collagen IV) (56). Collagen synthesis is complex, involving several intracellular and extracellular steps. Collagen is synthesized within the cells as a non-hydroxylated, non-triple helix structure. During the intracellular modification the first collagen triple helix structure "procollagen" is excreted to the extracellular space. Subsequently, procollagen processing occurs shortly after secretion followed by the assembly of fibrils. Finally, fibrils are stabilized by the formation of covalent cross-links (210). The strength and stability of collagen depends on this final step of collagen covalent cross-linking process which is initiated by lysyl oxidase (LOX) (Figure 4-1). Furthermore, the nature of the collagen cross-linking depends on the extent of hydroxylation of telopeptide lysine by lysyl hydroxylase2 (LH2) (211) (Figure 4-2). An increase in collagen cross-linking via the hydroxylysine pathway has been demonstrated to be a fibrotic phenomenon (127). Furthermore, small leucine-rich proteoglycans (SLRPs) such as decorin and biglycan were shown to have a role in collagen fibril assembly (151).

From chapter 3, it was demonstrated that mechanical strain enhanced the production of collagen by airway fibroblasts. TGFβ is one of the most potent profibrotic mediators characterized to date and plays an essential role in tissue fibrosis and structural remodelling. It has been demonstrated to up-regulate collagen gene expression both *in vivo* (85) and in *vitro* (212). It has also been shown to enhance the production and decrease the degradation of collagen secreted by rat fibroblasts (195). There are three TGFβ isoform identified in mammals: TGFβ1-3. Previous studies have shown increased TGFβ1 and TGFβ2 expression in asthmatic airways (80-82;213). TGFβ1 and TGFβ2 have been shown to equally regulate airway collagen deposition in an animal model (214). TGFβ2 will be used to stimulate airway fibroblasts in this chapter as human bronchial epithelial cells have been shown to predominantly release TGFβ2 (44).

As collagen strength depends on the amount of covalent cross-linking initiated by lysyl oxidase (LOX), this chapter has investigated the impact of TGFβ2 on the airway fibroblasts synthesis of lysyl oxidase (LOX) and lysyl hydroxylase2b (LH2b). Changes in, the small leucine-rich proteoglycans (SLRPs), decorin and biglycan have also been evaluated as it has been shown that they have a role in collagen fibril assembly. Furthermore, the effect of mechanical strain to airway fibroblasts in producing LOX and LH2b was studied.

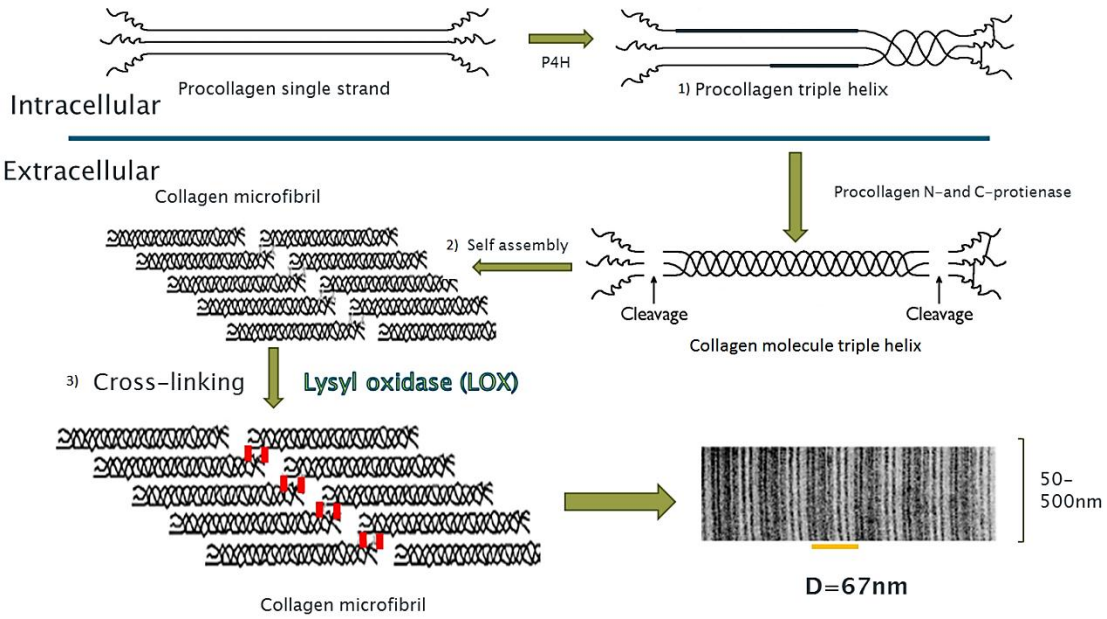

Figure 4-1: Collagen biosynthesis. Collagen is synthesized within the cells as a non-hydroxylated, non-triple helix structure. 1) During the intracellular modification the first collagen triple helix structure "procollagen" is excreted to the extracellular space. 2) Procollagen processing occurs shortly after secretion followed by the assembly of fibrils.3) Fibrils are stabilized by the formation of covalent cross-links. Collagen cross-linking gives rise the strength and stability for collagen. This figure was modified from Shoulders, MD et al Annu. Rev.Biochem.2009.78:929-58.

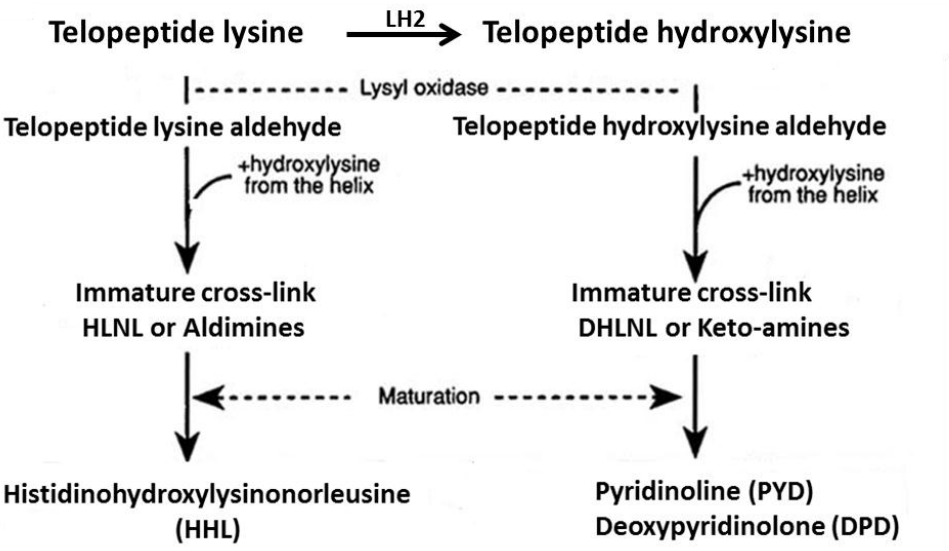

Figure 4-2: The collagen cross-linking pathway. Lysyl hydroxylase2 (LH2) hydroxylates telopeptide lysine to become telopeptide hydroxylysine. The subsequent cross-linking depends on the state of hydroxylation of telopeptide lysine (137).

4.2) Hypothesis

That TGFβ2 regulates airway fibroblasts in their production of collagen cross-linking enzymes.

4.3) Aims

- To investigate the effect of TGFβ2 on lysyl oxidase (LOX) mRNA expression and protein produced by airway fibroblasts.
- To investigate the effect of TGFβ2 on lysyl hydroxylase2b mRNA produced by airway fibroblasts.
- To investigate the effect of TGFβ2 on decorin and biglycan mRNA produced by airway fibroblasts.
- To investigate whether airway fibroblasts from asthmatic subjects respond to TGFβ differently from airway fibroblasts from healthy non-asthmatic subjects in these outcomes measured.
- To investigate the effect of mechanical strain on the generation of collagen cross-linking enzymes from airway fibroblasts.
- To investigate the level of collagen cross-linking enzymes in BAL fluid from healthy non-asthmatic and asthmatic subjects.

4.4) Methods

4.4.1) TGBβ2 stimulation of cultured fibroblasts

Airway fibroblasts from healthy non-asthmatic and asthmatic volunteers were seeded at a density of 100,000 cells/well in 12 well plates and incubated at 37˚C in the presence of 5% CO_2 until fully confluent. The cells were then treated with TGFβ2 (1 or 10ng/ml) in serum free or 0.4% (v/v) FBS in DMEM supplemented with 50 IU/ml penicillin, 50 mg/ml streptomycin, 2 mM L-glutamine, 1 mM Sodium pyruvate and 1 mM nonessential amino acids (NEAA) for 6h to 96h.

4.4.2) Subject characteristics

Airway fibroblasts from 6 healthy non-asthmatic and 6 asthmatic subjects were used to study the effect of TGFβ2 on the regulation of LOX expression. There was no statistical difference in age between non-asthmatic and asthmatic subjects. Asthmatic subjects, all of whom were on inhaled corticosteroids, had a significantly lower FEV_1 (%predicted) than healthy non-asthmatic subjects ($p < 0.01$). There was no significant difference in age between healthy and asthmatic subjects, but there was more female in asthmatic group than healthy group (Table 4-1).

Table 4-1: Characteristics of subjects who provided bronchial fibroblasts for the studies of the effect of TGFβ in the regulation of LOX expression

Disease	No.	Age (yrs)	Sex (F:M)	FEV_1 (%predicted)	Inhaled steroid (µg/day BDP equivalent)	Prednisolone (mg/day)
Healthy	6	38 (20-64)	2:4	111 (89.8-134)	0	0
Asthma	6	50 (28-67)	4:2	58.5* (19.8-101)	1720 (1000-4000)	5 (0-15)

Data are shown as mean with range in brackets. FEV_1= forced expiratory volume in 1 second. BDP= Beclomethasone Dipropionate. * $p < 0.01$.

Airway fibroblasts from 7 healthy non-asthmatic and 15 asthmatic subjects were used to study the effect of mechanical strain on the regulation of LOX expression. There was no statistical difference in age between healthy non-asthmatic and asthmatic subjects but there was more female in asthmatic group than healthy group. The asthmatic subjects had a significantly lower FEV_1 (% predicted) than healthy non-asthmatic subjects (Table 4-2).

Table 4-2: Subjects characteristics studied on mechanical strain in the regulation of LOX expression

Disease	No.	Age (yrs)	Sex (F:M)	FEV_1 (%predicted)	Inhaled steroid (µg/day BUD equivalent)	Prednisolone (mg/day)
Healthy	7	38 (20-64)	2:5	108.2 (89.8-133.8)	0	0
Asthma	15	41 (17-69)	9:6	80.6* (19.8-131)	1800 (0-4000)	5 (0-20)

Data shown as mean with range in brackets. FEV_1= forced expiratory volume in 1 second. BDP= Beclomethasone Dipropionate. * $p < 0.05$.

4.5) Results

4.5.1) Initial experiments

Initial experiments were undertaken using airway fibroblasts from one healthy non-asthmatic and one asthmatic donor to optimize the conditions for the further experiments. Since a previous study has shown that serum in the medium can alter the response of fibroblasts to cytokine stimulation (215), fibroblasts were treated with TGFβ2 at 1 or 10 ng/ml in serum free complete DMEM or complete DMEM containing 0.4% FBS for 6h to 96h.

4.5.1.a) The optimal duration for TGFβ2 stimulation

To find the optimal duration for TGFβ2 stimulation, airway fibroblasts from one healthy non-asthmatic and one asthmatic subject were treated with TGFβ2 (10 ng/ml) in serum free complete DMEM or complete DMEM containing 0.4% FBS for 6h to 96h. Total RNA was extracted and LOX mRNA expression was measured by RT-qPCR. LOX protein secreted by airway fibroblasts in the cell culture supernatants was concentrated using Strataclean® resin and analysed by SDS-PAGE and immunoblotted using anti lysyl oxidase (LOX) antibodies as detailed in section 2.4.14).

These analyses revealed that TGFβ2 up-regulated LOX mRNA expression by 24h and this was sustained for up to 96h above baseline (Figure 4-3). There did not appear to be a difference in the time-response behaviour between fibroblasts from either the healthy non-asthmatic or the asthmatic donor. Consistent with previous findings, serum in the media had an additive effect on LOX mRNA expression. Similar results were seen in protein expression. Thus both TGFβ2 and serum enhanced the production of the pro-LOX (50 kDa) but the effect of serum was less than the effect of TGFβ2. TGFβ2 enhanced the production of the active LOX (30 kDa) with the maximum effect being seen after 96hr treatment (Figure 4-4). However, after 96h treatment, the cells started to detach (Figure 4-5). As a result, it was not possible to evaluate changes beyond this time point. Serum alone also induced an activation of LOX, although this was much less than the effect of TGFβ2 alone. In combination, serum and TGFβ2 promoted an activation of LOX at an earlier time point, with the 30 kDa form being evident by 24h. As a result, further experiments were done at 24h for LOX mRNA and 48h for LOX protein measurement, so ensuring that cell viability was well maintained. In addition to the expected band at 50 and 30 kDa, bands at 37 kDa and 25 kDa were also recognized by the anti-LOX antibody. As a result further experiment was done to test the specificity of antibody.

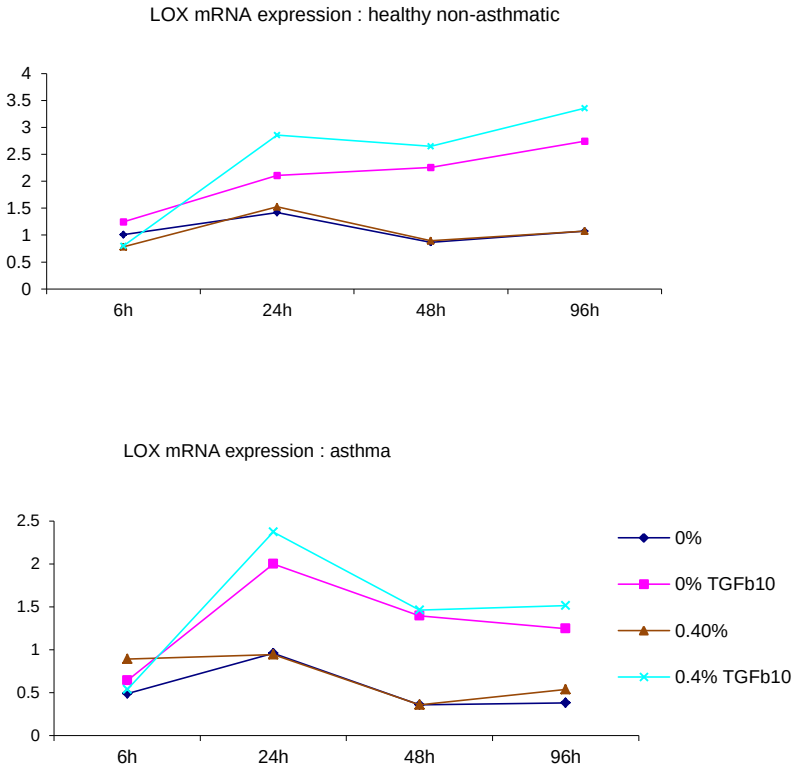

Figure 4-3: LOX mRNA expression in fibroblasts after treatment with TGFβ2. Airway fibroblasts from one healthy non-asthmatic and one asthmatic subject were treated with TGFβ2 (10ng/ml) for 6h-96h. Total RNA was extracted and analysed for LOX mRNA. The values were normalized to the geometric mean of UBC/A2 and expressed relative to the lowest expression observed in an untreated sample from a non-asthmatic subject at 6h. Graphs represent mean value of triplicate wells of fibroblasts from one subject. Blue line represents untreated samples in serum free medium, pink line represents TGFβ2 10ng/ml treated samples in serum free medium, yellow line represents untreated samples in medium containing 0.4% FBS, and green line represents TGFβ2 10ng/ml treated samples in medium containing 0.4% FBS.

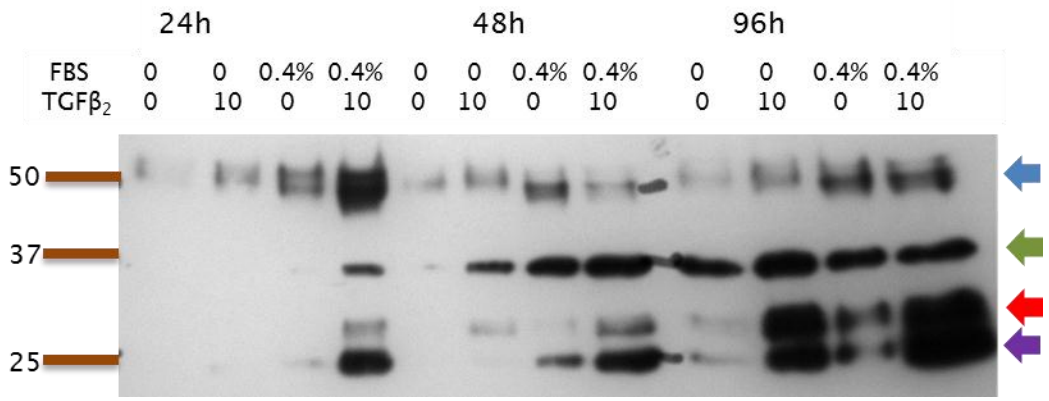

Figure 4-4: LOX protein western blots from culture supernatants of airway fibroblasts treated with TGFβ2 (10ng/ml) for 24h-96h in serum free DMEM medium or DMEM containing 0.4%FBS. Culture supernatants from experiments shown in Figure 4-3 were concentrated using Strataclean® resin and analysed by SDS-PAGE and immunoblotted using anti lysyl oxidase (LOX) antibodies. The blue arrow indicates Pro-LOX (50 kDa), the red arrow indicates active LOX (30 kDa), whereas the green and purple arrows indicate band at 37 kDa and at 25 kDa whose relation to LOX was the focus of more detailed analysis.

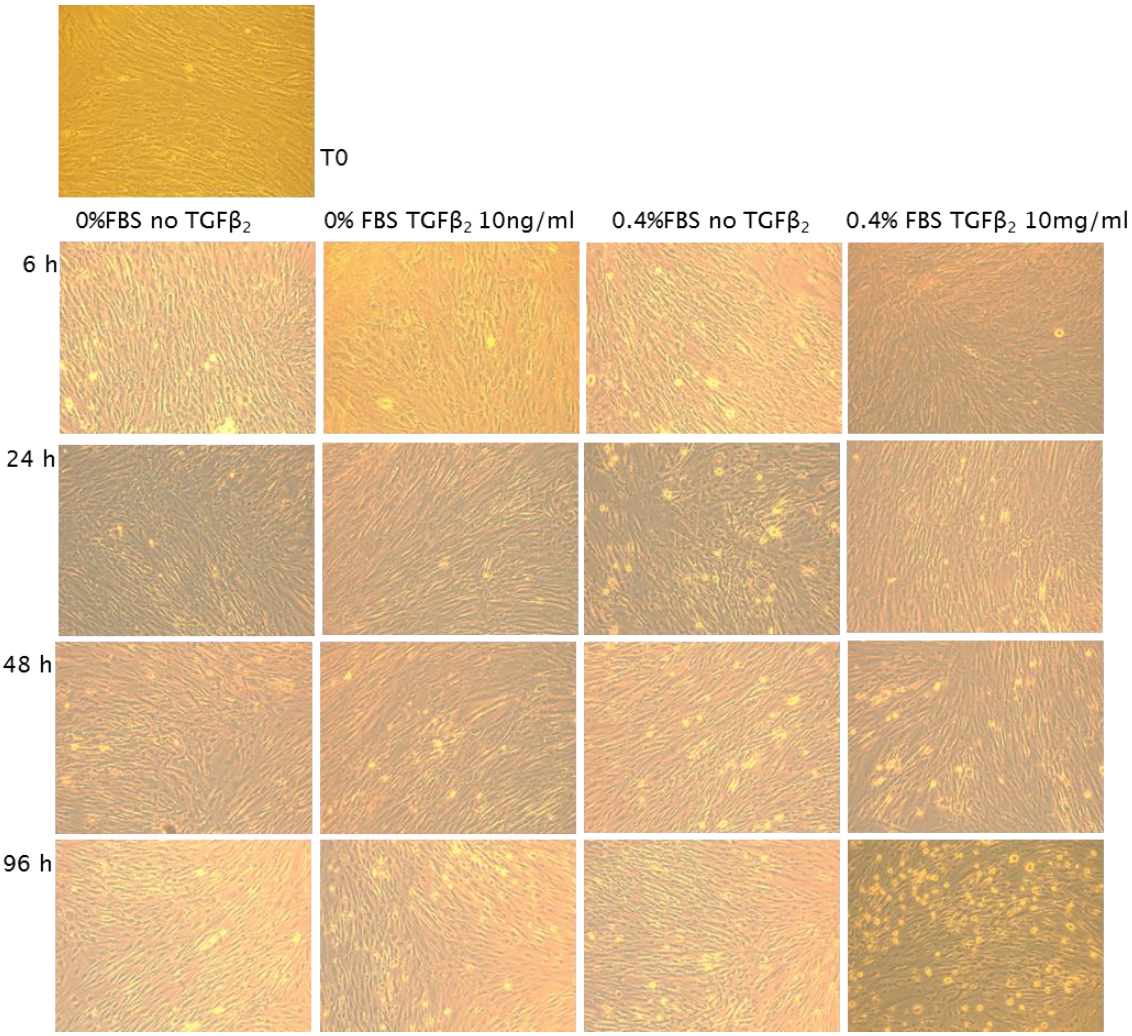

Figure 4-5: Photomicrograph of airway fibroblasts after treatment with TGFβ2 for 6h to 96h. Airway fibroblasts were treated without or with (TGFβ2 10ng/ml) in serum free or 0.4% FBS complete DMEM for 6h-96h as indicated. The cells were viewed by phase contrast light microscopy with the magnification X20.

4.5.1.b) The specificity of anti lysyl oxidase antibody

As indicated in section 4.5.1.a), western blot analysis of LOX protein in the culture supernatants showed the bands at 50 kDa (Pro-LOX) and 30 kDa (active LOX). There were also bands at 37 kDa and 25 kDa which did not correspond to any reported LOX protein isoform. To test the specificity of the antibody, control experiments were performed. Culture supernatants from one fibroblasts sample, after treatment with TGFβ2 (10 ng/ml) for 48h, were concentrated with Strataclean® resin and analysed by SDS-PAGE. After transfer, the membrane was cut into 4 pieces. The first two pieces were incubated with LOX antibody and then incubated with anti-rabbit HRP secondary antibody from two different companies. The third piece was incubated with rabbit IgG as a control for the primary antibody, at the same concentration used for LOX antibody, and then incubated with the anti-rabbit HRP secondary antibody. The last piece was incubated with the milk buffer used for diluting the primary antibody, and then the blot was incubated with anti-rabbit HRP secondary antibody. The 37 kDa band and 25 kDa band were present in the membranes that were incubated with LOX antibody and buffer of the anti-rabbit secondary antibodies. However, these bands were not detected in either the blot that was incubated with rabbit-IgG and anti-rabbit HRP secondary antibody or the blot that incubated with secondary antibody alone (Figure 4-6). After processing of 50 kDa Pro-LOX in the extracellular environment, the non-glycosylated 30 kDa catalytically active LOX and 18 kDa propeptide LOX are produced. The propeptide LOX is suggested to have a role in cancer suppression (216). Recent studies have reported bands at 35 kDa and 25 kDa as a glycosylated propeptide LOX (216;217). Therefore, the 37 kDa and 25 kDa band in the present work appear to be a glycosylated propeptide LOX that is secreted by airway fibroblasts during the process of TGFβ stimulation. However, these forms were not detected in supernatants from all fibroblasts. However, these forms were not detected in supernatants from all fibroblasts (Figure 4-7).

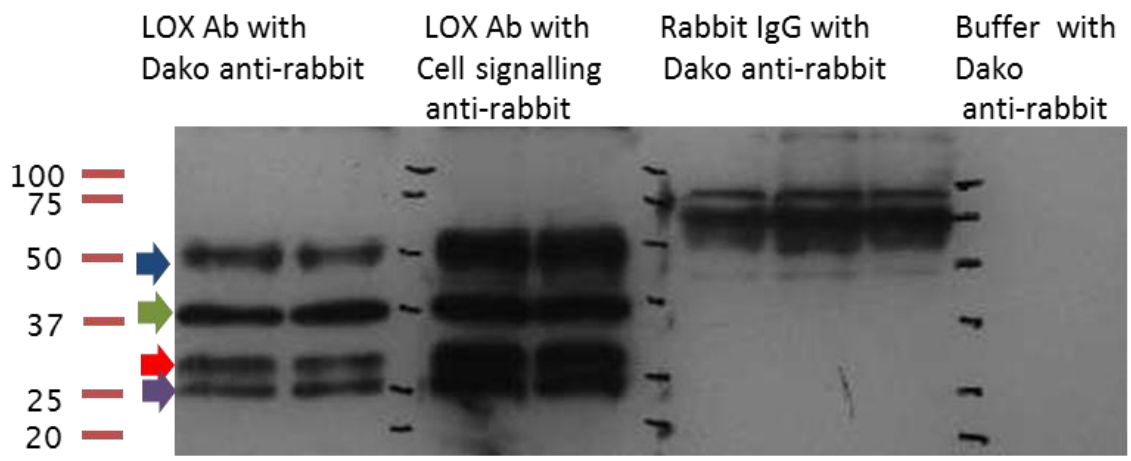

Figure 4-6: LOX antibody specificity. Fibroblasts were treated with TGFβ2 (10 ng/ml) for 48h and the culture supernatants were harvested and concentrated with Strataclean® resin for LOX western blot. After transfer, the membrane was cut into 4 parts. They were then incubated with 1) LOX Ab and Dako anti-rabbit Ab, 2) LOX Ab and Cell signalling ant-rabbit Ab, 3) Rabbit IgG and Dako anti-rabbit Ab and 4) Milk buffer and Dako anti-rabbit. The figure shows LOX western blot. The blue arrow indicates Pro-Lox (50 kDa), the red arrow indicates active LOX (30 kDa), the green arrow indicates 37 kDa protein band, and the purple arrow indicates 25 kDa protein band.

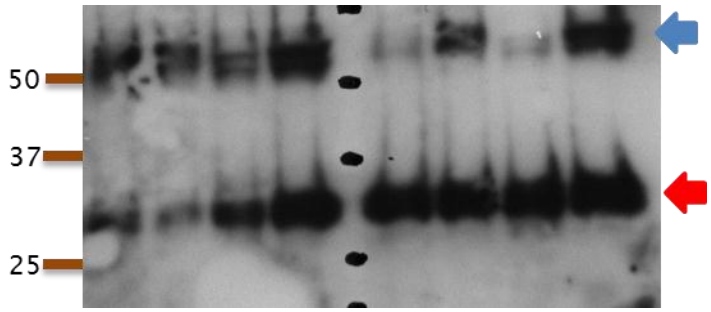

Figure 4-7: Representative western blots of Pro-LOX and active LOX. Fibroblasts from a different subject from Figure 4-6 were treated with TGFβ2 (10 ng/ml) for 48h and the culture supernatants were harvested and concentrated with Strataclean® resin for LOX western blot analysis. The figure shows LOX western blot. The blue arrow indicates Pro-Lox (50 kDa) and the red arrow indicates active LOX (30 kDa).

4.5.1.c) TGFβ2 up-regulated LOX mRNA in airway fibroblasts in a dose-dependent manner

To investigate the optimum dose of TGFβ2, airway fibroblasts were treated with TGFβ2 at 1ng/ml or 10 ng/ml for 24h. Total RNA was extracted and measured for LOX mRNA expression. This revealed that TGFβ2 up-regulated LOX mRNA in a dose-dependent manner both in serum free and 0.4% FBS complete DMEM (Figure 4-8).

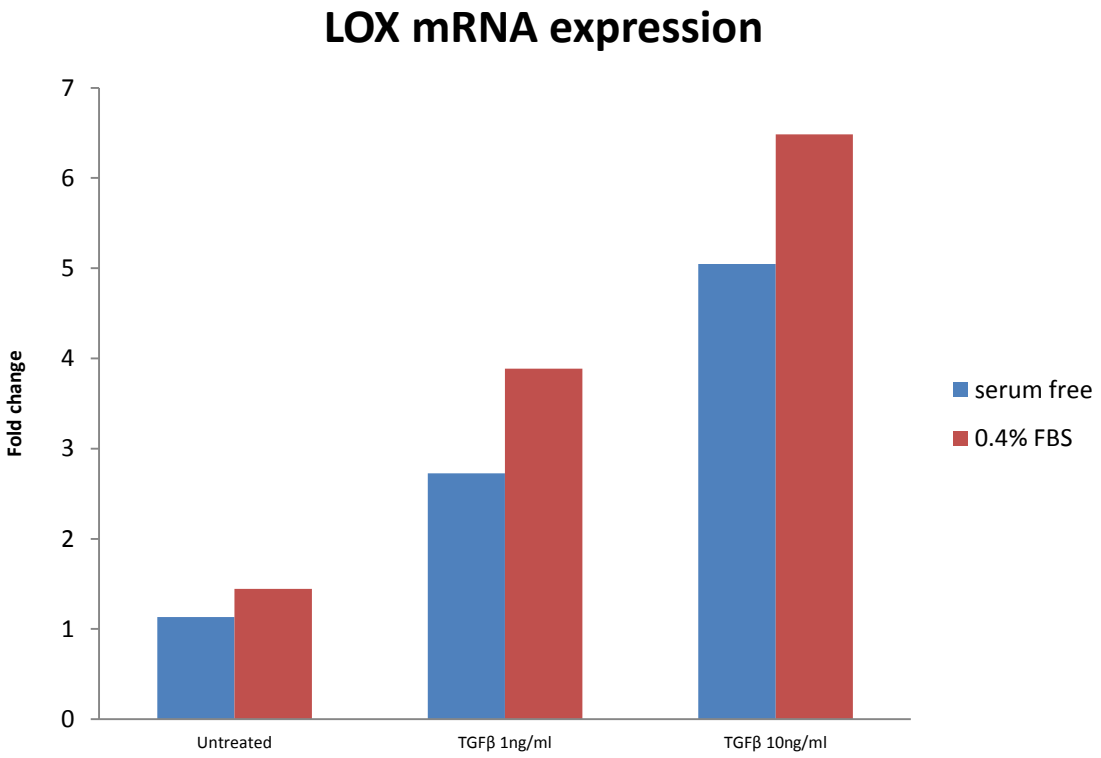

Figure 4-8: TGFβ2 up-regulated LOX mRNA expression. Airway fibroblasts were treated with TGFβ2 at 1 ng/ml or 10ng/ml in serum free or 0.4%FBS complete DMEM for 24h. Total RNA was extracted and analysed for LOX mRNA. The value was normalized to the geometric mean of UBC/A2 and relative to the expression observed in a serum free untreated sample. Graph shows the mean value of duplicate samples from one experiment.

4.5.2) **TGFβ2 stimulated airway fibroblasts to produce pro-and active LOX protein in a dose dependent manner**

To determine LOX protein secretion by airway fibroblasts following stimulation with TGFβ2 for 48h, culture supernatants were concentrated using Strataclean® and assessed for pro- and active LOX using western blotting. TGFβ2 stimulated airway fibroblasts to produce the 50-kDa proenzyme, the catalytically active enzyme 30 kDa which is consistent with LOX mRNA expression. TGFβ2 enhanced the production of LOX protein in a dose dependent manner both in serum free and 0.4% FBS media, the maximum effect was seen at 10 ng/ml in complete DMEM containing 0.4% FBS (Figure 4-9). Consequently further experiments were done with TGFβ2 at 10ng/ml.

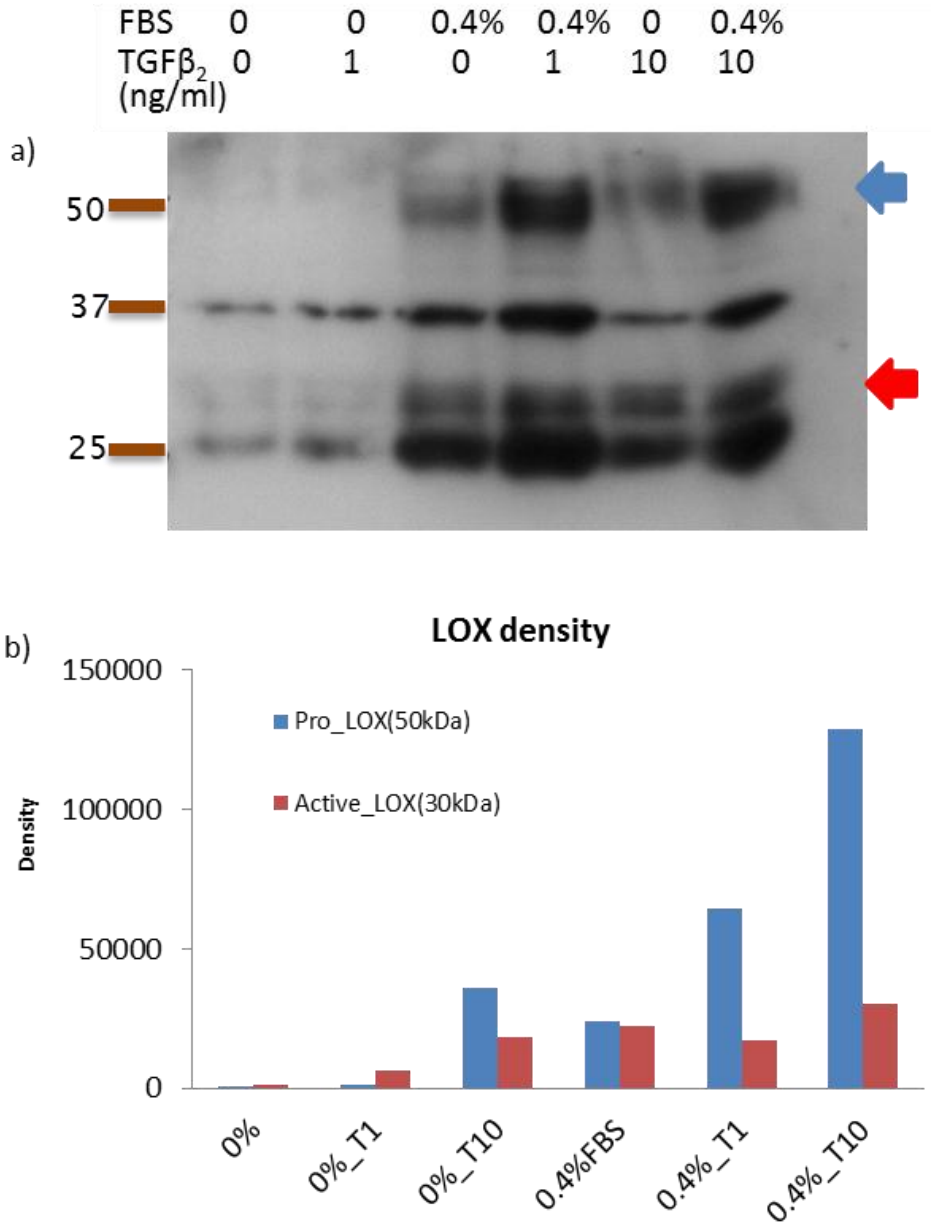

Figure 4-9: TGFβ2 enhanced the production of LOX protein. Airway fibroblasts were treated with TGFβ2 1ng/ml or 10ng/ml in serum free or 0.4%FBS DMEM for 48h. Culture supernatants were concentrated with Strataclean® resin and analysed by SDS-PAGE and immunoblotted using anti lysyl oxidase (LOX) antibodies. a) The figure shows western blot of LOX protein; blue arrow indicates Pro-LOX and red arrow indicates active LOX. In b) the protein bands of Pro-LOX and active LOX were quantified by densitometry using ImageJ. Graph shows the mean value of three densitometry measurements of one experiment. Blue bars demonstrate the density of Pro-LOX and red bars demonstrate the density of active-LOX.

4.5.3) TGFβ2 up-regulated LOX and LH2b mRNA expression in fibroblasts from healthy non-asthmatic and asthmatic airways

To investigate whether airway fibroblasts from healthy non-asthmatic and asthmatic subjects respond differently to TGFβ2, fibroblasts from 6 healthy non-asthmatic and 6 severe asthmatic subjects were treated with TGFβ2 for 24-48h and analysed for LOX and LH2b expression by RT-qPCR. This showed that TGFβ2 significantly up-regulated LOX (Figure 4-10) and LH2b mRNA expression (Figure 4-11) both in fibroblasts from healthy non-asthmatic and asthmatic subjects. This effect also maintained after 48h treatment. There was no significant difference in LOX and LH2b mRNA expression between serum free and 0.4% FBS media experiments. Comparing between healthy and asthmatic group, there was no significant difference in LOX and LH2b mRNA.

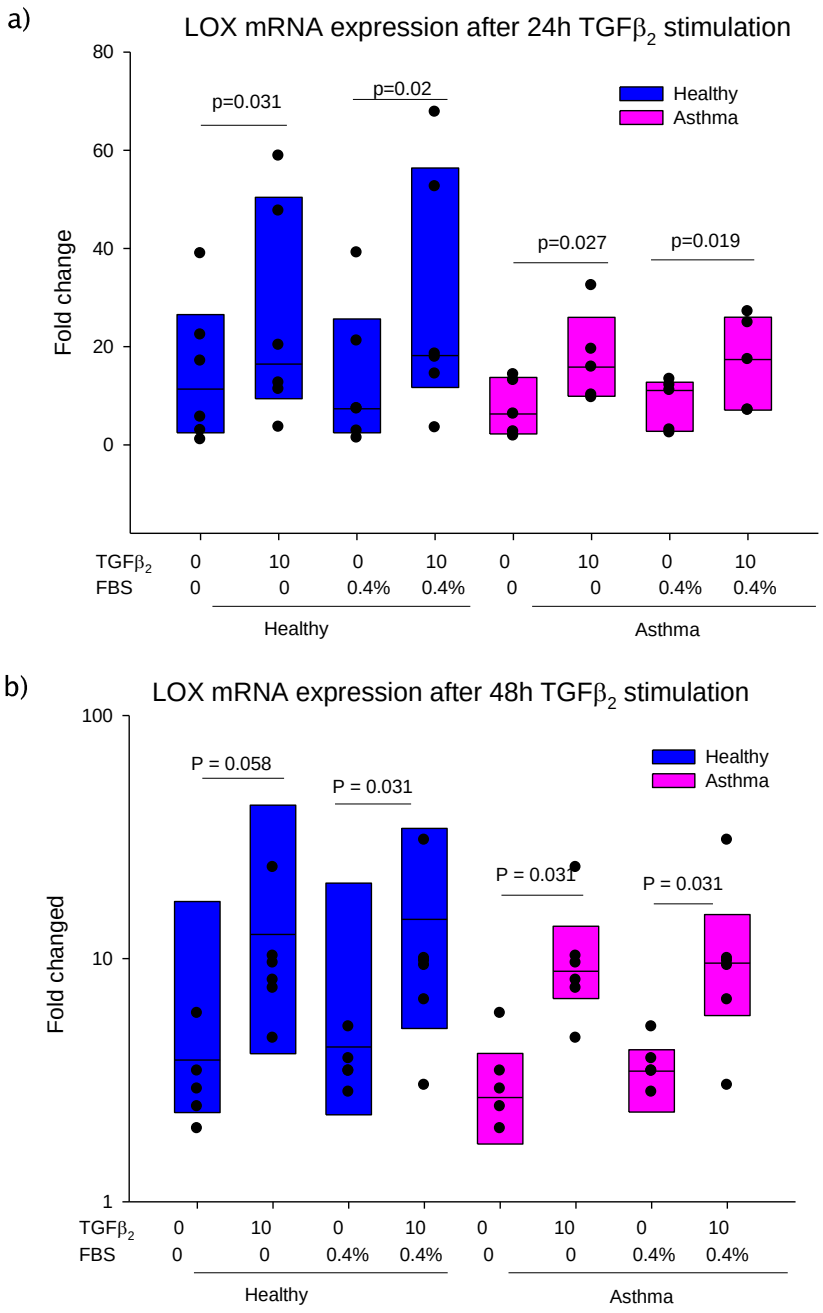

Figure 4-10: TGFβ2 up-regulated LOX mRNA expression in airway fibroblasts. Airway fibroblasts from 6 non-asthmatic and 6 asthmatic subjects were treated with TGFβ2 10ng/ml in serum free or 0.4% FBS DMEM for 24h-48h. Total RNA was extracted and analysed for LOX mRNA. The figure shows LOX mRNA expression after treatment with TGFβ2 for a) 24h and b) 48h. Blue boxes indicate data from fibroblasts from non-asthmatic subjects and pink boxes indicate those from asthmatic subjects. The values were normalized to the geometric mean of UBC/A2 and relative to the lowest expression observed in an untreated serum free untreated sample from a healthy non-asthmatic subject. The individual data points are superimposed on a box plot showing median and IQR. The data were tested for statistical significance using one way repeated measures ANOVA.

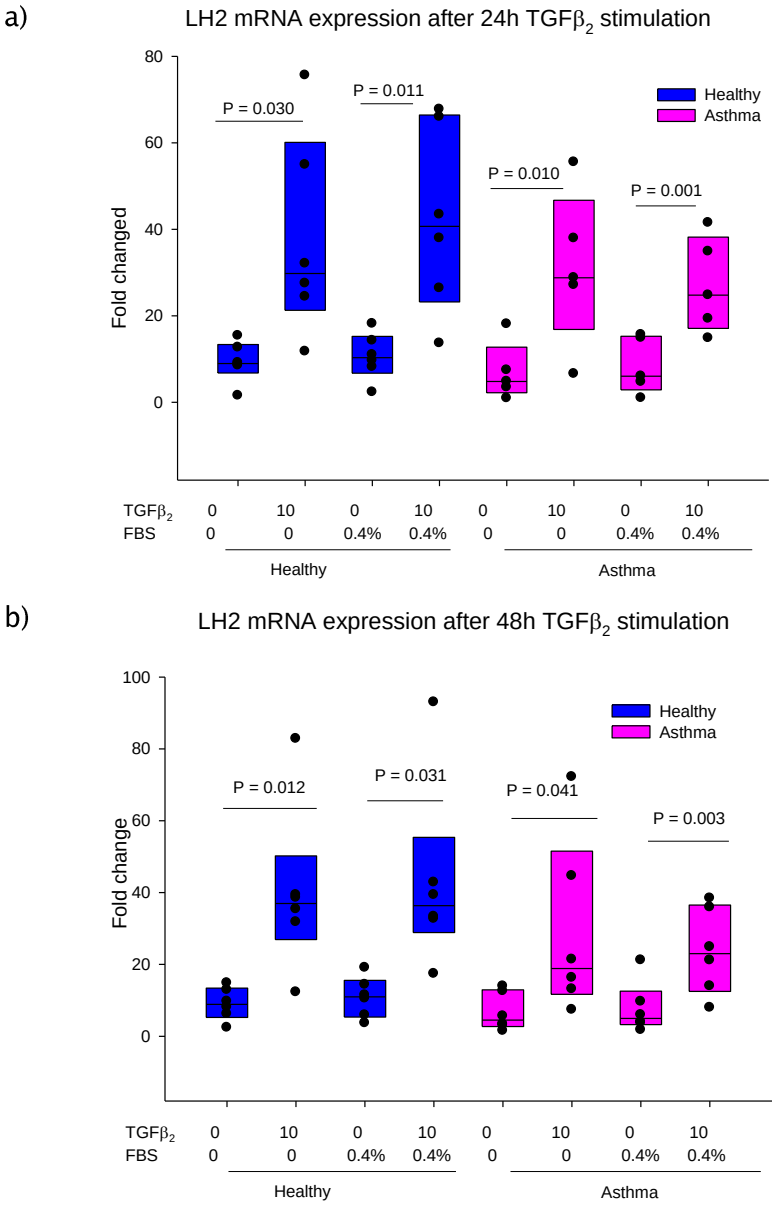

Figure 4-11: TGFβ2 up-regulated LH2b mRNA expression. Fibroblasts were treated as described in Figure 4-10 and LH2b expression was analysed by RT-qPCR. The graphs show a) LH2b mRNA expression after treatment with for 24h TGFβ2 treatment and b) LH2b mRNA expression after 48h TGFβ2 treatment. Blue boxes indicate data from fibroblasts from healthy non-asthmatic subjects and pink boxes indicate those from asthmatic subjects. The value was normalized to the geometric mean of UBC/A2 and relative to the lowest expression observed in an untreated serum free sample from a healthy non-asthmatic subject. The individual data points are superimposed on a box plot showing median and IQR. The data were tested for statistical significance using one way repeated measures ANOVA.

4.5.4) TGFβ2 stimulated airway fibroblasts to secrete Pro-LOX and active LOX

To determine whether airway fibroblasts from healthy non-asthmatic and asthmatic subjects secreted LOX protein differently, culture supernatants from fibroblasts treated with TGFβ2 for 48h were analysed for LOX protein production by western blot analysis. It was shown that TGFβ2 and serum enhanced the production of Pro-LOX (50 kDa) but the effect of serum alone was not greater than the effect of TGFβ2. Furthermore, TGFβ2 or serum could activate Pro-LOX to become active LOX (30 kDa). Combination of serum and TGFβ2 had the maximum effect on airway fibroblasts in promoting LOX protein production both of Pro-LOX (50 kDa) and active LOX (30 kDa) (Figure 4-12). The same response was seen both in fibroblasts from healthy non-asthmatic and asthmatic subjects.

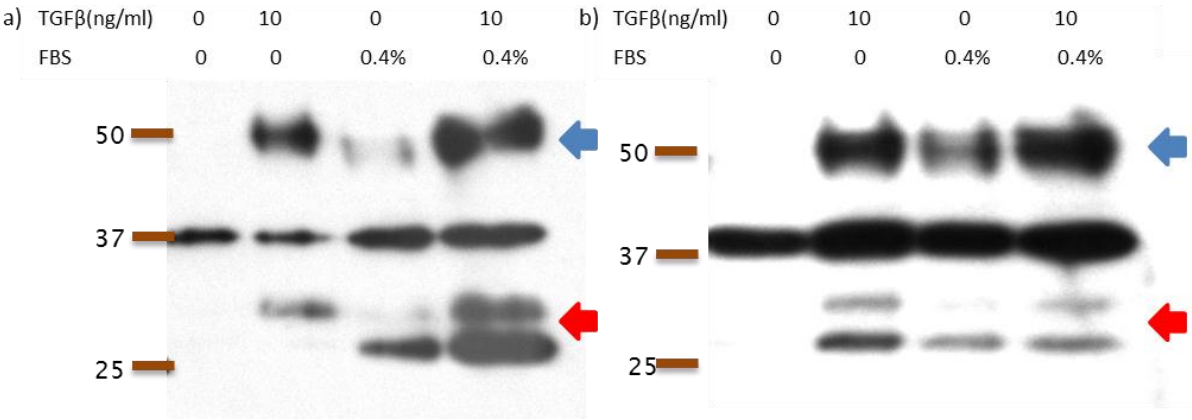

Figure 4-12: TGFβ2 enhanced airway fibroblasts to secret Pro-LOX and activated active LOX. Airway fibroblasts from healthy non-asthmatic and asthmatic subjects were treated with TGFβ2 (10ng/ml) in serum free or 0.4%FBS complete DMEM for 48h. Culture supernatants were concentrated and analysed by SDS-PAGE and immunoblotted using anti lysyl oxidase (LOX) antibodies. a) Representative of LOX western blot from healthy non-asthmatic fibroblasts. b) Representative of LOX western blot from asthmatic fibroblasts. The blue arrow indicates Pro-LOX (50 kDa) and the red arrow indicates active LOX (30 kDa).

4.5.5) TGFβ2 up-regulated collagen I mRNA expression

It was shown in previous sections that TGFβ2 induced airway fibroblasts to produce LOX. To investigate the effect of TGFβ2 on collagen mRNA expression in airway fibroblasts, cDNA samples from experiments described in section 4.5.3) were evaluated for collagen mRNA expression using RT-qPCR. This showed that TGFβ2 significantly up-regulated collagen I mRNA expression in fibroblasts from both healthy non-asthmatic and asthmatic subjects but there was no significant effect on collagen III mRNA expression after TGFβ2 48h stimulation (Figure 4-13). There was no significant difference in collagen mRNA expression between fibroblasts from healthy and asthmatic subjects.

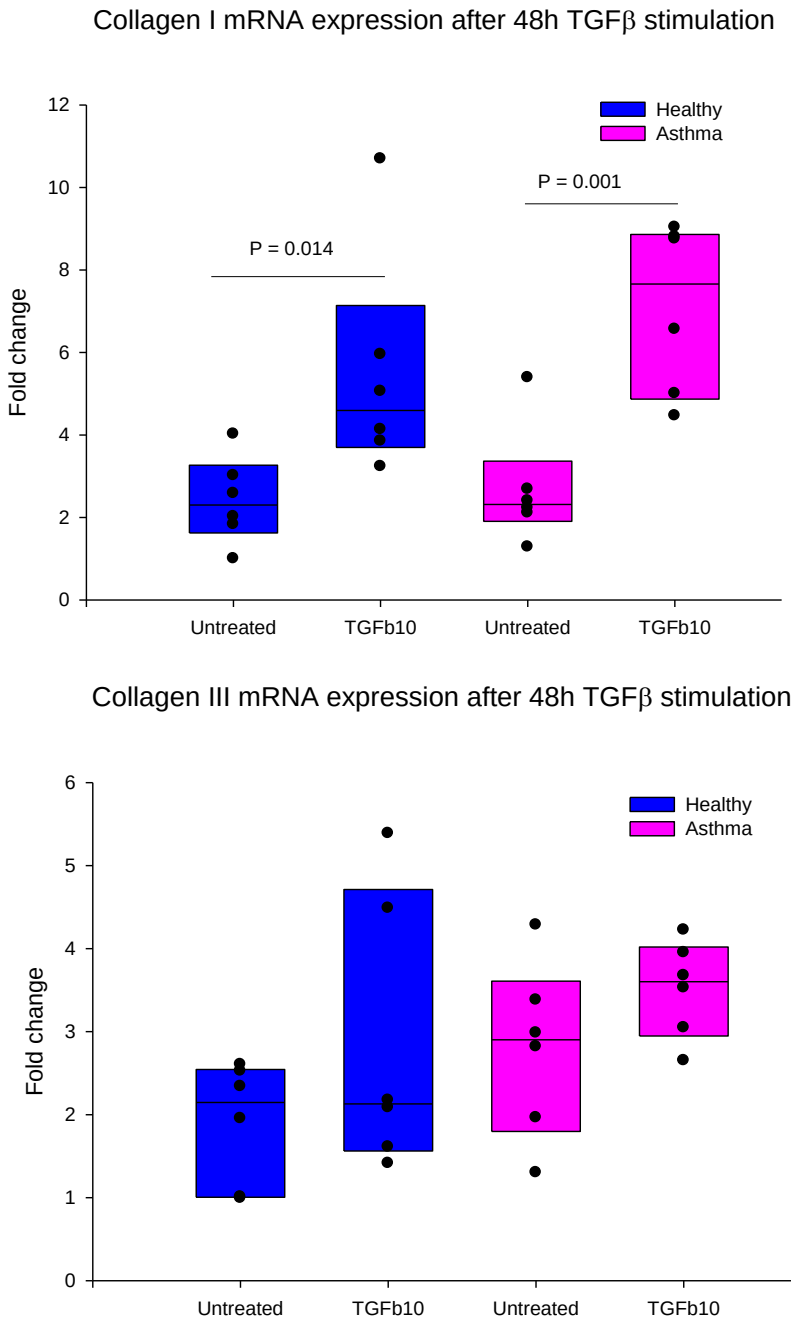

Figure 4-13: TGFβ2 up-regulated collagen I mRNA expression. cDNA from the experiments shown in Figure 4-10 experiment were analysed for collagen I and III mRNA using RT-qPCR. The values were normalized to the geometric mean of UBC/A2 and expressed relative to the lowest expression observed in an untreated serum free sample from a non-asthmatic subject. The individual data points are superimposed on a box plot showing median and IQR. Blue boxes indicate data from fibroblasts from healthy non-asthmatic subjects and pink boxes indicate those from asthmatic subjects. The data were tested for statistical significant using a paired *t*-test or Wilcoxon's Signed Rank Test for non-parametric data.

4.5.6) TGFβ2 up-regulated biglycan mRNA expression but suppressed decorin mRNA expression

Decorin and biglycan have been shown to have a role in collagen fibril assembly (151). Therefore, the effect of TGFβ2 on decorin and biglycan was investigated using the cDNA from experiments described in section 4.5.3). This revealed that TGFβ2 significantly up-regulated biglycan mRNA expression both in airway fibroblasts from healthy non-asthmatic and asthmatic subjects (Figure 4-14). In contrast to biglycan, decorin mRNA was suppressed by TGFβ2 (Figure 4-15). There was no significant difference in biglycan and decorin mRNA expression between fibroblasts from healthy and asthmatic subjects.

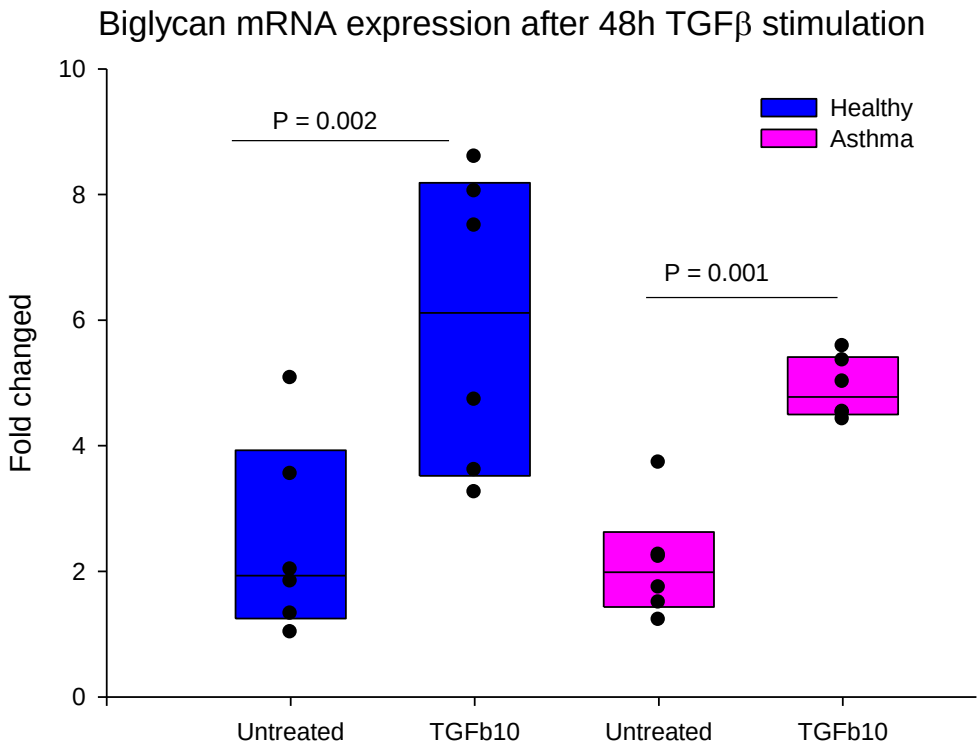

Figure 4-14: TGFβ2 up-regulated biglycan mRNA expression. cDNA from the experiments shown in Figure 4-10 were analysed for biglycan mRNA expression by RT-qPCR. The values were normalized to the geometric mean of UBC/A2 and expressed relative to the lowest expression observed in a serum free control from a non-asthmatic subject. The individual data points are superimposed on a box plot showing median and IQR. Blue boxes indicate data from fibroblasts from healthy non-asthmatic subjects and pink boxes indicate those from asthmatic subjects. The data were tested for statistical significance using a paired *t*-test.

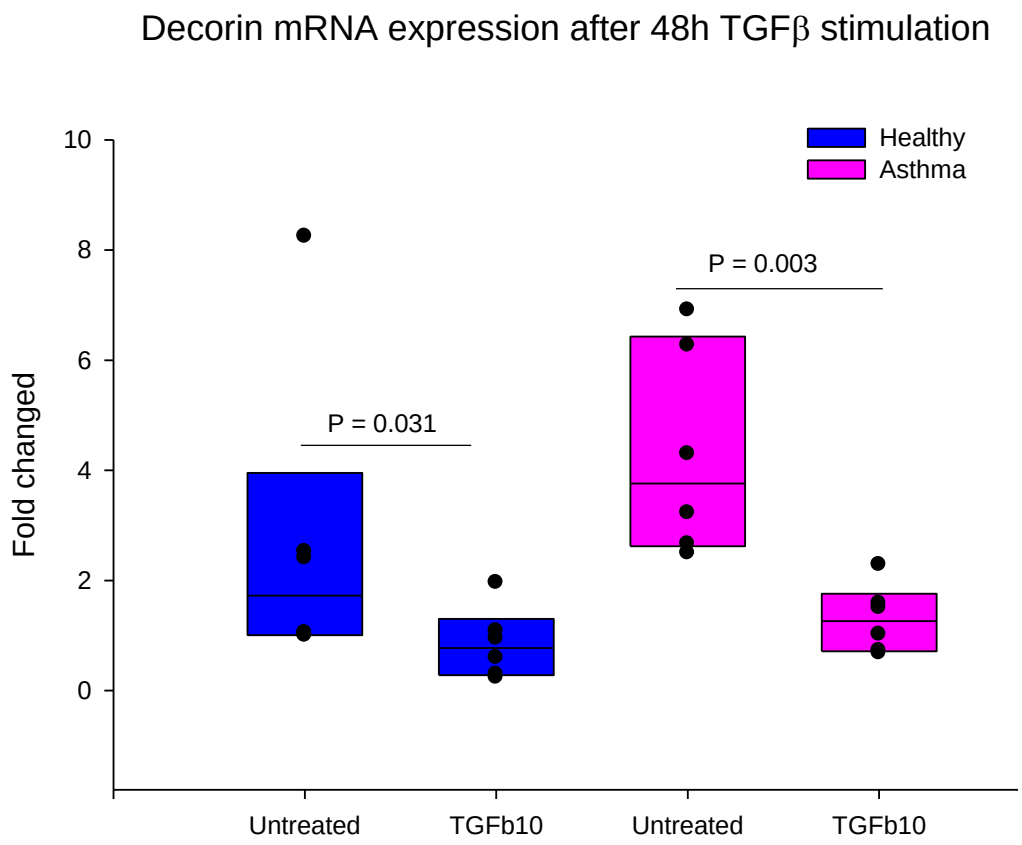

Figure 4-15: TGFβ2 suppressed decorin mRNA expression. cDNA from the experiments shown in Figure 4-10 were analysed for decorin mRNA expression by RT-qPCR. The values were normalized to the geometric mean of UBC/A2 and expressed relative to the lowest expression observed in a serum free control from a non-asthmatic subject. The individual data points are superimposed on a box plot showing median and IQR. Blue boxes indicate data from fibroblasts from healthy non-asthmatic subjects and pink boxes indicate those from asthmatic subjects. The data were tested for statistical significance using a paired *t*-test.

4.5.7) **Mechanical strain suppressed LOX mRNA**

It was shown in chapter 3 that mechanical strain to airway fibroblasts enhanced the production of collagen mRNA and protein. It was hypothesized that mechanical strain also regulated collagen cross-linking process. To investigate the impact of mechanical strain on LOX production, airway fibroblasts from 7 healthy non-asthmatic and 15 asthmatic subjects were subjected to mechanical strain (30% elongation, 12 cycles per minute) for 48 or 96h. The RNA was extracted and LOX mRNA was analysed using RT-qPCR. This revealed that mechanical strain significantly suppressed LOX mRNA expression both in fibroblasts from healthy non-asthmatic and asthmatic subjects after exposure to mechanical strain for 48h. However, after 96h mechanical strain, the significant suppression was seen in only in fibroblasts from asthmatic subjects (Figure 4-16). There was no significant difference in LOX mRNA expression between fibroblasts from healthy and asthmatic subjects.

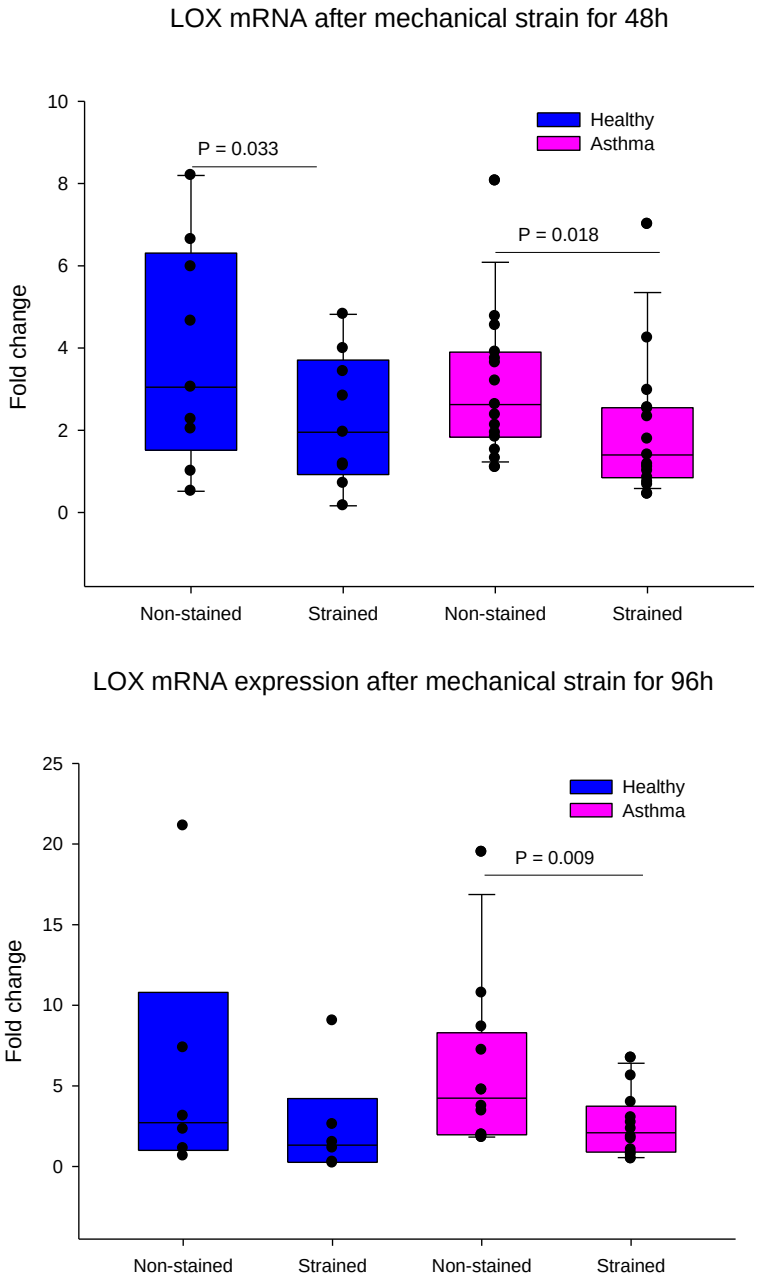

Figure 4-16: Mechanical strain suppressed LOX mRNA expression. Fibroblasts from healthy non-asthmatic and asthmatic subjects were subjected to mechanical strain 30% elongation, 12 cycles per minute for 48 or 96h. Total RNA was extracted and analysed for LOX mRNA. Blue boxes indicate data from fibroblasts from healthy non-asthmatic subjects and pink boxes indicate those from asthmatic subjects. The values were normalized to GAPDH and expressed relative to the lowest expression of a non-strained sample from a healthy non-asthmatic subject. The individual data points were superimposed on a box plot showing median and IQR. The data were tested for statistical significance using Wilcoxon Signed Rank Test.

4.5.8) Mechanical strain enhanced the production of LOX protein

To measure the level of LOX protein in culture supernatant after mechanical strain, fibroblasts from 3 healthy non-asthmatic and 3 asthmatic subjects were exposed to mechanical strain (30% elongation, 12 cycles per minute for 48h). The culture supernatants were then concentrated and LOX protein was measured by western blot. The density of LOX protein bands was calculated as a ratio with each non-strained pair per 10,000 cells. This revealed that mechanical strain enhanced the production of active LOX in relative to non-strained sample in both healthy non-asthmatic and asthmatic group. In contrast to active LOX, mechanical strain had a trend to enhance the production of Pro-LOX in healthy non-asthmatic group but suppressed Pro-LOX production in asthmatic group (Figure 4-17).

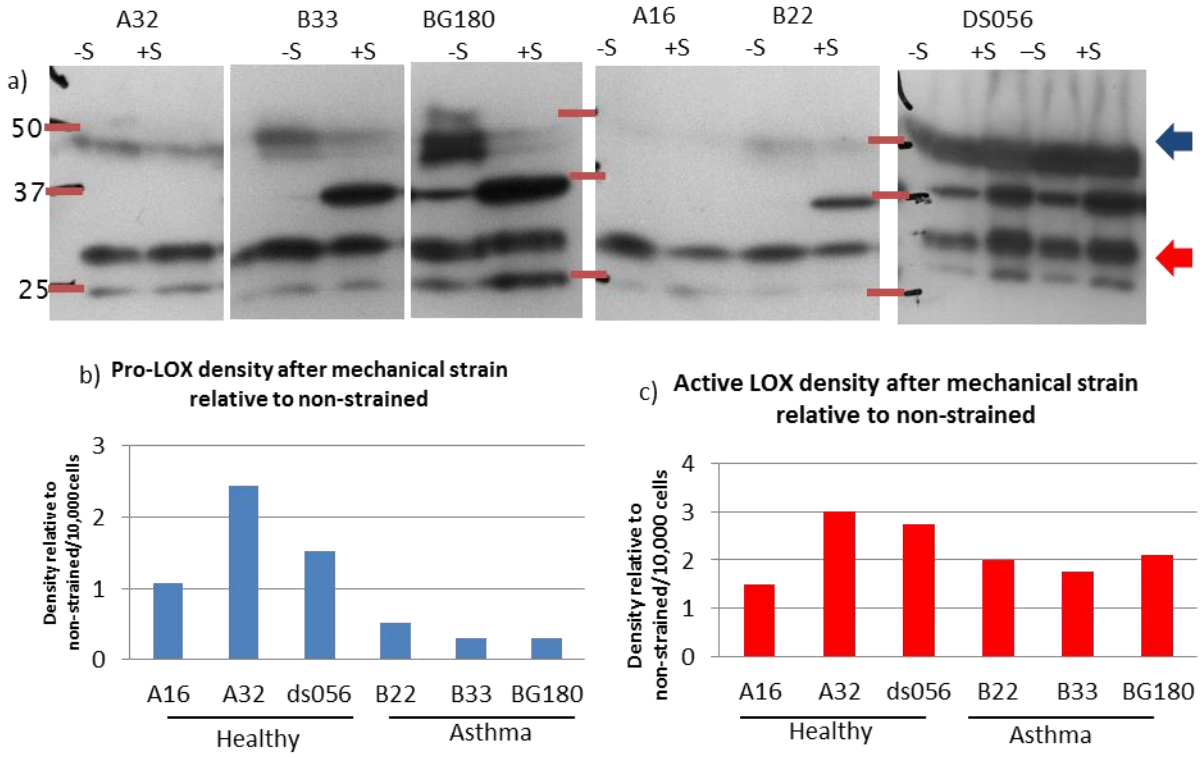

Figure 4-17: Mechanical strain enhanced the production of LOX protein. Airway fibroblasts from 3 healthy non-asthmatic and 3 asthmatic subjects were exposed to mechanical strain for 48h. Culture supernatants were concentrated and analysed by SDS-PAGE and immunoblotted using anti lysyl oxidase (LOX) antibodies. Pro-Lox and active LOX bands were quantified by densitometry using ImageJ. a) Representative LOX western blots. -S indicates non-strained cells, +S indicates strained cells, the blue arrow indicates Pro-LOX and the red arrow indicates active LOX. Graphs show a ratio density of strained to non-strained pair per 10,000 cells b) Pro-LOX and c) active LOX. The value more than 1 indicates increase production after mechanical strain.

4.5.9) Mechanical strain up-regulated LH2b mRNA expression

To examine the impact of mechanical strain on LH2b mRNA expression, cDNA from experiments described in section 4.5.7) were evaluated for LH2b mRNA using RT-qPCR. This showed that mechanical strain up-regulated LH2b mRNA expression only in fibroblasts from asthmatic subjects but not in fibroblasts from healthy non-asthmatic subjects after 96 h mechanical strain. The absence of significant changes in the healthy group may be explained from the low statistic power. There was no significant change of LH2b mRNA after 48h mechanical strain (Figure 4-18). There was no significant difference in LH2b mRNA expression between fibroblasts from healthy and asthmatic subjects.

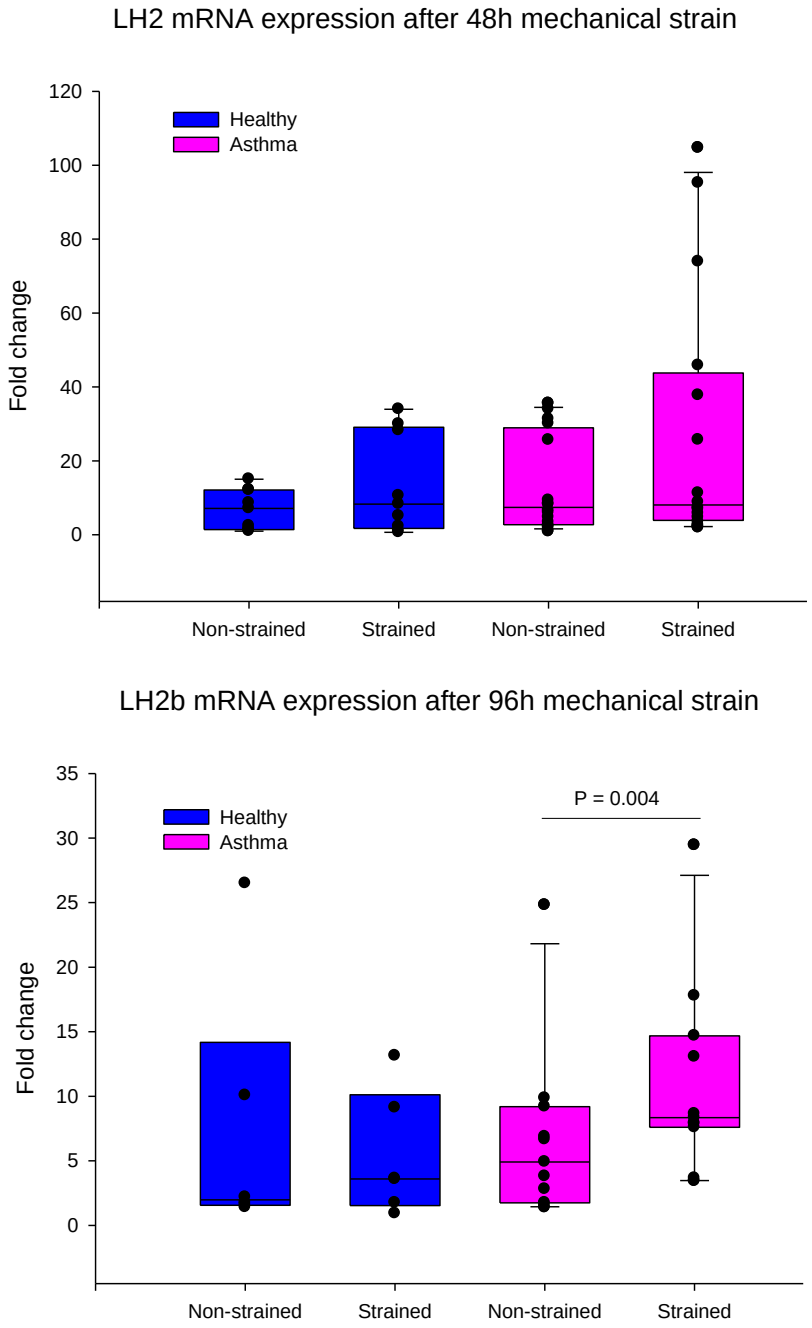

Figure 4-18: Mechanical strain up-regulated LH2b mRNA expression. cDNA from experiments shown in Figure 4-16 were analysed for LH2b mRNA using RT-qPCR. Blue boxes indicate data from fibroblasts from healthy non-asthmatic subjects and pink boxes indicate those from asthmatic subjects. The values were normalized to GAPDH and expressed relative to the lowest expression of a non-strained sample from a non-asthmatic subject. The individual data points were superimposed on a box plot showing median and IQR. The data were tested for statistical significance using Wilcoxons Signed Rank Test.

4.5.10) Mechanical strain up-regulated biglycan mRNA expression but suppressed decorin mRNA expression

As small leucine-rich proteoglycans (SLRPs) such as decorin and biglycan have a role in collagen fibril assembly, the effect of mechanical strain on biglycan and decorin expression was also evaluated. cDNA from experiments described in section 4.5.7) were processed for RT-qPCR analysis for biglycan and decorin mRNA. It was found that mechanical strain significantly up-regulated biglycan mRNA in fibroblasts from asthmatic subjects after mechanical strain for 48h. Decorin mRNA expression was significantly suppressed by mechanical strain in fibroblasts from healthy non-asthmatic subjects. There was a trend in suppression of decorin mRNA expression in fibroblasts from asthmatic subjects but it did not reach statistical significance (Figure 4-19). There was no significant difference in biglycan and decorin mRNA expression between fibroblasts from healthy and asthmatic subjects. The opposing effects of mechanical strain on decorin and biglycan mRNA expression were similar to the effect of TGFβ (Section 4.5.6).

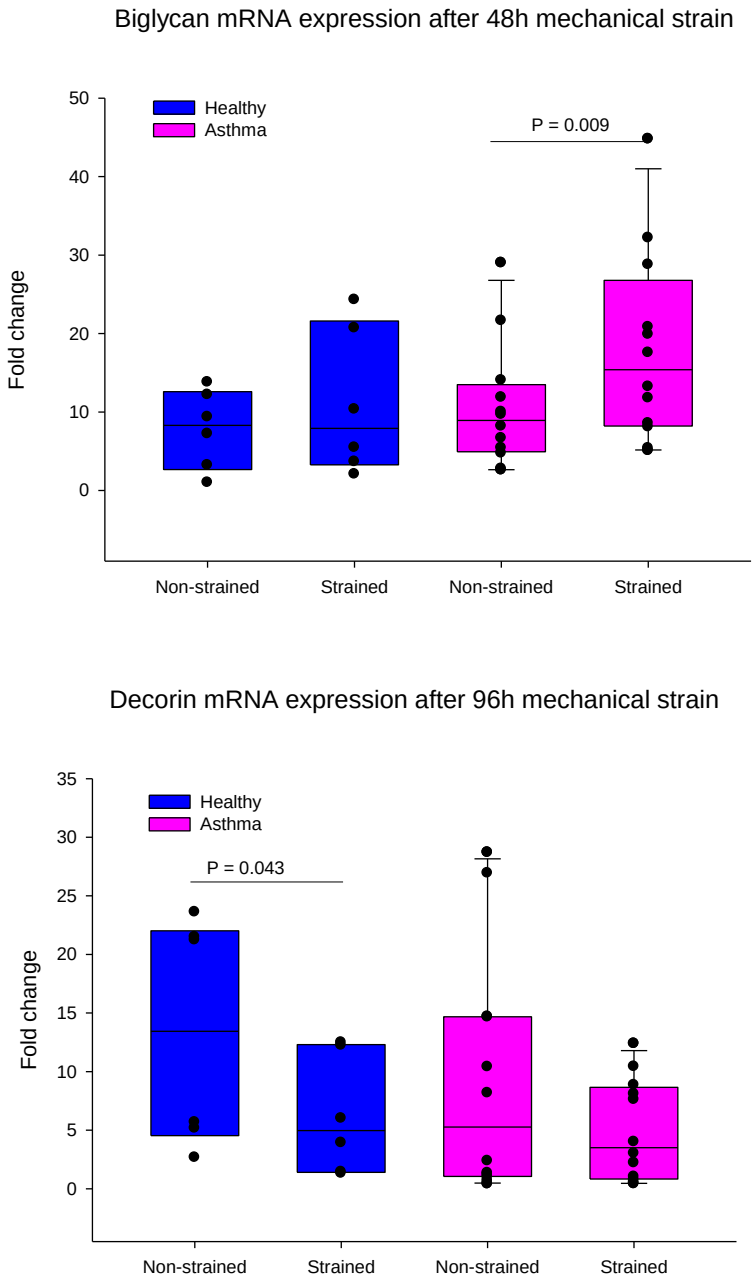

Figure 4-19: Mechanical strain up-regulated biglycan mRNA expression but suppressed decorin mRNA expression. cDNA from experiments shown in Figure 4-16 were analysed for biglycan and decorin mRNA. Blue boxes indicate data from fibroblasts from healthy non-asthmatic subjects and pink boxes indicate those from asthmatic subjects. The values were normalized to GAPDH and expressed relative to the lowest expression of a non-strained sample from a healthy non-asthmatic subject. The individual data points are superimposed on a box plot showing median and IQR. The data were tested for statistical significance using Wilcoxon's Signed Rank Test.

4.5.11) LOX western blot of BAL fluid from healthy non-asthmatic and asthmatic subjects

Since from previous sections, it was found that TGFβ2 and mechanical strain induced the production of LOX by airway fibroblasts. Several studies have demonstrated an elevation of TGFβ in BAL fluid of asthmatic patient (86;89). Then it was hypothesized that the same respond occurs *in vivo*. As a result, LOX protein in bronchoalveolar lavage (BAL) fluid from healthy non-asthmatic and asthmatic subjects was measured. BAL fluid from 10 healthy non-asthmatic, 10 mild asthmatic and 12 severe asthmatic subjects were concentrated with Strataclean® resin and measured for LOX protein by western blot analysis. This revealed that among 32 BAL fluid samples, only 5 samples demonstrated active LOX band at 30 kDa (Figure 4-20). Interestingly, all of these samples were BAL from severe asthmatic subjects. Furthermore, BAL fluids from severe asthmatic subjects had a significantly higher Pro-LOX density when compared to healthy non-asthmatic and mild asthmatic subjects.

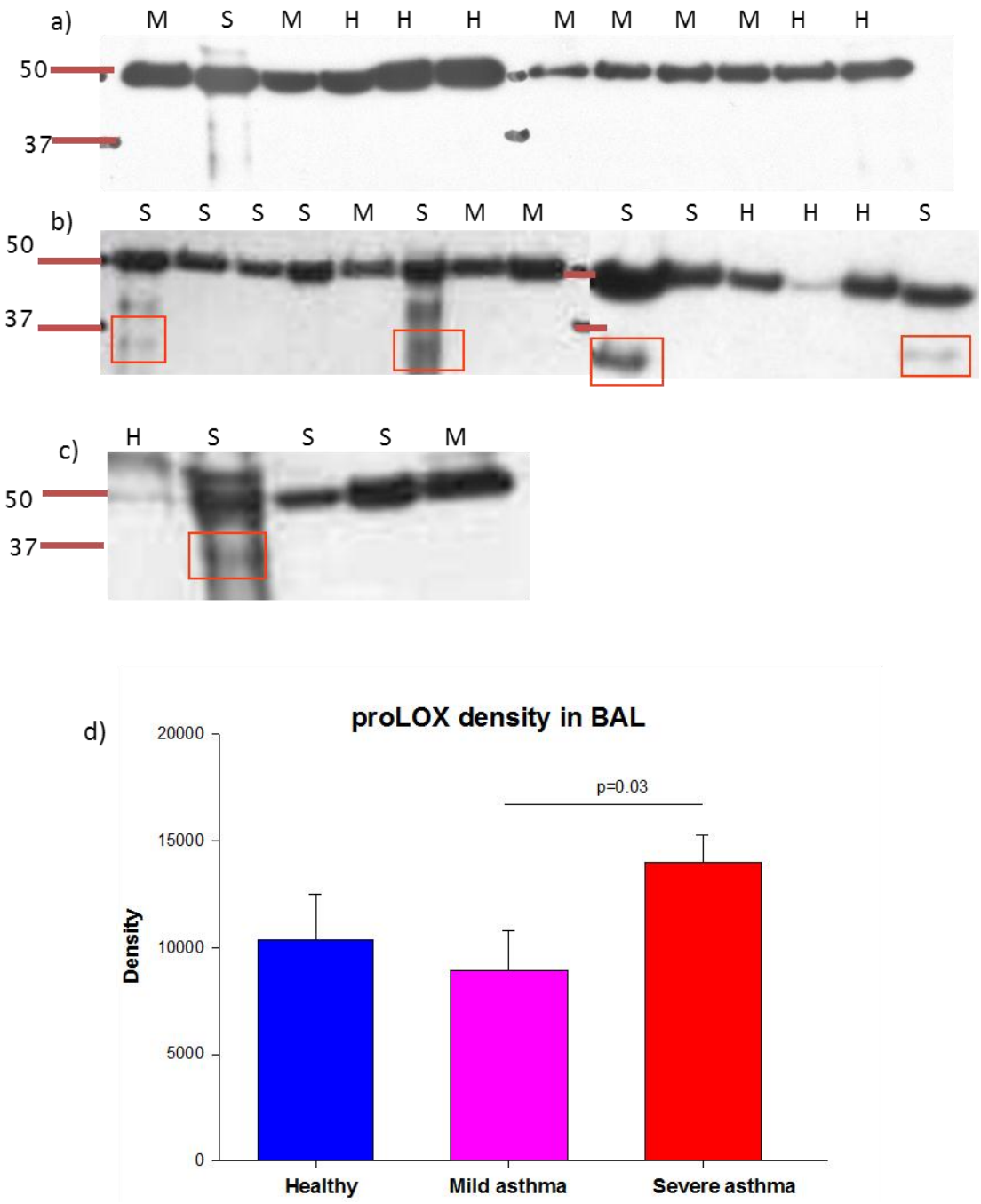

Figure 4-20: Representative western blots of LOX protein in BAL fluid from 10 healthy non-asthmatics, 10 mild asthmatic and 12 severe asthmatic subjects in a), b) and c). BAL fluid was concentrated and analysed by SDS-PAGE and immunoblotted using anti lysyl oxidase (LOX) antibodies. Pro-Lox band from BAL fluid of 10 non-asthmatic, 10 mild asthmatic, and 12 severe asthmatic subjects was quantified by densitometry using ImageJ. In d) graph represents the mean density of Pro-LOX and standard error. The difference among groups was tested for using a one way ANOVA. H=Healthy, M=mild asthma and S=severe asthma.

4.5.12) Comparison of the clinical data from severe asthmatic subjects with and without active LOX in BAL fluid

To investigate whether any factors may play roles in promoting release of active LOX into BAL fluid, the clinical data of the subjects with and without active LOX were compared. It was found that all healthy non-asthmatic and mild asthmatic subjects were atopic and non-smokers, whereas 3 subjects from severe asthma were current smokers. None of the mild asthma subjects were treated with inhaled corticosteroids. The mild asthma group had a significantly lower age when compared to the severe asthma (25.9±5.38 yr vs 41.5±2.85 yr) (Table 4-3). Comparing between the severe asthma subjects with and without active LOX in BAL fluid, the age of severe asthmatic subjects who presented active LOX was higher than those did not, but this was not statistically significant. Active LOX was detected in the group that had lower % reversibility but this failed to reach statistical significance. There was no difference in the dose of inhaled steroid or oral prednisolone between these two groups (Table 4-4). However, the severe asthma group was the only one that received corticosteroids for their treatment. Then it was hypothesized that corticosteroids may have an effect on LOX production by airway fibroblasts. This will be investigated in the following chapter.

Table 4-3: Clinical characteristic of subjects whose was analysed for LOX protein in BAL fluid

	Healthy (n=10)	Mild asthma (n=10)	Severe asthma (n=12)
Age (yr) (mean±sd)	30.83±13.44	25.9±5.38*	41.5±2.85
Sex (M:F)	4:6	4:6	3:9
Atopy:non-atopy	10:0	10:0	8:4
Current smoker	0	0	3
FEV_1%Predicted	99.7+10.9	98.98+18.02	61.5+19.2
Inhaled steroid (BDP equivalent µg/day)	0	0	2765
Prednisolone(mg/day)	0	0	7.25

* $p<0.05$. BDP= Beclomethasone Dipropionate

Table 4-4: Clinical characteristic of severe asthma with and without active LOX

Severe asthma with active LOX

Code	Age (yr)	Inhaled steroid BDP EQ (ug/day)	Prednisolone (mg/day)	FEV_1 %predicted	Reversibility (%)	Peak flow variability (%)	Sex	Current smoker
BG129	21	8000	25	60	14.98	30	F	No
BG157	40	2400	0	80	24.00	23	F	Yes
BG178	54	1600	10	19.8	0	15	F	No
DS070	42	2000	0	59	0	NA	F	No
DS075	28	2800	0	83	3.32	NA	M	No
Mean	37	3360	8.75	60.36	10.57	22.6		

Severe asthma without active LOX

Code	Age (yr)	Inhaled steroid BDP EQ (ug/day)	Prednisolone (mg/day)	FEV_1 %predicted	Reversibility (%)	Peak flow variability (%)	Sex	Current smoker
BG170	28	1320	0	34.9	71.43	NA	M	No
BG180	51	4000	15	29.7	25.00	53	F	No
BG173	32	2380	20	78.6	12.00	NA	F	Yes
BG225	50	3080	15	84.8	10.63	12.5	F	No
DS083	51	2400	0	76	4.02	NA	F	No
BG224	57	1600	0	64.9	25.00	31.9	M	No
DS077	45	1600	10	64	5.56	7	M	No
Mean	45	2340	8.57	61.84	21.94	26.10		

4.6) Discussion

Summary of findings

- TGFβ2 up-regulated collagen I mRNA expression in airway fibroblasts but not collagen III mRNA.
- TGFβ2 enhanced the production of lysyl oxidase (LOX) by airway fibroblasts in a dose dependent manner.
- TGFβ2 activated Pro-LOX to become active LOX.
- Serum also enhanced the production of pro-LOX and active LOX by airway fibroblasts.
- TGFβ2 up-regulated expression of lysyl hydroxylase 2b (LH2b) mRNA in airway fibroblasts.
- TGFβ2 up-regulated expression of biglycan but suppressed decorin mRNA expression in airway fibroblasts.
- Airway fibroblasts from healthy non-asthmatic and asthmatic subjects responded to TGFβ2 stimulation in the same pattern.
- Severe asthmatic subjects produced more LOX in BAL fluid when compared to healthy non-asthmatic and mild asthmatic subjects.
- Severe asthmatic subjects who presented active LOX in BAL fluid had a trend for more fixed airway obstruction than those with absent LOX in BAL fluid.
- Mechanical strain to airway fibroblasts suppressed LOX mRNA expression in airway fibroblasts.
- Active LOX protein production by airway fibroblasts was increased after exposure to mechanical strain.
- Mechanical strain up-regulated lysyl hydroxylase 2b (LH2b) mRNA in airway fibroblasts from asthmatic subjects.
- Mechanical strain up-regulated biglycan mRNA expression in fibroblasts from healthy non-asthmatic subjects but suppressed decorin mRNA expression in fibroblasts from asthmatic subjects.

Subepithelial thickening is a notable feature of airway remodelling in asthmatic airways and is attributable to an increase in extracellular matrix protein deposition particularly collagen. Airway fibroblasts are the crucial matrix producing cells in the submucosal layer and respond to diverse stimuli with an increase in collagen deposition. The biophysical strength of the collagen fibres depends on the cross-linking between collagen molecules within the fibrils by lysyl oxidase (LOX), resulting in the deposition of insoluble collagen within fibrils. Inhibition of this process can result in loss of strength of collagen. Furthermore, the nature of the collagen cross-linking depends on the extent of hydroxylation of the telopeptide in the collagen molecule which is catalysed by lysyl hydroxylase2b (LH2b) (211).

LOX is synthesized as a proenzyme that is secreted to the extracellular space where it is processed to the active enzyme. LOX production can be explored at three levels: synthesis of mRNA, Pro-LOX synthesis, and extracellular conversion of Pro-LOX to active LOX. Hypoxia-inducible factor-1α (HIF1-α) has been shown to increase the production of LOX both at the mRNA and protein level in adipose tissue (218). Several studies have demonstrated a role for TGFβ1 in the regulation of LOX (215;219-221). However, there are few studies that have focused on TGFβ2 which is the major isoform released by human bronchial epithelial cells (44). Pro-LOX has no enzymatic activity and needs to be additional processed to produce the catalytically active form. Several proteins have been shown to activate Pro-LOX ; these include procollagen C proteinase (222), Tolloid-like 1 protein (223), and Aminopeptidase B (224). Increases in LOX expression and LOX activity have been shown to result in increased collagen cross-linking in several organs such as heart (225), lung (226) and kidney (221). The present study has demonstrated that TGFβ2 up-regulated LOX mRNA and protein in airway fibroblasts from both healthy non-asthmatic and asthmatic subjects. TGFβ2 was also shown to activate Pro-LOX. Whereas in a previous study, TGFβ1 was not able to convert Pro-LOX to become active LOX (215). Serum was found to enhance the production of LOX protein but its effect was not greater than the effect of TGFβ2. However, as plasma protein exudation is a feature of airway inflammation encounter in asthma, the combination of effects of TGFβ and serum proteins may have added impact in clinical disease.

LH2b mRNA was also up-regulated in airway fibroblasts following treatment with TGFβ2. Additionally, airway fibroblasts subjected to mechanical strain that resemble deep breath also stimulated active LOX production. Mechanical strain also up-regulated LH2b mRNA, a collagen telopeptide lysine hydroxylation enzyme that helps collagen cross-linking shifting to a more fibrotic pathway (127). Interestingly, this effect was found only in asthmatic fibroblasts. Consequently, the net effect of applying mechanical strain to airway fibroblasts appears to direct fibroblasts from asthmatic subjects to produce more fibrotic collagen cross-linking end products.

It was also revealed that mechanical strain to airway fibroblasts suppressed LOX mRNA expression in airway fibroblasts, but it enhanced the production of active LOX. The inconsistent result between mRNA and protein can be explained from the modification of LOX as after secretion from fibroblasts, Pro-LOX needs to be activated. This result suggested that mechanical strain may have a role in activating Pro-LOX. The regulation of LOX at several different levels by TGFβ2 and mechanical strain is summarized in Figure 4-21.

However, there was no difference between airway fibroblasts from healthy non-asthmatic and asthmatic subjects in their responses to TGFβ2 and mechanical strain in producing LOX. This suggests that the response to TGFβ2 or mechanical strain is normal. However, the environment in the airway of asthmatic and healthy non-asthmatic subjects is not the same. Asthmatic airways are exposed to more TGFβ secreted by airway epithelial cells and inflammatory cells such as eosinophils following airway injury and inflammation. This was supported by an *in vitro* study: Goulet et al have reported that under the condition that mimicked inflammatory environment (5%FBS and/or TGFβ1), human lung fibroblasts produced more total ECMs and collagen when compared to a non-inflammatory condition (0.3% albumin) (227). In addition, asthmatic patients also cough more frequently than healthy non-asthmatic subjects. This may result in an increase in mechanical strain to the airways as it has been shown that patients with chronic cough without asthma had a thicker subepithelial basement membrane than healthy control subjects (207). Furthermore, it was found that LOX active form was demonstrated only in BAL fluid from severe asthmatic subjects but not in BAL fluid from healthy non-asthmatic and mild asthmatic subjects. All subjects in healthy non-asthmatic and mild asthmatic groups were corticosteroids naïve. Consequently, it is possible that corticosteroids may have a role in regulating LOX production in asthma. However, not all severe asthmatic samples demonstrated active LOX in BAL fluid; only 5 in 12 severe asthmatic samples had active LOX. Since it was found that mechanical strain enhanced the production of active LOX, the airways of severe asthmatic subjects who expressed active LOX in BAL fluid might be recently exposed to the mechanical strain (e.g. from asthmatic attack) or have more labile

airways with the greater peak flow variability. This may have resulted in enhancement of production of active LOX. However, due to the low number of samples studied, the present work was not able to demonstrate the difference in the percentage of the peak flow variability between subjects with or without active LOX in BAL fluid. More studies will be needed to explore the influence of acute asthma on LOX production. In addition, when the clinical characteristic of patients were compared, patients with active LOX tended to have more fixed airway than patients without active LOX (% reversibility 10.57 vs 21.94), although this failed to reach statistical significance because of the low number and high inter-subjects variation. This may highlight the role of collagen cross-linking in altering the biophysical property of asthmatic airways.

Collagen fibrils assembly depends, in part, on association with small leucine-rich proteoglycans: decorin (228-230) and biglycan (231;232). Decorin was shown to have a negative regulation on TGFβ both *in vitro* and *in vivo (84;233)*. In contrast, biglycan was shown to interfere with TGFβ bioactivity *in vitro*, but the same effect was not seen *in vivo (84)*. The present study found that TGFβ2 at the concentration of 10 ng/ml suppressed decorin mRNA but up-regulated biglycan mRNA expression in airway fibroblasts. Similar results were seen in a recent study that demonstrated the effect of TGFβ1 in increasing biglycan production with a trend to decrease decorin production by airway fibroblasts from non-asthmatic and asthmatic subjects (234). The differential regulation of TGFβ on decorin and biglycan production has previously been demonstrated in human embryonic lung fibroblasts (235), murine lungs (84), in a bleomycin induced pulmonary fibrosis animal model (236). This suggests an independent regulation of TGFβ on decorin and biglycan production in the airway. Furthermore, the response to TGFβ on decorin expression also depends on TGFβ isoform and the origin of fibroblasts studied. It was found that TGFβ1 increased decorin expression in murine lung fibroblasts as assessed by immunocytochemistry. However, there was no change in decorin expression after treatment with TGFβ2 up to 1 ng/ml in murine lung fibroblasts as demonstrated by immunocytochemistry (83). The present study also found an increase in biglycan mRNA expression but down regulation of decorin mRNA expression in airway fibroblasts after mechanical strain stimulation. This effect may explain from the effect of TGFβ1, since from chapter 3 it was found that the mechanical strain enhanced the production of active TGFβ1.

Taken together, this chapter has demonstrated a role for TGFβ2 and mechanical strain in regulating collagen cross-link processes and with the potential to affect collagen fibril assembly in airway fibroblasts. This includes enhancing the production LOX and regulating LH2b, decorin and biglycan mRNA. These will have a potential for increased cross-linking of collagen in the airways in asthma (Figure 4-21).

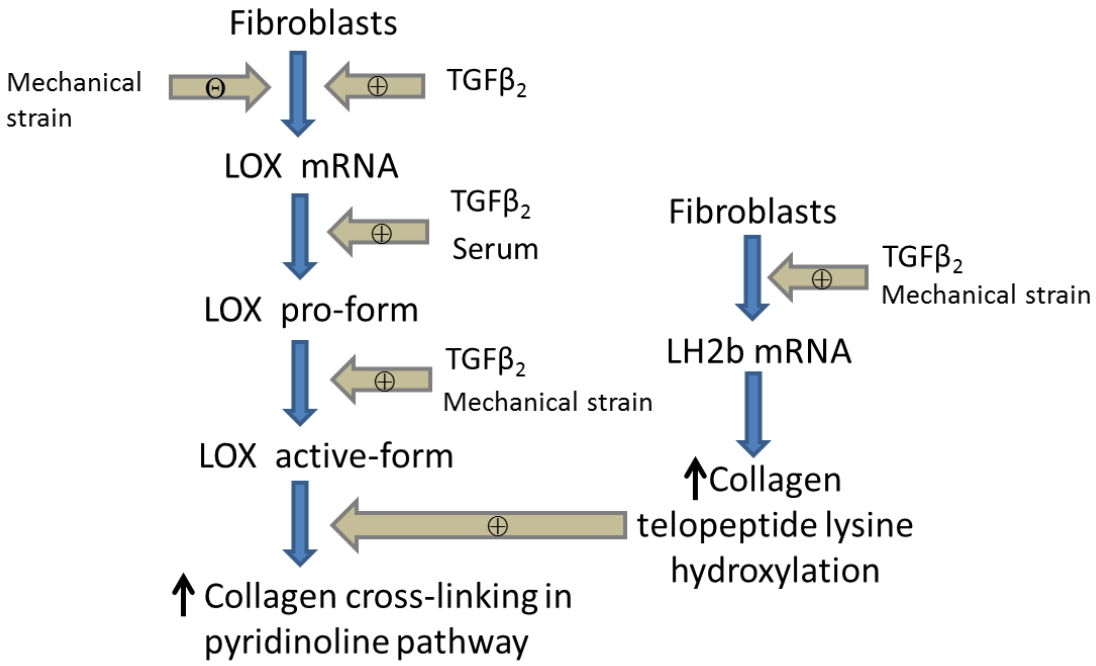

Figure 4-21: The diagram demonstrates the regulation of lysyl oxidase (LOX) and lysyl hydroxylase2b by TGFβ2 and mechanical strain in airway fibroblasts. This may result in an increase collagen cross-linking. ⊕=stimulation, Θ= inhibition and ↑=increase.

Chapter 5: Dexamethasone and Collagen Cross-linking Enzymes

5.1) Rationale

Asthma is a chronic inflammatory disorder of the airways which many inflammatory and structural cells including eosinophils, T lymphocyte, macrophages, mast cells, neutrophils, epithelial cells and fibroblasts are involved. These cells release several cytokines, chemokines, and growth factors in response to stimulation and various mechanical or physiological forms of stress resulting in a sustained chronic airway inflammation that leads to bronchoconstriction and structural changes of the airways such as airway remodelling. Medication to treat asthma can be classified into 2 categories: controller and relievers. Controller is medication taken daily on the long term basis to keep asthma under control by targeting airway inflammation. Relievers are medications used on an as-needed basis to relieve airway obstruction from smooth muscle contraction. Inhaled corticosteroids are suggested to be the most effective controller medications to treat airway inflammation in asthma (1). From chapter 4, it was demonstrated that the collagen cross-linking enzyme, lysyl oxidase (LOX), was up-regulated in airway fibroblasts following TGFβ2 stimulation. Furthermore, it was found that active LOX was only detectable in BAL fluid from severe asthmatic subjects who received high doses of inhaled corticosteroid whilst no active LOX was detected in BAL fluid from healthy non-asthmatic and mild asthmatic subjects who were not inhaled corticosteroid treated. Consequently, it was hypothesized that corticosteroids may play a role in regulating expression of the collagen cross-linking enzymes. In this chapter, airway fibroblasts from healthy non-asthmatic and asthmatic subjects were stimulated with dexamethasone in the presence or absence of TGFβ2. Changes in LOX, the collagen cross-linking enzyme, and LH2b, which catalyses the hydroxylation of collagen telopeptide lysines, as well as the small leucine-rich proteoglycans (SLRPs): decorin and biglycan, were evaluated. Furthermore, to allow comparison with a highly fibrotic disease, lung fibroblasts from an interstitial lung disease (ILD) subject were also stimulated with dexamethasone in the presence or absence of TGFβ2 and compared the response with airway fibroblasts from healthy non-asthmatic and asthmatic subjects.

5.2) Hypothesis

That dexamethasone stimulates airway fibroblasts to produce collagen cross-linking enzymes.

5.3) Aims

- To investigate the changes of lysyl oxidase (LOX) produced by airway fibroblasts following dexamethasone stimulation.
- To investigate the changes of lysyl hydroxylase2b (LH2b) mRNA produced by airway fibroblasts following dexamethasone stimulation.
- To investigate the changes of decorin and biglycan mRNA produced by airway fibroblasts following dexamethasone stimulation.
- To investigate whether airway fibroblasts from healthy non-asthmatic and asthmatic subjects respond to dexamethasone stimulation differently from lung fibroblasts from an ILD subject in producing collagen cross-linking enzymes.

5.4) Methods

5.4.1) Dexamethasone and TGBβ2 stimulation of cultured fibroblasts

Airway fibroblasts from healthy non-asthmatic and asthmatic volunteers and lung fibroblasts from a patient diagnosed with chronic bronchiolitis with constrictive obliterative bronchiolitis, an interstitial lung disease (ILD), were seeded at a density of 100,000 cells/well in 12 well plates and incubated in 37˚C in the presence of 5% CO_2 until fully confluent. The cells were then treated with dexamethasone 10-1000 nM in the presence or absence of TGFβ2 10ng/ml in 0.4% (v/v) FBS in complete DMEM for 24-48h.

5.4.2) Subject characteristics

Airway fibroblasts from 6 healthy non-asthmatic and 6 asthmatic subjects were used to study on the effect of dexamethasone in the regulation of LOX expression. There was no statistical difference in age between healthy non-asthmatic and asthmatic subjects but there was more female in asthmatic group. Asthmatic subjects had a significantly lower FEV_1 (%predicted) than healthy non-asthmatic subjects (p=0.002) (Table 5-1).

Table 5-1: Characteristics of subjects who provided bronchial fibroblasts for the studies of the effect of dexamethasone in the regulation of LOX expression

Disease	No.	Age (yrs)	Sex (F:M)	FEV_1 (%predicted)	Inhaled steroid (µg/day BDP equivalent)	Prednisolone (mg/day)
Healthy	6	36 (20-59)	2:4	112 (89.8-134)	0	0
Asthma	6	54 (28-67)	4:2	62.5* (19.8-101)	1800 (1000-4000)	5 (0-15)
ILD	1	67	F	64	800	0

* p=0.002. Data shown as mean with range in brackets. FEV_1= forced expiratory volume in 1 second. BDP= Beclomethasone Dipropionate

5.5) Results

5.5.1) Initial experiments

Initial experiments were undertaken in airway fibroblasts from one subject to optimize the conditions for the further experiments. Airway fibroblasts were treated with dexamethasone 10-1000nM and TGFβ2 (10ng/ml) as a positive control in complete DMEM containing 0.4% FBS for 24-48h.

5.5.1.a) The optimum duration to stimulate airway fibroblasts with dexamethasone

To optimize the duration of treatment with dexamethasone, airway fibroblasts were treated with dexamethasone at 500nM, 1000nM or TGFβ2 (10 ng/ml) as a positive control for 24-48 h. This showed a trend for increased LOX mRNA after 24 h treatment. After 48 h, LOX mRNA increased 2-3 fold following dexamethasone treatment (Figure 5-1). Then 48 h time point was chosen for further experiments. Photomicrograph of airway fibroblasts after treatment with dexamethasone was shown in Figure 5-2.

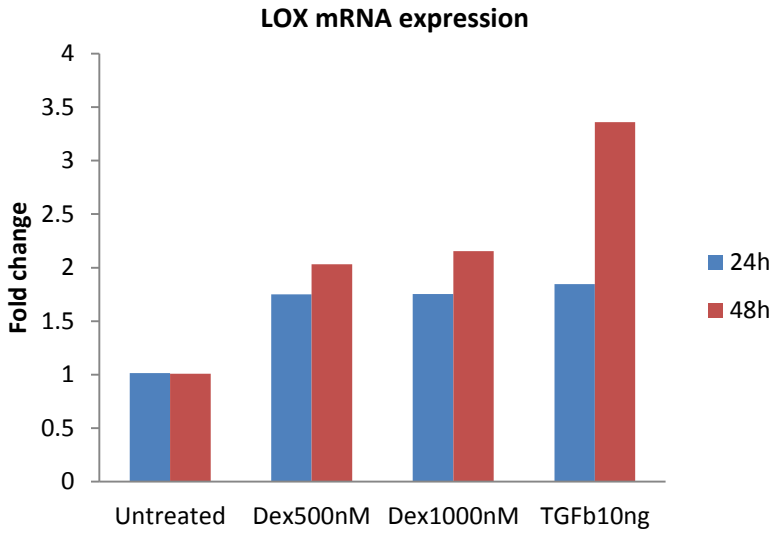

Figure 5-1: LOX mRNA expression after treatment with dexamethasone. Airway fibroblasts were treated with dexamethasone 500 nM, 1000 nM or TGFβ2 10ng/ml in 0.4% FBS complete DMEM for 24h or 48h. Total RNA was extracted and analysed for LOX mRNA. The values were normalized to the geometric mean of UBC/A2 and expressed relative to the expression observed in an untreated sample from a healthy non-asthmatic subject using the ΔΔCt method. Graphs represent mean value of triplicate wells of fibroblasts from one subject.

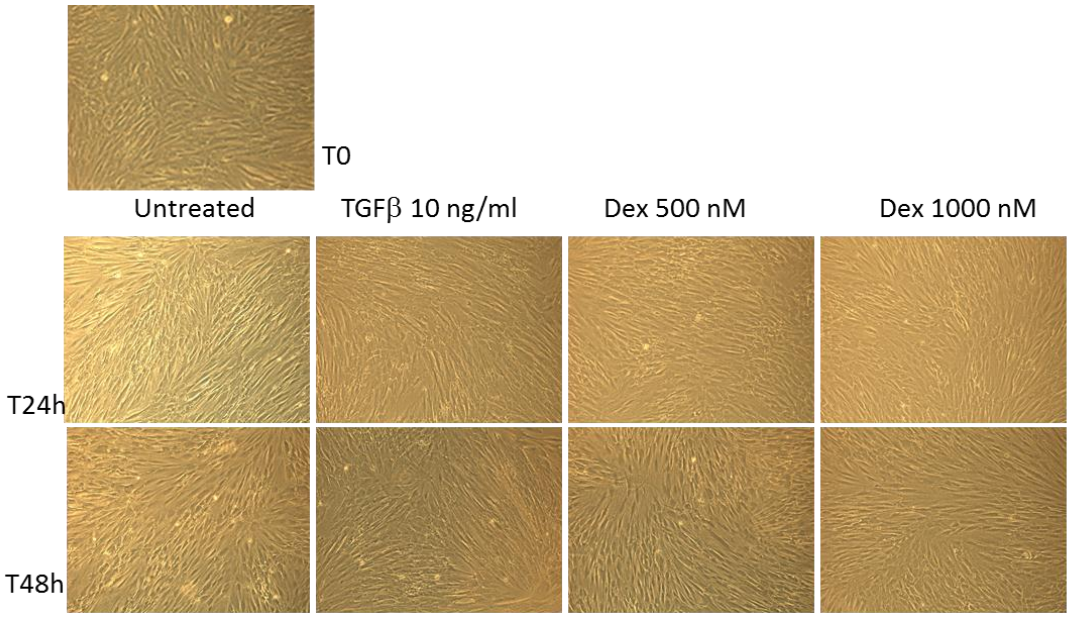

Figure 5-2: Photomicrographs of airway fibroblasts after treatment with TGFβ or dexamethasone for 24-48h. Fibroblasts from experiments shown in Figure 5-1 were imaged by phase contrast microscopy with the magnification X 20.

5.5.1.b) The optimum dose for treatment with dexamethasone

To investigate the optimum dose of dexamethasone required to induce LOX expression, airway fibroblasts were treated with dexamethasone 10-1000nM and TGFβ2 (10ng/ml) as a positive control for 48h. Total RNA was extracted for analysing LOX mRNA using RT-qPCR and LOX protein in culture supernatants were measured by western blot analysis. This revealed that dexamethasone up-regulated LOX mRNA in a dose dependent manner over the range 10-500 nM with the induction increasing by about 2.5 fold at doses between 100 nM and 500 nM, but the response decreased when dexamethasone was used at 1000 nM. However, the dexamethasone effect on LOX mRNA expression was not greater than the effect of TGFβ2 (Figure 5-3). This effect was confirmed in protein level: dexamethasone also enhanced the production of both Pro-LOX and active LOX, although the dose-dependently was not clear (Figure 5-4). Consequently, further experiments were done with dexamethasone at 100 and 500 nM.

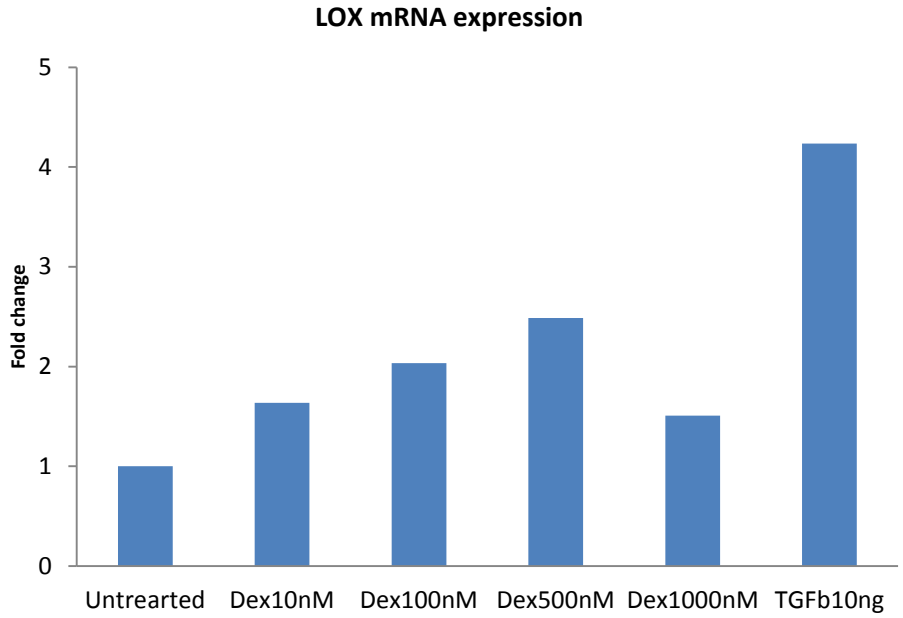

Figure 5-3: LOX mRNA expression after treatment of fibroblasts with dexamethasone 10-1000 nM. Airway fibroblasts were treated with dexamethasone 10 nM-1000 nM or TGFβ2 10 ng/ml in 0.4% FBS DMEM for 48h. Total RNA was extracted and analysed for LOX mRNA. The values were normalized to the geometric mean of UBC/A2 and expressed relative to the expression observed in an untreated sample from a non-asthmatic subject using the ΔΔCt method. Graphs represent mean value of triplicate wells of fibroblasts from one subject.

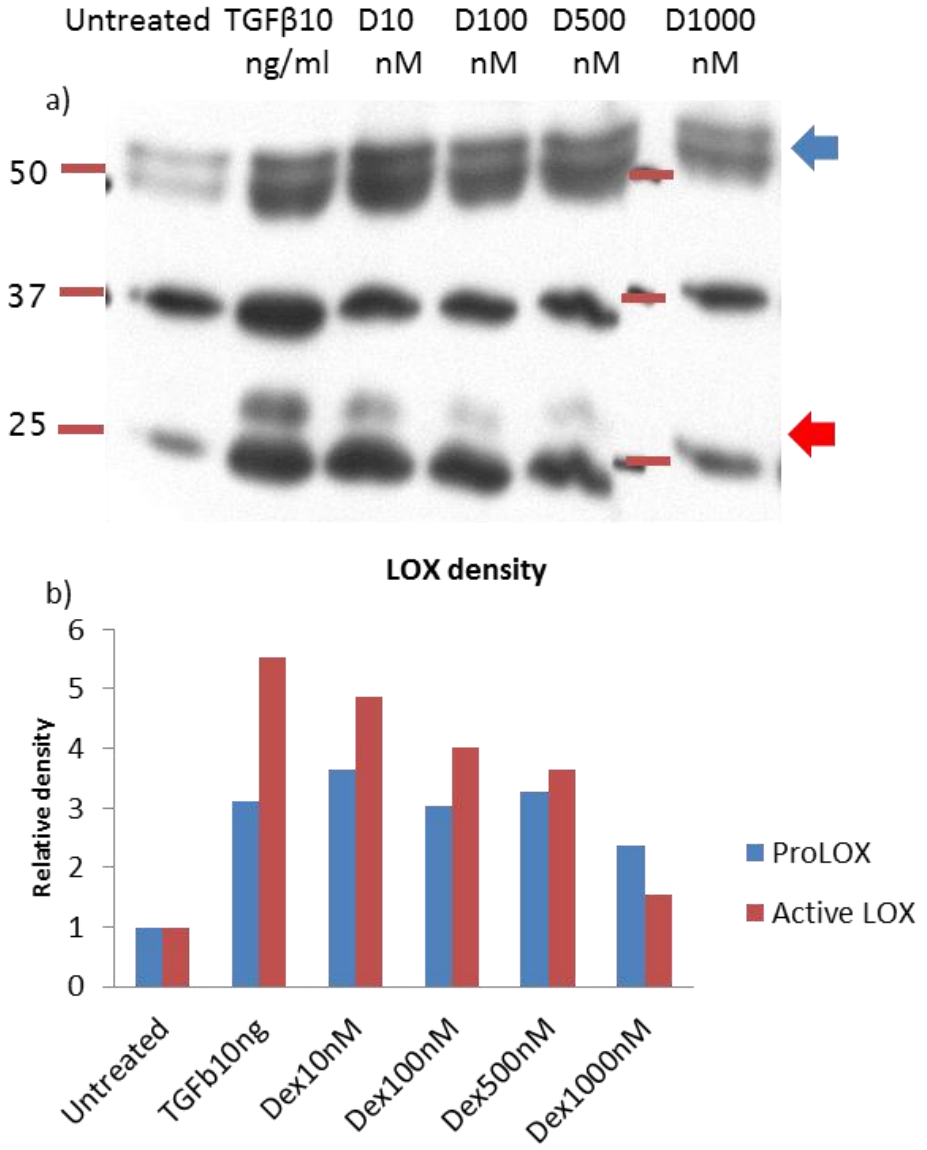

Figure 5-4: Dexamethasone enhanced the production of both Pro-LOX and active LOX. Airway fibroblasts were treated with TGFβ2 10ng/ml or dexamethasone 10-1000 nM in DMEM containing 0.4% FBS for 48h. Culture supernatants were concentrated with Strataclean® resin, then analysed by SDS-PAGE and immunoblotted using anti lysyl oxidase (LOX) antibodies. a) Representative LOX western blot of culture supernatants following dexamethasone treatment. The blue arrow indicates pro-LOX and the red arrow indicates active LOX. b) Pro-LOX and active LOX bands were quantified by densitometry using ImageJ and plotted as a ratio to the density of untreated samples. Graph shows the mean value of three densitometry measurements of one experiment. Blue bars demonstrate the density of Pro-LOX and red bars demonstrate the density of active LOX.

5.5.2) Dexamethasone up-regulated LOX mRNA in fibroblasts from asthmatic subjects but not in healthy non-asthmatic subjects

To compare the response between asthmatic and healthy non-asthmatic fibroblasts, airway fibroblasts from 6 healthy non-asthmatic and 6 severe asthmatic subjects (all were gifts from Dr David Summit and Dr Sarah Field) were treated with dexamethasone at 100 nM or 500 nM with or without TGFβ2 10 ng/ml for 48 h. By RT-qPCR, dexamethasone was found to significantly up-regulate LOX mRNA in fibroblasts from asthmatic subjects. There was a trend in up-regulation in fibroblasts from healthy non-asthmatic subjects but it did not reach statistical significance due to the inter-subjects variation. Furthermore, dexamethasone had an additive effect with TGFβ2 in up-regulating LOX mRNA in asthmatic fibroblasts (Figure 5-5). There was no significant difference in LOX mRNA expression between fibroblasts from healthy and asthmatic subjects.

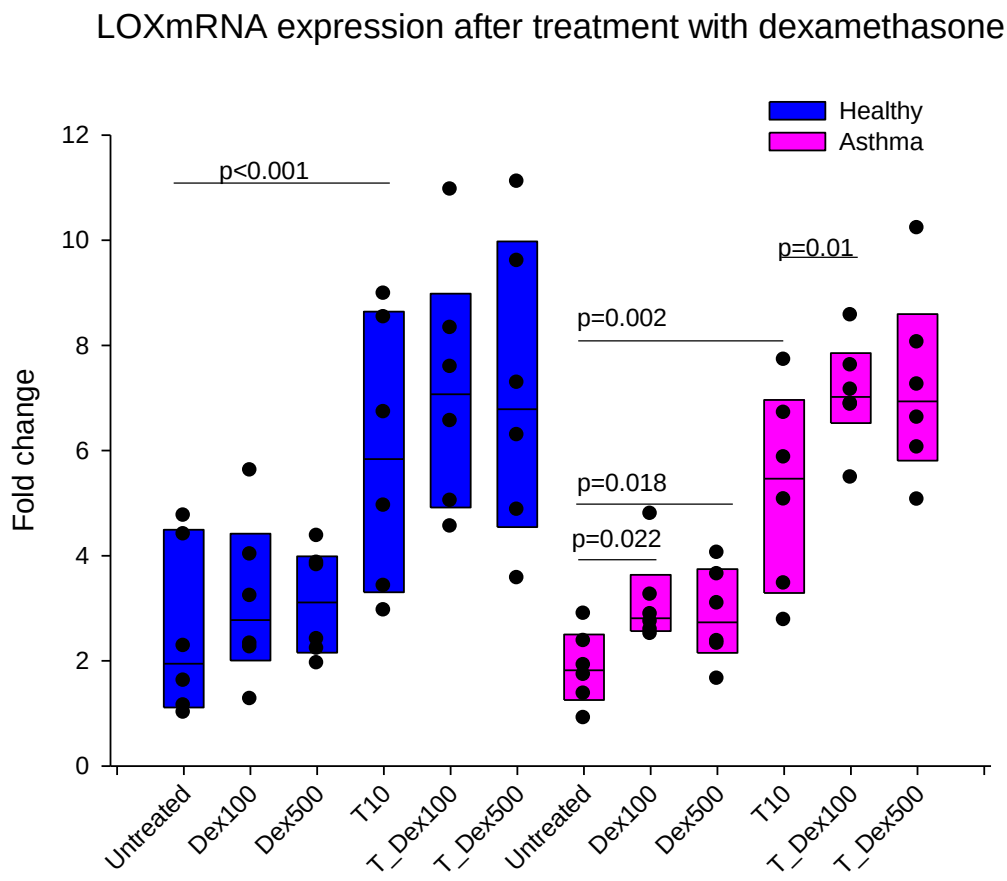

Figure 5-5: Dexamethasone up-regulated LOX mRNA expression in asthmatic fibroblasts but not in healthy non-asthmatic fibroblasts. Airway fibroblasts from 6 healthy non-asthmatic and 6 asthmatic subjects were treated with dexamethasone 100nM or 500nM in the presence or absence of TGFβ2 (10ng/ml) in 0.4% FBS complete DMEM for 48h. Total RNA was extracted and analysed for LOX mRNA. The values were normalized to the geometric mean of UBC/A2 and expressed relative to the lowest expression observed in an untreated sample from a healthy non-asthmatic subject using the ΔΔCt method. The individual data points are superimposed on a box plot showing median and IQR. Blue boxes indicate data from fibroblasts from healthy non-asthmatic subjects and pink boxes indicate those from asthmatic subjects. The data were tested for statistical significance using one way repeated measures ANOVA. Dex=Dexamethasone, T= TGFβ2 and T_Dex= TGFβ2+Dexamethasone.

5.5.3) Dexamethasone enhanced the production of LOX protein both in fibroblasts from healthy non-asthmatic and asthmatic subjects

To measure the level of LOX protein produced by airway fibroblasts from healthy non-asthmatic and asthmatic subjects, the culture supernatants from experiments from section 5.5.2) were measured for LOX protein by western blotting. Pro-LOX and active LOX bands were quantified by densitometry using ImageJ. The ratio of the density of Pro-LOX and active LOX to the paired untreated control sample was calculated. This revealed that in healthy non-asthmatic subjects, dexamethasone had a trend to enhance the production of Pro-LOX but it did not reach statistical significance. However, dexamethasone could activate Pro-LOX to become active LOX (Figure 5-6). In contrast, in asthmatic subjects, dexamethasone enhanced the production of both Pro-LOX and active LOX (Figure 5-7). This result is consistent with LOX mRNA result from section 5.5.2), which found that dexamethasone up-regulated LOX mRNA expression only in asthmatic fibroblasts. However, dexamethasone did not have an obvious effect over and above that of TGFβ2 in the production of LOX protein.

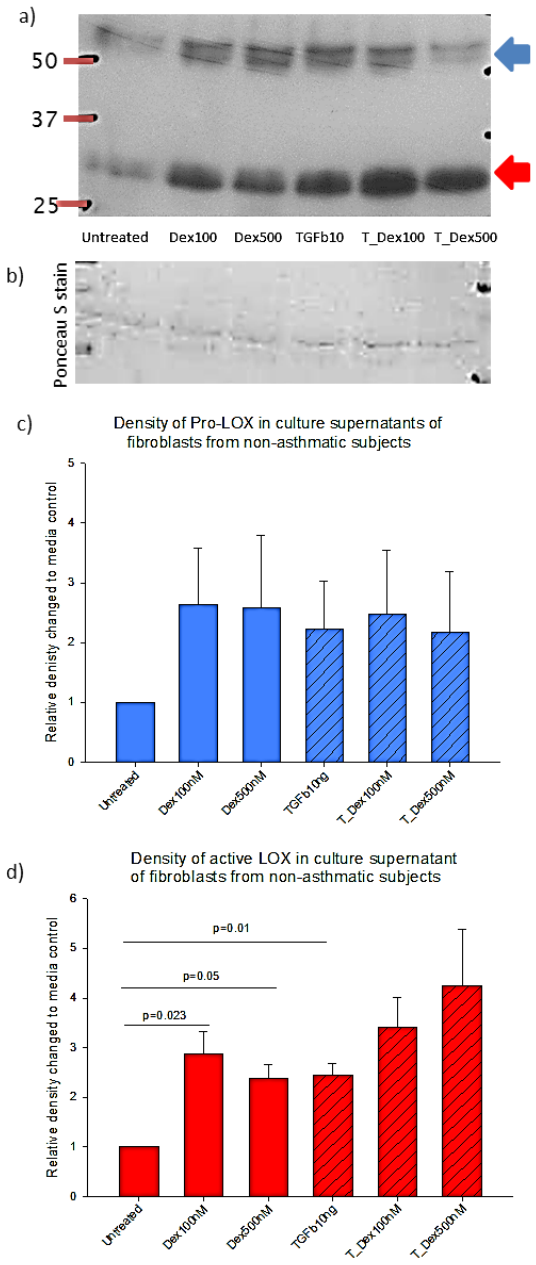

Figure 5-6: Dexamethasone enhanced the production of active LOX in fibroblasts from healthy non-asthmatic subjects. Culture supernatants of healthy non-asthmatic fibroblasts from experiments shown in Figure 5-5 were concentrated and analysed by SDS-PAGE and immunoblotted using anti lysyl oxidase (LOX) antibodies. Pro-LOX and active LOX bands were quantified by densitometry using ImageJ and plotted as the ratio of the density of each paired untreated sample. a) Representative LOX western blot. The blue arrow indicates Pro-LOX and the red arrow indicates active LOX. b) The blot was stained with Ponceau stain to show equal protein loading. Graphs show the mean ratio density of c) Pro-LOX and d) active LOX with standard error. Red bars indicate the density of active LOX. Blue bars indicate the density of Pro-LOX. Hatch bars indicate TGFβ treated experiments. The data were tested for statistical significance using one way repeated measures ANOVA.

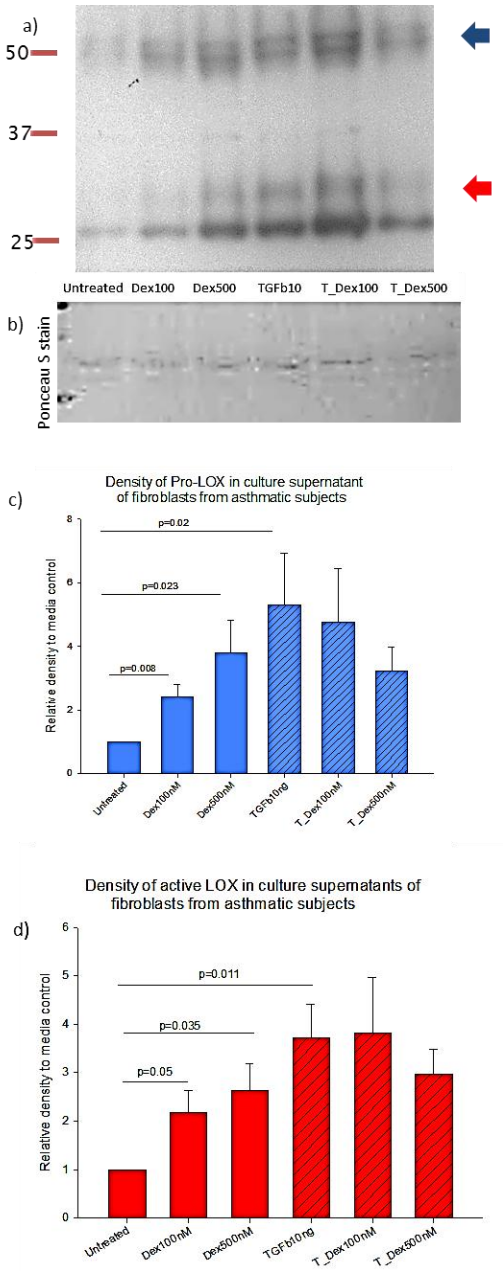

Figure 5-7: Dexamethasone enhanced the production of active LOX in fibroblasts from asthmatic subjects. Culture supernatants of asthmatic fibroblasts from experiments shown Figure 5-5 were concentrated and analysed by SDS-PAGE and immunoblotted using anti lysyl oxidase (LOX) antibodies. Pro-LOX and active LOX bands were quantified by densitometry using ImageJ and plotted as a ratio to the density of each paired untreated sample. a) Representative LOX western blot. The blue arrow indicates Pro-LOX and the red arrow indicates active LOX. b) The blot was stained with Ponceau stain to show equal protein loading. Graphs show the mean ratio density of c) Pro-LOX and d) active LOX with standard error. Red bars indicate the density of active LOX. Blue bars indicate the density of Pro-LOX. Hatch bars indicate TGFβ treated experiments. The data were tested for statistical significance using one way repeated measures ANOVA.

5.5.4) **Dexamethasone suppressed LH2b mRNA expression and suppressed the ability of TGFβ up-regulate LH2b mRNA in both fibroblasts from healthy non-asthmatic and asthmatic subjects**

It was shown from chapter 4 that TGFβ2 up-regulated LH2b mRNA both in fibroblasts from healthy non-asthmatic and asthmatic subjects. To determine the effect of dexamethasone on LH2b mRNA expression, cDNA from experiments described in section 5.5.2) were analysed for LH2b mRNA using RT-qPCR. This revealed that dexamethasone significantly suppressed LH2b mRNA expression in fibroblasts from asthmatic subjects but not in fibroblasts from healthy non-asthmatic subjects, although there was a trend for suppression in fibroblasts from healthy non-asthmatic subjects. Furthermore, the effect of TGFβ2 in up-regulating LH2b mRNA was significantly decreased after co-treatment with dexamethasone both in fibroblasts from healthy non-asthmatic and asthmatic subjects (Figurre5-8). There was no significant difference in LH2b mRNA expression between fibroblasts from healthy and asthmatic subjects.

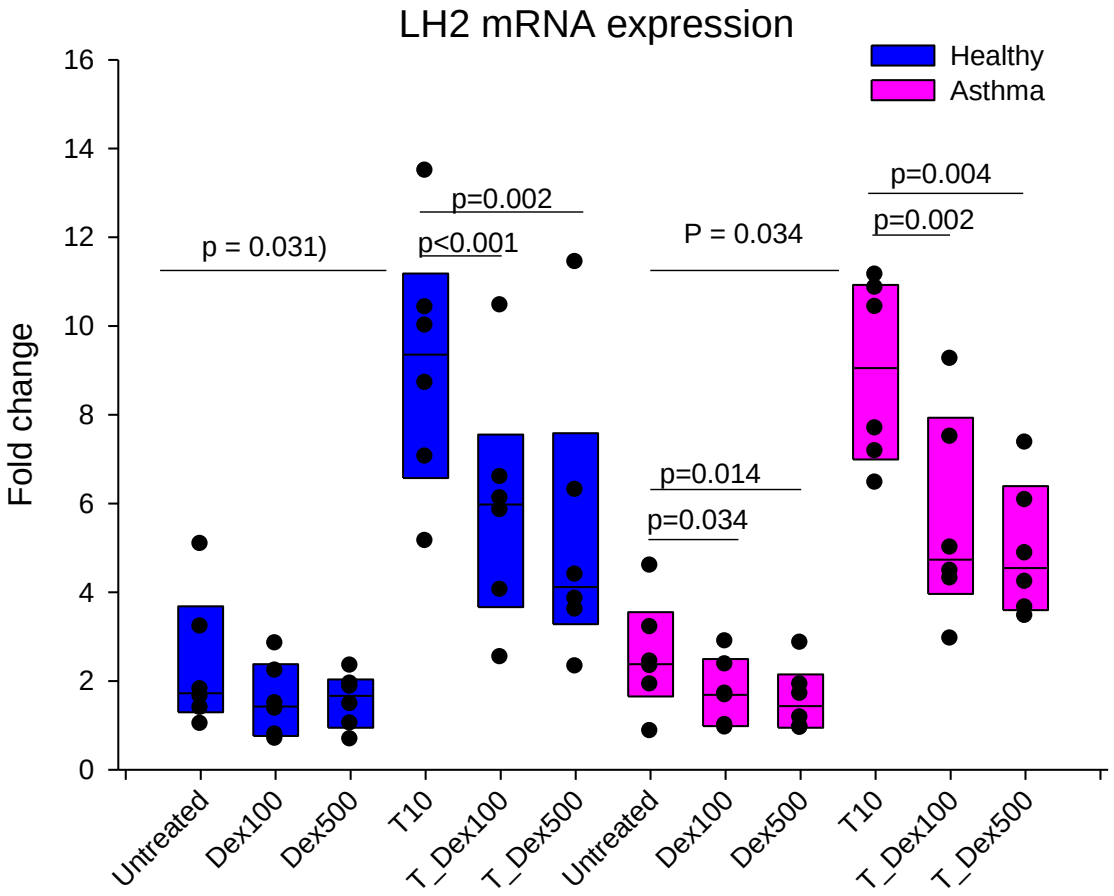

Figure 5-8: Dexamethasone suppressed LH2b mRNA expression and inhibited the ability of TGFβ2 up-regulate of LH2b mRNA. cDNA from experiments shown in Figure 5-5 were analysed for LH2b mRNA by RT-qPCR. The values were normalized to the geometric mean of UBC/A2 and expressed relative to the lowest expression observed in an untreated sample from a healthy non-asthmatic subject using the ΔΔCt method. The individual data points are superimposed on a box plot showing median and IQR. Blue boxes indicate data from fibroblasts from healthy non-asthmatic subjects and pink boxes indicate those from asthmatic subjects. The data were tested for statistical significance using one way repeated measures ANOVA. Dex=Dexamethasone, T= TGFβ2 and T_Dex= TGFβ2+Dexamethasone.

5.5.5) Dexamethasone had no effect on collagen mRNA expression in fibroblasts from healthy non-asthmatic and asthmatic subjects

Inhaled corticosteroids are a standard treatment for chronic asthma. Since collagen deposition in the airway is one of the characteristic of airway remodelling in asthma. The effect of dexamethasone on collagen mRNA expression was investigated. cDNA from experiments described in section 5.5.2) were analysed for collagen I and III mRNA expression. This revealed that TGFβ2 significantly up-regulated collagen I mRNA expression both in fibroblasts from healthy non-asthmatic and asthmatic subjects. However, there was no change of collagen I mRNA expression following treatment with dexamethasone. In addition, treatment with dexamethasone did not suppress up-regulation of collagen I mRNA expression by TGFβ2 (Figure 5-9). Dexamethasone and TGFβ2 had no effect on collagen III mRNA expression (Figure 5-10). There was no significant difference in collagen mRNA expression between fibroblasts from healthy and asthmatic subjects.

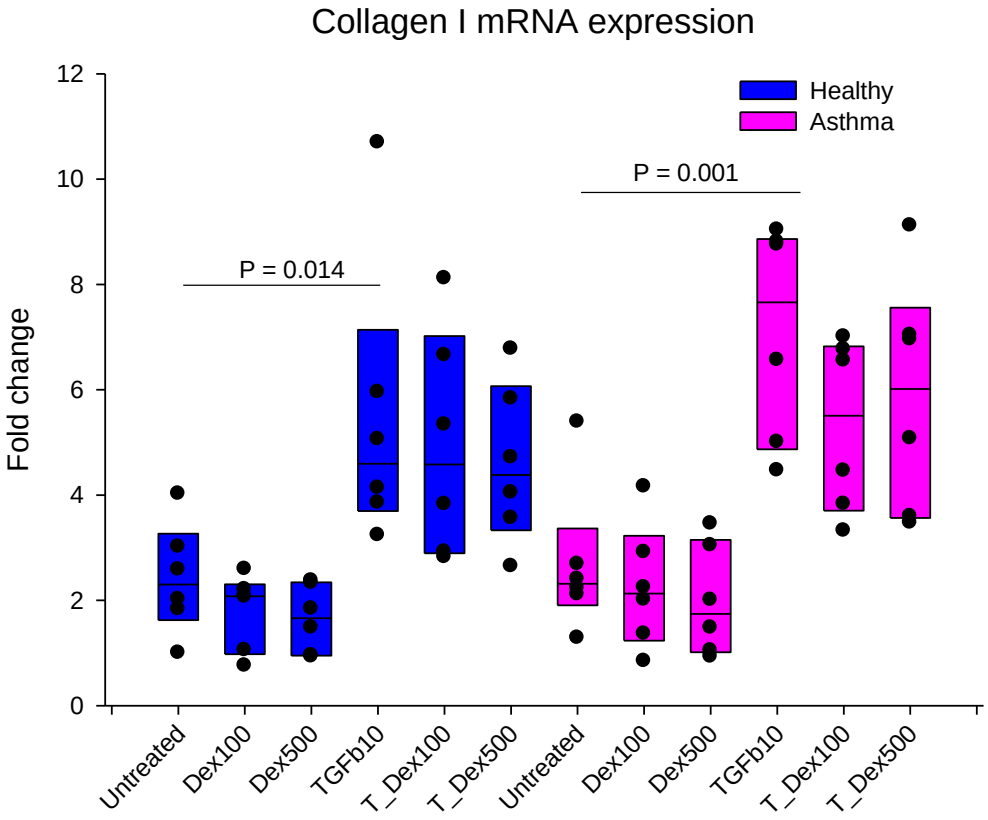

Figure 5-9: TGFβ2 up-regulated collagen I mRNA expression but dexamethasone had no effect on collagen I mRNA expression. The experiments are the same as shown in Figure 5-5. Collagen I mRNA was measured by RT-qPCR. The values were normalized to the geometric mean of UBC/A2 and expressed relative to the lowest expression observed in an untreated sample from a non-asthmatic subject using the ΔΔCt method. The individual data points are superimposed on a box plot showing median and IQR. Blue boxes indicate data from fibroblasts from healthy non-asthmatic subjects and pink boxes indicate those from asthmatic subjects. The data were tested for statistical significance using one way repeated measures ANOVA. Dex=Dexamethasone, T= TGFβ2 and T_Dex= TGFβ2+Dexamethasone.

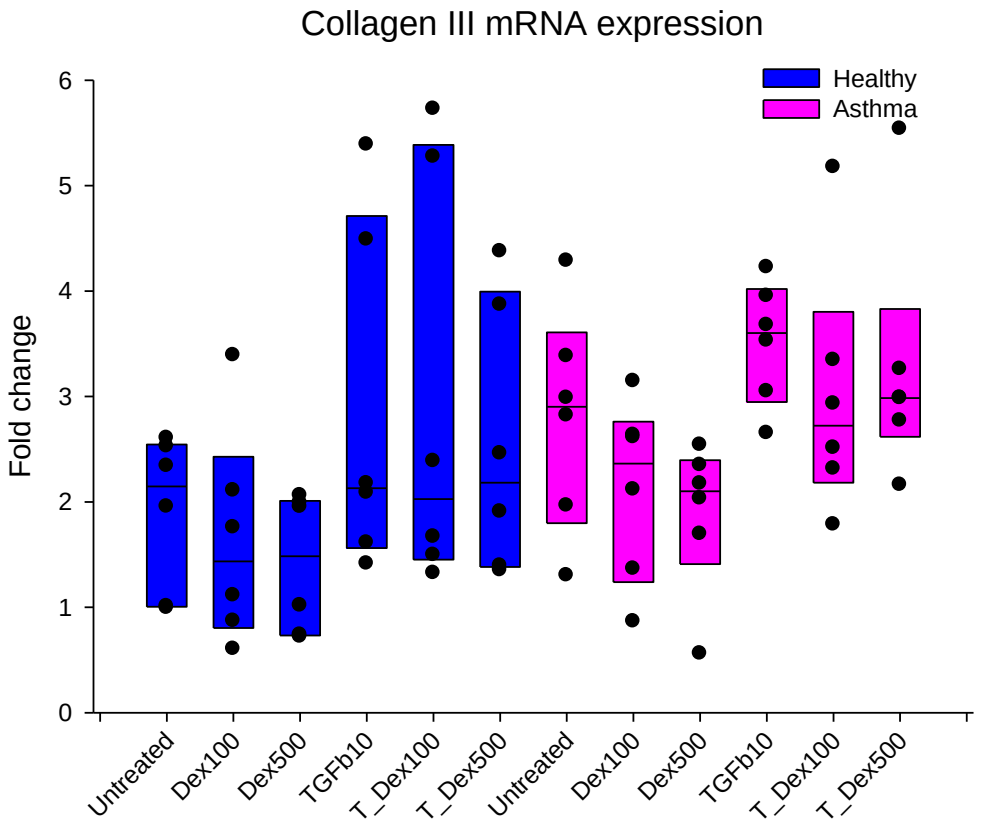

Figure 5-10: TGFβ2 and dexamethasone had no effect on collagen III mRNA expression. The experiments are the same as shown in Figure 5-5. Collagen III mRNA was measured by RT-qPCR. The values were normalized to the geometric mean of UBC/A2 and expressed relative to the lowest expression observed in an untreated sample from a non-asthmatic subject using the ΔΔCt method. The individual data points are superimposed on a box plot showing median and IQR. Blue boxes indicate data from fibroblasts from healthy non-asthmatic subjects and pink boxes indicate those from asthmatic subjects. The data were tested for statistical significance using one way repeated measures ANOVA. Dex=Dexamethasone, T= TGFβ2 and T_Dex= TGFβ2+Dexamethasone.

5.5.6) Dexamethasone suppressed up-regulation of biglycan mRNA expression by TGFβ2 in airway fibroblasts from healthy non-asthmatic and asthmatic subjects

Biglycan is involved in collagen fibril assembly, and it has been shown that TGFβ2 up-regulated biglycan mRNA in Chapter 4. Therefore, the effect of dexamethasone on biglycan mRNA expression was investigated using cDNA from experiment described in section 5.5.2). This revealed that dexamethasone suppressed the up-regulation of biglycan mRNA by TGFβ2 both in airway fibroblast from healthy non-asthmatic and asthmatic subjects (Figure 5-11). There was no significant difference in biglycan mRNA expression between fibroblasts from healthy and asthmatic subjects.

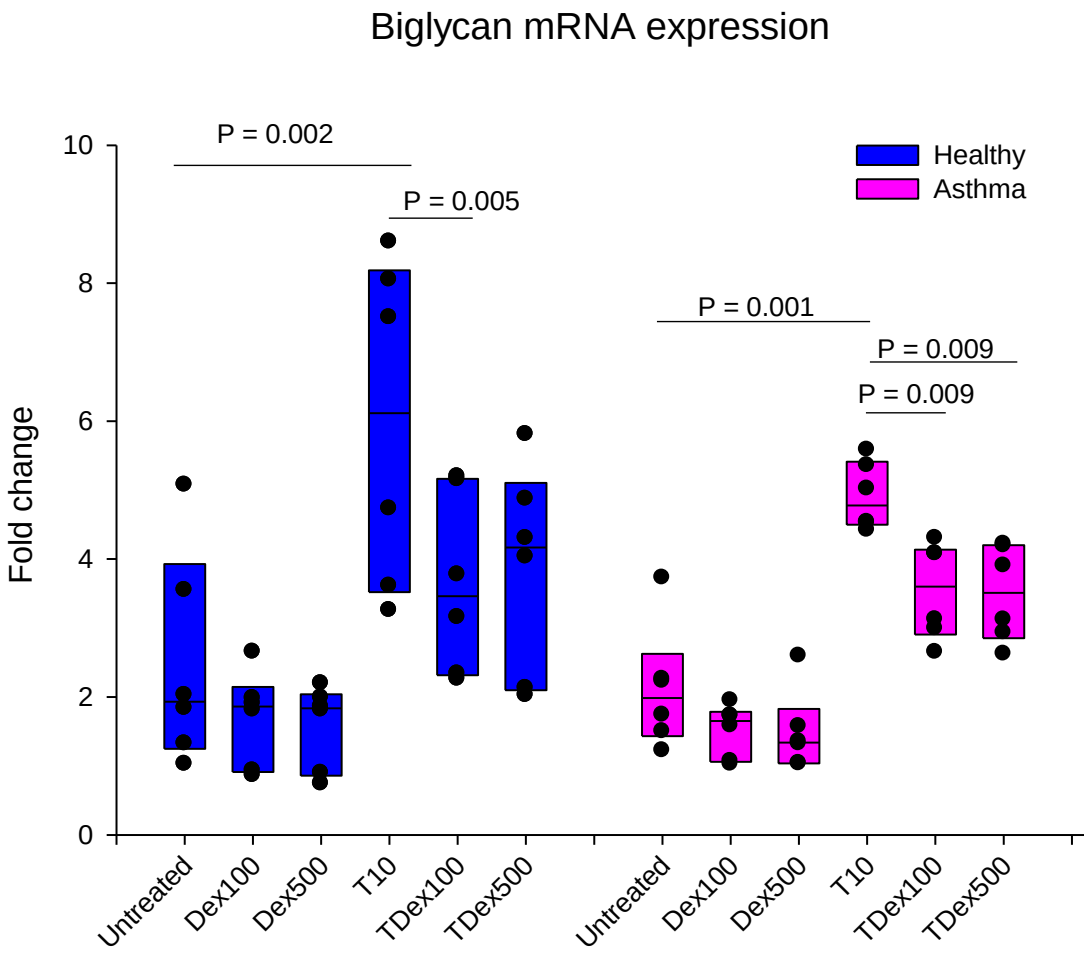

Figure 5-11: Dexamethasone suppressed biglycan mRNA up-regulation by TGFβ2. The experiments are the same as shown in Figure 5-5. Biglycan mRNA was measured by RT-qPCR. The values were normalized to the geometric mean of UBC/A2 and expressed relative to the lowest expression observed in an untreated sample from a healthy non-asthmatic subject using the ΔΔCt method. The individual data points are superimposed on a box plot showing median and IQR. Blue boxes indicate data from fibroblasts from healthy non-asthmatic subjects and pink boxes indicate those from asthmatic subjects. The data were tested for statistical significance using one way repeated measures ANOVA. Dex=Dexamethasone, T= TGFβ2 and T_Dex= TGFβ2+Dexamethasone.

5.5.7) Dexamethasone had no effect on the regulating of decorin in airway fibroblasts

Decorin also plays a role in collagen fibril assembly and its expression was suppressed by TGFβ2 as shown in Chapter 4. To investigate the effect of dexamethasone on decorin mRNA expression, cDNA from experiments described in section 5.5.2) were analysed for decorin mRNA by RT-qPCR. This revealed that dexamethasone had no effect on decorin mRNA expression in airway fibroblasts and did not affect the suppression effect of TGFβ2 on decorin mRNA expression. Co-treatment of cells with TGFβ2 and dexamethasone has similar effects on decorin mRNA expression as treatment with TGFβ2 alone (Figure 5-12). There was no significant difference in decorin mRNA expression between fibroblasts from healthy and asthmatic subjects.

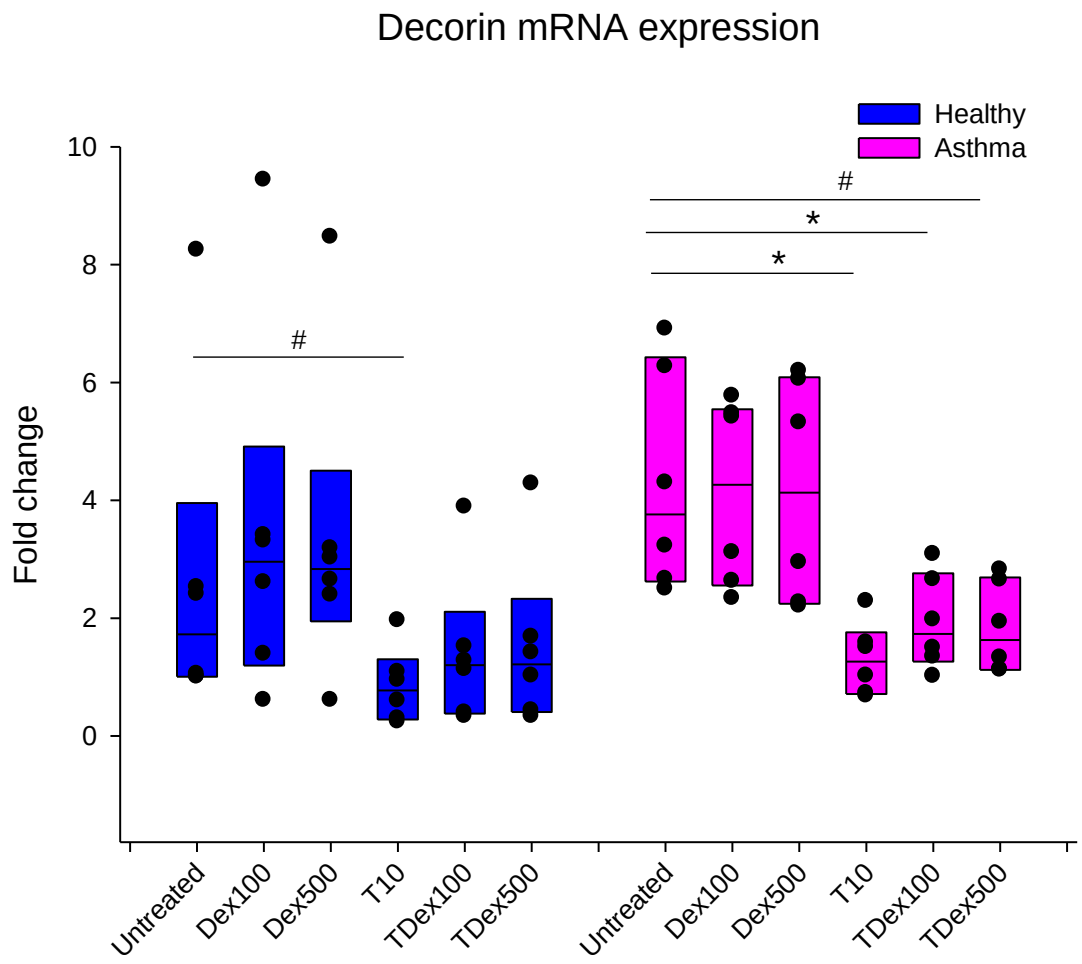

Figure 5-12: Dexamethasone had no effect on the regulation of decorin mRNA expression. The experiments are the same as shown in Figure 5-5. Decorin mRNA expression was measured by RT-qPCR. The values were normalized to the geometric mean of UBC/A2 and expressed relative to the lowest expression observed in an untreated sample from a healthy non-asthmatic subject using the ΔΔCt method. The individual data points are superimposed on a box plot showing median and IQR. Blue boxes indicate data from fibroblasts from healthy non-asthmatic subjects and pink boxes indicate those from asthmatic subjects. The data were tested for statistical significance using one way repeated measures ANOVA. Dex=Dexamethasone, T= TGFβ2 and T_Dex= TGFβ2+Dexamethasone. # $p < 0.03$, *$p<0.01$.

5.5.8) **The effect of dexamethasone and TGFβ2 on lung fibroblasts from a donor with interstitial lung disease**

Chronic bronchiolitis with constrictive obliterative bronchiolitis is one of the interstitial lung diseases (ILD) characterized by fibrosis occurring predominantly in the membranous and respiratory bronchioles (237). To compare the response of fibroblasts from fibrotic lungs with those from healthy non-asthmatic and asthmatic airways, fibroblasts from a patient diagnosed with chronic bronchiolitis with constrictive obliterative bronchiolitis were treated with dexamethasone 100 nM or 500nM and TGFβ2 (10 mg/ml) in complete DMEM containing 0.4% FBS for 24 or 48h. However, the cell viability was poor after 48 h stimulation (Figure 5-13). Consequently, further experiments were undertaken only at 24 h stimulation.

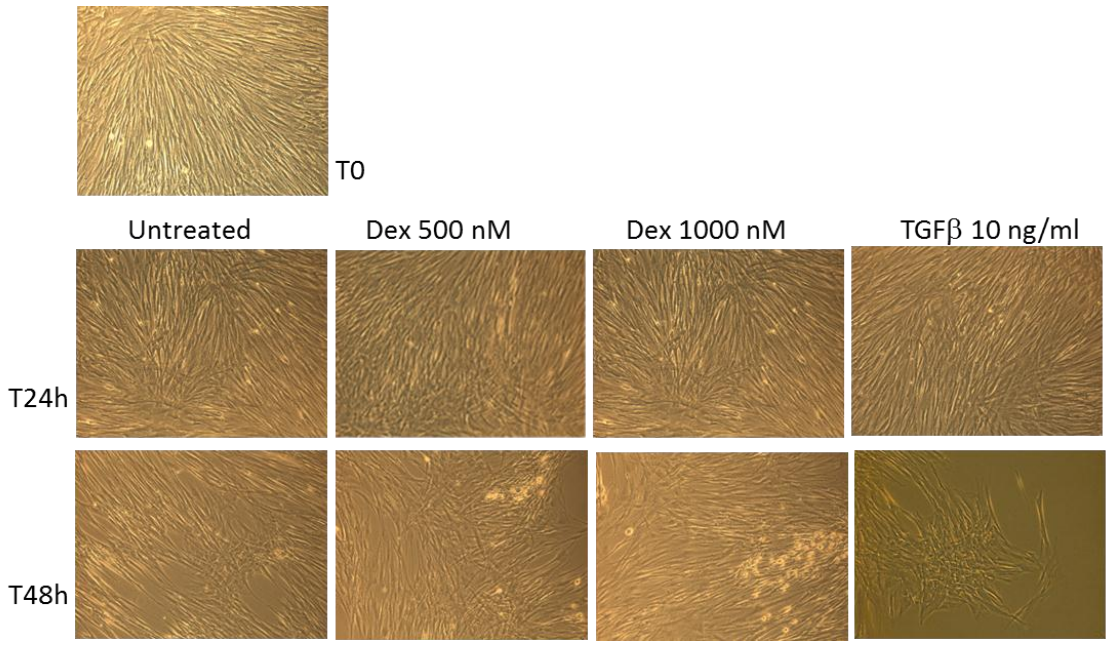

Figure 5-13: Photomicrographs of lung fibroblasts from an ILD patient after treatment with dexamethasone or TGFβ for 24-48h. Lung fibroblasts from an ILD patients were stimulated with dexamethasone 500 nM, 1000 nM or TGFβ 10 ng/ml in complete DMEM containing 0.4% FBS for 24h and 48h. The cells were viewed by phase contrast microscope with the magnification X20.

5.5.8.a) TGFβ2 and Dexamethasone up-regulated LOX mRNA in lung fibroblasts from the ILD subject

To evaluate the response of fibroblasts from fibrotic lungs, the fibroblasts were treated with dexamethasone 100 nM or 500 nM with or without TGFβ2 (10 ng/ml) for 24h. Total RNA was extracted and LOX mRNA was analysed using RT-qPCR. These results were compared to LOX mRNA expression of fibroblasts from healthy non-asthmatic healthy and asthmatic subjects from section 5.5.2). This revealed that TGFβ2 up-regulated LOX mRNA expression in all groups. Dexamethasone tended to up-regulate LOX mRNA expression in all group but this was significant only in fibroblasts from asthmatic and ILD subjects. Dexamethasone also had an additive effect to TGFβ2 in up-regulating LOX mRNA only in fibroblasts from asthmatic subjects. The similar trends of responses were seen in fibroblasts from the ILD patient but there was no statistical significance due to the low statistical power (Figure 5-14).

.

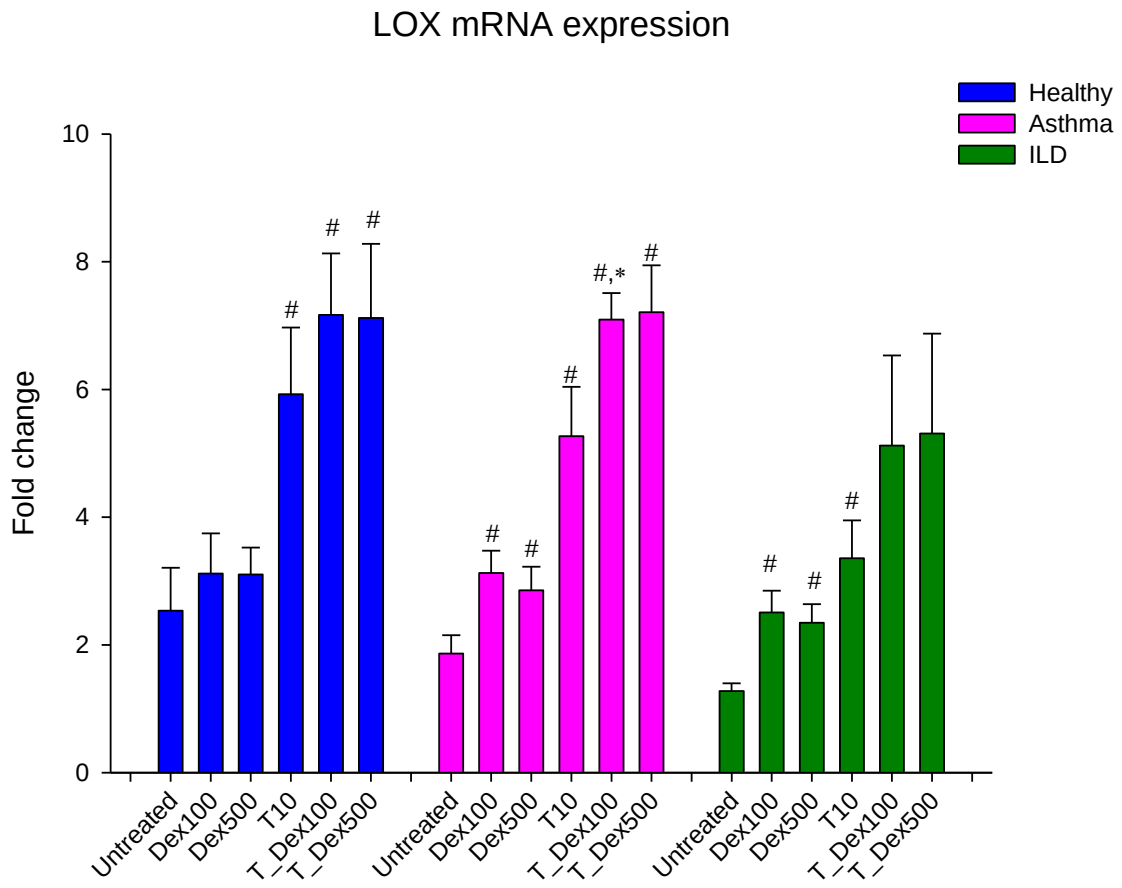

Figure 5-14: TGFβ2 up-regulated LOX mRNA expression in fibroblasts from healthy non-asthmatic, asthmatic airways and ILD lungs. The experiments for healthy non-asthmatic (N=6) and asthmatic subjects (N=6) are the same as shown in Figure 5-5, and lung fibroblasts from one ILD subject were treated with dexamethasone 100nM or 500nM in the presence or absence of TGFβ2 10ng/ml in 0.4% FBS DMEM for 24h. Total RNA was extracted and analysed for LOX mRNA using RT-qPCR. Data are from 3 separate experiments from one ILD subject. The values were normalized to the geometric mean of UBC/A2 and expressed relative to the lowest expression observed in an untreated sample of a healthy non-asthmatic subject using ΔΔCt method. The data are presented as mean and standard error and tested for statistical significance using one way repeated measures ANOVA. Blue boxes indicate data from fibroblasts from healthy non-asthmatic subjects, pink boxes indicate those from asthmatic subjects and green boxes indicate those from an ILD subject. # $p < 0.05$ when compared to untreated samples, *$p<0.05$ when compared to TGFβ2 treated samples.

5.5.8.b) TGFβ2 and Dexamethasone enhanced the production of LOX in lung fibroblasts from the ILD subject

To measure LOX protein secreted by lung fibroblasts from the ILD patient following TGFβ2 and dexamethasone stimulation, the culture supernatants from the experiments described in section 5.5.8.a) were concentrated using Strataclean® resin and measured for LOX protein using western blotting. The ratio of the density of Pro-LOX and active LOX to the paired untreated control samples was calculated. This revealed that TGFβ2 and dexamethasone had a trend to enhance the production of Pro-LOX and LOX active, but there was no statistical significance due to the low statistical power. Co- treatment of dexamethasone and TGFβ2 significantly enhanced the production of active LOX protein (Figure 5-15).

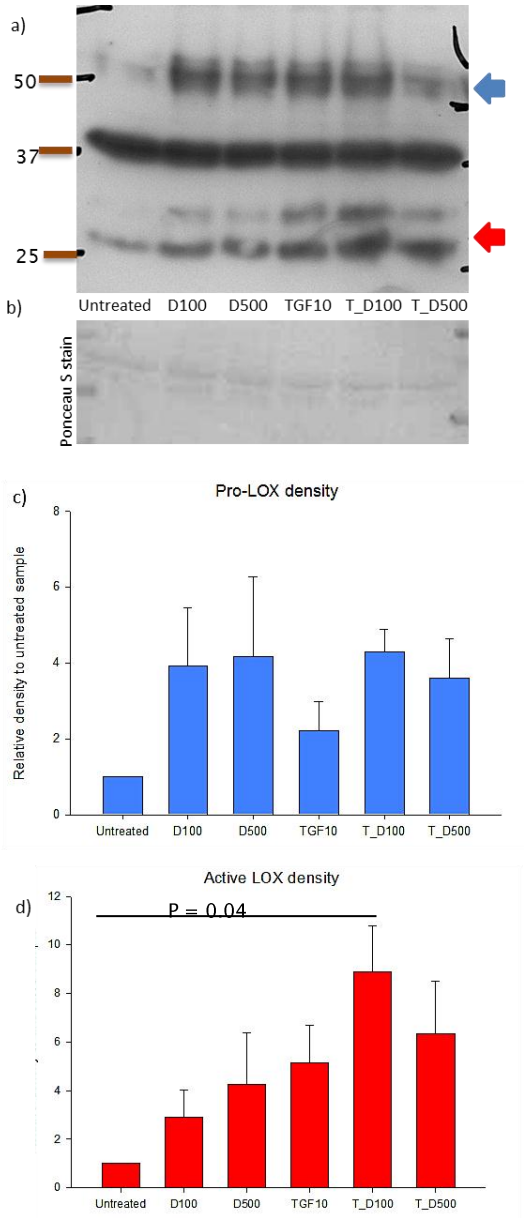

Figure 5-15: TGFβ2 and Dexamethasone enhanced the production of LOX by lung fibroblasts from a patient with interstitial lung disease. Culture supernatants from experiments shown in Figure 5-14 were concentrated and analysed by SDS-PAGE and immunoblotted using anti lysyl oxidase (LOX) antibodies. Pro-Lox and active LOX bands were quantified by densitometry using ImageJ and plotted as a ratio of the density of Pro-LOX and active LOX to the paired untreated control samples. a) Representative LOX western blot. b) The blot was stained with Ponceau stain to show equal protein loadings. Graphs show the mean ratio density with standard error of Pro-LOX in c) and active LOX in d). The blue arrow indicates Pro-LOX and the red arrow indicates active LOX. The data were tested for statistical significance using one way repeated measures ANOVA. Data are from 3 independent experiments from one subject. Dex=Dexamethasone, T= TGFβ2 and T_Dex= TGFβ2+Dexamethasone.

5.5.8.c) TGFβ2 up-regulated LH2b mRNA expression in lung fibroblasts from the ILD subject

To investigate LH2b mRNA expression in fibroblasts from fibrotic lungs following stimulation with TGFβ2 and dexamethasone, the cDNA samples from experiments described in section 5.5.8.a) were analysed for LH2b mRNA using RT-qPCR. The result was then compared to LH2b mRNA expression of fibroblasts from healthy non-asthmatic and asthmatic subjects from section 5.5.4). This revealed that TGFβ2 up-regulated LH2b mRNA expression in all groups. This effect was suppressed by dexamethasone when co-treatment with TGFβ2 in healthy non-asthmatic and asthmatic group. However, LH2b mRNA expression in fibroblasts stimulated with TGFβ2 and dexamethasone co-cultured was significantly higher than that in untreated fibroblasts. A similar trend was seen in an ILD subject but it did not reach statistically significant due to a low statistical power. In addition, dexamethasone modestly suppressed LH2b mRNA expression from approximately 3 fold increase to 1.5 fold increase only in fibroblasts from asthmatic subjects (Figure 5-16).

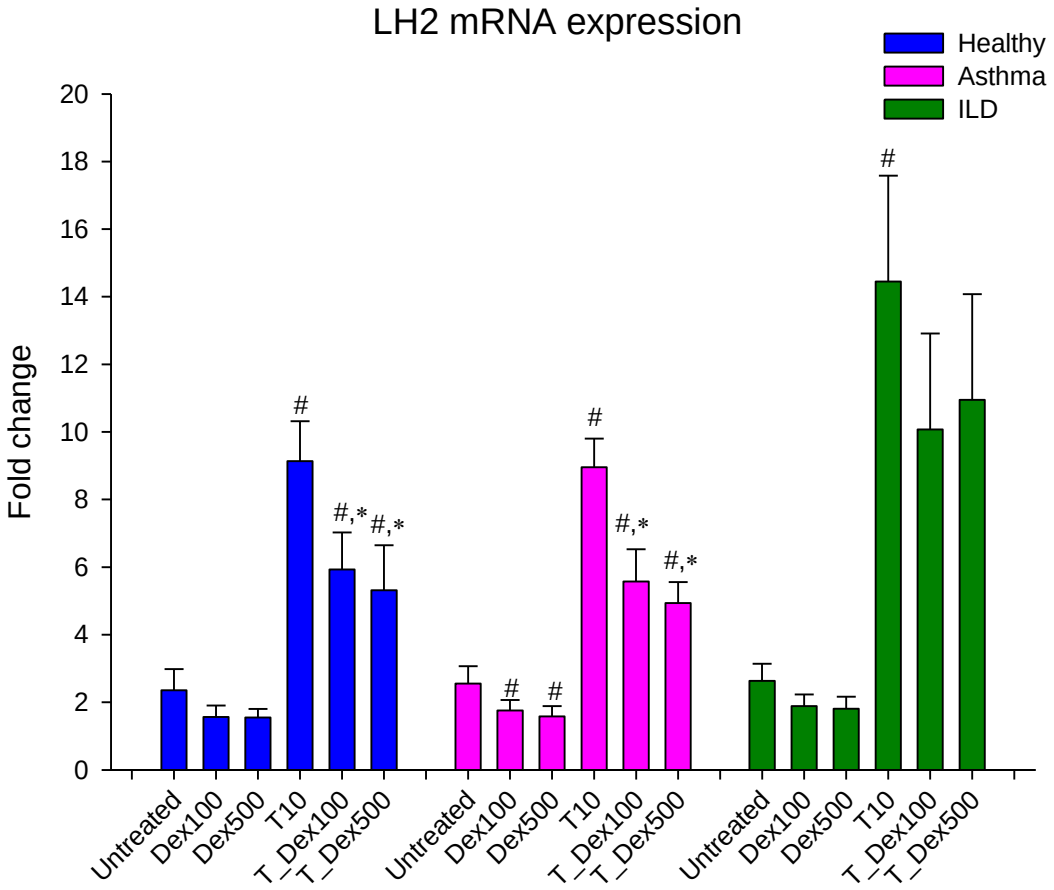

Figure 5-16: TGFβ2 up-regulated LH2b mRNA expression in fibroblasts from healthy non-asthmatic, asthmatic airways and ILD lungs. The experiments for fibroblasts from healthy non-asthmatic (N=6) and asthmatic subjects (N=6) are the same as shown in Figure 5-5, and those from an ILD patient are the same as Figure 5-14. The samples were analysed for LH2b mRNA using RT-qPCR. The values were normalized to the geometric mean of UBC/A2 and expressed relative to the lowest expression observed in an untreated sample of a healthy non-asthmatic subject using ΔΔCt method. The data are presented as mean and standard error and tested for statistical significance using one way repeated measures ANOVA. Blue boxes indicate data from fibroblasts from healthy non-asthmatic subjects, pink boxes indicate those from asthmatic subjects and green boxes indicate those from an ILD subject. # $p < 0.05$ when compared to untreated samples, *$p<0.05$ when compared to $TGF\beta_2$ treated samples. Dex=Dexamethasone, T= TGFβ2 and T_Dex= TGFβ2+Dexamethasone.

5.5.8.d) TGFβ2 up-regulated collagen mRNA expression but dexamethasone had no effect on collagen mRNA expression in fibroblasts from the ILD subject

Since the characteristic feature of fibrotic lung is an increase collagen deposition, collagen mRNA expression in fibroblasts from fibrotic lungs following stimulation with TGFβ2 and dexamethasone was compared with expression in fibroblasts from healthy non-asthmatic and asthmatic subjects. The samples from section 5.5.8.a) were analysed for collagen I and III mRNA expression using RT-qPCR. These results were then compared to collagen mRNA expression of fibroblasts from healthy non-asthmatic and asthmatic subjects from section 5.5.5). This revealed that TGFβ2 up-regulated collagen I mRNA expression in fibroblasts from healthy non-asthmatic and asthmatic subjects. A similar trend was seen in cells from the ILD subject but there was no statistical significance. In contrast to TGFβ2, dexamethasone had no effect on collagen I mRNA expression in all groups. Treatment with dexamethasone did not suppress collagen I gene up-regulation by TGFβ2 (Figure 5-17). Collagen III mRNA expression did not change following stimulation with TGFβ2 and dexamethasone in all groups (Figure 5-18).

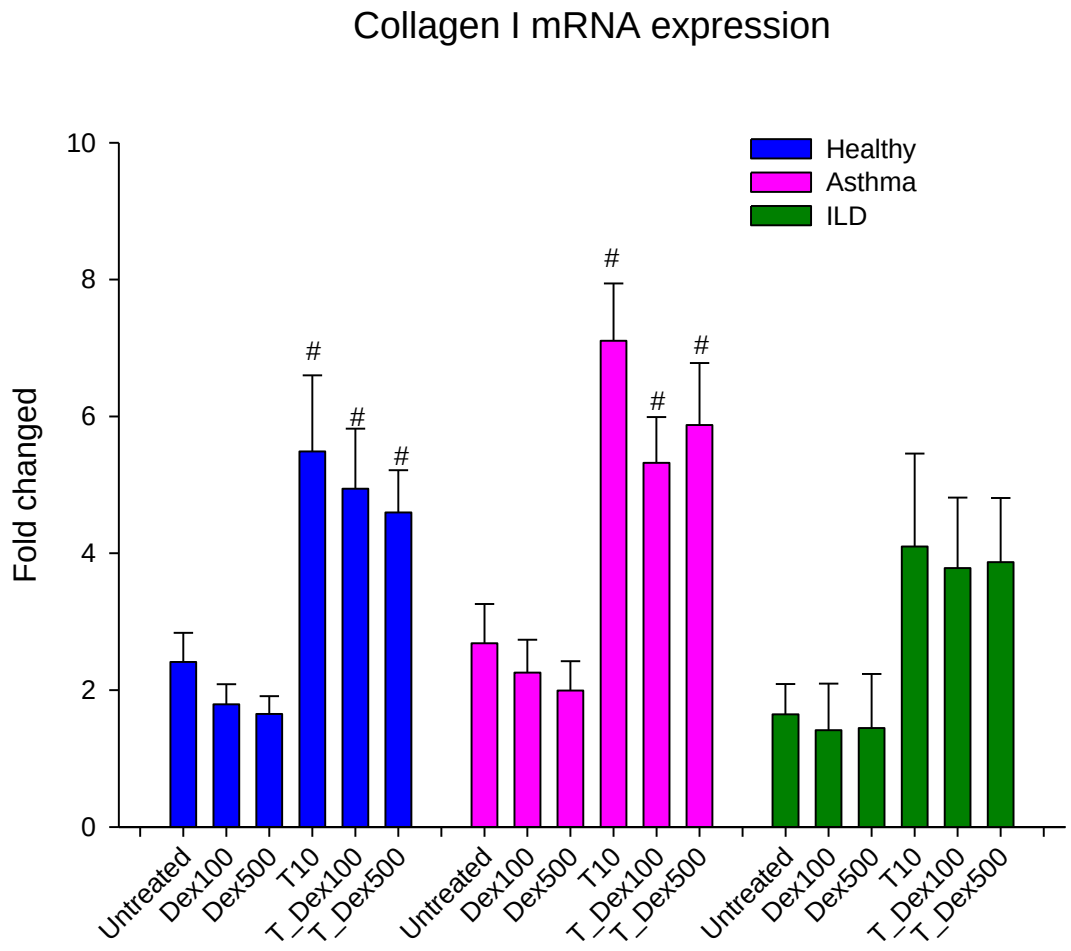

Figure 5-17: TGFβ2 up-regulated collagen I mRNA expression in fibroblasts from healthy non-asthmatic, asthmatic airways and ILD lungs. The experiments for fibroblasts from healthy non-asthmatic (N=6) and asthmatic subjects (N=6) are the same as Figure 5-5, and those from an ILD patient are the same as Figure 5-14. The samples were analysed for collagen I mRNA using RT-qPCR. The values were normalized to the geometric mean of UBC/A2 and expressed relative to the lowest expression observed in an untreated sample of a healthy non-asthmatic subject using ΔΔCt method. The data are presented as mean and standard error and tested for statistical significance using one way repeated measures ANOVA. Blue boxes indicate data from fibroblasts from healthy non-asthmatic subjects, pink boxes indicate those from asthmatic subjects and green boxes indicate those from an ILD subject. # $p < 0.05$ when compared to untreated samples. Dex=Dexamethasone, T= TGFβ2 and T_Dex= TGFβ2+Dexamethasone.

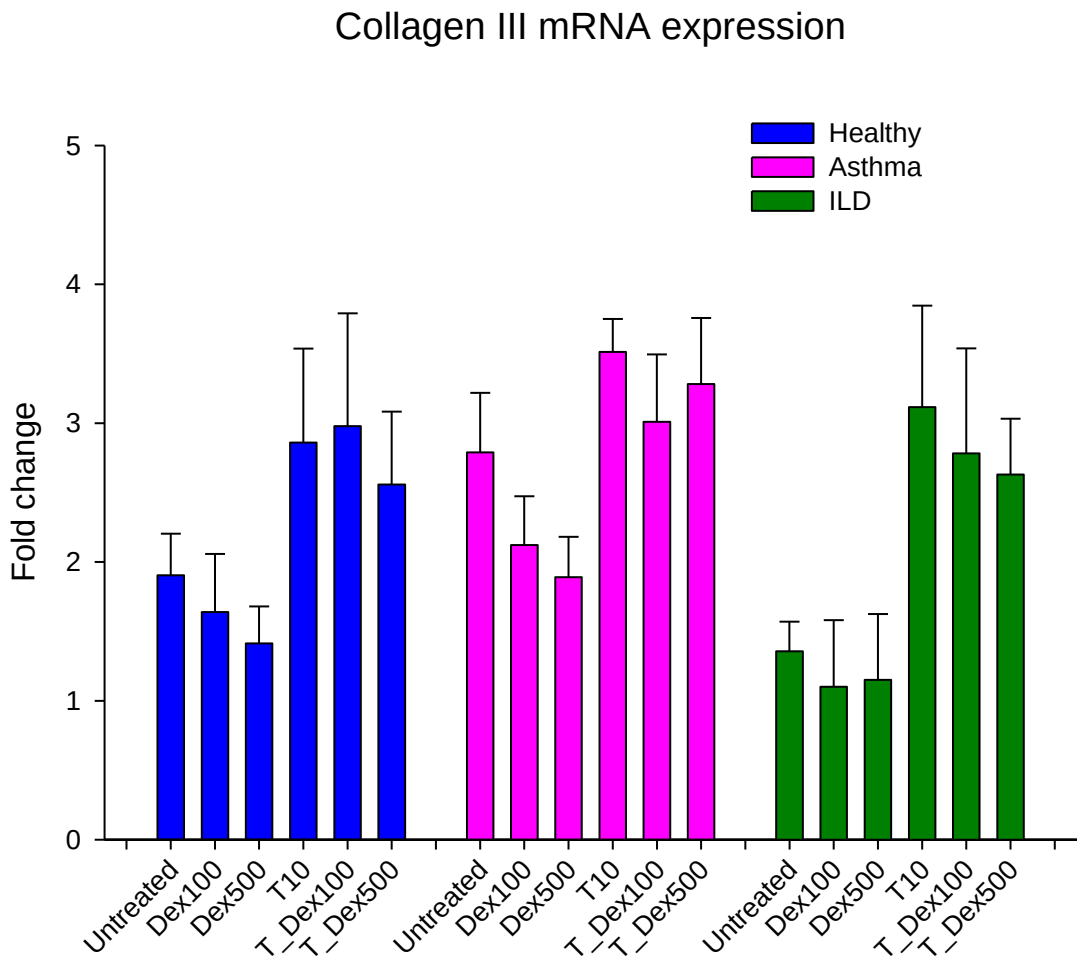

Figure 5-18: Collagen III mRNA expression in fibroblasts from healthy non-asthmatic, asthmatic airways and ILD lungs. The experiments for fibroblasts from healthy non-asthmatic (N=6) and asthmatic subjects (N=6) are the same as shown in Figure 5-5, and those from an ILD patient are the same as Figure 5-14. The samples were analysed for collagen III mRNA using RT-qPCR. The values were normalized to the geometric mean of UBC/A2 and expressed relative to the lowest expression observed in an untreated sample of a healthy non-asthmatic subject using ΔΔCt method. The data are presented as mean and standard error and tested for statistical significance using one way repeated measures ANOVA. Blue boxes indicate data from fibroblasts from healthy non-asthmatic subjects, pink boxes indicate those from asthmatic subjects and green boxes indicate those from an ILD subject. Dex=Dexamethasone, T= TGFβ2 and T_Dex= TGFβ2+Dexamethasone.

5.5.8.e) TGFβ2 suppressed decorin mRNA expression but dexamethasone had no effect in regulating decorin in lung fibroblasts from the ILD subject

To investigate decorin mRNA expression in fibroblasts from fibrotic lungs following stimulation with TGFβ2 and dexamethasone, the samples from section 5.5.8.a) were analysed for decorin mRNA using RT-qPCR. The result was then compared to decorin mRNA expression of fibroblasts from healthy non-asthmatic and asthmatic subjects from section 5.5.7). This showed that decorin mRNA expression was suppressed upon TGFβ2 stimulation in all groups. In contrast to TGFβ2, dexamethasone had no effect on decorin mRNA expression (Figure 5-19).

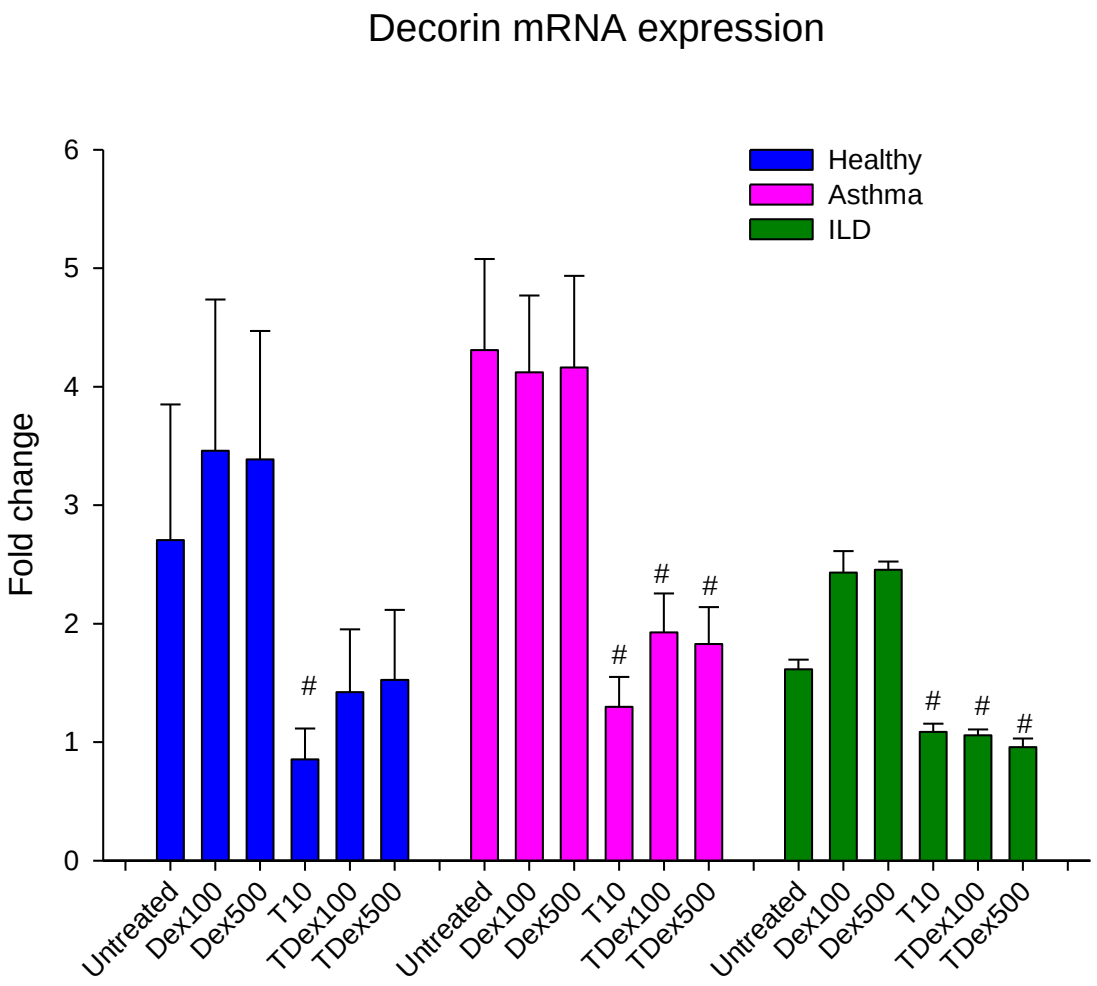

Figure 5-19: TGFβ2 suppressed decorin mRNA expression in fibroblasts from heathy non-asthmatic, asthmatic airways and ILD lungs. The experiments for fibroblasts from healthy non-asthmatic (N=6) and asthmatic subjects (N=6) are the same as shown in Figure 5-5, and those from an ILD patient are the same as Figure 5-14. The samples were analysed for decorin mRNA using RT-qPCR. The values were normalized to the geometric mean of UBC/A2 and expressed relative to the lowest expression observed in an untreated sample of a healthy non-asthmatic subject using ΔΔCt method. The data are presented as mean and standard error and tested for statistical significance using one way repeated measures ANOVA. Blue boxes indicate data from fibroblasts from healthy non-asthmatic subjects, pink boxes indicate those from asthmatic subjects and green boxes indicate those from an ILD subject. # $p < 0.05$ when compared to untreated samples. Dex=Dexamethasone, T= TGFβ2 and T_Dex= TGFβ2+Dexamethasone.

5.5.8.f) Dexamethasone suppressed biglycan mRNA up-regulation by TGFβ2 in lung fibroblasts from the ILD subject

Biglycan mRNA expression in fibroblasts from fibrotic lungs following stimulation with TGFβ2 and dexamethasone was compared with those from healthy non-asthmatic and asthmatic subjects. The samples from section 5.5.8.a) were analysed for biglycan mRNA expression using RT-qPCR. The results were then compared to biglycan mRNA expression of fibroblasts from healthy non-asthmatic and asthmatic subjects from section 5.5.6). This revealed that TGFβ2 up-regulated biglycan mRNA expression, but dexamethasone had no effect on biglycan mRNA expression in all groups. However, dexamethasone suppressed the TGFβ2 induced up-regulation of biglycan mRNA (Figure 5-20).

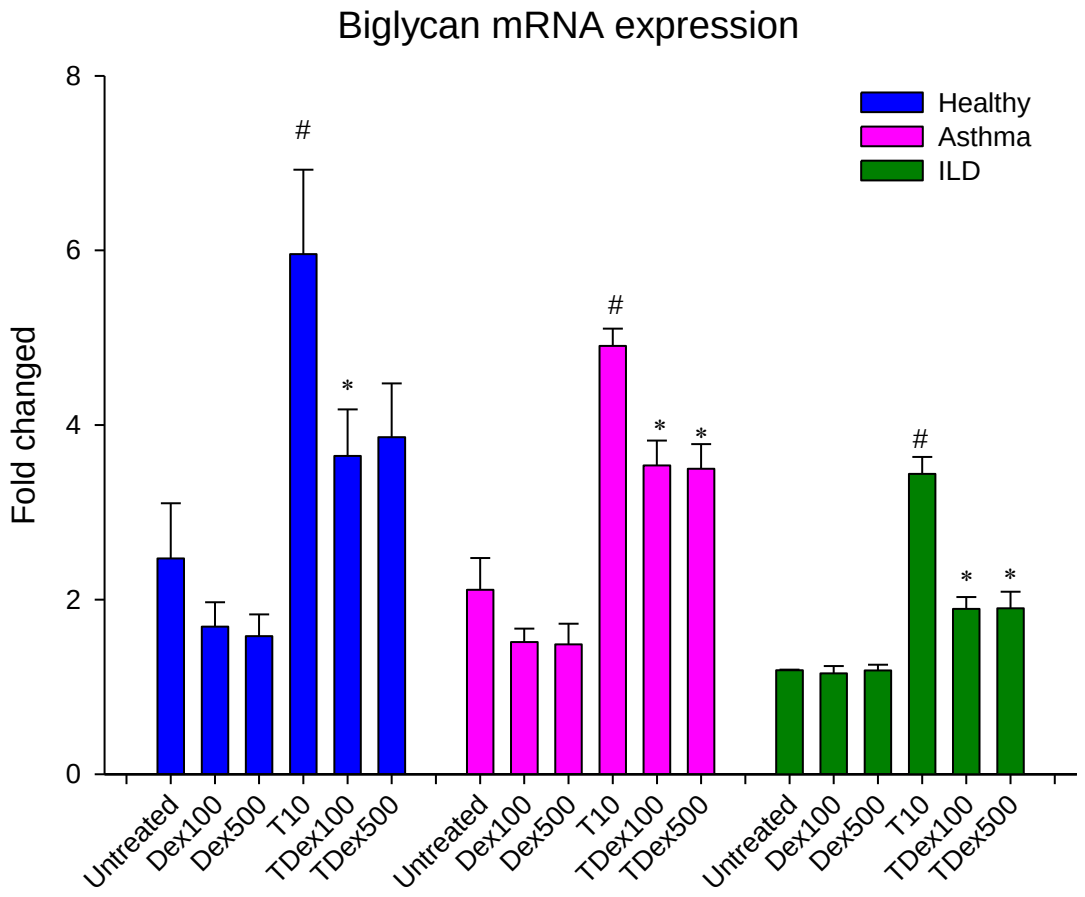

Figure 5-20: TGFβ2 up-regulated biglycan mRNA expression in fibroblasts from healthy non-asthmatic, asthmatic airways and ILD lungs. The experiments for fibroblasts from healthy non-asthmatic (N=6) and asthmatic subjects (N=6) are the same as shown in Figure 5-5, and those from an ILD patient are the same as Figure 5-14. The samples were analysed for biglycan mRNA using RT-qPCR. The values were normalized to the geometric mean of UBC/A2 and expressed relative to the lowest expression observed in an untreated sample of a healthy non-asthmatic subject using ΔΔCt method. The data are presented as mean and standard error and tested for statistical significance using one way repeated measures ANOVA. Blue boxes indicate data from fibroblasts from healthy non-asthmatic subjects, pink boxes indicate those from asthmatic subjects and green boxes indicate those from an ILD subject. # $p < 0.05$ when compared to untreated samples, *$p<0.05$ when compared to TGFβ2 treated samples. Dex=Dexamethasone, T= TGFβ2 and T_Dex= TGFβ2+Dexamethasone.

5.6) Discussion

Summary of findings

- Dexamethasone had no effect on collagen mRNA expression in airway fibroblasts and fibrotic lung fibroblasts.
- Dexamethasone up-regulated LOX mRNA expression only in fibroblasts from asthmatic airways and fibrotic lungs.
- Dexamethasone had an additive effect with TGFβ2 in regulating LOX mRNA only in fibroblasts from asthmatic subjects
- Dexamethasone enhanced the production of Pro-LOX only in airway fibroblasts from asthmatic subjects.
- Dexamethasone could activate pro LOX to become active LOX.
- Dexamethasone suppressed LH2b mRNA expression only in airway fibroblasts from asthmatic subjects.
- Dexamethasone suppressed the effect of TGFβ2 in up-regulating LH2b mRNA expression in airway fibroblasts.
- Dexamethasone had no effect on decorin mRNA expression.
- Dexamethasone suppressed the up-regulation of biglycan by TGFβ2.

.

Bronchial asthma is characterised by airway inflammation, airway hyperresponsiveness, and airway obstruction. Inhaled corticosteroids are suggested as currently the most effective anti-inflammatory medications for the treatment of chronic asthma (1). Several studies have demonstrated their efficacy in reducing asthma symptoms (238), improving in quality of life , improving in lung function , decreasing airway hyperresponsiveness (239-241), controlling airway inflammation(55;240), reducing asthma exacerbation(241;242), and reducing asthma mortality rate (243). However, it has been shown that after discontinuation of inhaled corticosteroids, airway hyperresponsiveness returns to baseline values within weeks, while changes in lung function and increases in asthma symptom occur within weeks to months (240;244-246). Furthermore, inhaled corticosteroids treatment in atopic children with recurrent wheezing has shown no effect on the loss of lung function or the natural history of asthma (30).

The role of corticosteroids in remodelling in asthma is still controversial. An *in vitro* study has demonstrated the anti-proliferative effect of corticosteroids on bovine airway smooth muscle cells (247). Apart from their apoptotic effect on airway epithelium cells (248), corticosteroids have been demonstrated to decrease airway fibroblast proliferation and cytokine release (249). However, studies regarding the efficacy of corticosteroids in reducing the subepithelial layer thickening are controversial. Treatment with inhaled corticosteroids has been shown to decrease the subepithelial layer thickness (250-252). However, other studies have reported a modest or no effect of inhaled corticosteroids on subepithelial layer thickness (109;253). Furthermore, inhaled corticosteroids have failed to establish an inhibitory effect on the decline in lung function in asthmatic patients after treatment (241;254).

Collagen cross-linking initiated by lysyl oxidase (LOX) is essential for collagen strength and stability. In chapter 4, it was shown that there is an increase in active LOX in BAL fluid of severe asthmatic subjects. Consequently, this chapter investigated the effect of corticosteroids on the expression of the collagen cross-linking enzyme in airway fibroblasts and fibrotic lung fibroblasts. This revealed that asthmatic airway fibroblasts and fibrotic lung fibroblasts respond to dexamethasone differently from healthy non-asthmatic airway fibroblasts. The up-regulation of LOX mRNA was seen only in airway fibroblasts and fibrotic lung fibroblasts. The additive effect of dexamethasone with TGFβ2 in up-regulating LOX mRNA and increased in pro-LOX was demonstrated only in asthmatic airway fibroblasts after stimulation with dexamethasone. However, dexamethasone was shown to activate pro-LOX to become the active-form in all groups. This may suggest that asthmatic airway fibroblasts have a potential to respond to corticosteroids more aggressively in producing LOX when compared to healthy non-asthmatic fibroblasts. This is supported by the findings from chapter 4 which found that active LOX was detected only in BAL fluid from some severe asthmatic subjects, but not in BAL fluid from mild asthmatic and healthy non-asthmatic subjects who are not corticosteroids treated.

In addition, in this chapter it was found that although dexamethasone had no effect on collagen mRNA expression in airway fibroblasts, it could not suppress the effect of TGFβ2 in up-regulating collagen I mRNA expression. This result may support the inconsistent efficacy of corticosteroid in decreasing subepithelial layer thickening in asthmatic airways (250-252). In addition, a recent study has reported that the effect of corticosteroids on collagen production by human lung fibroblasts depends on the environment that cells were exposed. Fibroblasts treated with dexamethasone in medium containing 5%FBS, which was proposed to mimic an inflammatory condition, produced more collagen, but collagen production was decreased in those were treated with dexamethasone under a 'non-inflammatory' condition (0.3% albumin) (227). This

underlines the importance of the environment that the cells are exposed. In the case of asthmatic airways, fibroblasts tend to be exposed to a highly inflammatory environment with more TGFβ present. If asthmatic airways are continually exposed to corticosteroids, this may induce airway fibroblasts to produce more LOX. This, in conjunction with its inability to suppress collagen production, may result in more cross-linked collagen deposited in the airways.

Another enzyme that plays an essential role in directing the collagen cross-linking pathway is lysyl hydroxylase2b (LH2b**).** LH2b is able to hydroxylate the collagen telopeptide lysine to form hydroxylysine allowing the collagen to be cross linked in the pyridinoline end product pathway. This pathway is seen predominantly in bone and cartilage whilst the telopeptide lysine pathway is seen predominantly in skin (137). It has been suggested that an increase in collagen cross-linking via the pyridinoline pathway is associated with a fibrotic phenomenon (127). However, this *in vitro* study found that dexamethasone suppressed LH2b mRNA expression in asthmatic group and also suppressed the effect of TGFβ2 in up-regulating LH2b mRNA in all groups. Dexamethasone modestly down regulated LH2b mRNA in asthmatic fibroblast from 3 fold increase in untreated samples to 1.5 fold increase in dexamethasone treated samples. The question is whether this small change in mRNA expression will have an effect on the protein level. If it has an effect on protein levels, the increase in LOX production by airway fibroblasts but the lower amount of LH2b may shift the collagen cross-linking to telopeptide lysine pathway which the end product is histidinohydroxylysinonorleucine (HHL).

Even though, dexamethasone could suppress LH2b mRNA expression in airway fibroblasts, LH2b mRNA expression in fibroblasts following TGFβ2 and dexamethasone co-treatment was still significantly higher than that in untreated fibroblasts (Figure 5-16). As discussed in chapter 4, asthmatic airways are exposed to more TGFβ than healthy non-asthmatic airways; the up-regulation effect of TGFβ on LH2b mRNA expression in asthmatic fibroblasts may overcome the suppression effect of dexamethasone which may result in shifting the collagen cross-linking pathway to pyridinoline pathway. However, there are no previous reports suggesting which collagen cross-inking pathway occurs predominantly in asthmatic airways. More studies evaluating the collagen cross-linking end product will answer these questions.

Biglycan and decorin are known to have a role in collagen fibril assembly both in vitro and *in vivo* (255). From chapter 4, it was found that both TGFβ2 and mechanical strain up-regulated biglycan mRNA expression but suppressed decorin mRNA expression in airway fibroblasts. However, the present work revealed that dexamethasone had no effect in regulating decorin mRNA in airway fibroblasts. In contrast to decorin, dexamethasone could suppress the effect of TGFβ2 in up-regulating biglycan mRNA expression in airway fibroblasts. A similar result has been seen in an *in vitro* study of asthmatic airway fibroblasts, where budesonide attenuated the ability of TGFβ to enhance the release of biglycan in culture supernatants (234). However, while decorin has been suggested to have a key role in collagen assembly (228), biglycan can provide a partial functional compensation for decorin deficiency (256). Consequently, corticosteroids may have a modest role in collagen fibril assembly by regulating biglycan mRNA expression.

This chapter has also evaluated the response of lung fibroblasts from interstitial lung disease (ILD), one of the fibrotic pulmonary diseases, and compared the results with airway fibroblasts from healthy non-asthmatic and asthmatic subjects. It was found the lung fibroblasts from an ILD patient responded to dexamethasone and TGFβ2 in a similar trend as airway fibroblasts from asthmatic subjects. Both dexamethasone and TGFβ2 enhance the production of LOX in fibrotic lung fibroblasts. TGFβ has been shown to be highly expressed in fibrotic lungs (257). As a result, in conjunction with the effects corticosteroids from treatment, this may exacerbate the fibrotic process of the disease by enhancing more cross-linking collagen deposited in the tissue. However, since the present result was from one ILD subject, more studies need to be done to confirm these findings.

In conclusion, this chapter has demonstrated a potentially detrimental role of dexamethasone on airway remodelling. Apart from its anti-inflammatory effect, dexamethasone also has a profibrotic effect in up-regulating lysyl oxidase (LOX), the collagen cross-linking enzyme. This may result in more collagens being cross-linked resulting in stiffer collagen being deposited in asthmatic airways which may affect airway wall mechanics. The balance between the anti-inflammatory effect and the profibrotic effect of dexamethasone should be considered in terms of disease chronicity. The role of dexamethasone on collagen cross-linking is summarized in Figure 5-21.

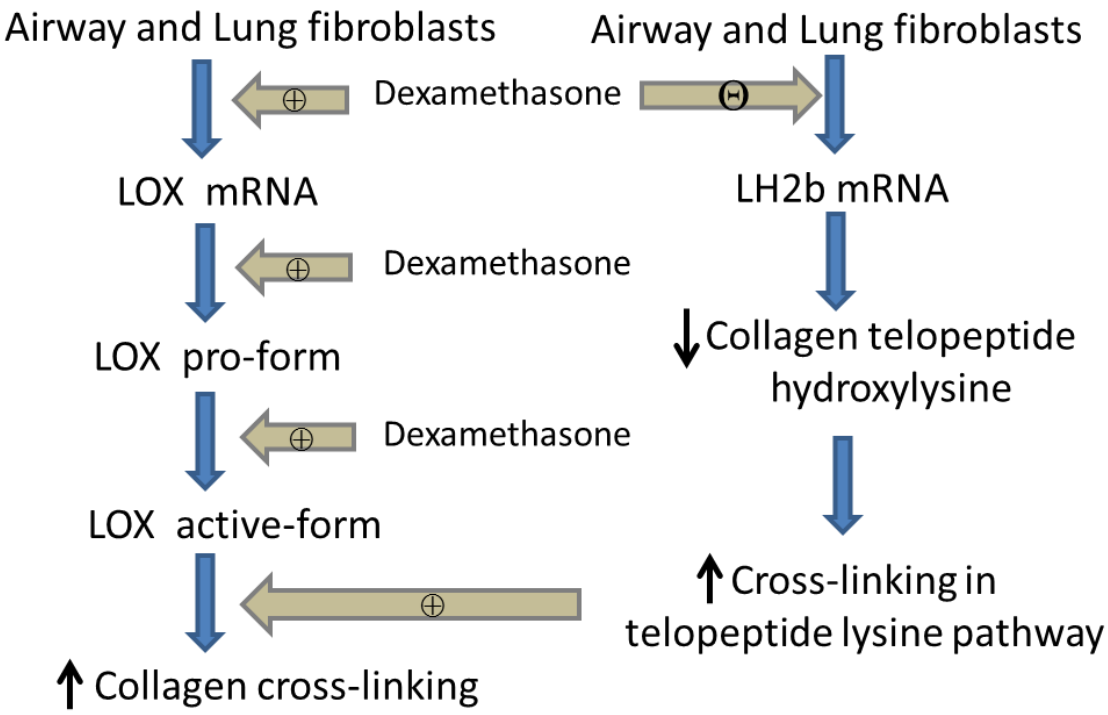

Figure 5-21: Diagram to show how dexamethasone regulates the collagen cross-linking enzymes: lysyl oxidase (LOX) and lysyl hydroxylase2b in airway and lung fibroblasts results in increased collagen cross-linking. ⊕=stimulation, Θ= inhibition and↑= increase.

Chapter 6: The structure and Mechanical Properties of Airway Collagen

6.1) Rationale

Extracellular matrix (ECM) is crucial for the mechanical properties of a tissue. Tissue stiffness can increase up to 3 times with an increase in ECM deposition (126). The most abundant and most critical ECM for structural integrity is collagen. The fibrillar collagens such as collagen I, II, III, V and XI maintain the structural framework of the tissue. Collagen I is found throughout the body except in cartilaginous tissue. An increase in collagen I synthesis has been demonstrated in response to tissue injury that leads to a fibrotic response. The lungs and airways contain mostly collagen I and III. Collagen IV is also expressed in the airway basement membrane. Much of what is currently known about collagen biology and ultrastructure has been done from studies focusing on collagen I in tendon and skin. There are limited studies regarding collagen nanoscale structure in the lungs and airways (56;258). Collagen also has a complex modification after synthesis. The first part of the collagen protein synthetic pathway is the secretion of soluble procollagen from cells. Procollagen is then converted into collagen by procollagen C and N-proteinase (Figure 6-1). The collagen molecules then further self-assemble to give rise to the typical offset of D-banding of 65-67 nm fibrillar structure (Figure 6-2) (259). This characteristic D banding can be demonstrated by electron microscopy and atomic force microscopy. The final step to stabilize the collagen fibrils is the covalent cross-linking initiated by lysyl oxidase (LOX) (Figure 6-1). The collagen cross-linking process is essential for collagen strength and stability. Consistent with this proposal, rats treated with β-aminopropionitrile (BAPN), an irreversibly lysyl oxidase inhibitor had reduced collagen stiffness. Measurement the mechanical properties of murine lung tissue using atomic force microscopy have demonstrated an increase in lung tissue stiffness with the evidence of increased collagen deposition in the murine induced fibrotic lung when compared to that from saline treated lungs (260). The change in tissue mechanical properties has been attributed to a reorganization of the collagen fibres. However, the organization and mechanical properties of individual collagen fibres has not been well studied. Additionally, there may be disease specific influences. It has been suggested that in asthmatic patients have a difference in the post translational modification of collagen from that in non-asthmatic subjects.

However, a comparative study has not identified any differences in non-asthmatic and disease between the production of procollagen from normal and asthmatic fibroblasts (135). This is consistent with the findings in chapter 3 which found no differences in soluble collagen produced by fibroblasts from healthy non-asthmatic and asthmatic subject.

From my work detailed in chapters 4 and 5, it was demonstrated that airway fibroblasts produced more collagen cross-linking enzyme following TGFβ2 and dexamethasone stimulation. Furthermore, it was shown that severe asthmatic subjects in whom there is active LOX in BAL fluid had a trend of having more fixed airway obstruction than those without active LOX. It was hypothesized that an increase in collagen cross-linking in asthma would result in altered mechanical properties of collagen within the airways. The aim of the work presented in this chapter was to evaluate collagen structure generated by airway fibroblasts *in vitro* and collagen extracted from airway tissue biopsies using the technique of atomic force microscopy. Their mechanical properties were also measured using nanoindentation by atomic force microscopy.

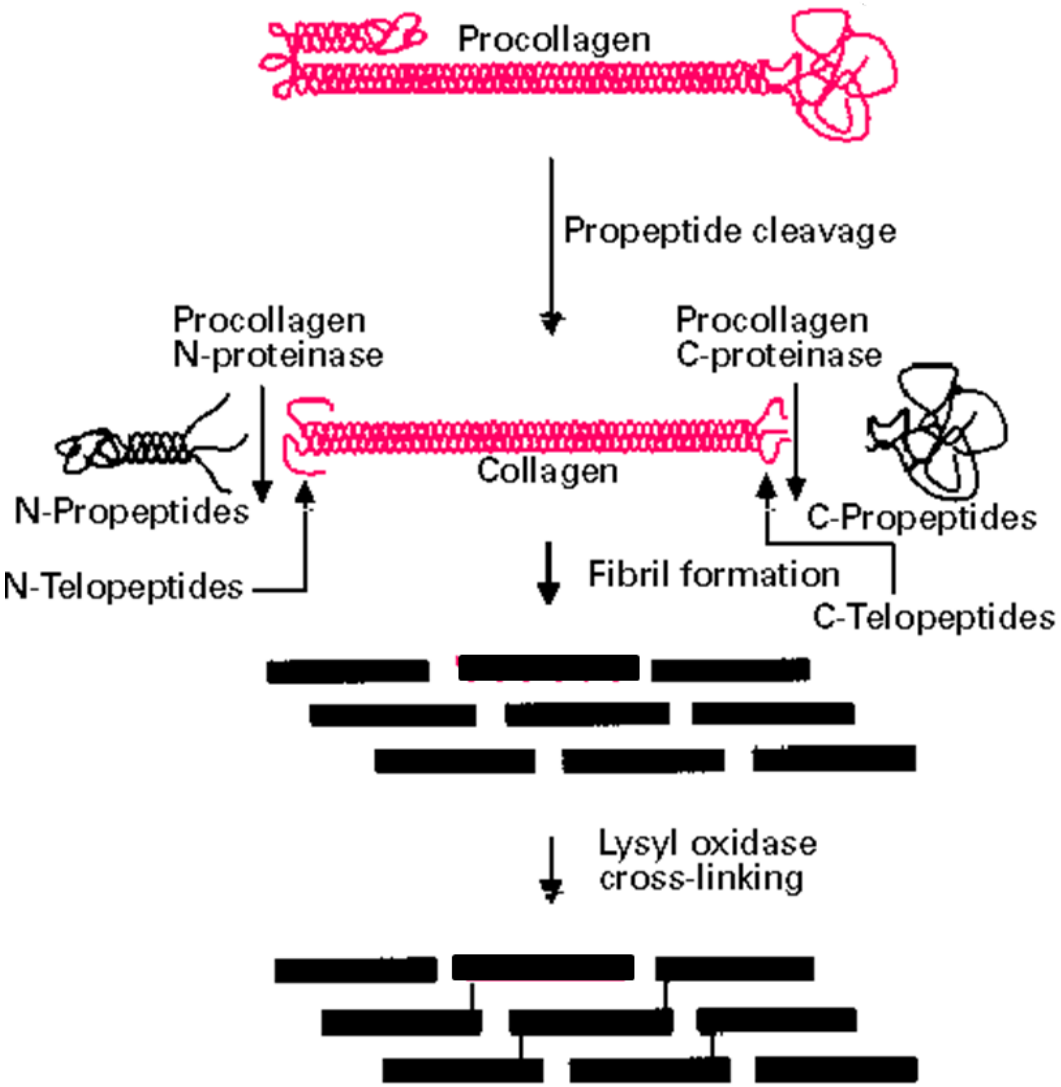

Figure 6-1: Synthesis of fibrillar collagen. 1) Procollagen is secreted from the cells and is converted to collagen by the removal of the N-and C-propetides by proteinase. Then the collagen proceeds to self-assemble into the fibrillar collagen with the typical D-banding pattern. The final stabilization of the fibrils is completed by covalent-cross-linking by lysyl oxidase. The image was reproduced with permission, from Kadler et al, 1996, Biochemical Journal, 316, 1-11 © the Biochemical Society.

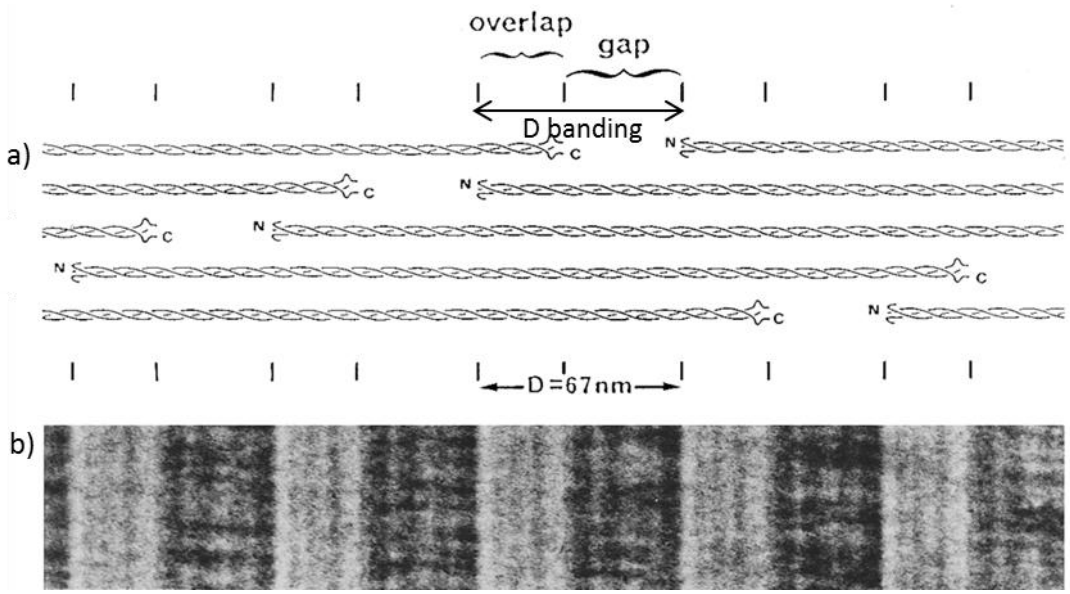

Figure 6-2: a) Schematic representation of the packing arrangement of collagen triple helix molecules into a fibril. b) TEM image of collagen fibril from calf skin collagen. The image was reproduced with permission, from Kadler et al, 1996, Biochemical Journal, 316, 1-11 © the Biochemical Society.

6.2) Hypothesis

That collagen in the airways of asthmatic subjects and collagen generated by fibroblasts from asthmatic airways has different mechano-structural properties from those from healthy non-asthmatic subjects.

6.3) Aims

- To optimize the method to extract collagen produced by airway fibroblasts in culture and collagen in airway tissue.
- To establish the structure of collagen produced by airway fibroblasts in culture and collagen in airway tissue using atomic force microscopy.
- To compare the airway collagen ultra-structural appearances in airway tissue.
- To measure the mechanical property of collagen fibrils from airway tissue by nanoindentation using atomic force microscopy.

6.4) Methods

6.4.1) Atomic force microscopy imaging

Atomic force microscopy (AFM) is a mechanical imaging device that measures the three-dimensional topography, as well as physical properties of a surface with a sharpened tip connected with a cantilever (191). While the tip is scanning across the surface, the machine will project the laser light to the cantilever then the laser light is reflected back to the photo-detector, allowing an image to be generated (Figure 6-3). Samples were put on glass slides and imaged by AC mode; collagen fibril indentation was done using an MFP-3D atomic force microscope (Asylum research, CA, USA). All measurements were taken in the air and at room temperature. All data analysis was performed with the Asylum Research software.

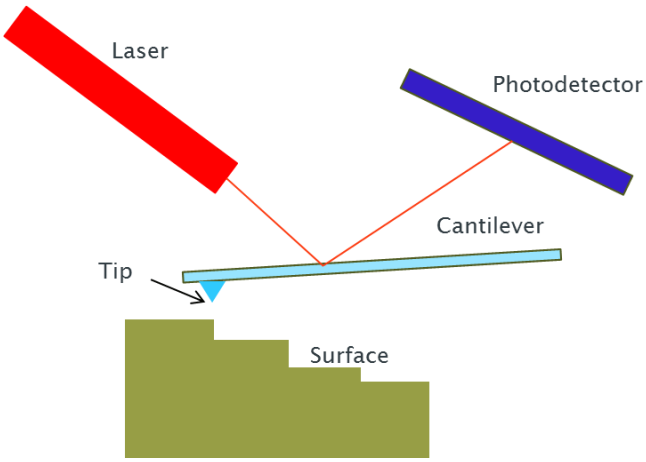

Figure 6-3: Schematic representation of how the AFM creates the image. A sharp tip connected to a cantilever will scan across the surface and the machine will project the laser light to the cantilever and reflect back to the photo-detector. The topographic image then can be generated.

Figure 6-4: Image of MFP-3D™ Stand Alone AFM

6.4.2) **Nanoindentation**

Nanoindentation involves application of a controlled force to the surface of the sample to induce surface deformation. The load and displacement curves are monitored during loading and unloading of the applied forces, and the mechanical properties such as stiffness and Young's modulus are calculated from the load and displacement curve using the method of Oliver and Pharr (192) (Figure 6-5). More detail of the calculation can be found in chapter 2, section 2.4.21.a)

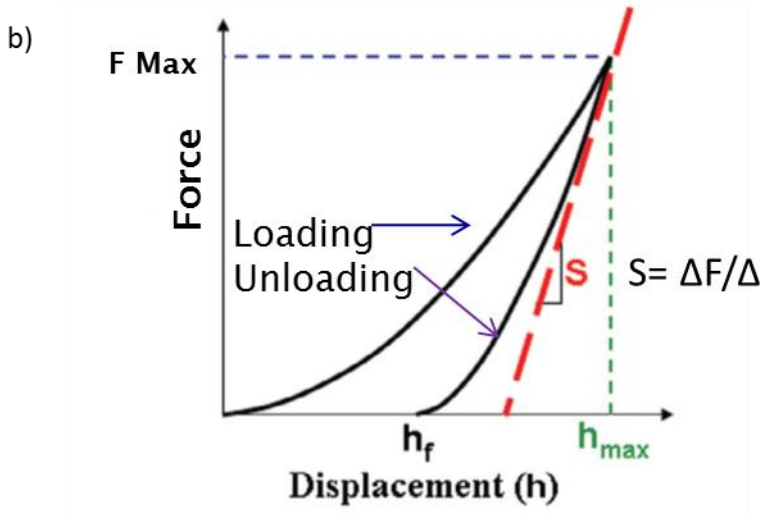

Figure 6-5: Nanoindentation of the sample surface and a typical load-displacement curve. In a) during indentation, the force will be applied to the tip then the tip is moved into the sample causing a deformity of the surface and in b) the load and displacement curve can be generated. The slope of unloading curve is stiffness. S=Stiffness.

6.4.3) **Subject characteristics of airway tissue samples**

To optimize the protocols to extraction of collagen from tissues, various lung and airways samples were studied. These were obtained from lung resection, nasal polyp and bronchial biopsies. The characteristics of the donors are shown in Table 6-1.

Table 6-1: Subjects characteristics studied on the structure of collagen

Code	Type of tissue	Disease	Age (Y)	Sex	FEV_1 % pred	Inhaled steroid (µg/day BDP equivalent)	Current Smoker
EV104	Lung parenchyma	Lung cancer	71	Female	38.9	0	Yes
HL162	Large Airway	COPD GOLD 2	67	Male	51.3	400	Ex-smoker
DS113	Bronchial biopsy	Healthy	54	Female	141	0	No
DS115	Bronchial biopsy	Severe asthma	37	Female	77	1000	Ex-smoker

A nasal polyp sample was donated by Dr Susan Wilson. The sample was collected as anonymised without clinical details.

6.5) Results

6.5.1) The structure of collagen by TEM negative staining

The typical D banding of collagen can be demonstrated by electron microscopy. For initial studies of collagen ultrastructure, bovine collagen was imaged by TEM using a negative staining method. 5 µl of bovine collagen I solution was put on the grid and negative stained with 1% ammonium molybdate. The samples were then imaged by TEM. The dark transverse bands were seen as the result of uptake of electron dense heavy metal ions from the staining solutions on to charged amino acid residue side chains of collagen (259). However, the typical dark and light area of D-banding pattern was not clearly observed (Figure 6-6). Following this evaluation, collagens generated by airway fibroblasts in pellet culture and stimulated with TGFβ were studied.

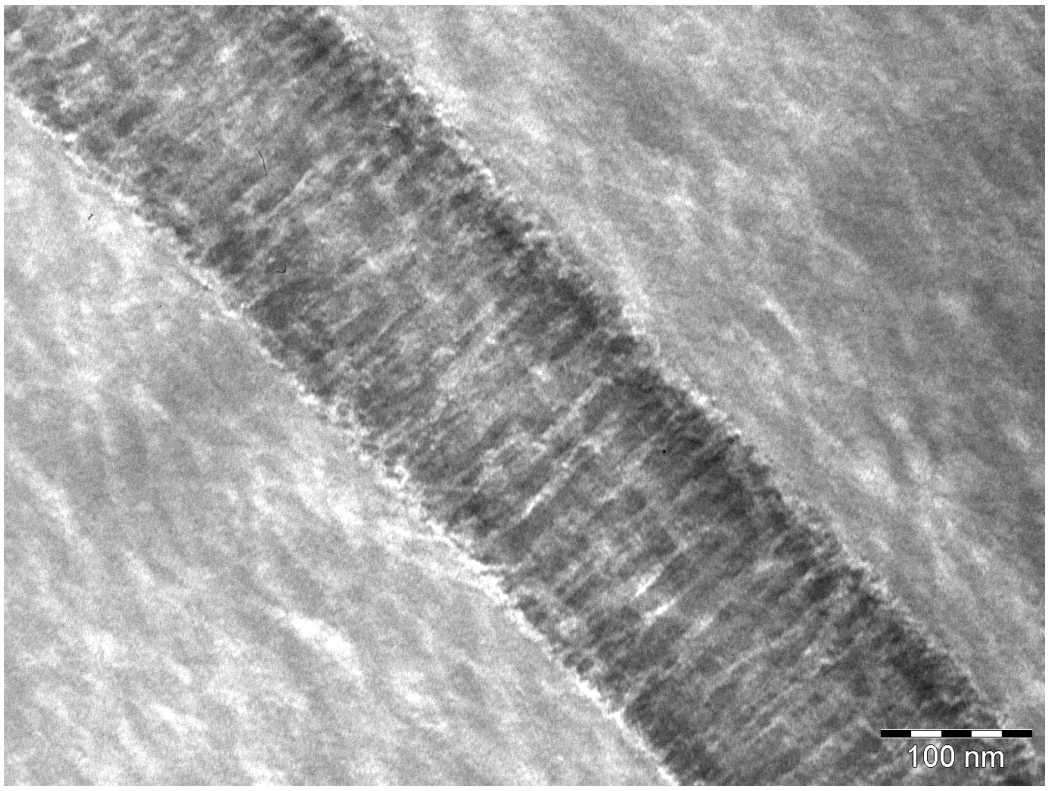

Figure 6-6 : Negative staining of bovine collagen. The dark transverse bands were seen as the result of uptake of electron dense heavy metal ions from the staining solutions on to charged amino acid residue side chains of collagen. Scale bar = 100 nm.

6.5.2) Extracellular matrix production by fibroblasts in pellet culture

To obtain collagen produced by airway fibroblasts, asthmatic airway fibroblasts in pellet culture was treated with TGFβ2 (10 ng/ml) for 1 week. After removing the medium, the pellets were then fixed with 3% glutaraldehyde and 4% formaldehyde in 0.1 M PIPES buffer pH 7.2 at room temperature for 1 hour and the samples were further processed by Dr Susan Wilson before imaging with TEM. From the TEM image, fibroblast with extracellular matrix (ECM) outside the cell was observed (Figure 6-7). However, the characteristic D-banding of collagen could not be demonstrated within the resolution of the microscope. However, the fibroblast pellet culture model could not be used for atomic force microscopy (AFM) imaging, as the samples needed to be put on a surface such as glass slide or mica disc. Therefore, further experiments were undertaken with airway fibroblasts monolayer cultured on the chamber glass slides.

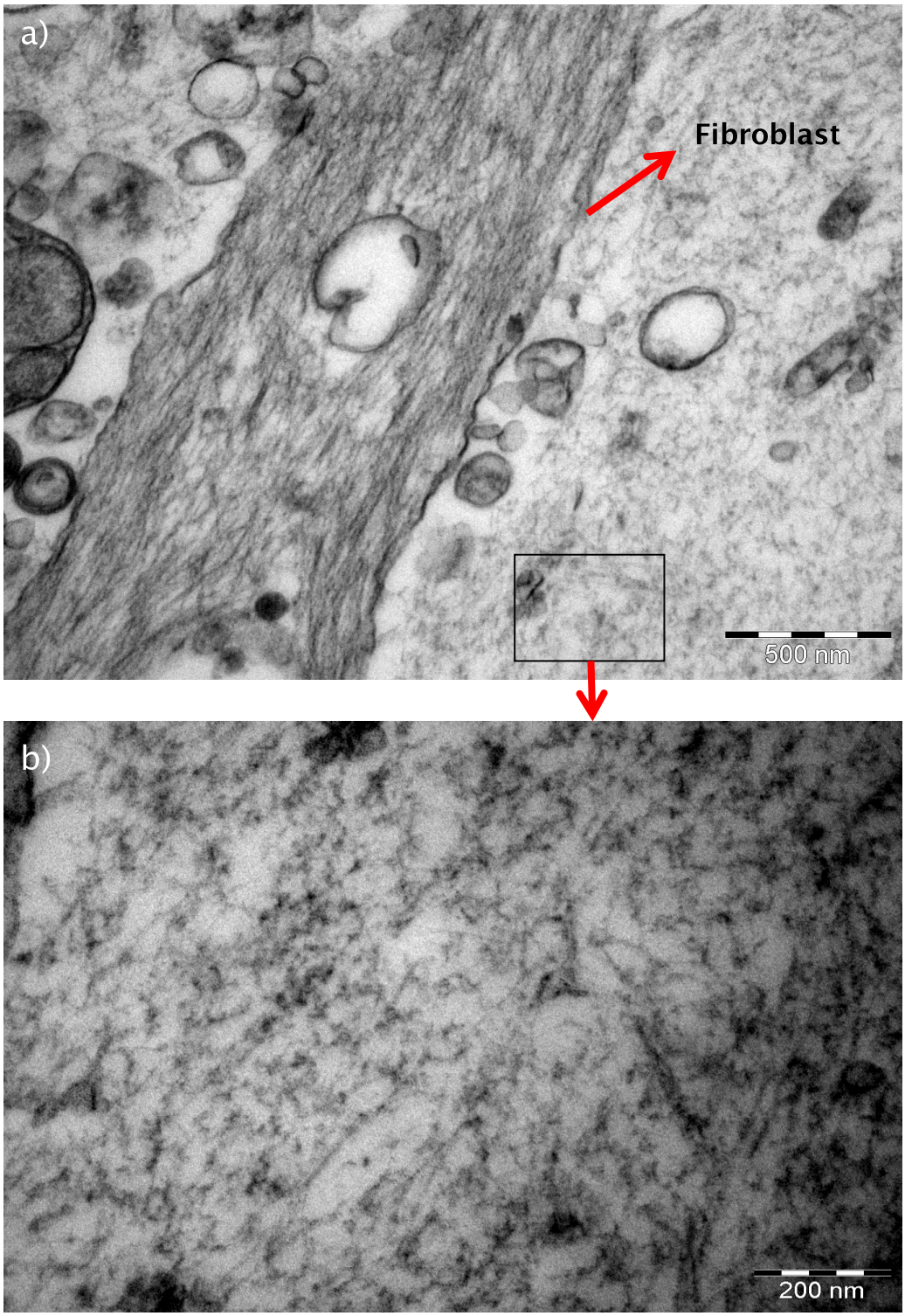

Figure 6-7: TEM images of airway fibroblasts pellet culture treated with TGFβ. Image a) demonstrates a fibroblast with ECM outside the cell, and image b) shows ECM in higher magnification of marked area. a) scale bar = 500 nm and b) scale bar = 200nm. (The samples were imaged with the help of Dr Susan Wilson)

6.5.3) **Image of fibroblasts and fibrils by AFM**

To allow AFM assessment of collagen produced by airway fibroblasts, airway fibroblasts were cultured in monolayer on chamber glass slides coated with bovine collagen I. Cells were stimulated with TGFβ2 (10 ng/ml) for 7 days. Following this, the culture medium was removed and the slides were left to dry overnight before imaging by AFM. From the AFM image, fibroblasts with fibrils located out of the cell were identified (Figure 6-8). However, the characteristic D-banding was not clearly demonstrated. As a consequence, following experiments were undertaken by removing the cells using different methods (section 6.5.4) before proceeding to image with AFM. All AFM images in this section were done with the help of Mr Orestis Katsamenis under the supervision of Dr Philipp Thurner.

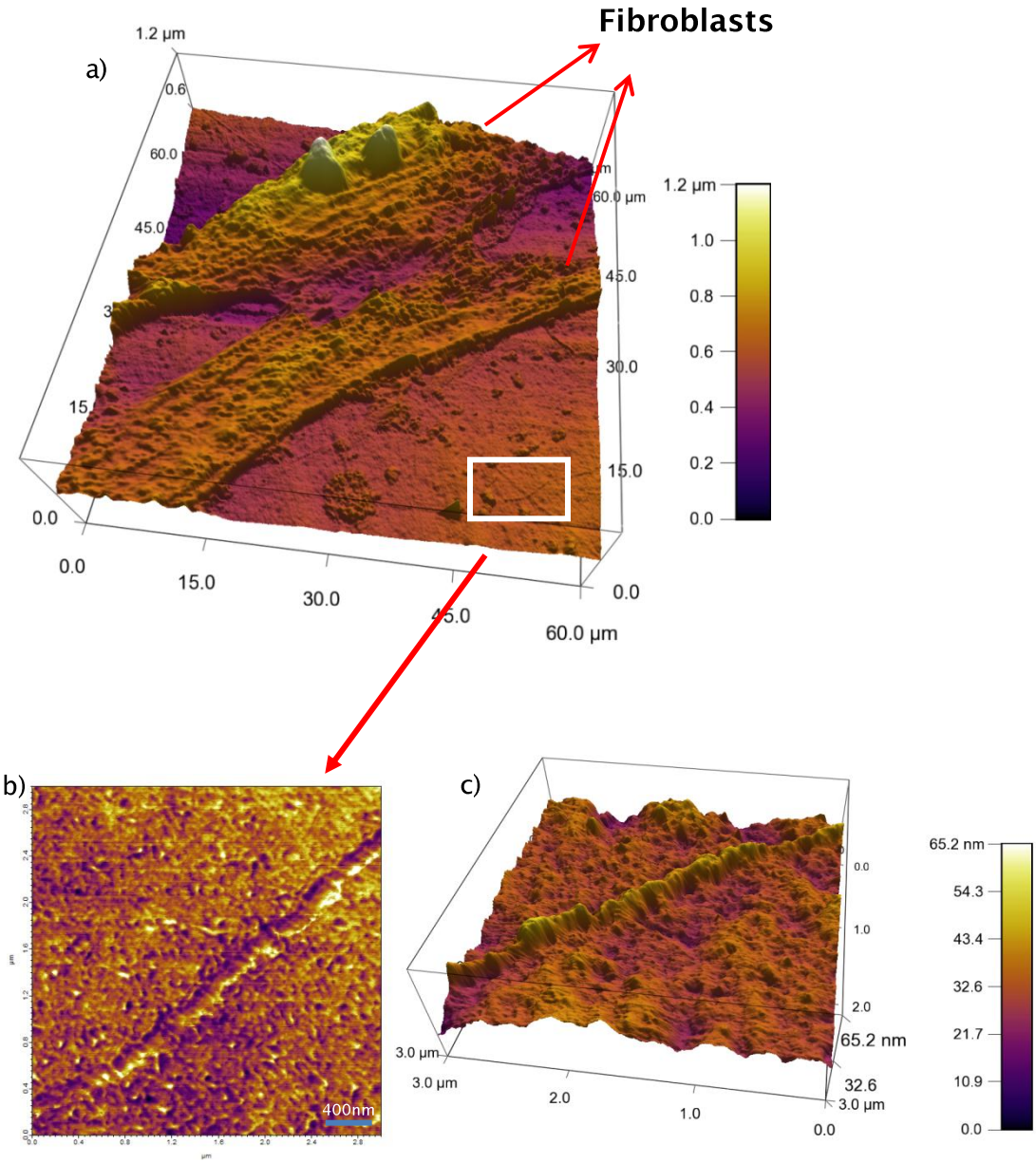

Figure 6-8: AFM images of fibroblast with fibrils outside the cell. Airway fibroblasts were treated with TGFβ2 (10 ng/ml) for 7 days on collagen coated glass slides. Image a) shows fibrils located extracellular of fibroblast, image b) demonstrates the fibril in higher magnification, and image c) shows 3D reconstruction image of image b). Image b) is 3 µm X 3 µm scan image. Scale bar = 400nm.

6.5.4) **Fibrillar structure from fibroblasts cultured in collagen coated glass slide**

To determine the best method to remove the cells and leave the collagen produced by fibroblasts in culture slides, airway fibroblasts were cultured on the glass chamber slides coated with collagen I and treated with TGFβ2 (10 ng/ml) for 1 week. Fibroblasts were then removed using each of the following methods:
1) 25 mmol/l NH_4OH for 10 minutes at room temperature (187).
2) 0.5% deoxycholate (DOC) in radio immunoprecipitation assay buffer (50 mM Tris, 150 mM NaCl, and 1% Nonidet P-40) for 5 minutes at 4°C under gentle shaking (188).
3) 5 mM EDTA in PBS for 5 minutes at 37°C (189).

For all methods, the complete cell detachment was checked under light microscope and detached cells were discarded and remaining ECM proteins attached to the surface of slides were washed with dH_20. The slides were then left to dry overnight before imaging by atomic force microscopy.

6.5.4.a) Image of ECM produced by cultured fibroblasts after removing the cell with NH_4OH

After removing fibroblasts with NH_4OH, ECM which was left in the slide was imaged using AFM. The image showed fibrils which has the same diameter as collagen (50-500nm) (Figure 6-9). However, the typical D banding pattern as seen in collagen from rat tail (Figure 6-10) was not demonstrated.

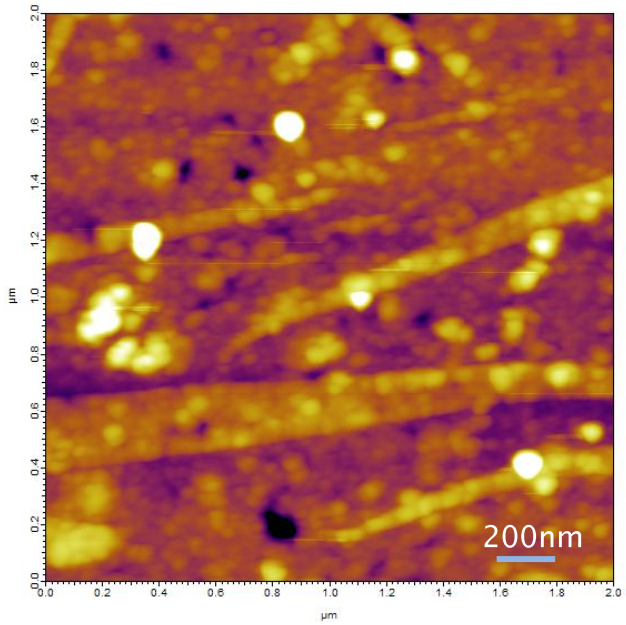

Figure 6-9: AFM image after removing fibroblasts with NH_4OH. The experiment was the same as Figure 6-8. The cells were removed using 25 mmol/l NH_4OH. The remaining ECM on slide was imaged by AFM. Image is 2 µm X 2 µm scan image. Scale bar = 200 nm

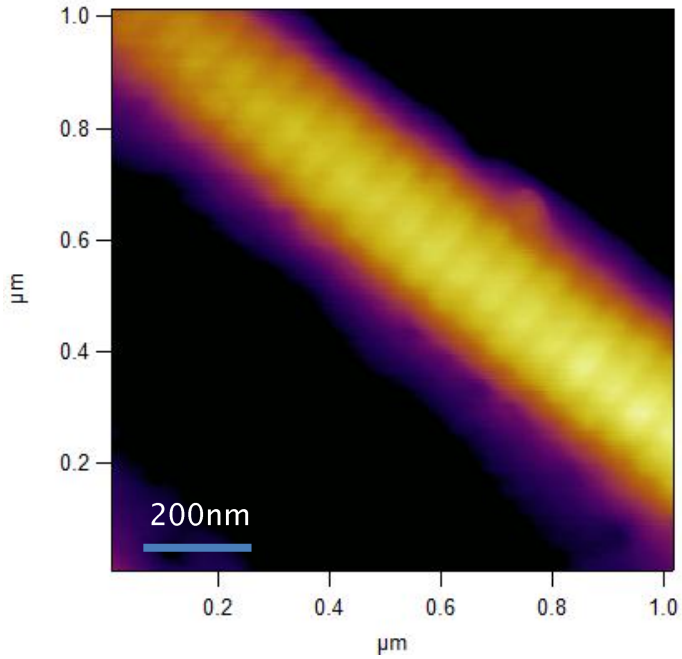

Figure 6-10: AFM image of collagen from rat tail with a characteristic D-banding pattern. Image is 1 µm X 1 µm scan image. Scale bar = 200 nm.

6.5.4.b) Image of ECM produced by cultured fibroblasts after removing the cell with DOC

As NH_4OH is a strong alkali which may disturb the structure of collagen, DOC protocol was then used to remove the cells. The same experiments as described in section 6.5.4) were done and the cells were removed using DOC. The samples were then imaged by AFM. This revealed the fibrillar structures, but again the banding pattern could not be demonstrated which suggested that these fibril structures may be intermediate filaments (Figure 6-11). As this protocol consists of several detergents which then resulted in solubilisation of the cell membrane and leave intermediate filaments on the surface. Consequently, EDTA was used to remove the cell layer.

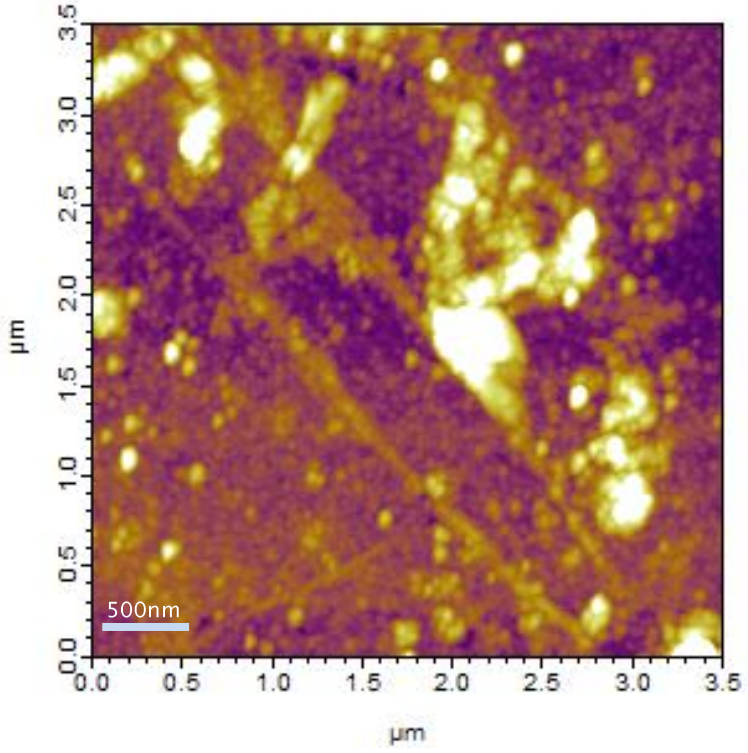

Figure 6-11: AFM image after removing fibroblasts with DOC. The experiment was the same as Figure 6-8. The cells were removed using 0.5% deoxycholate (DOC) in radio immunoprecipitation assay buffer (50 mM Tris pH8, 150 mM NaCl, and 1% Nonidet P-40) for 5 minutes. The remaining ECM on slide was imaged by AFM. Image is 3.5 µm X 3.5µm scan image, scale bar = 500 nm.

6.5.4.c) Image of ECM produced by cultured fibroblasts after removing the cell with EDTA

The same experiments as described in section 6.5.4) were done and the cells were removed using 5 mM EDTA. After removing fibroblasts with EDTA, fibrils with banding were observed by AFM but not by SEM (Figure 6-12). However, as the fibroblasts were grown on the slides coated with collagen, it would be difficult to distinguish between collagen produced by fibroblasts and collagen used for coating. As a result, the further experiments were changed to grow fibroblasts on plastic uncoated chamber slides.

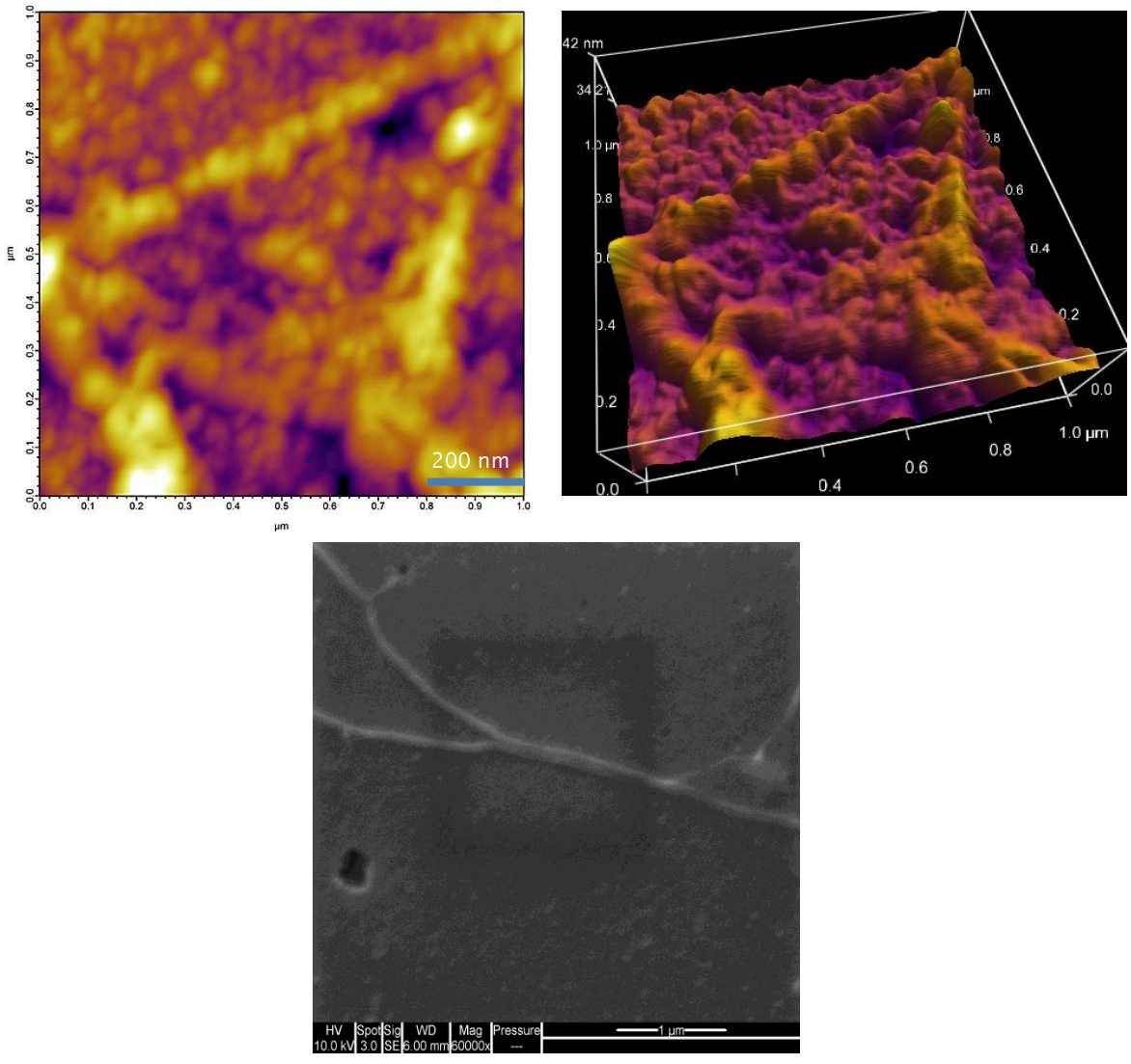

Figure 6-12: AFM and SEM images of fibrils after removing fibroblasts with 5mM EDTA. The experiment was the same as Figure 6-8. The cells were removed using 5mM EDTA Image a) shows 1 µmX1µm AFM scan image of the fibrils with banding, scale bar =200 nm, image b) is 3D reconstruction image of image a), and image c) shows SEM image of the same sample. scale bar = 1 µm.

6.5.5) Fibrillar structure from fibroblasts cultured in plastic slide

To determine the collagen produced by fibroblasts in culture, airway fibroblasts were cultured in plastic chamber slides and treated with TGFβ2 (10 ng/ml) for 1 week. Fibroblasts were then removed by incubating with 5mM EDTA in PBS for 5 minutes. The detached cells were discarded and remaining ECM proteins attached to the surface of slides were washed with dH_20. The slides were then left to dry overnight before imaging by atomic force microscopy. AFM image revealed fibrillar structures with banding. The fibrils diameter was around 100 nm with banding pattern but the background still was not clear (Figure 6-13).

In summary, the characteristic collagen structure could not be demonstrated unequivocally using fibroblasts in culture. This might be explained from the fact that fibroblasts in the tissue have a substantial and complex extracellular matrix. In monolayer culture, the cells have little associated matrix and are bathed in a large volume of culture media. Consequently, the further work was focused on assessment of the collagens from airway tissue.

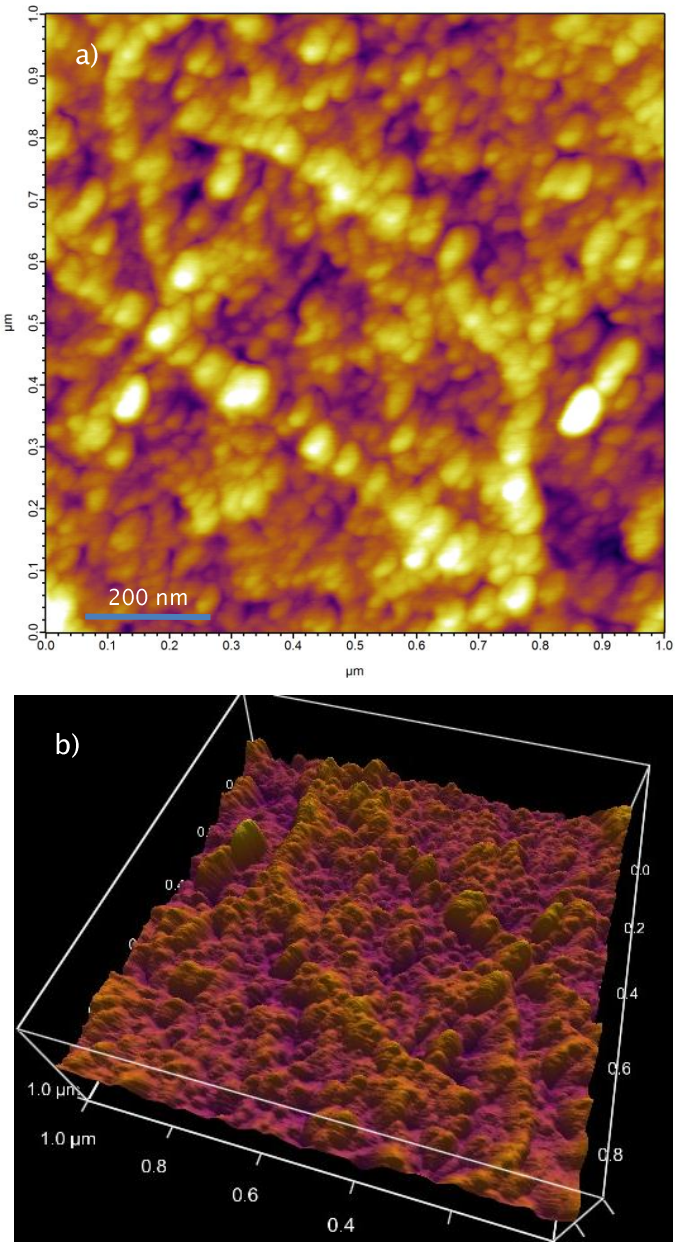

Figure 6-13: AFM images of fibrils after removing fibroblasts cultured with 5mM EDTA. Airway fibroblasts were treated with TGFβ2 (10 ng/ml) for 7 days on plastic chamber slide. The cells were removed using 5mM EDTA. Image a) is 1 µmX1µm AFM scan image of the fibrils with banding, scale bar =200 nm, and image b) is 3D reconstruction image of image a)

6.5.6) **Collagen ultrastructure from nasal polyp**

To optimize the method of extracting collagen in airway tissue, nasal polyp tissue samples were incubated with 1 mg/ml of hyaluronidase and 1mg/ml of trypsin in Sorensen's buffer pH 7.2 at 37°C for 24 h (190). After incubation, the samples were washed with dH2O for two times to remove the excess salt. The samples were then put on glass slides and left to dry overnight at room temperature before proceeding to image by the microscopy. This revealed that a fibrillar structures were observed by bright field and phase contrast microscope (Figure 6-14a and b).

As collagen has an auto-fluorescent property (excitation 280-450 nm, emission 310-530 nm), the samples were then imaged by fluorescent microscopy using a GFP filter (excitation 390-470 nm, emission 509-540 nm). The fibrils exhibited a fluorescent signal which suggested that these fibrils are likely to be collagen (Figure 6-14c). Next, the sample was imaged using AFM to determine whether the typical periodic banding of collagen fibrils was evident. The diameters of the bandings were measured using manufacturer's software. Figure 6-15 shows a 65 nm characteristic banding of collagen from nasal polyp. The same protocol was also used to evaluate and compare the structure of collagen from lung parenchyma and the airways.

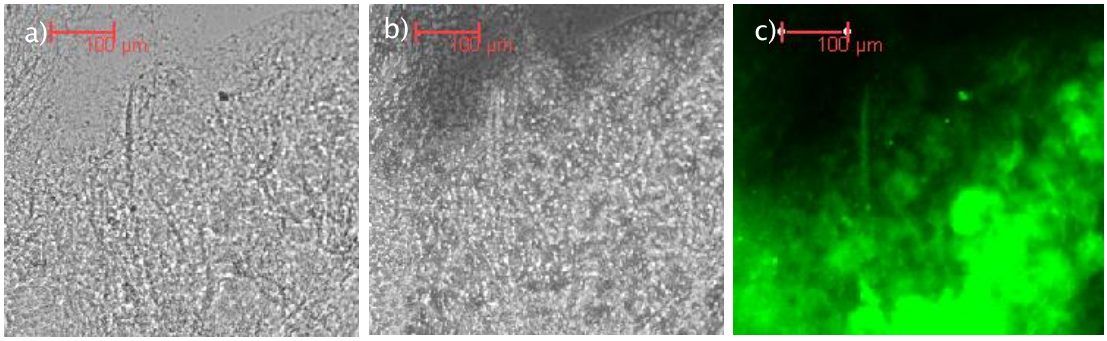

Figure 6-14: Nasal polyp samples were incubated with 1mg/ml of hyaluronidase and 1mg/ml of trypsin in Sorensen's buffer for 24 hr. After washing with dH2O, the samples were then put on glass slides and left to dry overnight before proceeding to image using a) bright field microscopy, b) phase contrast microscopy, and c) fluorescent microscopy with GFP filter.

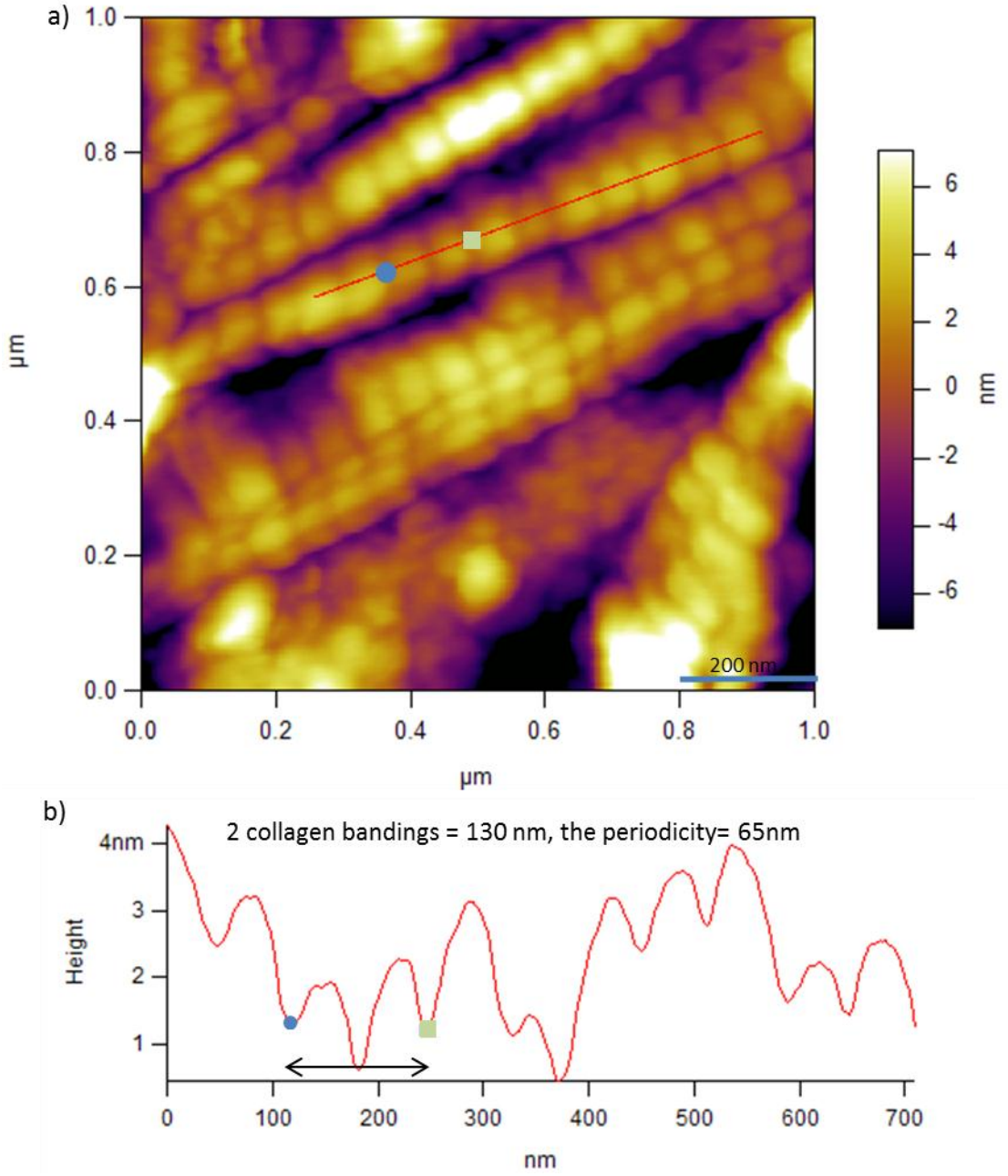

Figure 6-15: AFM image of collagen from nasal polyp. The same sample as Figure 6-14 was imaged using AFM. Image a) shows collagen structure from nasal polyp using AFM. The distance between the blue circle and the green square was measured for the diameter of banding using manufacturer's software. In b) graph shows the diameter of 2 collagen bandings between the blue circle and the green square. The images were acquired under the supervision of Dr Philipp Thurner. The collagen banding measurement was done by Dr Philipp Thurner.

6.5.7) **Image of collagen from the airway tissue**

To evaluate collagen structure from the airway tissue, the airway tissue from lung resection of a COPD patient, bronchial biopsies from a healthy non-asthmatic and an asthmatic subject were prepared as described in section 6.5.6) , then the samples were imaged with AFM. All AFM images in this section were done with the help of Mr Tsiloon Li under the supervision of Dr Philipp Thurner.

6.5.7.a) Image of collagen extracted from the airways of a COPD patient

Collagen extracted from the airways of a COPD patient illustrated a characteristic D banding (Figure 6-16).

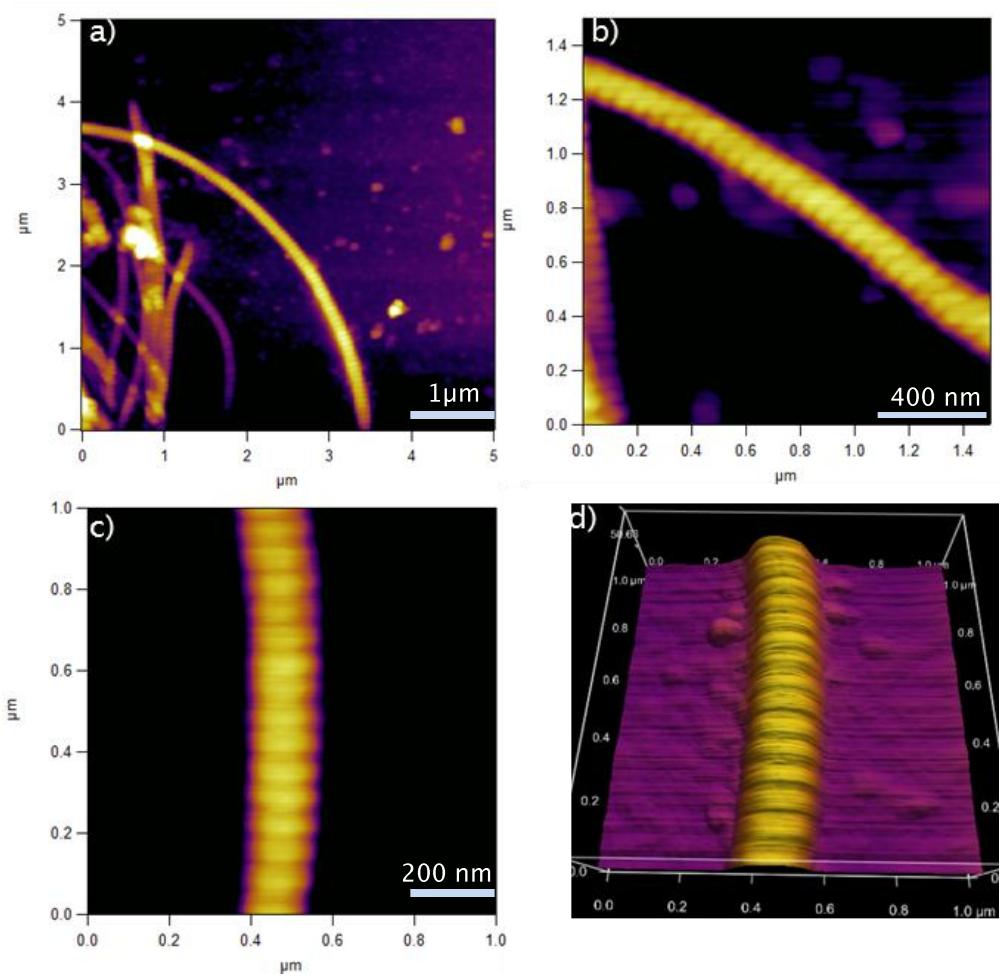

Figure 6-16: AFM images of collagen extracted from airways of a COPD patient. The samples were processed the same as Figure 6-14. Image a) is 5X5 µm scan image, scale bar=1µm, Image b) is 1.4X 1.4 µm scan image, scale bar=400nm, Image c) is 1X1 µm scan image, scale bar=200nm, and Image d) is 3D reconstruction of image c.

6.5.7.b) Image of collagen extracted from bronchial biopsies of a healthy non-asthmatic subject

A typical D banding pattern of collagen could be observed in collagen extracted from the airways of a healthy non-asthmatic subject (Figure 6-17).

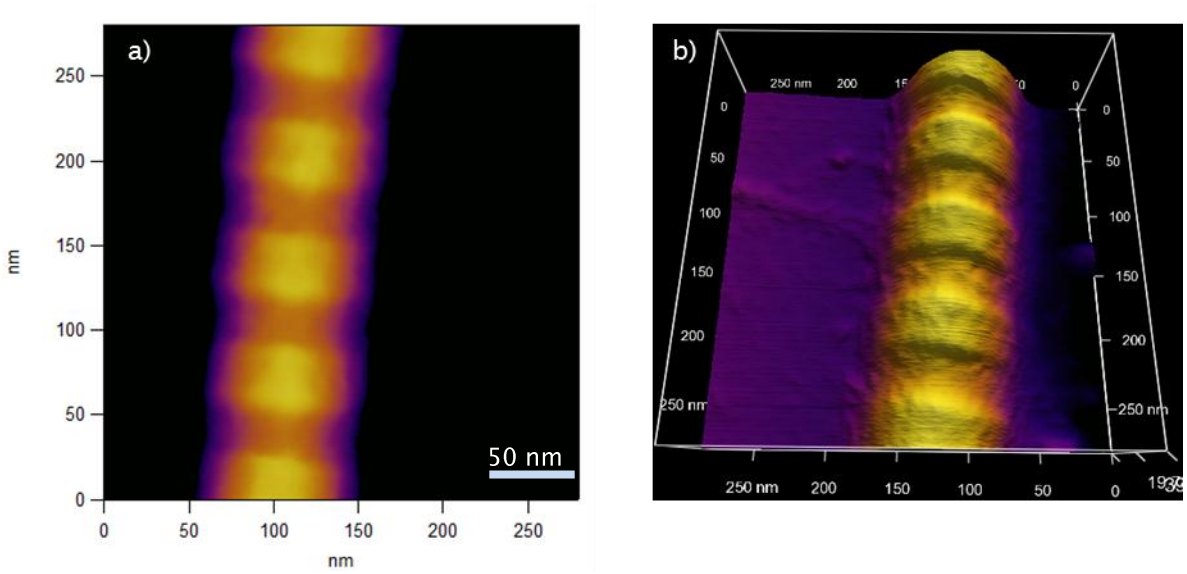

Figure 6-17: AFM images of airway collagen extracted from bronchial biopsies of a healthy non-asthmatic subject. The samples were processed the same as Figure 6-14. Image a) is 280X280 nm scan image, scale bar =50nm, and image b) is 3D reconstruction of image a). These collagen images were imaged using cypher AFM machine from Asylum Research UK during the machine's demonstration.

6.5.7.c) Image of collagen extracted from bronchial biopsies of an asthmatic subject

Collagen extracted from bronchial biopsies of an asthmatic subject also exhibited a typical D banding (Figure 6-18).

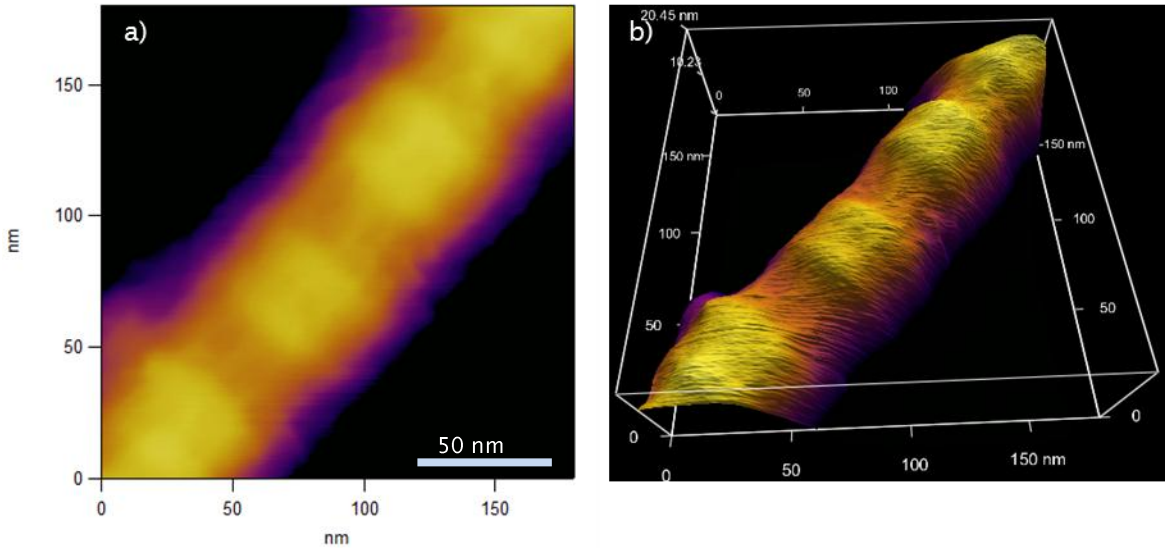

Figure 6-18: AFM images of collagen extracted from bronchial biopsies of an asthmatic subject. The samples were processed the same as Figure 6-14. Image a) is 180X180 nm scan image, scale bar=50nm and image b) is 3D reconstruction of image a. These collagen images were imaged using cypher AFM from Asylum Research UK during the machine's demonstration.

6.5.7.d) Image of collagen extracted from lung parenchyma

To evaluate the structure of collagen extracted from lung parenchyma, the lung samples from lung resection were prepared the same as section 6.5.6), then imaged with AFM. A typical banding periodic pattern was also observed in collagen extracted from lung parenchyma (Figure 6-19).

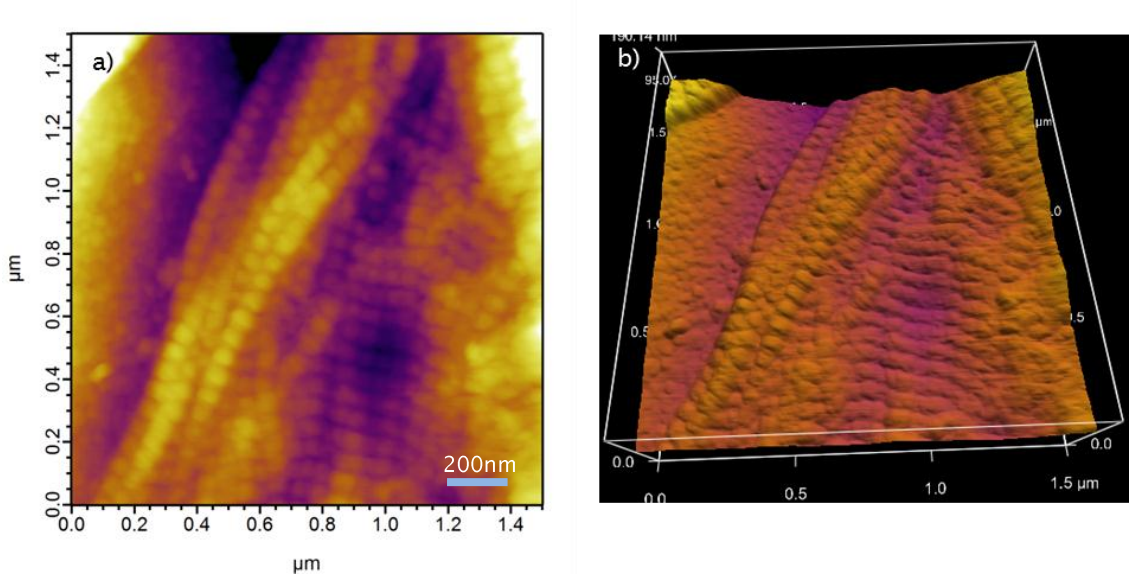

Figure 6-19: AFM images of collagen from lung parenchyma. The samples were processed the same as Figure 6-14. Image a) is 1.5X1.5 µm scan image, scale bar=200nm, and image b) is 3D reconstruction of image a.

6.5.8) **Comparison of the size of collagen fibrils extracted from upper airway, lower airway and lung parenchyma**

The mechanical properties of tendon have been show to relate the collagen fibril diameter distribution. To compare the size of collagen fibrils extracted from upper, lower airway, lung parenchyma, and rat tail collagen, all samples were imaged using 1X1μm scan image. It was shown that rat tail collagen was the largest when compared to collagen from the airways. Among collagen from the airways, collagen extracted from the COPD airways were the largest (Figure 6-20).

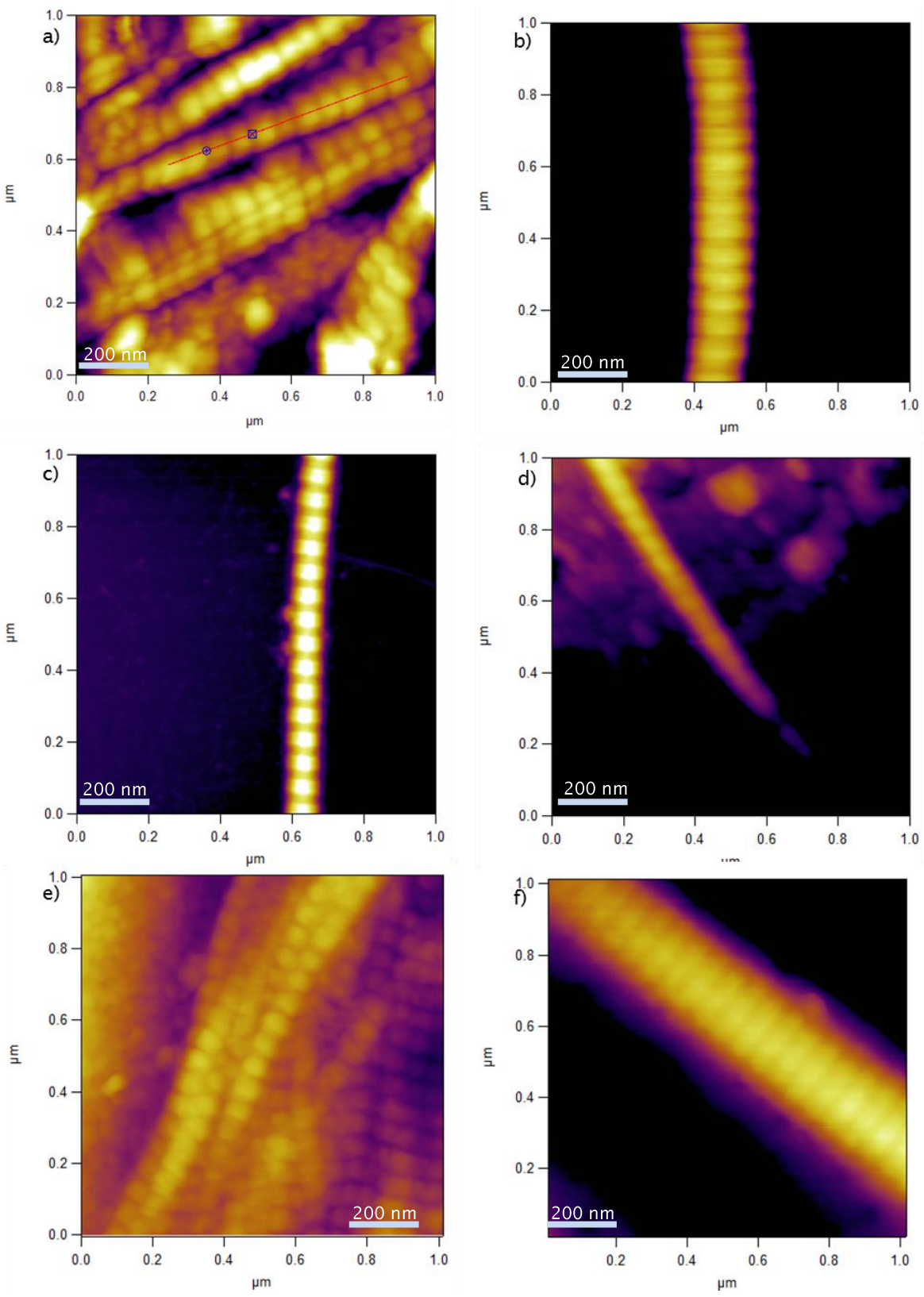

Figure 6-20: Images of collagen extracted from a) nasal polyp, b) COPD airway, c) healthy non-asthmatic airway, d) asthmatic airway, e) lung parenchyma, and f) rat tail. The samples were processed the same as Figure 6-14. All images are 1X1µm scan images, scale bar=200nm.

6.5.9) **Diameter of collagen fibril from the airways, lungs and rat tail**

Previous section, it was shown that collagen from the airway of a COPD subject had a largest size when compared to collagen from the airways of a healthy non-asthmatic and an asthmatic subject. To measure the diameter of collagen, images of single collagen fibril were selected for measurement of their diameters using manufacturer's software. The diameter of the fibril was measured by putting a red line perpendicular to the fibril and then a blue circle dot and a green square box were put out at the edge of each side of the fibril as shown in Figure 6-21a. The diameter was then measured from the graph reconstructed from the manufacturer's program. The distance between the blue circle dot and the green square box was the diameter of collagen fibril (Figure 6-21b). To compare the diameter of collagen fibrils, 10 collagen fibrils from each sample: nasal polyp, healthy non-asthmatic airways, asthmatic airways, COPD airways, lung parenchyma and rat tail were measured. This revealed that the mean diameter of collagen fibrils from nasal polyp was 63.7 + 14.4 nm, healthy non-asthmatic airways was 83.25 + 15.9 nm, asthmatic airways was 83.25 + 15.9 nm, COPD airways is 176.9 + 46.6 nm and, lung parenchyma is 70 + 9.6 nm. The diameter of collagen from COPD airways was significantly larger than other airway collagens ($p<0.001$). Comparison to airway collagens, the diameter of rat tail collagen was significantly larger (400.6 $\pm$ 168.2 nm) than collagens from the airways ($p<0.001$) (Figure 6-22). It is uncertain whether there are the disease related differences or whether the differences are related to different sampling techniques. Collagen extracted from COPD airway was obtained from lung resection, whereas collagens extracted from healthy non-asthmatic and asthmatic airways were obtained from bronchial biopsies. In addition, biopsies were taken from 3th and 4th airway carinae while the source of the COPD sample was less defined with respect to the size of the airway. Analysis of COPD biopsies instead of resection material, similar to asthmatic and non-asthmatic airway samples, would help to clarify whether differences were due to the site of the collagen extracted.

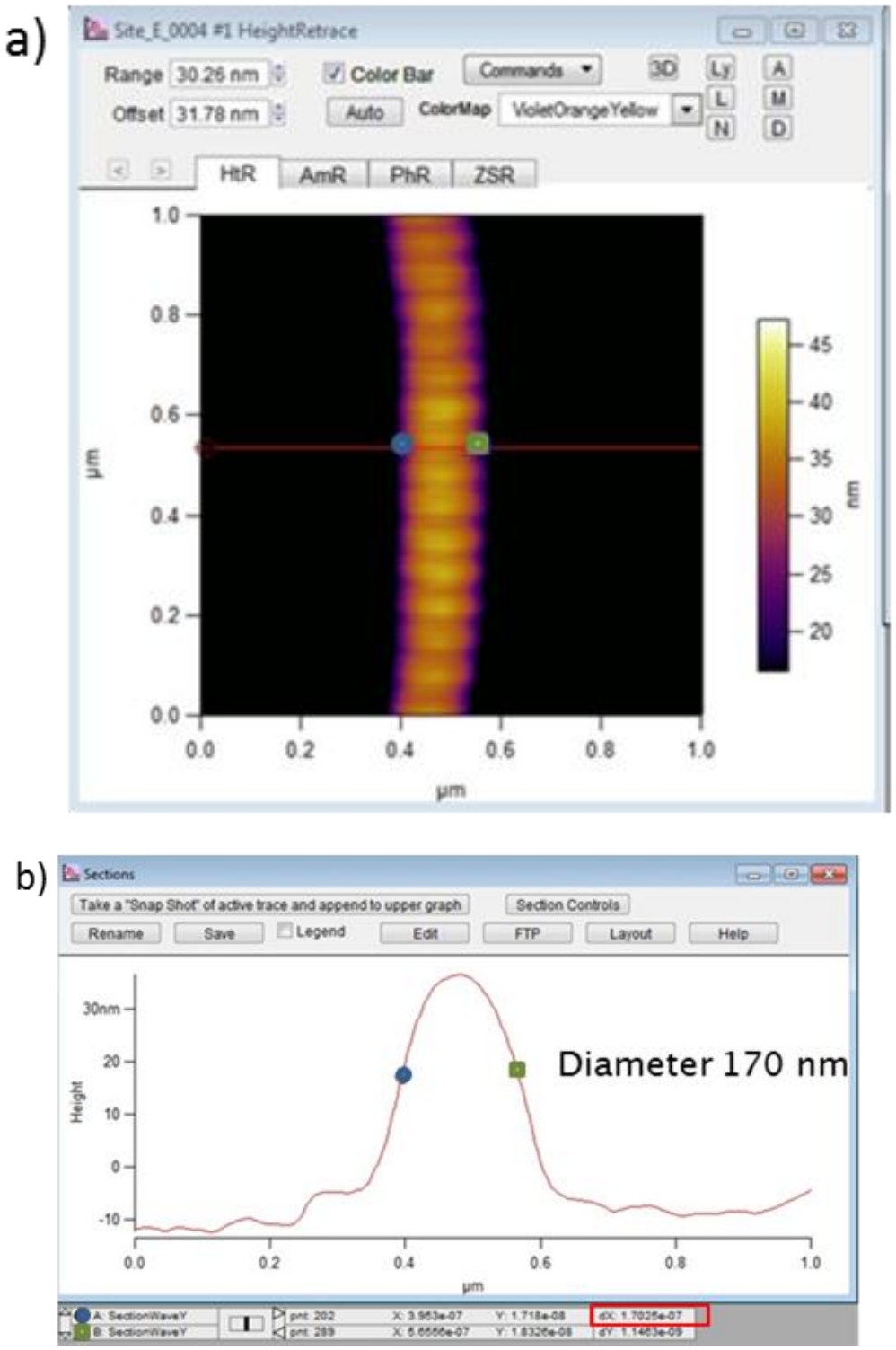

Figure 6-21: Collagen fibril diameter measurement. In a) the red line was put perpendicular on the collagen fibril, and a blue circle dot and a green square box were put at the edge of the fibril. In b) the diameter of the fibril can be calculated from the distance of between the blue circle dot and the green square box as highlighted in a red box.

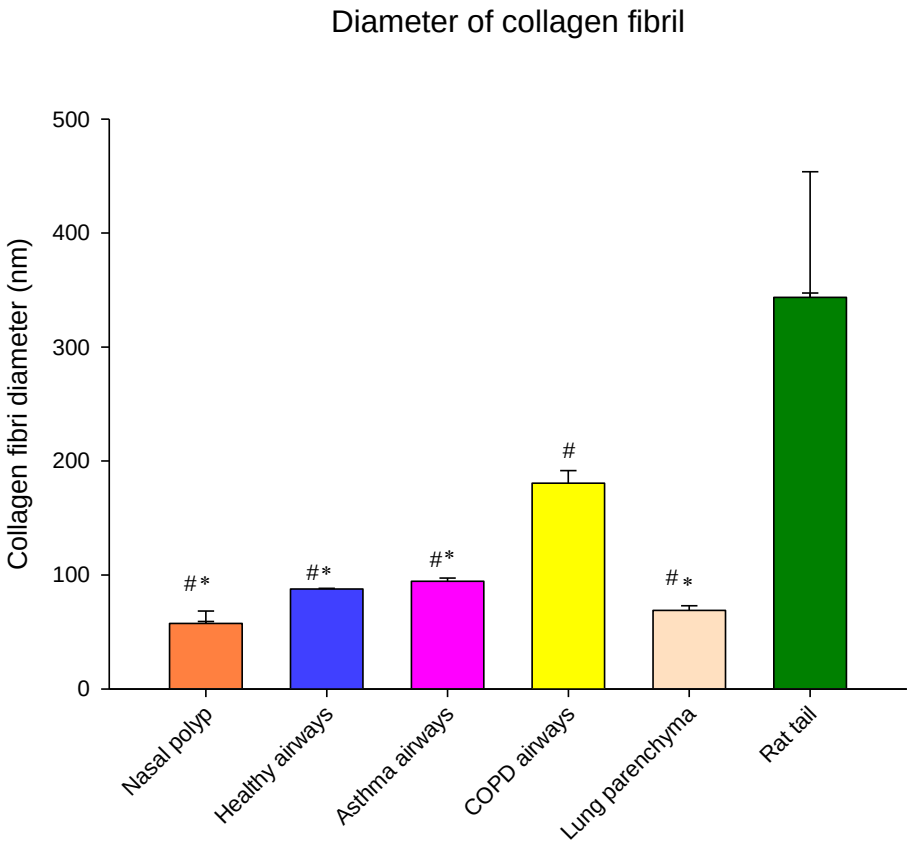

Figure 6-22: Diameter of collagen fibril extracted from nasal polyp, healthy airways, asthma airways, lung parenchyma and rat tail. 10 single collagen fibrils from nasal polyp, healthy airways, asthma airways, lung parenchyma and rat tail were measured for the diameter as described in Figure 6-21. The data are presented as mean and standard error and tested for statistical significance using one way ANOVA. # $p < 0.05$ when compared to collagen from rat tail, *$p<0.05$ when compared to collagen extracted from COPD airways.

6.5.10) **Mechanical properties of collagen from nasal polyp and rat tail**

As a typical collagen structure was observed for collagen extracted from nasal polyp samples, the same samples were then evaluated for their mechanical properties by nanoindentation using AFM as detailed in section 6.4.2). After indentation, the same fibril was imaged again to identify the indentation imprint mark on the fibrils which show the areas that have been measured for their mechanical properties (Figure 6-23). From the load and displacement curves (Figure 6-24), the stiffness of the collagen fibrils can be calculated from the slope of the unloading curve. Using this data, Young's modulus of the collagen fibrils can be further calculated by Asylum research software using the method of Oliver and Pharr (192). The mechanical property of collagen from a rat tail was also measured as a reference value (collagen rat tail image and indentation were done by Mr Tsiloon Li). Apart from rat tail collagen result, all indentation measurements were done with the help of Mr Tsiloon Li under the supervision of Dr Philipp Thurner. All the indentation curves were analysed for stiffness and Young's modulus by Mr Orestis Katsamenis. Please see details of the calculation of Young's modulus and stiffness in chapter 2 section 2.4.21.a)

These analyses revealed that collagen from nasal polyp had a significantly lower Young's modulus (E) than collagen from rat tail: young's modulus (E) were 0.96 ± 0.1(GPa) vs 1.43 ± 0.09 (GPa), $p=0.004$. However, there was no difference in the stiffness of collagen from nasal polyp and collagen from rat tail (94.8 ± 10.3 vs 93.5 ± 8.9 (N/m) (Figure 6-25). A previous study using the same technique has reported Young's modulus of collagen fibrils around 1-2 GPa (261). Consequently, the same nanoindentation technique was used to measure the mechanical properties of airway collagen extracted from an asthmatic and a healthy non-asthmatic subject.

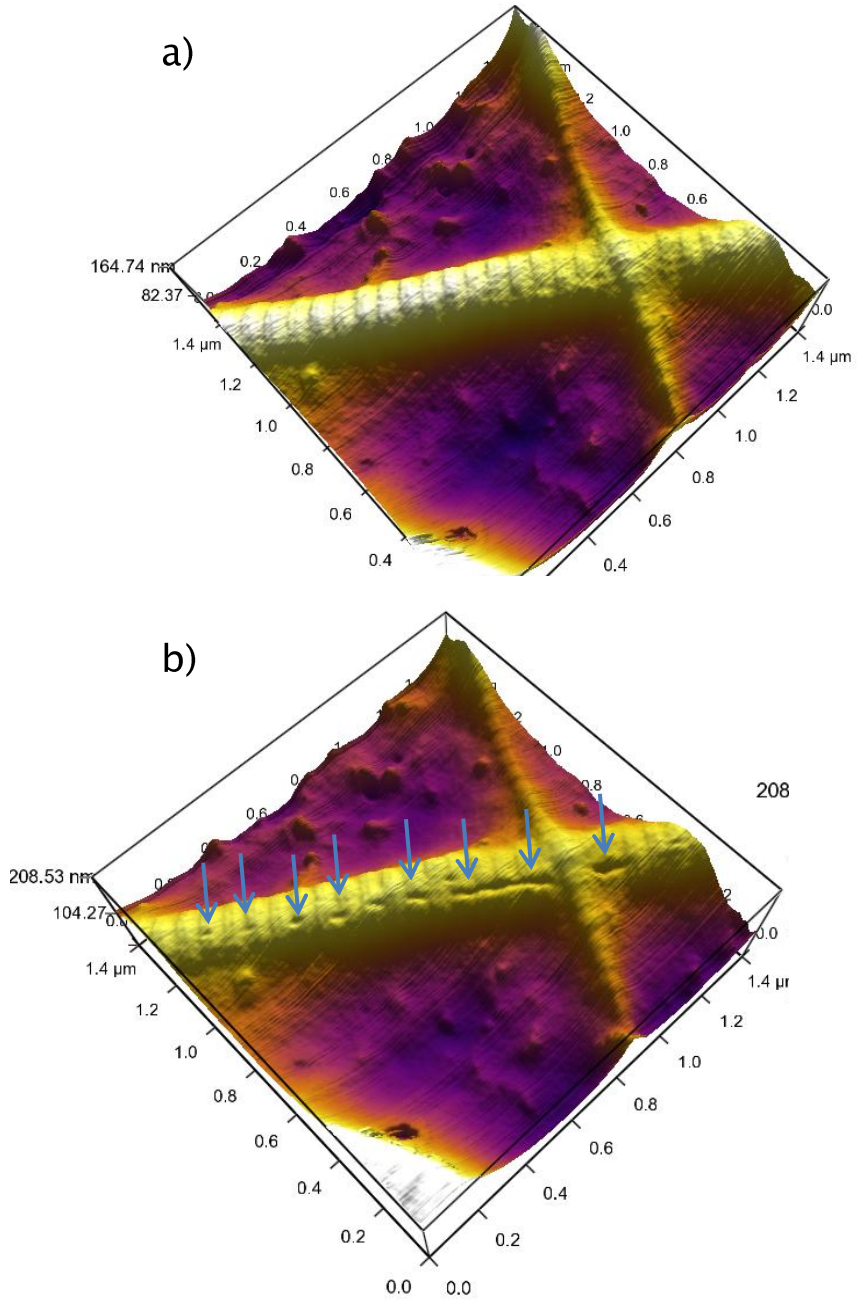

Figure 6-23: AFM images show a collagen fibril extracted from nasal polyp a) before and b) after nanoindentation. The sample from Figure 6-15 was measured for the mechanical properties using nanoindentation. The arrows show the areas that have been measured for the mechanical properties.

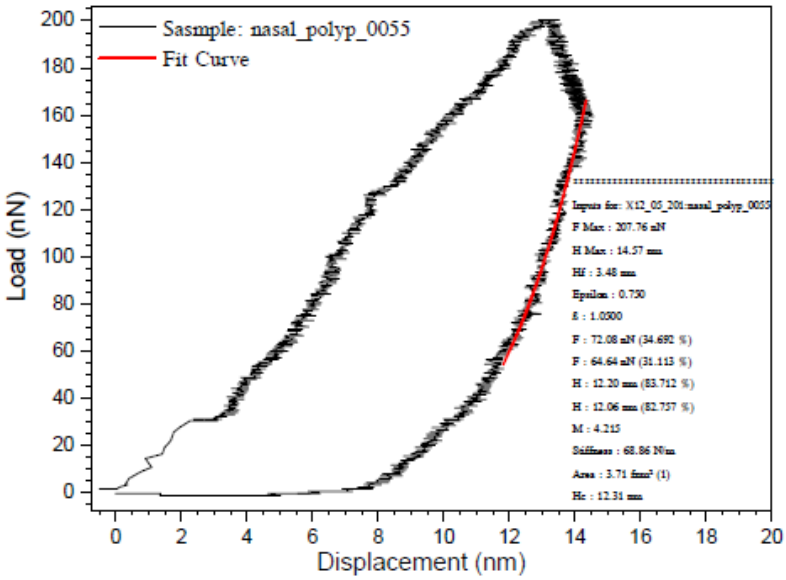

Figure 6-24: Load and displacement curve. The stiffness can be calculated from the slope of unloading curve (red line).

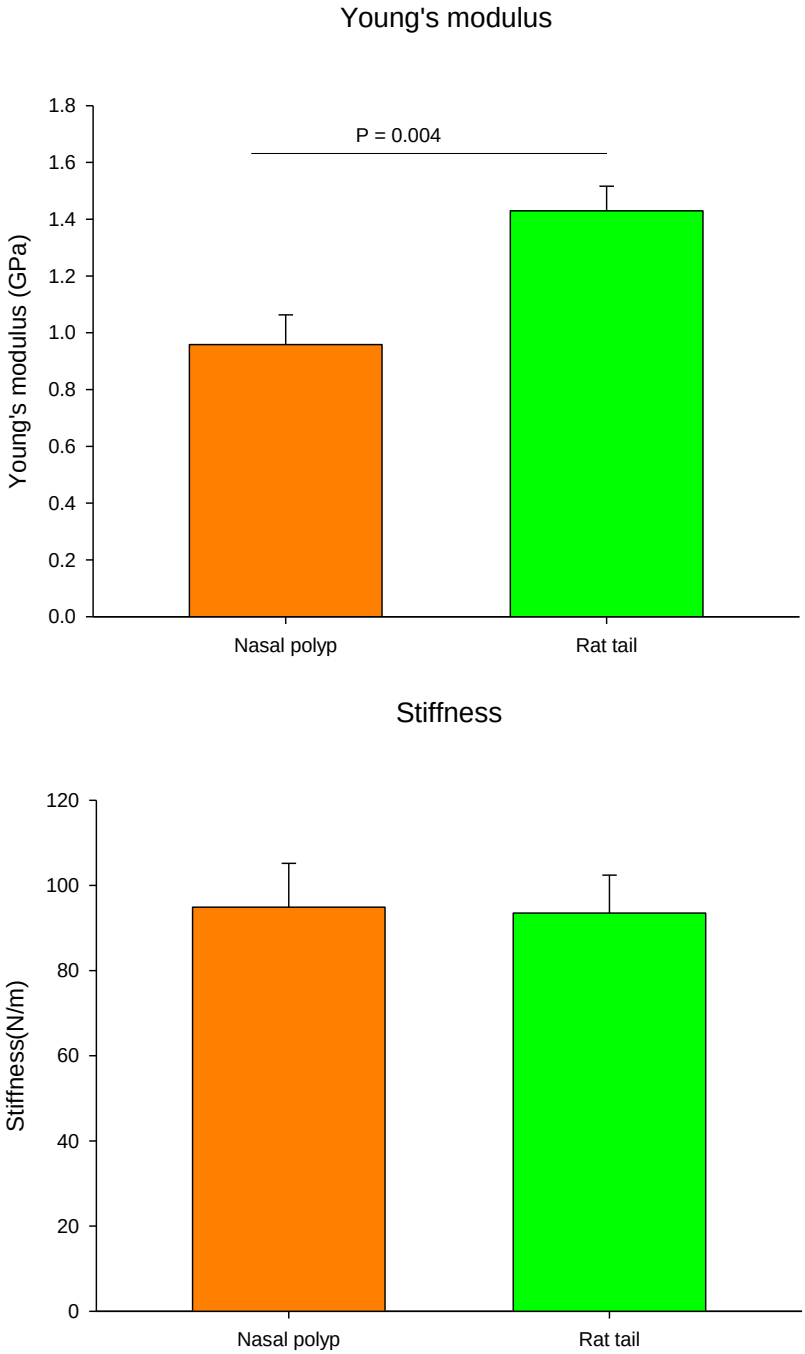

Figure 6-25: Young's modulus and stiffness of collagen from nasal polyp and rat rail collagen. a) Graph demonstrates mean and standard error of Young's modulus of collagen extracted from nasal polyp and rat tail collagen. b) Graph demonstrates mean and standard error of stiffness of collagen extracted from nasal polyp and rat tail collagen. The data were tested for statistical significance using unpaired *t*-test.

6.5.11) Mechanical properties of collagen from healthy non-asthmatic and asthmatic airways

To compare the mechanical properties of collagen extracted from the airways of a healthy non-asthmatic and an asthmatic subject, bronchial biopsies from bronchoscopy were processed the same as described in section 6.5.6) The samples were then imaged and measured for their mechanical properties using nanoindentation method. Calculation for stiffness and Young's modulus were performed as described. All the images and indentation measurements in this section were done with the help of Mr Orestis Antriotis under the supervision of Dr Philipp Thurner. All the indentation curves were analysed for stiffness and Young's modulus by Mr Orestis Antriotis.

It was shown that airway collagen from an asthmatic subject had a higher Young's modulus than collagen from a healthy non-asthmatic airway, but this difference did not reach statistical significance. The mean values of Young's modulus of collagen from healthy non-asthmatic and asthmatic airways were 0.98 ± 0.13 (GPa) and 1.2 ± 0.26 (GPa), respectively. However, airway collagen from an asthmatic subject had a significantly higher stiffness than collagen from a healthy non-asthmatic subject (29.9 ± 6.9 (N/m) vs 20.8 ± 3.9 (N/m), $p=0.02$) (Figure 6-26).

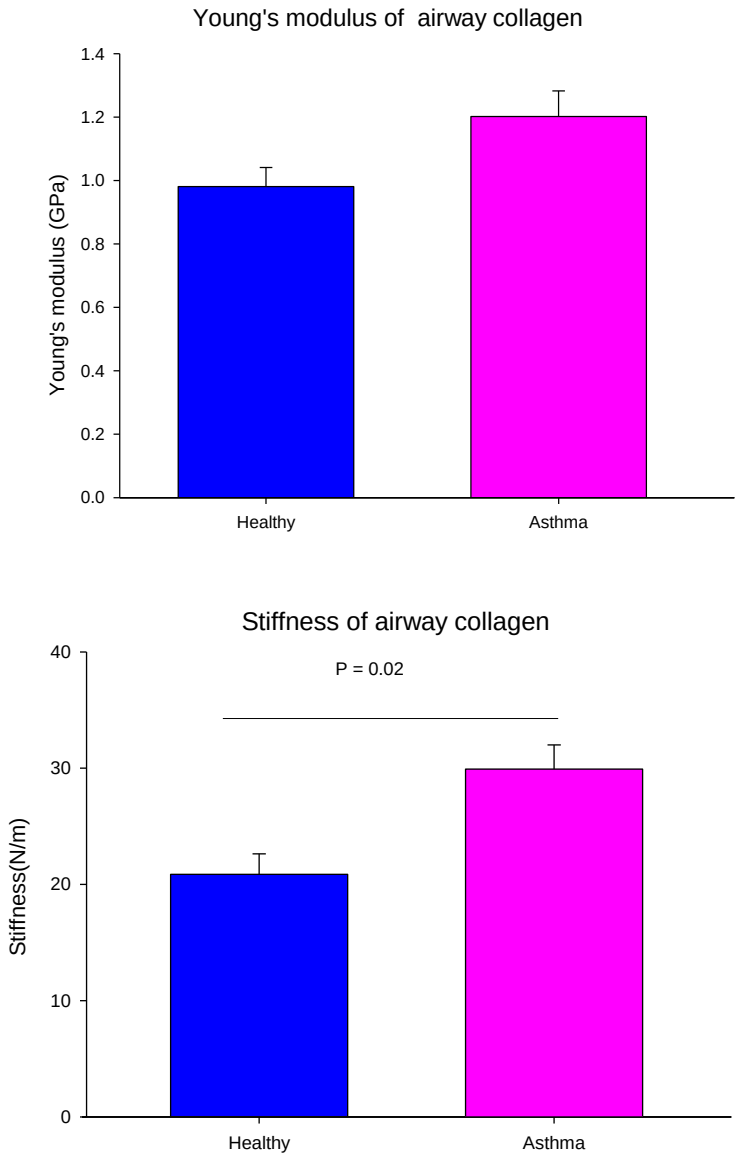

Figure 6-26: Mechanical properties of airway collagen from a healthy non-asthmatic and an asthmatic subject. Graph a) demonstrates mean and standard error of Young's modulus, and graph b) shows mean and standard error of stiffness. The data were tested for statistical significance using unpaired *t*-test.

6.6) Discussion

Summary of findings

- Atomic force microscopy is a good tool to investigate airway collagen structure and its mechanical properties.
- In pilot studies, collagen extracted from the airway of a COPD subject had a larger diameter than collagen extracted from nasal polyp, lung parenchyma, and healthy non-asthmatic and asthmatic airways.
- In pilot studies, collagen extracted from an asthmatic airway had a higher stiffness than collagen extracted from a healthy non-asthmatic airway.
- Collagen modification in cultured airway fibroblasts is incomplete. The characteristic banding structure cannot be demonstrated.

Subepithelial thickening from collagen deposition causes structural changes of the airways in asthma. These changes have been suggested to relate to the severity of asthma and may result in relatively irreversible narrowing of the airways (1). However, the role of collagen in the human airways has never been studied in detail regarding its structure and bio-physical property as on a nanoscale using atomic force microscopy before. The fibrillar collagens, collagen I and III are the main components of airway collagen. Fibrillar collagen is characterized by a hierarchical assembly of substructures. From triple helix, polypeptide collagen molecules assemble into collagen fibrils with a characteristic D-banding periodicity of 65-67 nm and then the fibrils are further assembled to into fibres with the interaction with proteoglycan (262;263).

In the present chapter, it was shown that use of hyaluronidase and trypsin is a reliable method to extract collagen fibrils from airway tissue. The characteristic D-banding pattern of collagen can be observed in collagen from airway tissue using atomic force microscopy. It has been suggested that collagen fibrils diameter depends on anatomical location and is age dependent. The lengths and diameter of the collagen fibrils also increase with maturation of tissue. In mature Achilles tendon, there is a bimodal distribution of thicker fibrils with the diameter of 150-250 nm and a group of thinner fibrils with the diameter of 50-80 nm. Skin has a homogeneous distribution of collagen fibrils of diameter 60 nm (151). However, there are no previous studies reporting about the diameter and mechanical properties of human airway collagen. It was proposed that the large fibrils are responsible for withstanding high tensile forces and the smaller fibrils have a role in resisting distortion under load or have more stiffness (151). The present chapter was found the evidence that disease status may influence on the diameter of airway collagen. Collagen extracted from COPD airway tissue was larger than collagen extracted from healthy non-asthmatic and asthmatic

bronchial biopsies. This can be explained from the fact that COPD patients have emphysematous lungs causing higher tensile forces to the airways. This may result in the larger collagen fibrils. However, the difference in diameter whether it is the age effect. Since the age of the COPD subject was higher than that of healthy and asthmatic subjects (67 yr vs 54 yr vs 37 yr). The present findings were from only one subject in each group. As a result, collagen extracted from more COPD, and asthmatic airways extracted from a similar age group need to be evaluated to answer these questions.

Young's modulus and stiffness are widely used to present the mechanical properties of the material in engineering science. Young's modulus describes the property of a material which is the resistance against deformation when exposed to a given force. Material with a higher Young's modulus needs a larger force to deform or bend. In contrast, stiffness is a property of a structure. It depends on the material, shape and boundary conditions (150). Consequently, most of the literatures used Young's modulus to compare a specific individual collagen fibril property.

The present work has found that Young's modulus of the collagen fibrils from nasal polyp, healthy non-asthmatic and asthmatic airways were 0.96 ± 0.1 (GPa), 0.98 ± 0.13 (GPa) and 1.2 ± 0.26 (GPa), respectively. Young's modulus of collagen fibril has been reported to range from 0.2-21.5 GPa depending on the method of measurement and the origin of the collagen (159). None of these studies has measured, however, the mechanical properties of collagen fibrils from the airway tissue. Therefore, it is difficult to compare these findings to previous studies because collagen has a tissue specific mechanical property. In different tissues with the same type and amount of collagen, the mechanical properties may differ (127). This suggests that in addition to varying the amounts of collagen present, even changes in the properties of the collagen (e.g. its cross-linking) can affect its mechanical properties. The current study was also found that the stiffness of collagen from nasal polyp, healthy non-asthmatic and asthmatic airways were 94.8 ± 10.3 (N/m), (29.9 ± 6.9(N/m) and 20.8 ± 3.9 (N/m), respectively. However, this work is a preliminary study, it is limited because the indentations were not done at the same time and the different parameters were used to optimize the methodology. Furthermore, analyses of the mechanical property calculations were not done by the same person. The parameters used for nanoindentation measurement of samples from healthy non-asthmatic and asthmatic airways were different from those used for nasal polyp and rat tail measurements. Furthermore, it is difficult to compare the stiffness of collagen from nasal polyp and collagen from the airways samples, because the derivation of the stiffness depends largely on the curve fit that used for the calculation which is subjective and was performed by 2 separate individual. However, it is reasonable to compare the mechanical properties of collagen extracted from nasal polyp with rat tail

and those from healthy non-asthmatic airways with asthmatic airways, because they were analysed by the same person and using the same parameters. In addition, it was found that collagen from the airways was much smaller than collagen from a rat tail. The parameter used for indentation of collagen from rat tail cannot be used for indentation of collagen from the airways because the smaller size of the collagen fibril from the airways needs to be taken into account when doing nanoindentation.

Interestingly, this preliminary work revealed that airway collagen from an asthmatic subject had a significant higher stiffness than that from a healthy non-asthmatic subject. Young's modulus of airway collagen from an asthmatic subject was also higher than that from a healthy non-asthmatic subject, but the difference was not statistically significant. The higher stiffness of collagen from an asthmatic airway is consistent with the results shown in chapter 4 and 5 which found an increase in the production of lysyl oxidase (LOX) following TGFβ2 and dexamethasone stimulation. In the airways, fibroblasts from asthmatic subjects would be exposed to a higher level of TGFβ and only asthmatic subjects received corticosteroid therapies. This may result in more collagens being cross-linked and this then has the potential to increase the mechanical properties of collagen. More measurements have to be done in more samples to confirm the difference of mechanical property between airway collagen from healthy non-asthmatic and asthmatic subjects using the same parameter and analysed by the same person.

Airway fibroblasts and myofibroblasts are the principal cells in producing the ECM especially collagen in the airway. In work presented here, it was found that collagen excreted from fibroblasts in culture was not further processed completely to be able to demonstrate the typical D-banding periodicity. This may be explained from the fact that the procollagen with the propedtide domain was not protelolytically removed then could not further processed to self-assembly to become fibrillar collagen. In addition, fibroblasts in the tissue are surrounded by ECM. In contrast, the cells in a monolayer cultured have little associated matrix and are bathed in a large volume of culture media. As a result, procollagen and partially processed intermediates accumulated in the culture media which is consistent with the findings in chapter 3 which found that mechanical strain enhanced airway fibroblasts to secrete soluble collagen into culture supernatants. Previous studies have shown that the processing of procollagen to fibrillar collagen of culture fibroblasts is incomplete and mostly secreted collagens are procollagen intermediate (264). It was shown that fibroblasts grown in medium containing less than 1 μg/ml of ascorbic acid were defective in collagen fibril formation and this was corrected after supplementation with 50 μg/ml of ascorbic acid (265). The absence of ascorbic acid supplement in culture medium in the present work may have a role in the incomplete collagen processing observed. In addition, a recent

study has suggested methods to accelerate collagen post-translational modification from procollagen to collagen in human lung fibroblasts by adding macromolecules such as negatively charged 500 kDa dextran sulphate or a mixture of neutral 70 and 400 kDa Ficoll™ in the culture medium (266).

The present work also demonstrated that imaging and measuring the mechanical properties of collagen fibrils from airway tissue using atomic force microscopy is feasible. However, collagen also has a complex hierarchical structure. The nature of how the collagen fibrils interact within a matrix of proteoglycan and the orientation of the fibrils plays a crucial role in the function and property of the tissue (151). For example, the collagen fibrils in skin and tendon have different nature of the distribution. Skin has a complex, closely interwoven fibril distribution which allows the resistance to strain occured within a two-dimensional plane. In contrast, tendons are supposed to withstand the strain only in the longitudinal axis, so the fibrils are arranged in parallel to each other. The collagen fibril network in the human lungs, as demonstrated by SEM, has been shown to be an interwoven network of collagen fibres in the pleural layer, and wavelike courses extend from one alveolar entrance to another. Furthermore, a ladder-like arrangement of collagen fibril network has been found within the collagen fibres network of alveolar septum (258). Previous studies using electron microscopy found a difference in collagen distribution in the airways of asthmatic and healthy non-asthmatic subjects. Beneath the subepithelial layer, there was a loose array of collagen fibrils formed in healthy non-asthmatic subjects. In contrast, there was a dense meshwork of collagen fibrils under the subepithelial layer in asthmatic subjects (56). A recent study using a multiphoton microscopy has demonstrated an increase in thickness and changing in collagen arrangement of airway collagen fibrils following house dust mite challenged in mice (267). These studies highlight the importance of collagen arrangement and distribution in asthmatic airways which would have an impact on the overall mechanical properties of the airways.

In conclusion, results in the present chapter have demonstrated the structure of collagen in nanoscale and the mechanical properties of collagen fibrils from the airways using atomic force microscopy. This will lead to more studies regarding the role of collagen in the airway wall mechanics, and then the decreased lung function and disease persistence in severe asthma can be clarified.

Chapter 7: Final discussion and future work

This present work has evaluated the role of mechanical forces and collagen in the pathogenesis of airway remodelling in asthma. Firstly, dynamic changes on extracellular matrix protein expression and inflammatory cytokine production by airway fibroblasts in response to cyclical mechanical strain were studied in chapter 3. Next, factors regulating collagen cross-linking involving lysyl oxidase (LOX) and lysyl hydroxylase2b (LH2b) produced by airway fibroblasts were evaluated in chapter 4 and 5. In addition, factors involved in collagen assembly such as small leucine-rich proteoglycans (SLRP): biglycan and decorin were also investigated. To relate these *in vitro* findings to *in vivo*, the level of LOX in BAL fluid of healthy non-asthmatic, mild and severe asthmatic subjects was measured. The responses of fibroblasts from healthy non-asthmatic and asthmatic airways were also compared with those from fibrotic lungs in chapter 5. Finally, the mechanical properties of collagen fibrils extracted from the airway tissue were measured using AFM in chapter 6.

7.1) Mechanical stimulation of airway fibroblasts

Summary of findings

- Mechanical strain enhanced the fibrotic response of airway fibroblasts by increasing the production of collagen and Pro MMP-2.
- Mechanical strain to airway fibroblasts did not promote myofibroblast differentiation but induced a synthetic phenotype.
- Mechanical strain regulated collagen cross-linking by activating Pro-LOX to become active LOX and up-regulated LH2b mRNA expression in airway fibroblasts.
- Mechanical strain promoted inflammatory response of airway fibroblasts by enhancing the production of IL-8.
- Airway fibroblasts from healthy non-asthmatic and asthmatic subjects responded to mechanical stimulation in the same pattern.

7.1.1) The role of mechanical stimulation of airway fibroblasts on airway remodelling

Fibroblasts and myofibroblasts are the principal cells in the airways that produce extracellular matrix protein (ECMs). Among ECMs in the airways, collagen is the most abundant and perhaps most critical for the structural integrity of the airways. This work has shown an increase in collagen production by primary bronchial fibroblasts after exposure to cyclical mechanical stimuli similar to deep breathing. However, it was shown that myofibroblasts are not responsible for this collagen production as there was no significant change of αSMA expression in mechanically exposed fibroblasts. Eches et al has proposed that mechanical stimulation induces a 'synthetic fibroblast phenotype' which is responsible for matrix synthesis (203). A recent study using the same model of mechanical stimulation has also shown that mechanical strain enhances the production of collagen in primary human embryonic lung fibroblasts (268). Apart from regulating collagen production, a similar model of mechanical stimulation to airway fibroblasts has been shown to regulate mRNA expression of the proteoglycans; versican and decorin (175;176). The amount of mechanical stimulation also has an impact on fibroblasts response. Blaauboer et al have shown a decrease in collagen mRNA expression after exposure of primary lung fibroblasts to a lower amount mechanical strain which is similar to normal breathing (202). Consequently, the increase in extracellular matrix production would be a fibrogenic response of airway fibroblasts only after exposure to a high level of mechanical stimulation. Furthermore, the interaction between cells and surrounding extracellular matrix component has an essential role in regulating cellular physiology and the cell-cycle kinetics which lead to the reorganization and remodelling of the ECM (127). It has been shown that airway fibroblast monolayers on membranes coated with different matrixes results in different responses to mechanical stimuli. After exposure of foetal lung fibroblasts to cyclical mechanical stimuli, procollagen I mRNA expression was up-regulated only when the cells were cultured on laminin and elastin coated membranes but the same response was not observed when grown the cells on fibronectin elastin coated membranes (177). Since, fibroblasts in the airways are surrounded by collagen. Collagen I was selected as the matrix for studying in the work presented here. The mechanical stimulation model used produces tensile stress to fibroblasts which can occur on the lungs and airways during deep breathing. However there are limitations to the model for example, during bronchoconstriction associated with asthma exacerbation, the airways are exposed mostly to compressive stress from the inner airway wall buckling into folds as a consequence of airway smooth muscle contraction (269).

In addition, the airway epithelium plays a crucial role in the response to airway injury by producing several cytokines, chemokines and growth factors resulting in regulation of the fibroblast responses (270) (Figure 1-1). An alternative model for studying the impact of mechanical stimuli on the airway during bronchoconstriction may be to grow fibroblasts in a collagen matrix with an epithelial layer on top, and then to expose the epithelial layer to compressive stress (122) (Figure 1-10b). However, in this model only the epithelial layer is exposed to mechanical stimulation. Choe et al. have proposed a three dimensional tissue-engineered model of the human airway wall (162). Utilizing differentiated normal human bronchial epithelial cells which were grown on top of a collagen gel containing human foetal lung fibroblasts (Figure 1-10c). These investigators were able to demonstrate increased collagen deposition and increased secretion of MMP-2 and 9 after exposure of the cell layer to lateral dynamic compression (172). The increase in collagen production and metalloproteinase secretion were also observed in fibroblasts exposure to lateral dynamic compression but the responses were less prominent when compared to epithelium-fibroblasts model (172). This may underline the role of epithelial cells in amplifying the response of fibroblasts on mechanical stimulation. However, even lack of the signal from epithelial cells, the present study has demonstrated that mechanical strain of airway fibroblasts enhanced collagen and metalloproteinase secretion. The role of mechanical stimulation of the airways in enhancing collagen production has been emphasized in a recent *in vivo* study. Grainge et al. have shown an increase in collagen deposition in the subepithelial layer after bronchoconstriction using methacholine challenge, a stimulus that did not affect airway inflammation (206). This emerging study has highlighted the role of mechanical stimuli in airway remodelling in asthma.

In contrast to the current findings, Choe et al. found increased myofibroblast differentiation after mechanical stimuli in their three dimensional epithelium and fibroblast co-culture model. This discrepancy might be explained by the presence of epithelial cells that secrete growth factors such as TGFβ in response mechanical stimuli to promote the myofibroblast differentiation. Even though in the present study, TGFβ was found to increase after mechanical strain to airway fibroblasts. Only 8 paired samples from 18 paired samples had a level of TGFβ1 that was high enough to detect. Furthermore, a recent study has demonstrated a suppressive effect of mechanical strain on TGFβ1 in up-regulation of αSMA expression in airway fibroblasts (202). The TGFβ produced by fibroblasts in the work presented here maybe not high enough to overcome the suppressive effect of mechanical strain resulting in decreased myofibroblast differentiation after mechanical stimuli. This suggests that in the present study the cells that are responsible for production of collagen after mechanical stimuli are fibroblasts that have adapted to be a 'synthetic phenotype'.

Mechanical strain also has a role in regulating collagen cross-linking. It can activate Pro-LOX to become active LOX, even though there was no significant change in Pro-LOX. Mechanical strain also up-regulated LH2b mRNA expression especially in fibroblasts from asthmatic subjects. An increase in LH2b would result in a shift of the collagen cross-linking pathway toward the telopeptide hydroxylysine pathway which is suggested to be a fibrotic response pathway (147). Further studies evaluating the effect on the collagen cross-linking end products need to be undertaken to explore this hypothesis. In summary, mechanical strain can promote airway fibroblasts to produce more collagen which has the potential to be cross-linked in a pro-fibrotic fashion. Asthmatic airways are exposed to a substantial amount of mechanical stress during acute exacerbations. This may result in more collagen deposition in the airways leading to remodelled airways. Thus, apart from the acute morbidity of acute asthma attacks in the clinical setting, bronchoconstriction also has a potential role to promote airway remodelling. This will support the findings in CAMP study which found that the progressive loss of lung function is associated with the frequency and severe asthma exacerbation (271). However, more *in vivo* studies evaluating the role of frequent asthma exacerbations on collagen cross-linking in airway tissues need to be investigated to explore this hypothesis.

7.1.2) The role of mechanical stimulation of airway fibroblasts on airway inflammation

Apart from the pro-fibrotic effect of mechanical strain, the present work also demonstrated an increase in IL-8 production by airway fibroblasts after exposure to cyclical mechanical strain. IL-8 is a potent neutrophil chemotactic factor. Neutrophilic airway inflammation is seen most commonly in patients with severe refractory asthma (272) and has been reported in autopsies of patients who died soon after the onset of a severe exacerbation (273). It also has been demonstrated in exercise induced bronchoconstriction (35;274). Neutrophilic airway inflammation has also been demonstrated in healthy non-asthmatic endurance athletes such as marathon, long distance swimming both at baseline and increases after heavy exercise (275;276). Boulet et al. have reported an association of airway neutrophilia with high-intensity training among airway hyperresponsive swimming athletes (277). The usual ventilatory response to exercise is an increase in tidal volume at low-to-moderate workloads, or an increase in respiratory frequency at high levels of exercise (274). This may result in increased mechanical stimulation to the airways causing more IL-8 to be produced, leading to more neutrophil infiltration into the airways. Consequently, the ability of mechanical strain to airway fibroblasts to trigger IL-8 production may contribute to the neutrophilic airway inflammation in athletes, severe fatal asthma, and exercise induced asthma.

7.2) Regulation of collagen cross-linking related enzymes in airway fibroblasts and fibrotic lung fibroblasts

Summary of findings

- TGFβ2 up-regulated collagen I mRNA expression but dexamethasone had no effect.
- TGFβ2 and dexamethasone enhanced the production of pro-LOX and active LOX.
- Dexamethasone up-regulated LOX mRNA expression only in fibroblasts from asthmatic airways and fibrotic lungs.
- Dexamethasone had an additive effect with TGFβ2 in regulating the production of LOX especially in fibroblasts from asthmatic subjects
- TGFβ2 up-regulated lysyl hydroxylase 2b (LH2b) mRNA expression but dexamethasone had the opposite effect and TGFβ2 up-regulating LH2b mRNA expression was also suppressed by dexamethasone
- Airway fibroblasts from healthy non-asthmatic and asthmatic subjects responded to TGFβ2 stimulation in the same pattern regarding to the production of LOX, LH2b and collagen mRNA expression.
- Severe asthmatic subjects who had a trend of more fixed airway obstruction produced more active LOX in BAL fluid when compared to healthy non-asthmatic and mild asthmatic subjects.

7.2.1) Regulation of Lysyl oxidase (LOX) in airway fibroblasts

Collagen is the most abundant ECMs protein and provides the structural integrity in the tissue. Lysyl oxidase (LOX) plays a key role in cross-linking of the collagen fibrils, resulting in the deposition of insoluble collagen fibres (278). The strength of collagen depends on the amount of crosslinking by lysyl oxidase (LOX). LOX is a copper dependent amine oxidase that belongs to a family of LOX proteins. The LOX family genes consist of LOX, LOXL-1, LOXL-2, LOXL-3 and LOXL-4. However, only LOX, LOXL-1 and LOXL-2 are expressed in the lungs and LOX has the highest expression (279). LOX is synthesized by fibroblasts as a 50-kDa proenzyme that is secreted out of the extracellular space where it was activated to form the 30-kDa catalytically active form. Therefore, LOX production can be regulated at the synthesis and the conversion to the active form level. It was previously reported that TGFβ1 or hypoxia-inducible factor-1 α (HIF-1 α) up-regulated LOX mRNA (278) whilst TNFα (280) and PGE2 (281) supressed LOX mRNA expression. Pro-LOX can be activated by procollagen C proteinase, Tolloid-like 1 protein, Aminopeptidase B and fibronectin (278).

The work present here has demonstrated the ability of TGFβ2, and dexamethasone to up-regulate LOX gene expression in airway fibroblasts. TGFβ2, serum, mechanical strain and dexamethasone also enhanced the production of LOX and also activated Pro-LOX to become active LOX. The up-regulation of LOX by corticosteroids was supported by the analysis of BAL fluid. It was shown there was an increase active LOX only in BAL fluid from a subset of corticosteroids treated asthmatic subjects, but not in those whom are corticosteroids untreated. Collagen strength derived from collagen cross-linking is essential for the structural integrity and function of tissue. Increased expression of LOX both at mRNA and protein levels were observed in several fibrotic models, including lungs [bronchopulmonary dysplasia (282), bleomycin-induced lung fibrosis (283)], heart (225), kidney (145) and skin (284). It has been shown that Lox knockout mice have substantial developmental problems in the lung as well as in the cardiovascular system and skin (284). A study in murine foetal lung organ cultures has found that dexamethasone up-regulated Lox gene expression and dexamethasone treated lungs developed thicker alveolar septa than untreated lungs (285). These previous studies emphasize the role of LOX via dexamethasone in accelerating maturation and differentiation of the developing foetal lung. However, continued exposure to corticosteroids in the lungs and airways may have an adverse effect on lungs and airway wall mechanics via promoting LOX production and resulting in increased collagen cross-linking. The role of dexamethasone in the regulation of LOX has never been studied in adult human airway before. The current *in vitro* study was able to demonstrate the ability of dexamethasone to up-regulate LOX mRNA

expression in airway fibroblasts, and enhance the production of both Pro-LOX and active LOX especially in fibroblasts from asthmatic subjects. As a result, continuing exposure to corticosteroids in the airways may promote the collagen cross-linking process via increasing the production of LOX. This may result in increased the stiffness of the airway as an unwanted side effect of anti-inflammatory treatment.

Apart from cross-linking collagen, LOX can also cross-link elastin which plays a crucial role in the development of alveolar space in the lung and elastic recoil of the lungs during expiration (286). Abnormal elastin metabolism is associated with several diseases of the lung, including pulmonary hypertension (287) and emphysema (288). It was shown that cigarette smoke condensate suppressed the production of LOX protein in cultured lung fibroblasts (289;290). Therefore, dysregulated LOX expression in the lung from smoking may play a role in emphysema in COPD patients.

7.2.2) Regulation of Lysyl hydroxylase2b (LH2b) in airway fibroblasts

Collagen cross-linking initiated by lysyl oxidase (LOX) has two different pathways, depending on the oxidative deamination of lysine or hydroxylysine residues in the telopeptide region of collagen molecules. The lysine pathway produces histidinohydroxylysinonorleucine (HHL) as a final end product, whilst the end products of the hydroxylysine pathway are pyridinoline (PYD) and deoxypyridinolone (DPD). An increase in pyridinoline has been suggested to be a fibrotic phenomenon as it has been documented in several fibrotic tissues (147). Lysyl hydroxylase2 (LH2) has been identified as a telopeptide lysyl hydroxylase which causes the cross-linking to be shifted to pyridinoline pathway. LH2 gene has 2 alternative RNA splice variants: LH2a and LH2b. van der Slot et al have reported an increase in LH2b mRNA expression in cultured fibroblast from hypertrophic scars, keloid and palmar fascia of Dupuytren's patients. These investigators also reported a concomitant formation of pyridinoline produced by the same fibroblast in culture (147). This suggests that LH2b is the primary regulator of the pattern of pyridinoline cross-linking in collagen. Several cytokines such as IL-4, activin A, and TNF-α have been shown to regulate LH2b mRNA expression in human skin fibroblasts in vitro (291;292). However, the role of TGFβ in regulating LH2b mRNA expression is controversial. Seitzer et al have reported a suppressive effect of TGFβ1 on LH2b mRNA expression in human osteoblast-like cells in vitro (293). On the contrary, van der Slota et al have shown that TGFβ1, 2 and 3 up-regulated LH2b mRNA expression in normal human skin fibroblasts in vitro (292). This suggests that TGFβ regulates LH2b mRNA expression differently in different cell types. The work presented here has demonstrated a regulatory effect of TGFβ2, mechanical strain and dexamethasone on LH2b mRNA expression in airway fibroblasts. TGFβ2 up-

regulated LH2b mRNA expression in airway both in fibroblasts from healthy non-asthmatic and asthmatic subjects, but mechanical strain up-regulated LH2b mRNA expression only in fibroblasts from asthmatic subjects. In contrast, dexamethasone modestly suppressed LH2b mRNA expression in fibroblasts from asthmatic subjects and also suppressed the up-regulation of LH2b mRNA expression by TGFβ2 both in fibroblasts from healthy non-asthmatic and asthmatic subjects. There is no previous report exploring the role of mechanical strain and dexamethasone in regulating LH2b mRNA expression before. Asthmatic airways are exposed to more TGFβ2 and frequent mechanical strain from asthma exacerbations. This may result in more LH2b expression leading to the collagen cross-liking via pyridinoline pathway. In corticosteroids treated asthmatic subjects, these effects may be opposed by their treatment. There is no previous report suggesting which collagen cross-linking pathway is dominant in asthmatic airways. Further measurement of the collagen cross-linking end products in airway tissue from healthy non-asthmatic, corticosteroid naïve, and corticosteroid treated asthmatic subjects will give us a better understanding in collagen cross-linking pathways in asthma.

In summary, the present in vitro study has demonstrated a role for TGFβ2, dexamethasone and mechanical strain in regulating collagen cross-linking related enzyme: LOX and LH2b. It was shown that collagen has the potential to be more cross-linked as a result of the increase in LOX expression after TGFβ2, dexamethasone and mechanical strain stimulations. However, more *in vivo* studies of LOX and LH2b protein expression and the collagen cross-linking end products in the airway tissue will help to translate this *in vitro* work into the clinical aspect.

7.2.3) Role of TGFβ2 and dexamethasone in regulating collagen cross-linking in ILD

The present work also evaluated the response of lung fibroblasts from a patient with chronic bronchiolitis with constrictive obliterative bronchiolitis. Chronic bronchiolitis with constrictive obliterative bronchiolitis is an interstitial lung disease (ILD) with prominent fibrosis in respiratory and membranous bronchioles (237). The role of TGFβ in this disease has been widely recognized in several studies (294-296). Increased lung collagen cross-linking has been shown both in a bleomycin induced lung fibrosis model (143) and ILD patients (141). In addition, it has been found that bleomycin enhances the production of LOX in human foetal lung fibroblasts (283). The present work has found that fibroblasts from one ILD subject produced more Pro-LOX and active LOX after stimulation with TGFβ2 and dexamethasone. Furthermore, dexamethasone had an additive effect to TGFβ2 in enhancing the production of LOX. Corticosteroids are one of the treatments for ILD patients. Consequently, from this in vitro results, apart from the anti-inflammatory effect of corticosteroids, these drugs may also had a detrimental effect in exacerbating the effect of TGFβ in promoting fibrotic process in interstitial lung diseases. However, more subjects need to be investigated to confirm that these responses are not the donor-specific effect.

TGFβ2 also significantly up-regulated LH2b mRNA expression in the fibroblasts from the ILD subject studied. However, the role of dexamethasone in regulating LH2b was not clearly seen in these fibroblasts. In contrast to the response observed in fibroblasts from the airways, dexamethasone had a less noticeable trend to suppress the up-regulation of LH2b mRNA by TGFβ2. This suggests that the predominant collagen cross-linking pathway in this ILD subject may be via pyridinoline pathway. This suggestion is supported by a previous study that reported an increase in pyridinoline collagen cross-link end product in lung tissue from patients with chronic fibrotic lung when compared to control subjects and patients with adult respiratory distress syndrome. These findings highlight the role TGFβ in promoting the fibrosis process in pulmonary fibrosis via up-regulating LH2b mRNA expression.

7.3) The role of decorin and biglycan on collagen fibrillogenesis

Summary of findings

- TGFβ2 and mechanical strain up-regulated biglycan mRNA expression but suppressed decorin mRNA expression.
- Dexamethasone suppressed the up-regulation of biglycan by TGFβ2 but it had no effect on decorin mRNA expression.

Small leucine -rich proteoglycans (SLRPs); decorin and biglycan have been recognized as regulators of collagen fibril assembly. They interact with collagen through specific binding sites and delay collagen fibril formation (297). However, the exact mechanism how SLRPs regulate collagen assembly is still unclear. It was proposed that SLRPs compete with collagens to bind to specific collagen binding site then prevent collagen assembly by preventing the further chemical reactions occurring during collagen fibrillogenesis (298). Different SLRPs have their own unique mechanism in competing for the collagen binding because they cannot compensate for the absence of each other as shown in knockout mice phenotypes. Decorin deficient mice suffer from skin fragility due to loosely packed collagen fibres (156) whilst biglycan knockout mice have a thin dermis with irregular collagen fibril (157). The present work has found that decorin mRNA expression in airway fibroblasts was suppressed by TGFβ2 and mechanical strain. Dexamethasone had no effect on decorin mRNA expression. It has been shown previously that TGFβ down-regulates decorin expression (299) and conversely decorin can inhibit TGFβ activity both *in vitro* and *in vivo (84;233)*. As a result, the role of decorin in regulating the collagen fibrillogenesis in the asthmatic airway may be complex because TGFβ and decorin can regulate each other activities.

In contrast to decorin, the present study revealed that biglycan mRNA expression was up-regulated by TGFβ2 and mechanical strain. Dexamethasone suppressed the up-regulation of biglycan by TGFβ2. Although decorin has been suggested to have a key role in collagen assembly (228), biglycan provides partial functional compensation for decorin deficiency (256). As a result, dexamethasone may have a limited role in affecting collagen assembly via regulation biglycan mRNA expression. The up-regulation of biglycan mRNA expression by TGFβ2 and mechanical strain may result in more biglycan deposited in asthmatic airways. This is consistent with the previous report showing an increase in biglycan staining in asthmatic airways when compared to non-asthmatic airways (300).

7.4) The role of corticosteroids and airway remodelling in asthma

Asthma is recognized as an inflammatory disease of the conducting airways which present functional and structural changes, leading to bronchial hyperresponsiveness (BHR) and airflow obstruction (45). Inhaled corticosteroids are suggested as currently the most effective anti-inflammatory medications for the treatment of chronic asthma (1). Even though inhaled corticosteroids have been shown to reduce asthma symptoms and exacerbations (238;241;242), they have failed to alter the natural history of disease. Thus, treatment atopic children with recurrent wheezing using inhaled corticosteroids have shown no effect on lung function or the natural history of asthma (30). The role of corticosteroids in reversing airway remodelling is controversial. Several studies have examined the effect of corticosteroids on subepithelial collagen thickness but the results were inconsistent (109;250;253). Inhaled corticosteroids have also failed to establish any inhibitory effect on the decline in lung function in asthmatic patients after treatment (241;254). Previous studies have demonstrated a suppressive effect of corticosteroids on collagen expression in fibroblasts (301;302). However, in the present study, it was not possible to demonstrate any changes in collagen mRNA in airway fibroblasts after stimulation with dexamethasone. Furthermore, apart from the commonly known anti-inflammatory effects of corticosteroids, the present study identified a potential role for dexamethasone in regulating collagen cross-linking in the airways. Thus, fibroblasts from asthmatic subjects were found to respond to dexamethasone differently from fibroblasts from healthy non-asthmatic subjects. It was shown that up-regulation of LOX mRNA, the additive effect to TGFβ on this up-regulation of LOX mRNA and the production of Pro-LOX were only detected in fibroblasts from asthmatic subjects. As asthmatic airways will be exposed to more corticosteroids as well as more TGFβ found in asthmatic airways than healthy non-asthmatic airways, this may further augment the response of fibroblasts to produce more LOX which may result in more cross-linked collagens deposited in asthmatic airways. Furthermore, it was shown that dexamethasone could activate pro-LOX to become active LOX both in fibroblasts from asthmatic and healthy non-asthmatic subjects. This highlights the potential detrimental effect of dexamethasone in promoting LOX production.

In the present study, it was found that dexamethasone down-regulated LH2b mRNA. This enzyme determines whether the final collagen cross-linking in the airways follows the lysine collagen cross-linking pathways which were suggested to be less fibrotic or the more fibrotic hydroxylysine pathways (127). However, there have been no previous studies focusing on the collagen cross-linking pathways in asthmatic airway before. Further studies on the relative levels of each collagen cross-linking end product in

asthmatic airways and their relationship with airway mechanics are needed to help understand better the role of collagen cross-linking on airway physiology. In addition, more studies regarding the impact of inhaled corticosteroid on collagen cross-linking in the airways need to be undertaken to determine whether the effect observed *in vitro* also occurs *in vivo* and whether it is a drug specific or class specific effect action or not.

Although, the combination of inhaled corticosteroids and long acting β2 agonist (LABA) are widely used in moderate to severe asthma, their ability to modulate airway remodelling is not well established. Goulet el al have investigated the effect of corticosteroids and LABA on collagen produced by human lung fibroblasts. These investigators have demonstrated that LABA (salmeterol and formoterol) suppressed collagen production by lung fibroblasts, but the opposite effects were shown in fibroblasts treated with fluticasone or budesonide, the commonly used inhaled corticosteroid (227). These investigators also reported that in combination of corticosteroids and LABA were able to suppress the corticosteroids induced increased in collagen production by human lung fibroblasts (227). A recent *in vitro* study has also found that co-treatment of airway fibroblasts from asthmatic subjects with budesonide and formoterol significantly suppressed the stimulatory effect of TGFβ in enhancing procollagen release from airway fibroblasts (234). Current asthma guideline also recommend leukotriene receptor antagonists as alternative controller therapy for chronic asthma (1). Therefore it is of interest that leukotriene receptor antagonist has been shown to reduce subepithelial layer thickening in a mouse asthma model (303-305). Based on these studies, it would be interesting to investigate the effect of inhaled steroids together with long acting beta2 agonist, or a leukotriene receptor antagonist on LOX production by airway fibroblasts. In addition, only BAL fluid samples from some severe asthmatic subjects presented active LOX. This subset of patients requires further investigation on the role of corticosteroids in regulating the collagen cross-linking processes in the airways and its potential link with fixed airflow obstruction.

7.5) Collagen fibril structure and mechanical properties as demonstrated by atomic force microscopy

Summary of finings

- Collagen extracted from the airways of a COPD patient had a larger diameter than collagen from nasal polyp, lung parenchyma, and healthy non-asthmatic and asthmatic airways.
- Collagen extracted from asthmatic airways had the highest Young's modulus when compared to collagen extracted from the nasal polyp and healthy non-asthmatic airways.
- Collagen extracted from asthmatic airways had a higher stiffness than collagen extracted from healthy non-asthmatic airways.

Collagen structure and distribution can be demonstrated by immunohistochemical techniques and electron microscopy. However, the routine sample preparation methods irreversibly denature the biomolecule by chemical fixation and staining, and also, during imaging from the electron beam interactions (306). This will affect the mechanical properties of the samples. Atomic force microscopy is a suitable method to determine collagen structure and its mechanical properties because fixation and staining are not required. In the present work, it was possible to demonstrate the structure of airway collagen and its mechanical properties using atomic force microscopy. It was found that collagen fibrils extracted from COPD airway tissue had the largest diameter when compared to collagen extracted from nasal polyp, lung parenchyma, and healthy non-asthmatic and asthmatic airways. It has been suggested that the mechanical properties of tendon are related to the collagen fibril diameter distribution: the large fibrils are responsible for withstanding high tensile forces and the smaller fibrils have a role in resisting distortion under load (151). However, in the present work a difference in the mechanical properties of airway collagen fibrils from healthy non-asthmatic and asthmatic subject was identified, but there was no difference in the diameter of these collagen fibrils. Published experiments monitoring collagen fibril diameters after mechanical loading of tendon *in vivo* have been inconclusive regarding the role of collagen fibril diameter and its mechanical loading properties. Patterson-Kane et al have evaluated the mechanical loading to superficial digital flexor tendon in horse using a specific defined training programme. This revealed a decrease in collagen fibril diameter in mechanically loaded tendon when compared to control (307). In contrast, Michna et al have evaluated collagen from mice skeletal tendon after exposure physical loading and it was found that the collagen fibril diameter in the control group was larger than in the physical loading group (308). It has been suggested that collagen in different tissue with similar collagen content can

exhibit different bio-mechanical properties depending on the specific need of the organs (127). This may suggest that apart from the tissue specific bio-mechanical properties of collagen, there may be other tissue specific effects on collagen bio-mechanical properties. As a result, it is difficult to compare the findings from the present work with previous reports, since most of the previously reported results are of collagen from rat tails or animal tendons, there are few studies exploring the collagen from airways and lung tissue (309) but none of these investigated the human airways and lung tissue samples.

In the present work, it was found that collagen fibrils from asthmatic airways had a higher Young's modulus than collagen from healthy non-asthmatic airways: 1.2 ± 0.26 (GPa) vs 0.98 ± 0.13 (GPa), respectively. Because of differences in methodology, the Young's modulus of collagen fibril has been reported to range from 1-11.5 GPa depending on the hydration status of the fibrils and indentation model used (159). As a result, it is necessary to use the same condition of indentation and hydration status to determine any differences in the mechanical property of the collagen fibrils. The data presented in the present study having established the structure of airway collagen on nanoscale are from one subject in each group. Therefore, more subjects need to be evaluated to confirm these findings. The next question is whether individual collagen fibril mechanical properties will represent the entire airway wall mechanical properties. The reorganization of collagen fibrils and type of collagen fibril is also responsible for changes in the tissue mechanical properties (127). Consequently, further studies in type of collagen fibril distributed in the airways using special staining (e.g. immunogold staining) and the collagen alignment in the airways using other imaging technique such as a multiphoton and second harmonic generation imaging need to be further investigated. In addition, there will need to be further investigation of how the mechanical properties of collagen fibrils in the airways affect the airway wall mechanics and have an impact on the airway physiology. However, there is no standard method in evaluating the airways and lung mechanics *in vivo*. A recent parameter, airway distensibility measured by forced oscillation technique (FOT) has been proposed to represent the airway mechanics (128).

7.6) Conclusions

Although the role of airway remodelling on excessive airway narrowing (193), and fixed airway obstruction, particularly in severe asthma has been well recognized (52), the pathogenesis of airway remodelling in asthma still remains under researched. The work in this thesis has demonstrated potential roles for both mechanical strain and dexamethasone on airway remodelling. It has been shown that mechanical strain can induce airway fibroblasts to produce more collagen and lysyl oxidase (LOX), the collagen cross-linking enzyme. Dexamethasone can also enhance the production of LOX by airway fibroblasts, similarly to TGFβ, a potent profibrotic cytokine. It has also been shown that fibroblasts from healthy and asthmatic airways and fibroblasts from fibrotic lung respond to TGFβ2 in similar ways. Furthermore, fibroblasts from asthmatic airways and fibrotic lung responded to dexamethasone different from healthy non-asthmatic subjects. Thus, up-regulation of LOX mRNA was demonstrated in fibroblasts from asthmatic airways and fibrotic lung but not those from healthy non-asthmatic subjects. The additive effect to TGFβ in up-regulation LOX mRNA and the production of Pro-LOX were also demonstrated only in fibroblasts from asthmatic subjects. Fibroblasts in asthmatic airways will be exposed to more TGFβ and only fibroblasts from asthmatic subjects will be exposed to corticosteroids. The overall effect in asthma may be an increase in LOX production and more cross-linked collagen deposited in the airways. This may also have an impact on collagen stiffness, as shown in the present work where collagen extracted from asthmatic airways has a higher stiffness than collagen fibrils from healthy non-asthmatic airways. The stiffer collagen deposited in the subepithelial layer will result in a stiffer airway that can resist or protect against airway smooth muscle contraction leading to decrease bronchial hyperresponsiveness (BHR) (193). The repeated exposure to mechanical stimulation during asthma exacerbations, together with increased TGFβ levels and treatment with high dose of corticosteroids especially in severe asthmatic subjects, the combine effect will result in an increased amount of stiff collagen deposited in the airways leading to fixed airway obstruction. These data support the need for more *in vivo* studies measuring the amount of collagen cross-linking and physiological evaluation of airway wall mechanics in asthmatic airways to confirm the role of collagen cross-linking on airway remodelling in asthma. A proposed schematic role of mechanical strain, TGFβ2 and dexamethasone and collagen in airway remodelling in asthma is summarized in Figure 7-1.

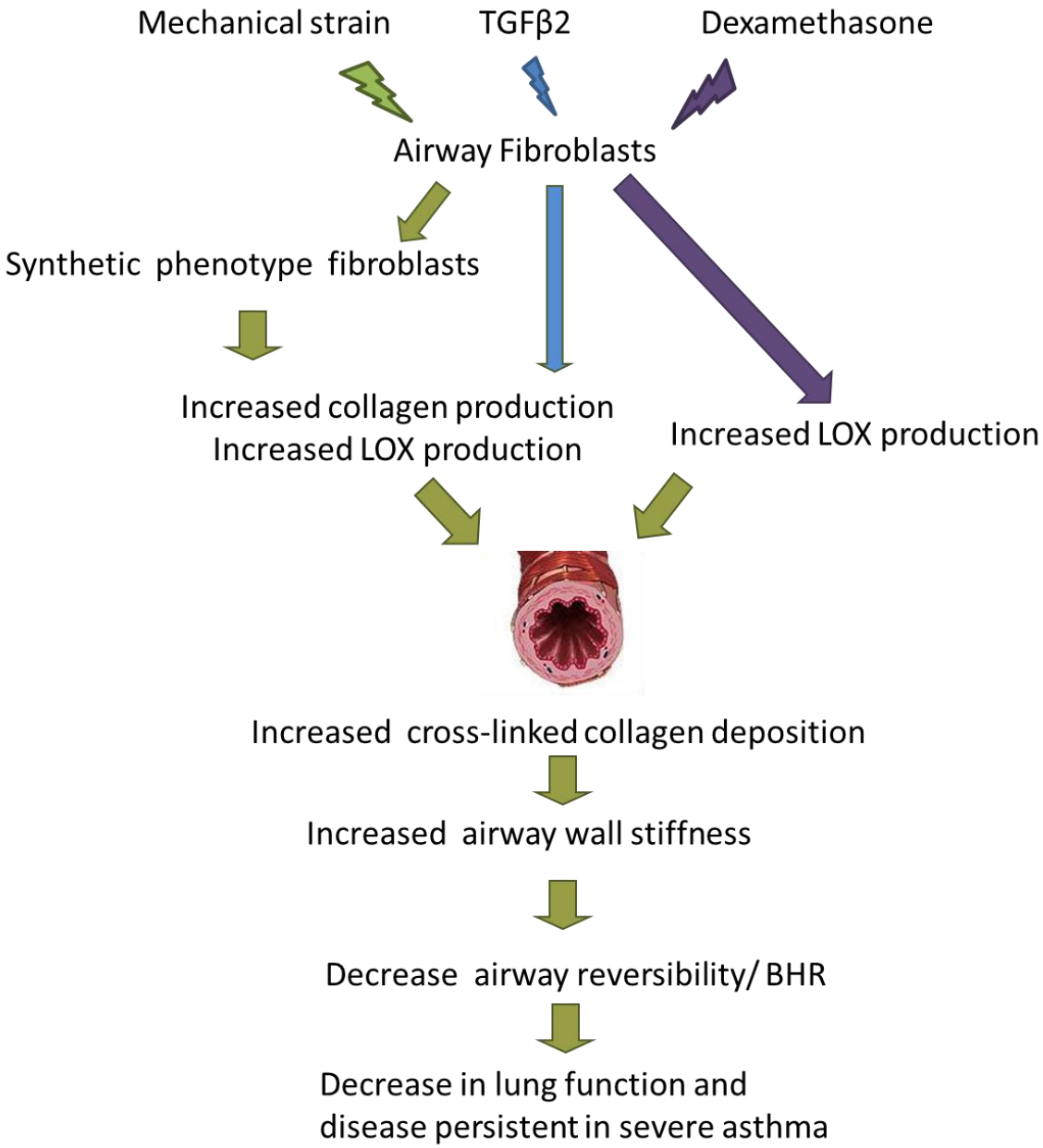

Figure 7-1: Schematic image summarizing the role of mechanical strain, TGFβ2 and dexamethasone on collagen cross-linking in the airways to result in increased airway wall stiffness which may oppose to airway smooth muscle contraction during bronchoconstriction resulting in decrease airway reversibility, this may explain the decrease in lung function and disease persistent in severe asthma.

Reference List

(1) the Global Strategy for Asthma Management and Prevention, Global Initiative for Asthma (GINA) 2010. [Internet] [cited 2010 June 20]. Available from http://www.ginasthma.org/.

(2) Holgate ST. A look at the pathogenesis of asthma: the need for a change in direction. Discov Med 2010 May;9(48):439-47.

(3) Holgate S, Bisgaard H, Bjermer L, Haahtela T, Haughney J, Horne R, et al. The Brussels Declaration: the need for change in asthma management. Eur Respir J 2008 Dec;32(6):1433-42.

(4) Henderson J, Sherriff A, Farrow A, Ayres JG. Household chemicals, persistent wheezing and lung function: effect modification by atopy? Eur Respir J 2008 Mar;31(3):547-54.

(5) Shaheen SO, Newson RB, Sherriff A, Henderson AJ, Heron JE, Burney PG, et al. Paracetamol use in pregnancy and wheezing in early childhood. Thorax 2002 Nov;57(11):958-63.

(6) Islam T, Gauderman WJ, Berhane K, McConnell R, Avol E, Peters JM, et al. Relationship between air pollution, lung function and asthma in adolescents. Thorax 2007 Nov;62(11):957-63.

(7) Chinn S. Obesity and asthma. Paediatr Respir Rev 2006 Sep;7(3):223-8.

(8) Arshad SH, Tariq SM, Matthews S, Hakim E. Sensitization to common allergens and its association with allergic disorders at age 4 years: a whole population birth cohort study. Pediatrics 2001 Aug;108(2):E33.

(9) Gilliland FD, Li YF, Peters JM. Effects of maternal smoking during pregnancy and environmental tobacco smoke on asthma and wheezing in children. Am J Respir Crit Care Med 2001 Feb;163(2):429-36.

(10) Flaherman V, Rutherford GW. A meta-analysis of the effect of high weight on asthma. Arch Dis Child 2006 Apr;91(4):334-9.

(11) Holloway JW, Yang IA, Holgate ST. Genetics of allergic disease. J Allergy Clin Immunol 2010 Feb;125(2 Suppl 2):S81-S94.

(12) Graves PE, Kabesch M, Halonen M, Holberg CJ, Baldini M, Fritzsch C, et al. A cluster of seven tightly linked polymorphisms in the IL-13 gene is associated with total serum IgE levels in three populations of white children. J Allergy Clin Immunol 2000 Mar;105(3):506-13.

(13) Weidinger S, Gieger C, Rodriguez E, Baurecht H, Mempel M, Klopp N, et al. Genome-wide scan on total serum IgE levels identifies FCER1A as novel susceptibility locus. PLoS Genet 2008 Aug;4(8):e1000166.

(14) van Diemen CC, Postma DS, Vonk JM, Bruinenberg M, Schouten JP, Boezen HM. A disintegrin and metalloprotease 33 polymorphisms and lung function decline in the general population. Am J Respir Crit Care Med 2005 Aug 1;172(3):329-33.

(15) Simpson A, Maniatis N, Jury F, Cakebread JA, Lowe LA, Holgate ST, et al. Polymorphisms in a disintegrin and metalloprotease 33 (ADAM33) predict impaired early-life lung function. Am J Respir Crit Care Med 2005;172(1):55-60.

(16) Holloway JW, Yang IA, Holgate ST. Interpatient variability in rates of asthma progression: can genetics provide an answer? J Allergy Clin Immunol 2008 Mar;121(3):573-9.

(17) Bieli C, Eder W, Frei R, Braun-Fahrlander C, Klimecki W, Waser M, et al. A polymorphism in CD14 modifies the effect of farm milk consumption on allergic diseases and CD14 gene expression. J Allergy Clin Immunol 2007 Dec;120(6):1308-15.

(18) Werner M, Topp R, Wimmer K, Richter K, Bischof W, Wjst M, et al. TLR4 gene variants modify endotoxin effects on asthma. J Allergy Clin Immunol 2003 Aug;112(2):323-30.

(19) Gilliland FD, Gauderman WJ, Vora H, Rappaport E, Dubeau L. Effects of glutathione-S-transferase M1, T1, and P1 on childhood lung function growth. Am J Respir Crit Care Med 2002 Sep 1;166(5):710-6.

(20) Gilliland FD, Li YF, Dubeau L, Berhane K, Avol E, McConnell R, et al. Effects of glutathione S-transferase M1, maternal smoking during pregnancy, and environmental tobacco smoke on asthma and wheezing in children. Am J Respir Crit Care Med 2002 Aug 15;166(4):457-63.

(21) Salam MT, Lin PC, Avol EL, Gauderman WJ, Gilliland FD. Microsomal epoxide hydrolase, glutathione S-transferase P1, traffic and childhood asthma. Thorax 2007 Dec;62(12):1050-7.

(22) Contopoulos-Ioannidis DG, Manoli EN, Ioannidis JP. Meta-analysis of the association of beta2-adrenergic receptor polymorphisms with asthma phenotypes. J Allergy Clin Immunol 2005 May;115(5):963-72.

(23) Holloway JW, Dunbar PR, Riley GA, Sawyer GM, Fitzharris PF, Pearce N, et al. Association of beta2-adrenergic receptor polymorphisms with severe asthma. Clin Exp Allergy 2000 Aug;30(8):1097-103.

(24) Chagani T, Pare PD, Zhu S, Weir TD, Bai TR, Behbehani NA, et al. Prevalence of tumor necrosis factor-alpha and angiotensin converting enzyme polymorphisms in mild/moderate and fatal/near-fatal asthma. Am J Respir Crit Care Med 1999 Jul;160(1):278-82.

(25) Moffatt MF, Gut IG, Demenais F, Strachan DP, Bouzigon E, Heath S, et al. A large-scale, consortium-based genomewide association study of asthma. N Engl J Med 2010 Sep 23;363(13):1211-21.

(26) Green RH, Brightling CE, McKenna S, Hargadon B, Parker D, Bradding P, et al. Asthma exacerbations and sputum eosinophil counts: a randomised controlled trial. Lancet 2002 Nov 30;360(9347):1715-21.

(27) Anderson GP. Endotyping asthma: new insights into key pathogenic mechanisms in a complex, heterogeneous disease. Lancet 2008;372(9643):1107-19.

(28) Leckie MJ, ten Brinke A, Khan J, Diamant Z, O'Connor BJ, Walls CM, et al. Effects of an interleukin-5 blocking monoclonal antibody on eosinophils, airway hyper-responsiveness, and the late asthmatic response. Lancet 2000;356(9248):2144-8.

(29) Bisgaard H, Hermansen MN, Loland L, Halkjaer LB, Buchvald F. Intermittent inhaled corticosteroids in infants with episodic wheezing. N Engl J Med 2006;354(19):1998-2005.

(30) Guilbert TW, Morgan WJ, Zeiger RS, Mauger DT, Boehmer SJ, Szefler SJ, et al. Long-term inhaled corticosteroids in preschool children at high risk for asthma. N Engl J Med 2006;354(19):1985-97.

(31) Murray CS, Woodcock A, Langley SJ, Morris J, Custovic A. Secondary prevention of asthma by the use of Inhaled Fluticasone propionate in Wheezy INfants (IFWIN): double-blind, randomised, controlled study. Lancet 2006;368(9537):754-62.

(32) Sears MR, Greene JM, Willan AR, Wiecek EM, Taylor DR, Flannery EM, et al. A longitudinal, population-based, cohort study of childhood asthma followed to adulthood. N Engl J Med 2003;349(15):1414-22.

(33) Wenzel SE, Szefler SJ, Leung DY, Sloan SI, Rex MD, Martin RJ. Bronchoscopic evaluation of severe asthma. Persistent inflammation associated with high dose glucocorticoids. Am J Respir Crit Care Med 1997 Sep;156(3 Pt 1):737-43.

(34) Shaw DE, Berry MA, Hargadon B, McKenna S, Shelley MJ, Green RH, et al. Association between neutrophilic airway inflammation and airflow limitation in adults with asthma. Chest 2007 Dec;132(6):1871-5.

(35) Busse W, O'Byrne PM, Holgate ST. Asthma Pathogenesis. In: Franklin NFJ, Bochner BS, Busse WW, Holgate ST, Lemanske RF, Jr., editors. Middleton's allergy : principles & practice. 6th ed. Philadelphia : Mosby; 2003. p. 1175-208.

(36) O'Byrne PM. Leukotriene bronchoconstriction induced by allergen and exercise. Am J Respir Crit Care Med 2000 Feb;161(2 Pt 2):S68-S72.

(37) Martin RJ, Cicutto LC, Smith HR, Ballard RD, Szefler SJ. Airways inflammation in nocturnal asthma. Am Rev Respir Dis 1991 Feb;143(2):351-7.

(38) Macedo P, Hew M, Torrego A, Jouneau S, Oates T, Durham A, et al. Inflammatory biomarkers in airways of patients with severe asthma compared with non-severe asthma. Clin Exp Allergy 2009 Nov;39(11):1668-76.

(39) Fahy JV, Kim KW, Liu J, Boushey HA. Prominent neutrophilic inflammation in sputum from subjects with asthma exacerbation. J Allergy Clin Immunol 1995 Apr;95(4):843-52.

(40) Davies DE, Wicks J, Powell RM, Puddicombe SM, Holgate ST. Airway remodeling in asthma: new insights. J Allergy Clin Immunol 2003;111(2):215-25.

(41) Bayram H, Rusznak C, Khair OA, Sapsford RJ, Abdelaziz MM. Effect of ozone and nitrogen dioxide on the permeability of bronchial epithelial cell cultures of non-asthmatic and asthmatic subjects. Clin Exp Allergy 2002;32(9):1285-92.

(42) Bucchieri F, Puddicombe SM, Lordan JL, Richter A, Buchanan D, Wilson SJ, et al. Asthmatic bronchial epithelium is more susceptible to oxidant-induced apoptosis. Am J Respir Cell Mol Biol 2002;27(2):179-85.

(43) Howat WJ, Holgate ST, Lackie PM. TGF-beta isoform release and activation during in vitro bronchial epithelial wound repair. Am J Physiol Lung Cell Mol Physiol 2002;282(1):L115-L123.

(44) Zhang S, Smartt H, Holgate ST, Roche WR. Growth factors secreted by bronchial epithelial cells control myofibroblast proliferation: an in vitro co-culture model of airway remodeling in asthma. Lab Invest 1999;79(4):395-405.

(45) Holgate ST. Pathogenesis of asthma. Clin Exp Allergy 2008;38(6):872-97.

(46) Bergeron C, Boulet LP. Structural changes in airway diseases: characteristics, mechanisms, consequences, and pharmacologic modulation. Chest 2006;129(4):1068-87.

(47) Fedorov IA, Wilson SJ, Davies DE, Holgate ST. Epithelial stress and structural remodelling in childhood asthma. Thorax 2005;60(5):389-94.

(48) Saglani S, Payne DN, Zhu J, Wang Z, Nicholson AG, Bush A, et al. Early detection of airway wall remodeling and eosinophilic inflammation in preschool wheezers. Am J Respir Crit Care Med 2007;176(9):858-64.

(49) Barbato A, Turato G, Baraldo S, Bazzan E, Calabrese F, Panizzolo C, et al. Epithelial damage and angiogenesis in the airways of children with asthma. Am J Respir Crit Care Med 2006 Nov 1;174(9):975-81.

(50) Payne DN, Rogers AV, Adelroth E, Bandi V, Guntupalli KK, Bush A, et al. Early thickening of the reticular basement membrane in children with difficult asthma. Am J Respir Crit Care Med 2003;167(1):78-82.

(51) Turato G, Barbato A, Baraldo S, Zanin ME, Bazzan E, Lokar-Oliani K, et al. Nonatopic children with multitrigger wheezing have airway pathology comparable to atopic asthma. Am J Respir Crit Care Med 2008;178(5):476-82.

(52) Durrani SR, Viswanathan RK, Busse WW. What effect does asthma treatment have on airway remodeling? Current perspectives. J Allergy Clin Immunol 2011 Sep;128(3):439-48.

(53) Holgate ST. Epithelium dysfunction in asthma. J Allergy Clin Immunol 2007 Dec;120(6):1233-44.

(54) Callerame ML, Condemi JJ, Bohrod MG, Vaughan JH. Immunologic reactions of bronchial tissues in asthma. N Engl J Med 1971 Mar 4;284(9):459-64.

(55) Jeffery PK, Godfrey RW, Adelroth E, Nelson F, Rogers A, Johansson SA. Effects of treatment on airway inflammation and thickening of basement membrane reticular collagen in asthma. A quantitative light and electron microscopic study. Am Rev Respir Dis 1992 Apr;145(4 Pt 1):890-9.

(56) Roche WR, Beasley R, Williams JH, Holgate ST. Subepithelial fibrosis in the bronchi of asthmatics. Lancet 1989;1(8637):520-4.

(57) Brewster CE, Howarth PH, Djukanovic R, Wilson J, Holgate ST, Roche WR. Myofibroblasts and subepithelial fibrosis in bronchial asthma. Am J Respir Cell Mol Biol 1990;3(5):507-11.

(58) Postma DS, Timens W. Remodeling in asthma and chronic obstructive pulmonary disease. Proc Am Thorac Soc 2006;3(5):434-9.

(59) Fernandes DJ, Bonacci JV, Stewart AG. Extracellular matrix, integrins, and mesenchymal cell function in the airways. Curr Drug Targets 2006;7(5):567-77.

(60) Holgate ST, Lackie PM, Howarth PH, Roche WR, Puddicombe SM, Richter A, et al. Invited lecture: activation of the epithelial mesenchymal trophic unit in the pathogenesis of asthma. Int Arch Allergy Immunol 2001 Jan;124(1-3):253-8.

(61) Hostettler KE, Roth M, Burgess JK, Gencay MM, Gambazzi F, Black JL, et al. Airway epithelium-derived transforming growth factor-beta is a regulator of fibroblast proliferation in both fibrotic and normal subjects. Clin Exp Allergy 2008;38(8):1309-17.

(62) Westergren-Thorsson G, Chakir J, Lafreniere-Allard MJ, Boulet LP, Tremblay GM. Correlation between airway responsiveness and proteoglycan production by bronchial fibroblasts from normal and asthmatic subjects. Int J Biochem Cell Biol 2002;34(10):1256-67.

(63) Chetta A, Foresi A, Del DM, Bertorelli G, Pesci A, Olivieri D. Airways remodeling is a distinctive feature of asthma and is related to severity of disease. Chest 1997 Apr;111(4):852-7.

(64) Bai TR, Cooper J, Koelmeyer T, Pare PD, Weir TD. The effect of age and duration of disease on airway structure in fatal asthma. Am J Respir Crit Care Med 2000 Aug;162(2 Pt 1):663-9.

(65) Bumbacea D, Campbell D, Nguyen L, Carr D, Barnes PJ, Robinson D, et al. Parameters associated with persistent airflow obstruction in chronic severe asthma. Eur Respir J 2004;24(1):122-8.

(66) Jain N, Covar RA, Gleason MC, Newell JD, Jr., Gelfand EW, Spahn JD. Quantitative computed tomography detects peripheral airway disease in asthmatic children. Pediatr Pulmonol 2005;40(3):211-8.

(67) Niimi A, Matsumoto H, Takemura M, Ueda T, Chin K, Mishima M. Relationship of airway wall thickness to airway sensitivity and airway reactivity in asthma. Am J Respir Crit Care Med 2003;168(8):983-8.

(68) Milanese M, Crimi E, Scordamaglia A, Riccio A, Pellegrino R, Canonica GW, et al. On the functional consequences of bronchial basement membrane thickening. J Appl Physiol 2001;91(3):1035-40.

(69) Paganin F, Seneterre E, Chanez P, Daures JP, Bruel JM, Michel FB, et al. Computed tomography of the lungs in asthma: influence of disease severity and etiology. Am J Respir Crit Care Med 1996 Jan;153(1):110-4.

(70) Al-Muhsen S, Johnson JR, Hamid Q. Remodeling in asthma. J Allergy Clin Immunol 2011 May 31.

(71) Kelly MM, O'Connor TM, Leigh R, Otis J, Gwozd C, Gauvreau GM, et al. Effects of budesonide and formoterol on allergen-induced airway responses, inflammation, and airway remodeling in asthma. J Allergy Clin Immunol 2010 Feb;125(2):349-56.

(72) McParland BE, Macklem PT, Pare PD. Airway wall remodeling: friend or foe? J Appl Physiol 2003 Jul;95(1):426-34.

(73) Kazi AS, Lotfi S, Goncharova EA, Tliba O, Amrani Y, Krymskaya VP, et al. Vascular endothelial growth factor-induced secretion of fibronectin is ERK dependent. Am J Physiol Lung Cell Mol Physiol 2004;286(3):L539-L545.

(74) Coutts A, Chen G, Stephens N, Hirst S, Douglas D, Eichholtz T, et al. Release of biologically active TGF-beta from airway smooth muscle cells induces autocrine synthesis of collagen. Am J Physiol Lung Cell Mol Physiol 2001;280(5):L999-1008.

(75) Johnson PR, Black JL, Carlin S, Ge Q, Underwood PA. The production of extracellular matrix proteins by human passively sensitized airway smooth-muscle cells in culture: the effect of beclomethasone. Am J Respir Crit Care Med 2000;162(6):2145-51.

(76) Johnson PR, Burgess JK, Underwood PA, Au W, Poniris MH, Tamm M, et al. Extracellular matrix proteins modulate asthmatic airway smooth muscle cell proliferation via an autocrine mechanism. J Allergy Clin Immunol 2004;113(4):690-6.

(77) Boxall C, Holgate ST, Davies DE. The contribution of transforming growth factor-beta and epidermal growth factor signalling to airway remodelling in chronic asthma. Eur Respir J 2006;27(1):208-29.

(78) Howell JE, McAnulty RJ. TGF-beta: its role in asthma and therapeutic potential. Curr Drug Targets 2006;7(5):547-65.

(79) Chu HW, Balzar S, Seedorf GJ, Westcott JY, Trudeau JB, Silkoff P, et al. Transforming growth factor-beta2 induces bronchial epithelial mucin expression in asthma. Am J Pathol 2004 Oct;165(4):1097-106.

(80) Chakir J, Shannon J, Molet S, Fukakusa M, Elias J, Laviolette M, et al. Airway remodeling-associated mediators in moderate to severe asthma: effect of steroids on TGF-beta, IL-11, IL-17, and type I and type III collagen expression. J Allergy Clin Immunol 2003 Jun;111(6):1293-8.

(81) Aubert JD, Dalal BI, Bai TR, Roberts CR, Hayashi S, Hogg JC. Transforming growth factor beta 1 gene expression in human airways. Thorax 1994 Mar;49(3):225-32.

(82) Coker RK, Laurent GJ, Jeffery PK, du Bois RM, Black CM, McAnulty RJ. Localisation of transforming growth factor beta1 and beta3 mRNA transcripts in normal and fibrotic human lung. Thorax 2001 Jul;56(7):549-56.

(83) Bottoms SE, Howell JE, Reinhardt AK, Evans IC, McAnulty RJ. Tgf-Beta isoform specific regulation of airway inflammation and remodelling in a murine model of asthma. PLoS One 2010;5(3):e9674.

(84) Kolb M, Margetts PJ, Sime PJ, Gauldie J. Proteoglycans decorin and biglycan differentially modulate TGF-beta-mediated fibrotic responses in the lung. Am J Physiol Lung Cell Mol Physiol 2001 Jun;280(6):L1327-L1334.

(85) Kenyon NJ, Ward RW, McGrew G, Last JA. TGF-beta1 causes airway fibrosis and increased collagen I and III mRNA in mice. Thorax 2003;58(9):772-7.

(86) Batra V, Musani AI, Hastie AT, Khurana S, Carpenter KA, Zangrilli JG, et al. Bronchoalveolar lavage fluid concentrations of transforming growth factor (TGF)-beta1, TGF-beta2, interleukin (IL)-4 and IL-13 after segmental allergen challenge and their effects on alpha-smooth muscle actin and collagen III synthesis by primary human lung fibroblasts. Clin Exp Allergy 2004;34(3):437-44.

(87) Willis BC, Borok Z. TGF-beta-induced EMT: mechanisms and implications for fibrotic lung disease. Am J Physiol Lung Cell Mol Physiol 2007;293(3):L525-L534.

(88) Hackett TL, Warner SM, Stefanowicz D, Shaheen F, Pechkovsky DV, Murray LA, et al. Induction of epithelial-mesenchymal transition in primary airway epithelial cells from patients with asthma by transforming growth factor-beta1. Am J Respir Crit Care Med 2009 Jul 15;180(2):122-33.

(89) Redington AE, Madden J, Frew AJ, Djukanovic R, Roche WR, Holgate ST, et al. Transforming growth factor-beta 1 in asthma. Measurement in bronchoalveolar lavage fluid. Am J Respir Crit Care Med 1997;156(2 Pt 1):642-7.

(90) Tschumperlin DJ, Shively JD, Kikuchi T, Drazen JM. Mechanical stress triggers selective release of fibrotic mediators from bronchial epithelium. Am J Respir Cell Mol Biol 2003;28(2):142-9.

(91) Thompson HG, Mih JD, Krasieva TB, Tromberg BJ, George SC. Epithelial-derived TGF-beta2 modulates basal and wound-healing subepithelial matrix homeostasis. Am J Physiol Lung Cell Mol Physiol 2006;291(6):L1277-L1285.

(92) Zhang HY, Phan SH. Inhibition of myofibroblast apoptosis by transforming growth factor beta(1). Am J Respir Cell Mol Biol 1999;21(6):658-65.

(93) Desmouliere A, Geinoz A, Gabbiani F, Gabbiani G. Transforming growth factor-beta 1 induces alpha-smooth muscle actin expression in granulation tissue myofibroblasts and in quiescent and growing cultured fibroblasts. J Cell Biol 1993;122(1):103-11.

(94) Wicks J, Haitchi HM, Holgate ST, Davies DE, Powell RM. Enhanced upregulation of smooth muscle related transcripts by TGF beta2 in asthmatic (myo) fibroblasts. Thorax 2006;61(4):313-9.

(95) McAnulty RJ. Fibroblasts and myofibroblasts: their source, function and role in disease. Int J Biochem Cell Biol 2007;39(4):666-71.

(96) Wen FQ, Kohyama T, Skold CM, Zhu YK, Liu X, Romberger DJ, et al. Glucocorticoids modulate TGF-beta production by human fetal lung fibroblasts. Inflammation 2003;27(1):9-19.

(97) Miller M, Cho JY, McElwain K, McElwain S, Shim JY, Manni M, et al. Corticosteroids prevent myofibroblast accumulation and airway remodeling in mice. Am J Physiol Lung Cell Mol Physiol 2006;290(1):L162-L169.

(98) McMillan SJ, Xanthou G, Lloyd CM. Manipulation of allergen-induced airway remodeling by treatment with anti-TGF-beta antibody: effect on the Smad signaling pathway. J Immunol 2005;174(9):5774-80.

(99) Study of GC1008 in Patients With Idiopathic Pulmonary Fibrosis (IPF). [Internet] [Updated 2009 June 28;cited2011 August 23]. Available from http://clinicaltrials.gov/ct/show/NCT00125385

(100) Cordeiro MF, Mead A, Ali RR, Alexander RA, Murray S, Chen C, et al. Novel antisense oligonucleotides targeting TGF-beta inhibit in vivo scarring and improve surgical outcome. Gene Ther 2003 Jan;10(1):59-71.

(101) Lloyd CM, Hawrylowicz CM. Regulatory T cells in asthma. Immunity 2009 Sep 18;31(3):438-49.

(102) Zhu Z, Homer RJ, Wang Z, Chen Q, Geba GP, Wang J, et al. Pulmonary expression of interleukin-13 causes inflammation, mucus hypersecretion, subepithelial fibrosis, physiologic abnormalities, and eotaxin production. J Clin Invest 1999;103(6):779-88.

(103) Rankin JA, Picarella DE, Geba GP, Temann UA, Prasad B, DiCosmo B, et al. Phenotypic and physiologic characterization of transgenic mice expressing interleukin 4 in the lung: lymphocytic and eosinophilic inflammation without airway hyperreactivity. Proc Natl Acad Sci U S A 1996;93(15):7821-5.

(104) Lee CG, Kang HR, Homer RJ, Chupp G, Elias JA. Transgenic modeling of transforming growth factor-beta(1): role of apoptosis in fibrosis and alveolar remodeling. Proc Am Thorac Soc 2006;3(5):418-23.

(105) Saito A, Okazaki H, Sugawara I, Yamamoto K, Takizawa H. Potential action of IL-4 and IL-13 as fibrogenic factors on lung fibroblasts in vitro. Int Arch Allergy Immunol 2003;132(2):168-76.

(106) Borowski A, Kuepper M, Horn U, Knupfer U, Zissel G, Hohne K, et al. Interleukin-13 acts as an apoptotic effector on lung epithelial cells and induces pro-fibrotic gene expression in lung fibroblasts. Clin Exp Allergy 2008;38(4):619-28.

(107) Wen FQ, Kohyama T, Liu X, Zhu YK, Wang H, Kim HJ, et al. Interleukin-4- and interleukin-13-enhanced transforming growth factor-beta2 production in cultured human bronchial epithelial cells is attenuated by interferon-gamma. Am J Respir Cell Mol Biol 2002;26(4):484-90.

(108) Richter A, Puddicombe SM, Lordan JL, Bucchieri F, Wilson SJ, Djukanovic R, et al. The contribution of interleukin (IL)-4 and IL-13 to the epithelial-mesenchymal trophic unit in asthma. Am J Respir Cell Mol Biol 2001;25(3):385-91.

(109) Ward C, Pais M, Bish R, Reid D, Feltis B, Johns D, et al. Airway inflammation, basement membrane thickening and bronchial hyperresponsiveness in asthma. Thorax 2002 Apr;57(4):309-16.

(110) Cho JY, Miller M, Baek KJ, Han JW, Nayar J, Lee SY, et al. Inhibition of airway remodeling in IL-5-deficient mice. J Clin Invest 2004;113(4):551-60.

(111) Flood-Page P, Menzies-Gow A, Phipps S, Ying S, Wangoo A, Ludwig MS, et al. Anti-IL-5 treatment reduces deposition of ECM proteins in the bronchial subepithelial basement membrane of mild atopic asthmatics. J Clin Invest 2003;112(7):1029-36.

(112) Haldar P, Brightling CE, Hargadon B, Gupta S, Monteiro W, Sousa A, et al. Mepolizumab and exacerbations of refractory eosinophilic asthma. N Engl J Med 2009 Mar 5;360(10):973-84.

(113) Nair P, Pizzichini MM, Kjarsgaard M, Inman MD, Efthimiadis A, Pizzichini E, et al. Mepolizumab for prednisone-dependent asthma with sputum eosinophilia. N Engl J Med 2009 Mar 5;360(10):985-93.

(114) Gueders MM, Foidart JM, Noel A, Cataldo DD. Matrix metalloproteinases (MMPs) and tissue inhibitors of MMPs in the respiratory tract: potential implications in asthma and other lung diseases. Eur J Pharmacol 2006 Mar 8;533(1-3):133-44.

(115) Chakrabarti S, Patel KD. Matrix metalloproteinase-2 (MMP-2) and MMP-9 in pulmonary pathology. Exp Lung Res 2005 Jul;31(6):599-621.

(116) Johnson S, Knox A. Autocrine production of matrix metalloproteinase-2 is required for human airway smooth muscle proliferation. Am J Physiol 1999 Dec;277(6 Pt 1):L1109-L1117.

(117) Cataldo D, Munaut C, Noel A, Frankenne F, Bartsch P, Foidart JM, et al. Matrix metalloproteinases and TIMP-1 production by peripheral blood granulocytes from COPD patients and asthmatics. Allergy 2001 Feb;56(2):145-51.

(118) Rajah R, Nachajon RV, Collins MH, Hakonarson H, Grunstein MM, Cohen P. Elevated levels of the IGF-binding protein protease MMP-1 in asthmatic airway smooth muscle. Am J Respir Cell Mol Biol 1999 Feb;20(2):199-208.

(119) Huang CD, Lin SM, Chang PJ, Liu WT, Wang CH, Liu CY, et al. Matrix metalloproteinase-1 polymorphism is associated with persistent airway obstruction in asthma in the Taiwanese population. J Asthma 2009 Feb;46(1):41-6.

(120) Prikk K, Maisi P, Pirila E, Reintam MA, Salo T, Sorsa T, et al. Airway obstruction correlates with collagenase-2 (MMP-8) expression and activation in bronchial asthma. Lab Invest 2002 Nov;82(11):1535-45.

(121) Chu EK, Cheng J, Foley JS, Mecham BH, Owen CA, Haley KJ, et al. Induction of the plasminogen activator system by mechanical stimulation of human bronchial epithelial cells. Am J Respir Cell Mol Biol 2006;35(6):628-38.

(122) Swartz MA, Tschumperlin DJ, Kamm RD, Drazen JM. Mechanical stress is communicated between different cell types to elicit matrix remodeling. Proc Natl Acad Sci U S A 2001;98(11):6180-5.

(123) Bosse M, Chakir J, Rouabhia M, Boulet LP, Audette M, Laviolette M. Serum matrix metalloproteinase-9:Tissue inhibitor of metalloproteinase-1 ratio correlates with steroid responsiveness in moderate to severe asthma. Am J Respir Crit Care Med 1999 Feb;159(2):596-602.

(124) Matsumoto H, Niimi A, Takemura M, Ueda T, Minakuchi M, Tabuena R, et al. Relationship of airway wall thickening to an imbalance between matrix metalloproteinase-9 and its inhibitor in asthma. Thorax 2005 Apr;60(4):277-81.

(125) Dolhnikoff M, Mauad T, Ludwig MS. Extracellular matrix and oscillatory mechanics of rat lung parenchyma in bleomycin-induced fibrosis. Am J Respir Crit Care Med 1999 Nov;160(5 Pt 1):1750-7.

(126) Ebihara T, Venkatesan N, Tanaka R, Ludwig MS. Changes in extracellular matrix and tissue viscoelasticity in bleomycin-induced lung fibrosis. Temporal aspects. Am J Respir Crit Care Med 2000 Oct;162(4 Pt 1):1569-76.

(127) Suki B, Bates JH. Extracellular matrix mechanics in lung parenchymal diseases. Respir Physiol Neurobiol 2008 Nov 30;163(1-3):33-43.

(128) Ward C, Johns DP, Bish R, Pais M, Reid DW, Ingram C, et al. Reduced airway distensibility, fixed airflow limitation, and airway wall remodeling in asthma. Am J Respir Crit Care Med 2001 Nov 1;164(9):1718-21.

(129) Johns DP, Wilson J, Harding R, Walters EH. Airway distensibility in healthy and asthmatic subjects: effect of lung volume history. J Appl Physiol 2000 Apr;88(4):1413-20.

(130) Wilson JW, Li X, Pain MC. The lack of distensibility of asthmatic airways. Am Rev Respir Dis 1993 Sep;148(3):806-9.

(131) Brackel HJ, Pedersen OF, Mulder PG, Overbeek SE, Kerrebijn KF, Bogaard JM. Central airways behave more stiffly during forced expiration in patients with asthma. Am J Respir Crit Care Med 2000 Sep;162(3 Pt 1):896-904.

(132) Brown NJ, Thorpe CW, Thompson B, Berend N, Downie S, Verbanck S, et al. A comparison of two methods for measuring airway distensibility: nitrogen washout and the forced oscillation technique. Physiol Meas 2004 Aug;25(4):1067-75.

(133) Brown NJ, Salome CM, Berend N, Thorpe CW, King GG. Airway distensibility in adults with asthma and healthy adults, measured by forced oscillation technique. Am J Respir Crit Care Med 2007 Jul 15;176(2):129-37.

(134) Shoulders MD, Raines RT. Collagen structure and stability. Annu Rev Biochem 2009;78:929-58.

(135) Dube J, Chakir J, Laviolette M, Saint MS, Boutet M, Desrochers C, et al. In vitro procollagen synthesis and proliferative phenotype of bronchial fibroblasts from normal and asthmatic subjects. Lab Invest 1998 Mar;78(3):297-307.

(136) Bruel A, Ortoft G, Oxlund H. Inhibition of cross-links in collagen is associated with reduced stiffness of the aorta in young rats. Atherosclerosis 1998 Sep;140(1):135-45.

(137) Robins SP. Biochemistry and functional significance of collagen cross-linking. Biochem Soc Trans 2007 Nov;35(Pt 5):849-52.

(138) Uzawa K, Marshall MK, Katz EP, Tanzawa H, Yeowell HN, Yamauchi M. Altered posttranslational modifications of collagen in keloid. Biochem Biophys Res Commun 1998 Aug 28;249(3):652-5.

(139) Bailey AJ, Bazin S, Sims TJ, Le LM, Nicoletis C, Delaunay A. Characterization of the collagen of human hypertrophic and normal scars. Biochim Biophys Acta 1975 Oct 20;405(2):412-21.

(140) Brinckmann J, Neess CM, Gaber Y, Sobhi H, Notbohm H, Hunzelmann N, et al. Different pattern of collagen cross-links in two sclerotic skin diseases: lipodermatosclerosis and circumscribed scleroderma. J Invest Dermatol 2001 Aug;117(2):269-73.

(141) Last JA, King TE, Jr., Nerlich AG, Reiser KM. Collagen cross-linking in adult patients with acute and chronic fibrotic lung disease. Molecular markers for fibrotic collagen. Am Rev Respir Dis 1990 Feb;141(2):307-13.

(142) Reiser KM, Last JA. A molecular marker for fibrotic collagen in lungs of infants with respiratory distress syndrome. Biochem Med Metab Biol 1987 Feb;37(1):16-21.

(143) Gerriets JE, Reiser KM, Last JA. Lung collagen cross-links in rats with experimentally induced pulmonary fibrosis. Biochim Biophys Acta 1996 Jun 7;1316(2):121-31.

(144) Brenner DA, Waterboer T, Choi SK, Lindquist JN, Stefanovic B, Burchardt E, et al. New aspects of hepatic fibrosis. J Hepatol 2000;32(1 Suppl):32-8.

(145) Di DA, Ghiggeri GM, Di DM, Jivotenko E, Acinni R, Campolo J, et al. Lysyl oxidase expression and collagen cross-linking during chronic adriamycin nephropathy. Nephron 1997;76(2):192-200.

(146) Takaluoma K, Lantto J, Myllyharju J. Lysyl hydroxylase 2 is a specific telopeptide hydroxylase, while all three isoenzymes hydroxylate collagenous sequences. Matrix Biol 2007 Jun;26(5):396-403.

(147) van der Slot AJ, Zuurmond AM, van den Bogaerdt AJ, Ulrich MM, Middelkoop E, Boers W, et al. Increased formation of pyridinoline cross-links due to higher telopeptide lysyl hydroxylase levels is a general fibrotic phenomenon. Matrix Biol 2004 Jul;23(4):251-7.

(148) Keene DR, Sakai LY, Bachinger HP, Burgeson RE. Type III collagen can be present on banded collagen fibrils regardless of fibril diameter. J Cell Biol 1987 Nov;105(5):2393-402.

(149) Cameron GJ, Alberts IL, Laing JH, Wess TJ. Structure of type I and type III heterotypic collagen fibrils: an X-ray diffraction study. J Struct Biol 2002 Jan;137(1-2):15-22.

(150) Fratz P. Collgen: Structure and Mechanics, an Introduction. In: Peter Fratzl, editor. Collagen Structure and Mechanics. 1st ed. New York USA: Springer Science+Business Media; 2008. p. 1-13.

(151) Wess TJ. Collagen Fibrilar Structure and Hierarchies. In: Peter Fratzl, editor. Collagen Structure and Mechanics. 1st ed. New York: Springer Science+Business Media, LLC; 2008. p. 49-80.

(152) Parry DA, Barnes GR, Craig AS. A comparison of the size distribution of collagen fibrils in connective tissues as a function of age and a possible relation between fibril size distribution and mechanical properties. Proc R Soc Lond B Biol Sci 1978 Dec 18;203(1152):305-21.

(153) McEwan PA, Scott PG, Bishop PN, Bella J. Structural correlations in the family of small leucine-rich repeat proteins and proteoglycans. J Struct Biol 2006 Aug;155(2):294-305.

(154) Neame PJ, Kay CJ, McQuillan DJ, Beales MP, Hassell JR. Independent modulation of collagen fibrillogenesis by decorin and lumican. Cell Mol Life Sci 2000 May;57(5):859-63.

(155) Geng Y, McQuillan D, Roughley PJ. SLRP interaction can protect collagen fibrils from cleavage by collagenases. Matrix Biol 2006 Oct;25(8):484-91.

(156) Danielson KG, Baribault H, Holmes DF, Graham H, Kadler KE, Iozzo RV. Targeted disruption of decorin leads to abnormal collagen fibril morphology and skin fragility. J Cell Biol 1997 Feb 10;136(3):729-43.

(157) Graham HK, Holmes DF, Watson RB, Kadler KE. Identification of collagen fibril fusion during vertebrate tendon morphogenesis. The process relies on unipolar fibrils and is regulated by collagen-proteoglycan interaction. J Mol Biol 2000 Jan 28;295(4):891-902.

(158) Corsi A, Xu T, Chen XD, Boyde A, Liang J, Mankani M, et al. Phenotypic effects of biglycan deficiency are linked to collagen fibril abnormalities, are synergized by decorin deficiency, and mimic Ehlers-Danlos-like changes in bone and other connective tissues. J Bone Miner Res 2002 Jul;17(7):1180-9.

(159) Wenger MP, Bozec L, Horton MA, Mesquida P. Mechanical properties of collagen fibrils. Biophys J 2007 Aug 15;93(4):1255-63.

(160) Tschumperlin DJ, Drazen JM. Chronic effects of mechanical force on airways. Annu Rev Physiol 2006;68:563-83.

(161) Wang JH, Thampatty BP. An introductory review of cell mechanobiology. Biomech Model Mechanobiol 2006;5(1):1-16.

(162) Choe MM, Sporn PH, Swartz MA. An in vitro airway wall model of remodeling. Am J Physiol Lung Cell Mol Physiol 2003;285(2):L427-L433.

(163) Savla U, Waters CM. Mechanical strain inhibits repair of airway epithelium in vitro. Am J Physiol 1998;274(6 Pt 1):L883-L892.

(164) Park JA, Tschumperlin DJ. Chronic Intermittent Mechanical Stress Increases MUC5AC Protein Expression. Am J Respir Cell Mol Biol 2009.

(165) Chu EK, Foley JS, Cheng J, Patel AS, Drazen JM, Tschumperlin DJ. Bronchial epithelial compression regulates epidermal growth factor receptor family ligand expression in an autocrine manner. Am J Respir Cell Mol Biol 2005;32(5):373-80.

(166) Chapman KE, Sinclair SE, Zhuang D, Hassid A, Desai LP, Waters CM. Cyclic mechanical strain increases reactive oxygen species production in pulmonary epithelial cells. Am J Physiol Lung Cell Mol Physiol 2005;289(5):L834-L841.

(167) Savla U, Sporn PH, Waters CM. Cyclic stretch of airway epithelium inhibits prostanoid synthesis. Am J Physiol 1997 Nov;273(5 Pt 1):L1013-L1019.

(168) McAnulty RJ, Chambers RC, Laurent GJ. Regulation of fibroblast procollagen production. Transforming growth factor-beta 1 induces prostaglandin E2 but not procollagen synthesis via a pertussis toxin-sensitive G-protein. Biochem J 1995 Apr 1;307 (Pt 1):63-8.

(169) McAnulty RJ, Hernandez-Rodriguez NA, Mutsaers SE, Coker RK, Laurent GJ. Indomethacin suppresses the anti-proliferative effects of transforming growth factor-beta isoforms on fibroblast cell cultures. Biochem J 1997 Feb 1;321 (Pt 3):639-43.

(170) Liu M, Xu J, Souza P, Tanswell B, Tanswell AK, Post M. The effect of mechanical strain on fetal rat lung cell proliferation: comparison of two- and three-dimensional culture systems. In Vitro Cell Dev Biol Anim 1995;31(11):858-66.

(171) Morishima Y, Nomura A, Uchida Y, Noguchi Y, Sakamoto T, Ishii Y, et al. Triggering the induction of myofibroblast and fibrogenesis by airway epithelial shedding. Am J Respir Cell Mol Biol 2001;24(1):1-11.

(172) Choe MM, Sporn PH, Swartz MA. Extracellular matrix remodeling by dynamic strain in a three-dimensional tissue-engineered human airway wall model. Am J Respir Cell Mol Biol 2006;35(3):306-13.

(173) Mourgeon E, Xu J, Tanswell AK, Liu M, Post M. Mechanical strain-induced posttranscriptional regulation of fibronectin production in fetal lung cells. Am J Physiol 1999;277(1 Pt 1):L142-L149.

(174) Wang JH, Thampatty BP, Lin JS, Im HJ. Mechanoregulation of gene expression in fibroblasts. Gene 2007;391(1-2):1-15.

(175) Le Bellego F, Perera H, Plante S, Chakir J, Hamid Q, Ludwig MS. Mechanical strain increases cytokine and chemokine production in bronchial fibroblasts from asthmatic patients. Allergy 2009;64(1):32-9.

(176) Ludwig MS, Ftouhi-Paquin N, Huang W, Page N, Chakir J, Hamid Q. Mechanical strain enhances proteoglycan message in fibroblasts from asthmatic subjects. Clin Exp Allergy 2004;34(6):926-30.

(177) Breen EC. Mechanical strain increases type I collagen expression in pulmonary fibroblasts in vitro. J Appl Physiol 2000;88(1):203-9.

(178) Bishop JE, Mitchell JJ, Absher PM, Baldor L, Geller HA, Woodcock-Mitchell J, et al. Cyclic mechanical deformation stimulates human lung fibroblast proliferation and autocrine growth factor activity. Am J Respir Cell Mol Biol 1993;9(2):126-33.

(179) Sanchez-Esteban J, Wang Y, Cicchiello LA, Rubin LP. Cyclic mechanical stretch inhibits cell proliferation and induces apoptosis in fetal rat lung fibroblasts. Am J Physiol Lung Cell Mol Physiol 2002;282(3):L448-L456.

(180) Wang L, Pare PD. Deep inspiration and airway smooth muscle adaptation to length change. Respir Physiol Neurobiol 2003;137(2-3):169-78.

(181) Allon AA, Schneider R, Lotz JC. Co-culture of Adult Mesenchymal Stem Cells and Nucleus Pulposus Cells in Bilaminar Pellets for Intervertebral Disc Regeneration. SAS Journal 2009;3:41-9.

(182) Kubista M, Andrade JM, Bengtsson M, Forootan A, Jonak J, Lind K, et al. The real-time polymerase chain reaction. Mol Aspects Med 2006 Apr;27(2-3):95-125.

(183) Livak KJ, Schmittgen TD. Analysis of relative gene expression data using real-time quantitative PCR and the 2(-Delta Delta C(T)) Method. Methods 2001;25(4):402-8.

(184) Sircol Soluble Collagen assay. 5th ed. Biocolor Ltd; 2007.

(185) Ziegler J, Vogt T, Miersch O, Strack D. Concentration of dilute protein solutions prior to sodium dodecyl sulfate-polyacrylamide gel electrophoresis. Anal Biochem 1997 Aug 1;250(2):257-60.

(186) Snoek-van Beurden PA, Von den Hoff JW. Zymographic techniques for the analysis of matrix metalloproteinases and their inhibitors. Biotechniques 2005 Jan;38(1):73-83.

(187) Watson KE, Parhami F, Shin V, Demer LL. Fibronectin and collagen I matrixes promote calcification of vascular cells in vitro, whereas collagen IV matrix is inhibitory. Arterioscler Thromb Vasc Biol 1998 Dec;18(12):1964-71.

(188) Wipff PJ, Rifkin DB, Meister JJ, Hinz B. Myofibroblast contraction activates latent TGF-beta1 from the extracellular matrix. J Cell Biol 2007 Dec 17;179(6):1311-23.

(189) Turoverova LV, Khotin MG, Iudintseva NM, Magnusson KE, Blinova MI, Pinaev GP, et al. [Analysis of extracellular matrix proteins produced by cultured cells]. Tsitologiia 2009;51(8):691-6.

(190) Stolz M, Gottardi R, Raiteri R, Miot S, Martin I, Imer R, et al. Early detection of aging cartilage and osteoarthritis in mice and patient samples using atomic force microscopy. Nat Nanotechnol 2009 Mar;4(3):186-92.

(191) Paul West. Introduction to Atomic Force Microscopy Theory Practices Applications. Paul West, editor. 2009. [cited 2011 June 20] Available form http://www.paulwestphd.com/index.html

(192) Oliver W.C. PGM. An improved technique for determining hardness and elastic modulus using load and displacement snsing indentation experiments. J Mater Res 1992;7(6):1564-83.

(193) Pare PD, McParland BE, Seow CY. Structural basis for exaggerated airway narrowing. Can J Physiol Pharmacol 2007 Jul;85(7):653-8.

(194) Iba T, Sumpio BE. Tissue plasminogen activator expression in endothelial cells exposed to cyclic strain in vitro. Cell Transplant 1992;1(1):43-50.

(195) McAnulty RJ, Campa JS, Cambrey AD, Laurent GJ. The effect of transforming growth factor beta on rates of procollagen synthesis and degradation in vitro. Biochim Biophys Acta 1991 Jan 31;1091(2):231-5.

(196) Ingber D. Integrins as mechanochemical transducers. Curr Opin Cell Biol 1991 Oct;3(5):841-8.

(197) Royce SG, Tan L, Koek AA, Tang ML. Effect of extracellular matrix composition on airway epithelial cell and fibroblast structure: implications for airway remodeling in asthma. Ann Allergy Asthma Immunol 2009 Mar;102(3):238-46.

(198) Atkinson JJ, Senior RM. Matrix metalloproteinase-9 in lung remodeling. Am J Respir Cell Mol Biol 2003 Jan;28(1):12-24.

(199) Hawwa RL, Hokenson MA, Wang Y, Huang Z, Sharma S, Sanchez-Esteban J. Differential Expression of MMP-2 and -9 and their Inhibitors in Fetal Lung Cells Exposed to Mechanical Stretch: Regulation by IL-10. Lung 2011 Jun 24.

(200) Abe M, Harpel JG, Metz CN, Nunes I, Loskutoff DJ, Rifkin DB. An assay for transforming growth factor-beta using cells transfected with a plasminogen activator inhibitor-1 promoter-luciferase construct. Anal Biochem 1994 Feb 1;216(2):276-84.

(201) Lindahl GE, Chambers RC, Papakrivopoulou J, Dawson SJ, Jacobsen MC, Bishop JE, et al. Activation of fibroblast procollagen alpha 1(I) transcription by mechanical strain is transforming growth factor-beta-dependent and involves increased binding of CCAAT-binding factor (CBF/NF-Y) at the proximal promoter. J Biol Chem 2002 Feb 22;277(8):6153-61.

(202) Blaauboer ME, Smit TH, Hanemaaijer R, Stoop R, Everts V. Cyclic mechanical stretch reduces myofibroblast differentiation of primary lung fibroblasts. Biochem Biophys Res Commun 2011 Jan 7;404(1):23-7.

(203) Eckes B, Zweers MC, Zhang ZG, Hallinger R, Mauch C, Aumailley M, et al. Mechanical tension and integrin alpha 2 beta 1 regulate fibroblast functions. J Investig Dermatol Symp Proc 2006 Sep;11(1):66-72.

(204) Qiu Y, Zhu J, Bandi V, Guntupalli KK, Jeffery PK. Bronchial mucosal inflammation and upregulation of CXC chemoattractants and receptors in severe exacerbations of asthma. Thorax 2007 Jun;62(6):475-82.

(205) Kikuchi S, Kikuchi I, Takaku Y, Kobayashi T, Hagiwara K, Kanazawa M, et al. Neutrophilic inflammation and CXC chemokines in patients with refractory asthma. Int Arch Allergy Immunol 2009;149 Suppl 1:87-93.

(206) Grainge CL, Lau LC, Ward JA, Dulay V, Lahiff G, Wilson S, et al. Effect of bronchoconstriction on airway remodeling in asthma. N Engl J Med 2011 May 26;364(21):2006-15.

(207) Niimi A, Torrego A, Nicholson AG, Cosio BG, Oates TB, Chung KF. Nature of airway inflammation and remodeling in chronic cough. J Allergy Clin Immunol 2005 Sep;116(3):565-70.

(208) Grymes RA, Sawyer C. A novel culture morphology resulting from applied mechanical strain. In Vitro Cell Dev Biol Anim 1997 May;33(5):392-7.

(209) Nishimura K, Blume P, Ohgi S, Sumpio BE. Effect of different frequencies of tensile strain on human dermal fibroblast proliferation and survival. Wound Repair Regen 2007 Sep;15(5):646-56.

(210) Hulmes DJS. Collagen Diversity, Synthesis and Assembly. In: Fratz P., editor. Collagen Structure and Mechanics. 1st ed. New York: Springer Science+Bussiness Media, LLC; 2008. p. 15-47.

(211) Avery N.C., Bailey A.J. Restraining Cross-Links Responsible for the Mechanical Properties of Collagen Fibers: Natural and Artificial. In: Peter Fratzl, editor. Collagen Structure and Mechanics. 1 ed. New York: Springer Science+Bussiness Media,LLC; 2008. p. 81-110.

(212) Coker RK, Laurent GJ, Shahzeidi S, Lympany PA, du Bois RM, Jeffery PK, et al. Transforming growth factors-beta 1, -beta 2, and -beta 3 stimulate fibroblast procollagen production in vitro but are differentially expressed during bleomycin-induced lung fibrosis. Am J Pathol 1997;150(3):981-91.

(213) Chu HW, Balzar S, Seedorf GJ, Westcott JY, Trudeau JB, Silkoff P, et al. Transforming growth factor-beta2 induces bronchial epithelial mucin expression in asthma. Am J Pathol 2004 Oct;165(4):1097-106.

(214) Bottoms SE, Howell JE, Reinhardt AK, Evans IC, McAnulty RJ. Tgf-Beta isoform specific regulation of airway inflammation and remodelling in a murine model of asthma. PLoS One 2010;5(3):e9674.

(215) Boak AM, Roy R, Berk J, Taylor L, Polgar P, Goldstein RH, et al. Regulation of lysyl oxidase expression in lung fibroblasts by transforming growth factor-beta 1 and prostaglandin E2. Am J Respir Cell Mol Biol 1994 Dec;11(6):751-5.

(216) Wu M, Min C, Wang X, Yu Z, Kirsch KH, Trackman PC, et al. Repression of BCL2 by the tumor suppressor activity of the lysyl oxidase propeptide inhibits transformed phenotype of lung and pancreatic cancer cells. Cancer Res 2007 Jul 1;67(13):6278-85.

(217) Guo Y, Pischon N, Palamakumbura AH, Trackman PC. Intracellular distribution of the lysyl oxidase propeptide in osteoblastic cells. Am J Physiol Cell Physiol 2007 Jun;292(6):C2095-C2102.

(218) Halberg N, Khan T, Trujillo ME, Wernstedt-Asterholm I, Attie AD, Sherwani S, et al. Hypoxia-inducible factor 1alpha induces fibrosis and insulin resistance in white adipose tissue. Mol Cell Biol 2009 Aug;29(16):4467-83.

(219) Shanley CJ, Gharaee-Kermani M, Sarkar R, Welling TH, Kriegel A, Ford JW, et al. Transforming growth factor-beta 1 increases lysyl oxidase enzyme activity and mRNA in rat aortic smooth muscle cells. J Vasc Surg 1997 Mar;25(3):446-52.

(220) Hong HH, Uzel MI, Duan C, Sheff MC, Trackman PC. Regulation of lysyl oxidase, collagen, and connective tissue growth factor by TGF-beta1 and detection in human gingiva. Lab Invest 1999 Dec;79(12):1655-67.

(221) Goto Y, Uchio-Yamada K, Anan S, Yamamoto Y, Ogura A, Manabe N. Transforming growth factor-beta1 mediated up-regulation of lysyl oxidase in the kidneys of hereditary nephrotic mouse with chronic renal fibrosis. Virchows Arch 2005 Nov;447(5):859-68.

(222) Uzel MI, Scott IC, Babakhanlou-Chase H, Palamakumbura AH, Pappano WN, Hong HH, et al. Multiple bone morphogenetic protein 1-related mammalian metalloproteinases process pro-lysyl oxidase at the correct physiological site and control lysyl oxidase activation in mouse embryo fibroblast cultures. J Biol Chem 2001 Jun 22;276(25):22537-43.

(223) Uzel MI, Shih SD, Gross H, Kessler E, Gerstenfeld LC, Trackman PC. Molecular events that contribute to lysyl oxidase enzyme activity and insoluble collagen accumulation in osteosarcoma cell clones. J Bone Miner Res 2000 Jun;15(6):1189-97.

(224) Lijnen PJ, Petrov VV, Turner M, Fagard RH. Collagen production in cardiac fibroblasts during inhibition of aminopeptidase B. J Renin Angiotensin Aldosterone Syst 2005 Sep;6(2):69-77.

(225) Adam O, Theobald K, Lavall D, Grube M, Kroemer HK, Ameling S, et al. Increased lysyl oxidase expression and collagen cross-linking during atrial fibrillation. J Mol Cell Cardiol 2011 Apr;50(4):678-85.

(226) Counts DF, Evans JN, Dipetrillo TA, Sterling KM, Jr., Kelley J. Collagen lysyl oxidase activity in the lung increases during bleomycin-induced lung fibrosis. J Pharmacol Exp Ther 1981 Dec;219(3):675-8.

(227) Goulet S, Bihl MP, Gambazzi F, Tamm M, Roth M. Opposite effect of corticosteroids and long-acting beta(2)-agonists on serum- and TGF-beta(1)-induced extracellular matrix deposition by primary human lung fibroblasts. J Cell Physiol 2007 Jan;210(1):167-76.

(228) Zhang G, Ezura Y, Chervoneva I, Robinson PS, Beason DP, Carine ET, et al. Decorin regulates assembly of collagen fibrils and acquisition of biomechanical properties during tendon development. J Cell Biochem 2006 Aug 15;98(6):1436-49.

(229) Fust A, LeBellego F, Iozzo RV, Roughley PJ, Ludwig MS. Alterations in lung mechanics in decorin-deficient mice. Am J Physiol Lung Cell Mol Physiol 2005 Jan;288(1):L159-L166.

(230) Jarvelainen H, Puolakkainen P, Pakkanen S, Brown EL, Hook M, Iozzo RV, et al. A role for decorin in cutaneous wound healing and angiogenesis. Wound Repair Regen 2006 Jul;14(4):443-52.

(231) Heegaard AM, Corsi A, Danielsen CC, Nielsen KL, Jorgensen HL, Riminucci M, et al. Biglycan deficiency causes spontaneous aortic dissection and rupture in mice. Circulation 2007 May 29;115(21):2731-8.

(232) Campbell PH, Hunt DL, Jones Y, Harwood F, Amiel D, Omens JH, et al. Effects of biglycan deficiency on myocardial infarct structure and mechanics. Mol Cell Biomech 2008 Mar;5(1):27-35.

(233) Yamaguchi Y, Mann DM, Ruoslahti E. Negative regulation of transforming growth factor-beta by the proteoglycan decorin. Nature 1990 Jul 19;346(6281):281-4.

(234) Todorova L, Bjermer L, Westergren-Thorsson G, Miller-Larsson A. TGFbeta-induced matrix production by bronchial fibroblasts in asthma: Budesonide and formoterol effects. Respir Med 2011 Sep;105(9):1296-307.

(235) Romaris M, Heredia A, Molist A, Bassols A. Differential effect of transforming growth factor beta on proteoglycan synthesis in human embryonic lung fibroblasts. Biochim Biophys Acta 1991 Jul 10;1093(2-3):229-33.

(236) Westergren-Thorsson G, Hernnas J, Sarnstrand B, Oldberg A, Heinegard D, Malmstrom A. Altered expression of small proteoglycans, collagen, and transforming growth factor-beta 1 in developing bleomycin-induced pulmonary fibrosis in rats. J Clin Invest 1993 Aug;92(2):632-7.

(237) Schlesinger C, Meyer CA, Veeraraghavan S, Koss MN. Constrictive (obliterative) bronchiolitis: diagnosis, etiology, and a critical review of the literature. Ann Diagn Pathol 1998 Oct;2(5):321-34.

(238) Juniper EF, Kline PA, Vanzieleghem MA, Ramsdale EH, O'Byrne PM, Hargreave FE. Effect of long-term treatment with an inhaled corticosteroid (budesonide) on airway hyperresponsiveness and clinical asthma in nonsteroid-dependent asthmatics. Am Rev Respir Dis 1990 Oct;142(4):832-6.

(239) Sovijarvi AR, Haahtela T, Ekroos HJ, Lindqvist A, Saarinen A, Poussa T, et al. Sustained reduction in bronchial hyperresponsiveness with inhaled fluticasone propionate within three days in mild asthma: time course after onset and cessation of treatment. Thorax 2003 Jun;58(6):500-4.

(240) Gershman NH, Wong HH, Liu JT, Fahy JV. Low- and high-dose fluticasone propionate in asthma; effects during and after treatment. Eur Respir J 2000 Jan;15(1):11-8.

(241) Long-term effects of budesonide or nedocromil in children with asthma. The Childhood Asthma Management Program Research Group. N Engl J Med 2000 Oct 12;343(15):1054-63.

(242) Pauwels RA, Lofdahl CG, Postma DS, Tattersfield AE, O'Byrne P, Barnes PJ, et al. Effect of inhaled formoterol and budesonide on exacerbations of asthma. Formoterol and Corticosteroids Establishing Therapy (FACET) International Study Group. N Engl J Med 1997 Nov 13;337(20):1405-11.

(243) Suissa S, Ernst P, Benayoun S, Baltzan M, Cai B. Low-dose inhaled corticosteroids and the prevention of death from asthma. N Engl J Med 2000 Aug 3;343(5):332-6.

(244) Khor YH, Feltis BN, Reid DW, Ward C, Johns DP, Wood-Baker R, et al. Airway cell and cytokine changes in early asthma deterioration after inhaled corticosteroid reduction. Clin Exp Allergy 2007 Aug;37(8):1189-98.

(245) Takaku Y, Nakagome K, Kobayashi T, Yamaguchi T, Nishihara F, Soma T, et al. Changes in airway inflammation and hyperresponsiveness after inhaled corticosteroid cessation in allergic asthma. Int Arch Allergy Immunol 2010;152 Suppl 1:41-6.

(246) Waalkens HJ, Van Essen-Zandvliet EE, Hughes MD, Gerritsen J, Duiverman EJ, Knol K, et al. Cessation of long-term treatment with inhaled corticosteroid (budesonide) in children with asthma results in deterioration. The Dutch CNSLD Study Group. Am Rev Respir Dis 1993 Nov;148(5):1252-7.

(247) Young PG, Skinner SJ, Black PN. Effects of glucocorticoids and beta-adrenoceptor agonists on the proliferation of airway smooth muscle. Eur J Pharmacol 1995 Jan 24;273(1-2):137-43.

(248) Dorscheid DR, Wojcik KR, Sun S, Marroquin B, White SR. Apoptosis of airway epithelial cells induced by corticosteroids. Am J Respir Crit Care Med 2001 Nov 15;164(10 Pt 1):1939-47.

(249) Descalzi D, Folli C, Nicolini G, Riccio AM, Gamalero C, Scordamaglia F, et al. Anti-proliferative and anti-remodelling effect of beclomethasone dipropionate, formoterol and salbutamol alone or in combination in primary human bronchial fibroblasts. Allergy 2008 Apr;63(4):432-7.

(250) Sont JK, Willems LN, Bel EH, van Krieken JH, Vandenbroucke JP, Sterk PJ. Clinical control and histopathologic outcome of asthma when using airway hyperresponsiveness as an additional guide to long-term treatment. The AMPUL Study Group. Am J Respir Crit Care Med 1999 Apr;159(4 Pt 1):1043-51.

(251) Olivieri D, Chetta A, Del DM, Bertorelli G, Casalini A, Pesci A, et al. Effect of short-term treatment with low-dose inhaled fluticasone propionate on airway inflammation and remodeling in mild asthma: a placebo-controlled study. Am J Respir Crit Care Med 1997 Jun;155(6):1864-71.

(252) Trigg CJ, Manolitsas ND, Wang J, Calderon MA, McAulay A, Jordan SE, et al. Placebo-controlled immunopathologic study of four months of inhaled corticosteroids in asthma. Am J Respir Crit Care Med 1994 Jul;150(1):17-22.

(253) Boulet LP, Turcotte H, Laviolette M, Naud F, Bernier MC, Martel S, et al. Airway hyperresponsiveness, inflammation, and subepithelial collagen deposition in recently diagnosed versus long-standing mild asthma. Influence of inhaled corticosteroids. Am J Respir Crit Care Med 2000 Oct;162(4 Pt 1):1308-13.

(254) Grol MH, Gerritsen J, Vonk JM, Schouten JP, Koeter GH, Rijcken B, et al. Risk factors for growth and decline of lung function in asthmatic individuals up to age 42 years. A 30-year follow-up study. Am J Respir Crit Care Med 1999 Dec;160(6):1830-7.

(255) Merline R, Schaefer RM, Schaefer L. The matricellular functions of small leucine-rich proteoglycans (SLRPs). J Cell Commun Signal 2009 Dec;3(3-4):323-35.

(256) Sanches JC, Jones CJ, Aplin JD, Iozzo RV, Zorn TM, Oliveira SF. Collagen fibril organization in the pregnant endometrium of decorin-deficient mice. J Anat 2010 Jan;216(1):144-55.

(257) Khalil N, Greenberg AH. The role of TGF-beta in pulmonary fibrosis. Ciba Found Symp 1991;157:194-207.

(258) Toshima M, Ohtani Y, Ohtani O. Three-dimensional architecture of elastin and collagen fiber networks in the human and rat lung. Arch Histol Cytol 2004 Mar;67(1):31-40.

(259) Kadler KE, Holmes DF, Trotter JA, Chapman JA. Collagen fibril formation. Biochem J 1996 May 15;316 (Pt 1):1-11.

(260) Liu F, Tschumperlin DJ. Micro-mechanical characterization of lung tissue using atomic force microscopy. J Vis Exp 2011;(54).

(261) Heim AaMW. Determination of the elastic modulus of native collagen fibrils via radial indentation. Appl Phys Lett 2006;89:181902-1-181902-2.

(262) Silver FH, Freeman JW, Seehra GP. Collagen self-assembly and the development of tendon mechanical properties. J Biomech 2003 Oct;36(10):1529-53.

(263) Ottani V, Martini D, Franchi M, Ruggeri A, Raspanti M. Hierarchical structures in fibrillar collagens. Micron 2002;33(7-8):587-96.

(264) Goldberg B, Sherr CJ. Secretion and extracellular processing of procollagen by cultured human fibroblasts. Proc Natl Acad Sci U S A 1973 Feb;70(2):361-5.

(265) Schafer IA, Silverman L, Sullivan JC, Robertson WV. Ascorbic acid deficiency in cultured human fibroblasts. J Cell Biol 1967 Jul;34(1):83-95.

(266) Chen CZ, Peng YX, Wang ZB, Fish PV, Kaar JL, Koepsel RR, et al. The Scar-in-a-Jar: studying potential antifibrotic compounds from the epigenetic to extracellular level in a single well. Br J Pharmacol 2009 Nov;158(5):1196-209.

(267) Abraham T, Hirota JA, Wadsworth S, Knight DA. Minimally invasive multiphoton and harmonic generation imaging of extracellular matrix structures in lung airway and related diseases. Pulm Pharmacol Ther 2011 Apr 7.

(268) Noto A, Manuyakorn W, Haitchi HM, Bucchieri F, Davies DE. Cyclical Mechanical Stertch Enhances the Profibrotic Response of Primary Embryonic Foetal fibroblasts, but not ADAM33 Expression. Thorax 2010;65:A17.

(269) Ressler B, Lee RT, Randell SH, Drazen JM, Kamm RD. Molecular responses of rat tracheal epithelial cells to transmembrane pressure. Am J Physiol Lung Cell Mol Physiol 2000 Jun;278(6):L1264-L1272.

(270) Davies DE. The role of the epithelium in airway remodeling in asthma. Proc Am Thorac Soc 2009 Dec;6(8):678-82.

(271) Covar RA, Spahn JD, Murphy JR, Szefler SJ. Progression of asthma measured by lung function in the childhood asthma management program. Am J Respir Crit Care Med 2004 Aug 1;170(3):234-41.

(272) Wenzel SE. Asthma: defining of the persistent adult phenotypes. Lancet 2006 Aug 26;368(9537):804-13.

(273) James AL, Elliot JG, Abramson MJ, Walters EH. Time to death, airway wall inflammation and remodelling in fatal asthma. Eur Respir J 2005 Sep;26(3):429-34.

(274) Carlsen KH, Anderson SD, Bjermer L, Bonini S, Brusasco V, Canonica W, et al. Exercise-induced asthma, respiratory and allergic disorders in elite athletes: epidemiology, mechanisms and diagnosis: part I of the report from the Joint Task Force of the European Respiratory Society (ERS) and the European Academy of Allergy and Clinical Immunology (EAACI) in cooperation with GA2LEN. Allergy 2008 Apr;63(4):387-403.

(275) Bonsignore MR, Morici G, Riccobono L, Insalaco G, Bonanno A, Profita M, et al. Airway inflammation in nonasthmatic amateur runners. Am J Physiol Lung Cell Mol Physiol 2001 Sep;281(3):L668-L676.

(276) Bonsignore MR, Morici G, Riccobono L, Profita M, Bonanno A, Paterno A, et al. Airway cells after swimming outdoors or in the sea in nonasthmatic athletes. Med Sci Sports Exerc 2003 Jul;35(7):1146-52.

(277) Boulet LP, Turcotte H, Langdeau JB, Bernier MC. Lower airway inflammatory responses to high-intensity training in athletes. Clin Invest Med 2005 Feb;28(1):15-22.

(278) Lopez B, Gonzalez A, Hermida N, Valencia F, de TE, Diez J. Role of lysyl oxidase in myocardial fibrosis: from basic science to clinical aspects. Am J Physiol Heart Circ Physiol 2010 Jul;299(1):H1-H9.

(279) Hayashi K, Fong KS, Mercier F, Boyd CD, Csiszar K, Hayashi M. Comparative immunocytochemical localization of lysyl oxidase (LOX) and the lysyl oxidase-like (LOXL) proteins: changes in the expression of LOXL during development and growth of mouse tissues. J Mol Histol 2004 Nov;35(8-9):845-55.

(280) Rodriguez C, Alcudia JF, Martinez-Gonzalez J, Raposo B, Navarro MA, Badimon L. Lysyl oxidase (LOX) down-regulation by TNFalpha: a new mechanism underlying TNFalpha-induced endothelial dysfunction. Atherosclerosis 2008 Feb;196(2):558-64.

(281) Boak AM, Roy R, Berk J, Taylor L, Polgar P, Goldstein RH, et al. Regulation of lysyl oxidase expression in lung fibroblasts by transforming growth factor-beta 1 and prostaglandin E2. Am J Respir Cell Mol Biol 1994 Dec;11(6):751-5.

(282) Kumarasamy A, Schmitt I, Nave AH, Reiss I, van dH, I, Dony E, et al. Lysyl oxidase activity is dysregulated during impaired alveolarization of mouse and human lungs. Am J Respir Crit Care Med 2009 Dec 15;180(12):1239-52.

(283) Chen LJ, Li WD, Li SF, Su XW, Lin GY, Huang YJ, et al. Bleomycin induces upregulation of lysyl oxidase in cultured human fetal lung fibroblasts. Acta Pharmacol Sin 2010 May;31(5):554-9.

(284) Maki JM, Sormunen R, Lippo S, Kaarteenaho-Wiik R, Soininen R, Myllyharju J. Lysyl oxidase is essential for normal development and function of the respiratory system and for the integrity of elastic and collagen fibers in various tissues. Am J Pathol 2005 Oct;167(4):927-36.

(285) Chinoy MR, Zgleszewski SE, Cilley RE, Krummel TM. Dexamethasone enhances ras-recision gene expression in cultured murine fetal lungs: role in development. Am J Physiol Lung Cell Mol Physiol 2000 Aug;279(2):L312-L318.

(286) Warburton D, Shi W. Lo, and the niche is knit: lysyl oxidase activity and maintenance of lung, aorta, and skin integrity. Am J Pathol 2005 Oct;167(4):921-2.

(287) Mecham RP, Whitehouse LA, Wrenn DS, Parks WC, Griffin GL, Senior RM, et al. Smooth muscle-mediated connective tissue remodeling in pulmonary hypertension. Science 1987 Jul 24;237(4813):423-6.

(288) Davidson JM. Biochemistry and turnover of lung interstitium. Eur Respir J 1990 Oct;3(9):1048-63.

(289) Chen LJ, Zhao Y, Gao S, Chou IN, Toselli P, Stone P, et al. Downregulation of lysyl oxidase and upregulation of cellular thiols in rat fetal lung fibroblasts treated with cigarette smoke condensate. Toxicol Sci 2005 Feb;83(2):372-9.

(290) Zhao Y, Gao S, Chou IN, Toselli P, Stone P, Li W. Inhibition of the expression of lysyl oxidase and its substrates in cadmium-resistant rat fetal lung fibroblasts. Toxicol Sci 2006 Apr;90(2):478-89.

(291) Brinckmann J, Kim S, Wu J, Reinhardt DP, Batmunkh C, Metzen E, et al. Interleukin 4 and prolonged hypoxia induce a higher gene expression of lysyl hydroxylase 2 and an altered cross-link pattern: important pathogenetic steps in early and late stage of systemic scleroderma? Matrix Biol 2005 Oct;24(7):459-68.

(292) van der Slot AJ, van Dura EA, de Wit EC, De GJ, Huizinga TW, Bank RA, et al. Elevated formation of pyridinoline cross-links by profibrotic cytokines is associated with enhanced lysyl hydroxylase 2b levels. Biochim Biophys Acta 2005 Jun 30;1741(1-2):95-102.

(293) Seitzer U, Batge B, Acil Y, Muller PK. Transforming growth factor beta 1 influences lysyl hydroxylation of collagen I and reduces steady-state levels of lysyl hydroxylase mRNA in human osteoblast-like cells. Eur J Clin Invest 1995 Dec;25(12):959-66.

(294) Bonniaud P, Kolb M, Galt T, Robertson J, Robbins C, Stampfli M, et al. Smad3 null mice develop airspace enlargement and are resistant to TGF-beta-mediated pulmonary fibrosis. J Immunol 2004 Aug 1;173(3):2099-108.

(295) Sime PJ, Xing Z, Graham FL, Csaky KG, Gauldie J. Adenovector-mediated gene transfer of active transforming growth factor-beta1 induces prolonged severe fibrosis in rat lung. J Clin Invest 1997 Aug 15;100(4):768-76.

(296) Wilson MS, Wynn TA. Pulmonary fibrosis: pathogenesis, etiology and regulation. Mucosal Immunol 2009 Mar;2(2):103-21.

(297) Rada JA, Cornuet PK, Hassell JR. Regulation of corneal collagen fibrillogenesis in vitro by corneal proteoglycan (lumican and decorin) core proteins. Exp Eye Res 1993 Jun;56(6):635-48.

(298) Kalamajski S, Oldberg A. The role of small leucine-rich proteoglycans in collagen fibrillogenesis. Matrix Biol 2010 May;29(4):248-53.

(299) Barnard JA, Lyons RM, Moses HL. The cell biology of transforming growth factor beta. Biochim Biophys Acta 1990 Jun 1;1032(1):79-87.

(300) Huang J, Olivenstein R, Taha R, Hamid Q, Ludwig M. Enhanced proteoglycan deposition in the airway wall of atopic asthmatics. Am J Respir Crit Care Med 1999;160(2):725-9.

(301) Sterling KM, Jr., Harris MJ, Mitchell JJ, DiPetrillo TA, Delaney GL, Cutroneo KR. Dexamethasone decreases the amounts of type I procollagen mRNAs in vivo and in fibroblast cell cultures. J Biol Chem 1983 Jun 25;258(12):7644-7.

(302) Shull S, Cutroneo KR. Glucocorticoids coordinately regulate procollagens type I and type III synthesis. J Biol Chem 1983 Mar 10;258(5):3364-9.

(303) Muz MH, Deveci F, Bulut Y, Ilhan N, Yekeler H, Turgut T. The effects of low dose leukotriene receptor antagonist therapy on airway remodeling and cysteinyl leukotriene expression in a mouse asthma model. Exp Mol Med 2006 Apr 30;38(2):109-18.

(304) Henderson WR, Jr., Chiang GK, Tien YT, Chi EY. Reversal of allergen-induced airway remodeling by CysLT1 receptor blockade. Am J Respir Crit Care Med 2006 Apr 1;173(7):718-28.

(305) Henderson WR, Jr., Tang LO, Chu SJ, Tsao SM, Chiang GK, Jones F, et al. A role for cysteinyl leukotrienes in airway remodeling in a mouse asthma model. Am J Respir Crit Care Med 2002 Jan 1;165(1):108-16.

(306) Ruprecht J, Nield J. Determining the structure of biological macromolecules by transmission electron microscopy, single particle analysis and 3D reconstruction. Prog Biophys Mol Biol 2001;75(3):121-64.

(307) Patterson-Kane JC, Wilson AM, Firth EC, Parry DA, Goodship AE. Comparison of collagen fibril populations in the superficial digital flexor tendons of exercised and nonexercised thoroughbreds. Equine Vet J 1997 Mar;29(2):121-5.

(308) Michna H. Morphometric analysis of loading-induced changes in collagen-fibril populations in young tendons. Cell Tissue Res 1984;236(2):465-70.

(309) Tschumperlin DJ, Boudreault F, Liu F. Recent advances and new opportunities in lung mechanobiology. J Biomech 2010 Jan 5;43(1):99-107.